PHD

Optimising the control of a passenger car diesel engine and continuously variable transmission

Deacon, Michael

Award date:
1996

Awarding institution:
University of Bath

OPTIMISING THE CONTROL OF A PASSENGER CAR DIESEL ENGINE AND CONTINUOUSLY VARIABLE TRANSMISSION

submitted by Michael Deacon
for the degree of PhD
of the University of Bath
1996

ACKNOWLEDGEMENTS

I would like to thank Dr Nick Vaughan for his invaluable help and guidance and for his keen interest in my work. I am also very grateful to my colleague Chris Brace, with whom I enjoyed working on the industry and government funded powertrain project. He worked enthusiastically on a parallel project which provided support for my work. My thanks also go to Prof Cliff Burrows for his guidance and valuable support of the powertrain project, and to Dr Steve Charlton who was involved with the setting up of the project and its initial running.

H Jones, Alan Jeffries and Don Blake all made essential contributions in their building of the test rig facility and the installation of the powertrain into the test vehicle. Their ongoing support during the experimental work proved invaluable. Peter Prest, Phil Burney, Paul Philips and Toby Bedding were responsible for the test rig instrumentation and for the data acquisition and I would like to thank them all for their contribution which was clearly essential. For assistance and advice in the modelling work I would like to thank all of the Bath*fp* team and for support and help with general computing issues I would like to thank Dave Barker.

I would like to acknowledge all of the assistance and support for the Diesel CTX powertrain project (which ran simultaneously with this work) given by colleagues at the Ford Motor Company, Lucas Automotive, Johnson Matthey and the DTI.

With gratitude, I think of my family and friends, and thank them for their encouragement and support.

Finally, and especially, I would like to thank Marion, my wife, for all that she has done to support and encourage me, throughout this work and during our first years together.

SUMMARY

The work described here involved the use of a Diesel engine and continuously variable transmission, installed onto a test rig and into a test vehicle. The objective was a substantial improvement in emissions and economy in the passenger car application, without a deterioration in drivability.

The use and history of automotive applications of continuously variable transmissions were surveyed and alternative approaches to CVT driveline control considered. A vehicle drivability appraisal was organised and subjective data compared with objective test results in order to investigate the implications on CVT powertrain control. Computer models of the drivetrain components were written and validated against experimental data. The complete driveline model was used for the evaluation of newly designed alternative control strategies and investigative work concerning powertrain efficiency. Simulation model performance was used in the prediction of drivecycle emissions and dynamic controller action.

The engine and transmission were installed onto a transient test rig with full emissions capability and into a vehicle. This allowed the evaluation of controller and drivetrain performance both in terms of emissions and economy and vehicle drivability. The transient test rig and a chassis dynamometer were used for emissions drivecycle tests. A second vehicle appraisal was completed to assess the drivability performances associated with the new controllers. The newly designed strategies included knowledge based approaches motivated by the field of artificial intelligence. These strategies, implemented experimentally, had structures which enabled the calibrated control action to be highly flexible and tuneable. The controllers were shown to enable lower vehicle drivecycle emissions and higher economy with acceptable drivability when compared with both the original CVT controller and equivalent vehicles with manual stepped ratio transmissions.

CONTENTS

NOMENCLATURE

a	Vehicle acceleration	m / s^2
A_b	Scaled measurement of accelerator busyness	-
A_c	Area of clutch actuator	m^2
a_{err}	Error between predicted and actual vehicle acceleration	m / s^2
AP	Accelerator position signal	-
AP_0	Accelerator position signal at start of transient	-
AP_n	Accelerator position signal on current controller iteration	-
AP_{n-1}	Accelerator position signal on last controller iteration	-
C_f	Coefficient of clutch friction during engagement	-
d	Scaled fuel injection system demand	-
F_{A_b}	Flag to regulate frequency of accelerator busyness calculation	-
F_b	Vehicle braking force	N
F_d	Vehicle driving force	N
HI	Fuzzy term 'high'	-
I_n	Scaled input 'n' to the fuzzification process	-
J	Flywheel inertia	kgm^2
k_1	Spring damper plate damping constant	N/(rad/s)
k_2	Spring damper plate spring constant	N/rad
k_n	Gain term associated with fuzzy rule 'n'	-
k_{slew}	Engine speed slew rate gain	-
k_T	Overall torque change gain term	-
L_t	Scaled distance from start to target during transient	-
LO	Fuzzy term 'low'	-
M_v	Vehicle mass	kg
N_{dem}	Demanded engine speed	rev/min
N_{ideal}	Ideal engine speed	rev/min
N_p	Number of clutch plates	-
N_{slew}	Demanded engine speed slew rate	rev/min/s
P_c	Clutch hydraulic pressure	bar
P_{dem}	Ideal power demand	kW
$P_{gradient}$	Gradient value of power demand equation	-
$P_{intercept}$	Intercept value of power demand equation	-
Ps_{dem}	Secondary pressure demand	bar
r	Spring damper plate rotational deflection	rad
R_e	External radius of clutch plates	m
R_i	Internal radius of clutch plates	m
R_n	Output of fuzzy rule 'n'	-
R_w	Dynamic vehicle wheel radius	m
$\sin(Gr)$	Sin of the road gradient	-
t	Time	s
t_0	Time at start of transient change	s

t_s	Time from the start of the transient change	s
T	Engine torque	Nm
T_{dem1}	Torque demand 1 (Transient shaping controller)	Nm
$T_{dem1lag}$	Time lagged value of Torque demand 1	Nm
T_{dem2}	Torque demand 2 (Transient shaping controller)	Nm
T_{dem_n}	Torque demand at controller iteration 'n'	Nm
T_e	Maximum torque transmissible by the clutch	Nm
T_g	Torque trim gain	-
T_{max}	Maximum engine torque	Nm
T_L	Flywheel load torque	Nm
T_{res}	Spring damper plate resultant torque	Nm
v	Vehicle speed	km/h
W_v	Vehicle weight	N
α_1	Accelerator term in demanded acceleration algorithm	-
α_2	Vehicle speed term in demanded acceleration algorithm	-
δ	Pure time delay before start of transient change	s
ΔT	Incremental change in torque demand	Nm
τ_1	Engine first order lag time constant	s
τ_2	First order lag term defining transient rate change	s
ω	Engine speed	rev/min
ω_1	Spring damper plate loading speed	rad/s
ω_2	Spring damper plate driving speed	rad/s
ω_p	Primary pulley speed	rad/s
ω_s	Secondary pulley speed	rad/s

LIST OF FIGURES AND TABLES

FIGURES **PAGE**

TABLES

1. INTRODUCTION

The focus of the research described in this thesis was the design, development and testing of an optimised drivetrain controller for a passenger car powertrain comprising an electronically governed Diesel engine and an electrohydraulically controlled continuously variable transmission. Optimisation of the controller was for low engine emissions and high vehicle economy, whilst maintaining vehicle drivability.

The work was undertaken as part of a larger research project, the aim of which was to exploit the potential for emission reduction and efficiency improvement of a passenger car by integrating electronic control of a Diesel engine and a continuously variable transmission (CVT). The research was multi-disciplined and involved consideration of issues of thermodynamics, fluid power, transmission and control engineering.

Background

Various reports of the effects of emissions upon both human beings and the environment, (DoE, 1993, Guibet and Douaud, 1992, Hopfner, 1991), have raised the public awareness of these issues. As a result there has been increasing pressure on legislative bodies to take action to reduce emissions production. A significant proportion of environmental emissions are due to the use of passenger cars and there is clearly a need to improve vehicle economy and to reduce exhaust emission levels. The resulting and ever tightening emissions legislation has forced vehicle manufacturers to consider every conceivable approach to emissions reduction. More efficient engines have been designed. Improved engine control has been achieved through the use of fuel injection equipment and electronic mapping of timing advance in petrol engines and electronic control of Diesel fuel injection equipment. Catalysts for treatment of exhaust products are now required by law on all petrol passenger cars sold in the UK. Oxidising catalysts are now fitted to some Diesel engines and research has continued into the use of particulate traps and lean NOx catalysts. Future improvements in emissions will be made by means of better engine design but immediate improvements can be made by alternative approaches. In addition to improving engine design, legislation has caused vehicle manufacturers to look more widely at the whole vehicle powertrain rather than at the engine alone. Improvements have been made by better control and matching of the engine and transmission, (Cuypers, 1984, Hendriks, 1993), and there is further scope for work in this area.

The Diesel engine was chosen for this work because it is the most efficient prime mover for passenger car applications. This is due to its high compression ratio and lack of throttling. Engine efficiencies of 36% to 40% are readily achieved and drive cycle fuel consumptions of 50 - 70 miles per gallon are commonplace. Considerable benefits can be obtained by the adoption of an engine control strategy such that the required output power is always produced in the most advantageous region of the torque speed map. This implies the use of an engine ideal operating line and requires the use of a continuously variable transmission to decouple the fixed relationship which would otherwise exist between vehicle and engine speed with a stepped ratio transmission. The operating strategy of such a powertrain must be based upon a compromise between drivability and economy and emissions.

1.1 Objective

The objective of the work described here was the design and implementation of a control system for the passenger car powertrain comprising the electronically governed Diesel engine and the electro-hydraulically controlled continuously variable transmission. The controller was to be optimised for low engine emissions and high vehicle economy, whilst maintaining vehicle drivability.

To meet this objective it was necessary to develop a specification for the controller operation. This necessitated the study of both the operation of the powertrain and the effect of powertrain operation on the driver's assessment of vehicle drivability.

1.2 Structure of this document

The first section of this chapter has introduced and justified the subject of this thesis. Section 1.3 reviews the recent trends in automotive transmissions. The discussion centres on the use of CVTs, contrasting these with alternative automatic and manual transmissions. The automatic control of various transmissions is discussed. Section 1.4 completes this chapter with a review of control methodologies. The field of multivariable control is discussed in the first part of this section. Following this, alternative methods of control are reviewed and their suitability for application to vehicle powertrains is examined.

The research and progress of the work can be considered in three stages: Firstly, various alternative controller strategies were designed which took into account theoretical powertrain issues and consideration of the conclusions of a vehicle drivability study. The strategies were developed using theoretical and empirical computer models of the complete vehicle powertrain. Secondly, testing of the strategies was performed on a transient powertrain test rig with facilities for the evaluation of engine emissions and economy. Finally, the controller strategies were evaluated in a test vehicle. This allowed assessment of the drivability by comparison with an earlier study and also provided the opportunity for chassis dynamometer emissions tests. The organisation of this thesis is described below.

In Chapter 2, the chosen powertrain is described. Installation of the powertrain on to the test rig and into the test vehicle is also discussed in this chapter. The test and data acquisition equipment used in both applications are described here. A drivability study is described in Chapter 3. The findings of this and the implications for CVT powertrain control are also discussed. Chapter 4 deals with the powertrain simulation work. The chosen simulation package is described and details of each of the powertrain component models are given. Some of the basic model validation work is also discussed here. In Chapter 5 the design considerations for the powertrain controller are discussed and the chosen approach to an overall controller architecture is described. Alternative designs of controller within the chosen architecture are described in Chapter 6. Their modes of operation are contrasted with the operation of the production hydromechanical controller. The implementations of the alternative controllers on the test rig and in the test vehicle are described. Chapter 7 discusses the results of the simulation studies. Chapter 8 includes description of both the test rig and test vehicle work. Both chapters include examinations of the characteristic performances of each of the alternative controllers. The experimental emissions test work is discussed in Chapter 8 and an analysis of a drivability appraisal of three alternative controller calibrations is also included. Chapter 9 concludes this thesis with a general discussion and some consideration of possible future work. The achievements of this work and its context within the field of automotive powertrain control and within the more general automotive field are discussed.

1.3 Continuously variable transmissions

In this section the development of continuously variable transmissions is considered. Their background and present position within the automotive transmission market place are discussed. The most recent CVTs are compared with manual and alternative automatic transmissions in terms of their efficiency and operation, cost of production and the customer perception of the resulting vehicle drivability. The Van Doorne CVT, used for the work presented here is examined in detail. Finally, current powertrain control approaches to both CVTs and alternative transmissions and the trends towards the use of electrohydraulic control are considered.

1.3.1 Advantages of CVTs

The advantages of CVTs when compared with stepped ratio manual or conventional automatic transmissions depend somewhat upon the CVT in question. Generally, as discussed in Section 1, CVTs enable the decoupling of the engine speed from the vehicle speed. This enables a greater freedom in the choice of an engine operating point and gives greater ability to follow an ideal operating line, certainly during steady state conditions and when not limited by the CVT ratio.

Always ensuring strict adherence of the engine to an ideal operating line would not, however, be satisfactory in terms of the vehicle's transient performance. It is therefore necessary to allow the engine to deviate from the ideal operating line during vehicle transients, the length and duration of the deviation being dependent mostly on the driver's demand. Due to the lack of gear changes, an additional advantage is the absence of interruptions in transmitted power. Depending upon the type of CVT, there may not be a need for a starting device due to the inherent inclusion of a geared neutral.

The motivations for the development of CVTs, namely the benefits of lower vehicle emissions, higher economy and improved drivability, have been discussed above. However, the technical challenges have been long-standing. To date, no low cost, easily controllable CVT has been developed with high operational efficiency and a ratio range large enough to enable all engine speeds at all vehicle speeds.

Current CVTs are disadvantaged in the two main areas discussed below. These are the resulting drivability of CVT vehicles and the efficiency of the transmissions themselves. CVTs are also more complex and more difficult to manufacture than alternative transmissions. However, much progress has and is being made in all of these areas, and the use of CVTs is becoming increasingly popular, (Autocar & Motor, 1992, Van Doorne Transmissie b.v., 1994).

<u>Drivability/performance</u>

The drivability, performance and the associated customer acceptance of CVT vehicles have historically been some of the greatest problems faced by powertrain engineers. The difficulties have been caused partly by the need for both transmission ratio control and control of the engine power output simultaneously. Added to these has been the challenge of the design and precise control of a device to enable the vehicle to start from rest.

Problems to be resolved in the areas of drivability and performance of CVT vehicles may be classified by association with vehicle acceleration, deceleration, steady state operation and starting and stopping. The challenges associated with customer acceptance may be divided into the areas of firstly perception and subjective assessment of powertrain behaviour, and secondly the resulting need to translate customer comment and desire into a practical control strategy.

Engine ideal operating lines have usually been biased towards the high torque low speed area of the engine map. This has produced the better vehicle fuel consumption performance, but inherent in this strategy is the delay in achieving full power while the engine is accelerated from low to high speed. During this delay the vehicle may be either accelerated more gradually, maintained at constant speed or worse, decelerated.

During vehicle deceleration, the engine speed may be kept high to enable engine braking. In addition to this effect, high engine speeds enable fast engine power delivery response if the accelerator pedal is suddenly pressed during the deceleration. However, high engine speeds are also generally associated with higher fuel consumption and emissions and higher noise levels. These arguments promote lowering the engine speed during deceleration to a value limited only by the transmission ratio. Engine speed control during deceleration is thus a compromise dependent upon these factors.

When at constant speed, the best operating point for combined engine and transmission efficiency may be used. As discussed above, this is generally towards the high torque, low speed area of the engine torque speed map which is also better for low powertrain noise. However, if the chosen point is a low power point close to the engine limiting torque curve, there may be considerable delay in moving the engine to a higher power delivery point. This is due to there not being sufficient extra torque available to accelerate the engine quickly to higher speed.

Starting from rest requires the use of a starting device. Van Doorne based transmissions have to date used both clutches and torque converters for this purpose, (Hendriks, 1993). Some hysteresis is needed in the control of the starting device. Swift acceleration from rest is achieved by running the engine at high speed and power, the speed difference at the transmission input being handled by the starting device. However, the starting device must be locked up during steady state powertrain operation and low vehicle acceleration to enable operation of the engine at lower speed. This leads to improved emissions and economy. In the case of a gradual acceleration from rest, synchronisation of the starting device input and output speeds should occur at a lower engine speed than in the case of a rapid acceleration from rest. Torque and hence power delivery is less in this case and the power lost in the starting device is also lower.

Hysteresis in the starting device is also an important factor when considering control of the transmission as the vehicle comes to rest. As the vehicle comes to rest the transmission is likely to have reached the lowest ratio enabling the lowest possible engine speed. The starting device will be locked up due to the probable small torques present across it. As the vehicle comes to rest it is necessary for the starting device to disengage either partially or completely and for the transmission to change to the highest ratio ready for the next start. These procedures must be completed without causing an unacceptable variation in the perceived deceleration rate of the vehicle.

Fuel consumption/emissions

The fuel consumption of CVT vehicles using the Van Doorne based transmission tend to be worse than those using conventional stepped ratio manual gearboxes, (DoT, 1994). The efficiency of vehicles fitted with the Van Doorne based transmission is affected by factors such as the hydraulic pump size and the design of the hydraulic circuit (Guebeli, 1993, Micklem 1991). The overall powertrain control strategy in terms of where the engine operates for various demanded powers is also important in determining the vehicle fuel consumption. Emissions performance is related to fuel consumption performance. Carbon dioxide production is directly related to the amount of fuel burned. Other gaseous and solid emissions vary across the engine torque speed map. Vehicle emissions are generally measured per distance travelled. The amount of vehicle acceleration and braking over the distance clearly has an effect on the overall emissions, but in addition to this the steady state engine torque and speed for a given vehicle speed also has an effect. Therefore the choice of engine operating line for steady state use and the allowable deviation from this line during acceleration and deceleration is vital in enabling low vehicle emissions.

1.3.2 Comparison of CVTs with manual and alternative automatic transmissions

Manual and stepped ratio (conventional) automatic transmissions have the largest share of the automotive transmission market. The following paragraphs describe the current trends in manual and conventional automatic transmissions. In this way, the discussion reviews the state of the market place in which automotive CVTs are promoted.

Developments in materials, manufacturing techniques and lubrication technology have enabled improved overall efficiencies in all types of vehicle transmissions. In addition, there has been a move towards the use of a greater number of ratios in both manual and conventional stepped ratio automatic transmissions. These two factors have led to generally improved vehicle efficiency and performance (DoT, 1994).

Manual transmissions

Over the last few years there have been no great changes in manual transmission design. Manual gearboxes are highly efficient in transmitting torque across a large range of ratios. This gives them an advantage over conventional automatic transmissions and current CVTs in terms of overall vehicle economy and emissions levels. However, there is a trend towards automatic control of conventional manual transmissions, (Watanabe et al, 1984, Page, 1985, Kasai et al, 1986), using actuators to control the clutch and gear change and these types of automated transmissions will have efficiencies approaching those of manual gearboxes.

Conventional automatic stepped ratio transmissions

The developments in automatic stepped ratio transmissions have also been driven by the goal of greater efficiency and performance. Four speed transmissions are now usual (DoT, 1994). Intelligent interpretation of the driver's intentions and electronic control of the ratio selection have all led to greater refinement and performance. Better matching of the transmission with the engine, improved regimes of starting device operation, for example, torque converter lockup and freewheeling capability on the overrun, and measurement and interpretation of such variables as driving style are all becoming commonplace in the current market.

Alternative automatic stepped ratio transmissions

The basic disadvantage of the energy lost to the torque converter has led manufacturers to look to other types of drive as an alternative for use in an automatic stepped ratio transmission. The efficiency advantages of geared drives over other types of transmission have caused a recent trend in manufacturers attempting to automate manual stepped ratio geared transmissions. If this was easily possible, there would be an argument (offset against one of cost) to increase the number of ratios available which would move the ratio capability of the transmission towards that of CVTs. However, there are still challenges to be met in the areas of clutch and engine management during the gear shift. Lees (1992) believes that Automotive Products has overcome the gear shift problem in an Automatic Clutch System (ACS) which comes in a range of levels, the most automated using a conventional design of clutch and gearbox. In the past Automotive Products worked with Porsche to develop a two-clutch gearbox which worked using the clutches alternately to progress through the gears (Scott, 1983).

1.3.3 Development of CVTs

CVTs for passenger cars have been under investigation for most of this century. However, it is only over the last twenty years that the significant and commercially viable developments have taken place.

Christenson (1975) described the toroidal drive and the hydrostatic split power transmission as those CVTs showing most promise for use in medium to large size cars of the future. At this time the DAF, manufactured in Holland, was the only production car making use of a CVT. It used two V-belts in tension, one for each driven wheel, each with variable sheaves to allow continuous change of the speed ratio. However, the DAF was a small, low powered car and the transmission system was not thought suitable for more demanding applications.

By 1980 the metal push-belt variable speed unit (VSU) had been developed to such a level that it was shown by Horowitz (1980) to be the only CVT design sufficiently practical and efficient to be used for automotive applications. Horowitz compared many types of transmissions including continuously variable belt, chain and traction drives and geared and timing belt drives. The significance of his paper has been shown by the fact that the metal belt CVT is the only automotive CVT currently in production. There are still, however, challenges in the areas of efficiency and transient control.

At present, the metal push belt design, described by Hendriks (1988) continues to gain ground in its share of the automatic transmission market. It is supplied as a variable speed unit by Van Doorne Transmissie b.v. Early problems in belt reliability which appear to have been linked to manufacturing techniques seem to have been solved and the Van Doorne V-belt variable speed unit (VSU) now has a life expectancy equal to that of the other major components of a car.

Over the last decade the Van Doorne metal thrust belt VSU has been incorporated into several transmissions by European motor vehicle manufacturers. Ford developed the CTX, (Roper and Simon, 1987), the VSU being under the supervision of a hydraulic controller which also controlled the operation of two wet clutches. Fiat, (Howard, 1992), and Rover went into production with vehicles equipped with CVTs similar to the CTX. Meanwhile both Subaru and Nissan developed electronically controlled transmissions based on the Van Doorne VSU (Sakai, 1988, Narumi et al, 1990). Section 1.3.4 gives more detail on the Van Doorne VSU and its use in various manufacturer's transmissions.

There have been many other belt and chain CVT drives which have been developed from the times of the first motor cars. These belt drives can be classified by whether their method of operation is dependent upon tension or compression. Cuypers (1984) compares two metal V-chains with the Van Doorne metal V-belt in his discussion of traction drives. He relates forces acting on individual belt and chain elements to overall unit efficiencies and concludes that V-belts have advantages over V-chains in terms of higher power density at large diameters and lower operating noise levels. Cuypers draws attention to the manufacturing challenges of the V-belt. An electrohydraulically controlled tension belt CVT is presented by Schneider (1989) in his paper. The system is designed such that the speed of the engine is controlled by the transmission ratio. The engine fuel is then scheduled according to the engine speed. This can be done with a focus on optimising efficiency or performance. Drivability considerations are taken into account, by, for example, limiting the engine speed set point as a function of vehicle speed above, say, 70 % throttle demand.

Kumm and Kraver (1986) discuss a flat-belt CVT in their paper. The efficiency characteristic of the unit is investigated with reference to the output speed and the ratio. Economy Mode and Sport Mode engine operating lines are described. However, since it is ultimately the efficiency of the whole vehicle which is important, it is clear that any engine ideal economy line must be combined with an efficiency map of the transmission so that an overall powertrain efficiency map can be obtained. The work presented by Kumm and Kraver did not indicate that they had analysed the overall powertrain efficiency. If this was done, then the powertrain efficiency map could be used for generation of the ideal operating point. In the steady state, the system would be operated at this point. However, due to the need for good vehicle drivability, it would be necessary to deviate from this line during a vehicle transient. Control of the rate of ratio change of the CVT in response to pedal movements would play an important role in the amount of this deviation from the ideal operating line and hence would be a critical factor affecting vehicle drivability.

As the use of the push belt CVT has grown, the toroidal drive, described as having much potential by Christenson (1975), has been developed further. One of the most well known toroidal traction drives is the Perbury Transmission (Perry, 1980, Stubbs 1981), first developed by Hayes. Stubbs describes the transmission in terms of the acceptable drivability performance of a test car. The vehicle was also found to have improved acceleration and fuel economy compared with a vehicle fitted with a conventional stepped ratio automatic transmission. It was concluded that the toroidal drive had good potential for future applications but that the challenges of transient control still required attention.

The development was continued over many years by Perbury Engineering, Leyland Cars, Leyland Vehicles and most recently Torotrak (Development) Ltd., who installed the transmission into a Rover

820i saloon car for the purpose of evaluation (Smith, 1992). Results indicated that by using a strategy that governed the engine to operate on a 'predetermined control line' savings of 10 % in economy and 20 % in carbon based emissions could be made compared with the manual transmission vehicle over the US emissions drivecycle. The types of control strategy used are described in more detail by Ironside and Stubbs (1980). The significance of the control of the Perbury CVT is the use of a proportional solenoid valve to regulate the torque transmitted by the CVT rather than the CVT ratio. It is this feature which enables the geared neutral to be workable. Ironside and Stubbs (1980) also make particular reference to an 'ideal operating line' for a 60 kW Otto engine and to deviations of the operating point from this line during vehicle transients. It is emphasised that when an increase in pedal demand occurs, a compromise must be made between using the available excess torque at the current engine speed to accelerate the vehicle and using this torque to accelerate the engine to a new higher speed where more power can be developed.

Hydrostatic transmissions, which consist of an hydraulic pump connected hydraulically to a motor, are attractive due to the wide ratio range possible, the existence of a geared neutral and the ease of installation into the vehicle. They are particularly suited to vehicles needing four wheel drive and large ground clearance. The disadvantages, however, are due to the low operating efficiencies obtained in at least part of the speed / power range. Despite this, work by Luo et al (1986) has predicted average efficiencies of 92 to 94 % using various control strategies in a project involving such a system on a vehicle of mass 1360 kg powered by a 1.8 L engine. Their control strategy made use of both a torque and a power control regime. By switching between the two and ensuring that the engine was close to its most efficient operating point for the required power output, an optimised overall system resulted.

Control of CVTs is a very different problem from that of control of a conventional stepped ratio transmission. The issues involved are discussed with clarity by Yang, Guo and Frank (1985). The control of the acceleration of a non - CVT vehicle can be performed by varying the throttle or the amount of fuel injected. On a vehicle with a CVT, however, acceleration may also be affected by controlling the rate of change of the transmission ratio. This most important difference between vehicles with conventional stepped ratio transmissions and vehicles with CVTs is the key to achieving good drivability. It also leads to the possibility of controlling the vehicle acceleration by control of the ratio alone, whilst scheduling the fuel injected or throttle position automatically according to the values of the demanded and actual engine speeds. Although different CVTs may be more or less easy to control, all of them may be used in the type of strategy described above. Section 1.3.5 discusses the control of transmissions in more depth.

1.3.4 Detail of the Van Doorne CVT

The Van Doorne based transmission is manufactured under licence by several of the largest of the world's car producing companies. Van Doorne supplies the push belt CVT variable speed unit, the principle of operation being the same in all cases. The differences occur in the choice and type of starting device, the output gearing, the casing and the control strategies and their implementation. Control is through the use of hydraulic valves which vary the clutch and primary and secondary pulley pressures. The operation and hydraulic control of Ford's version of the Van Doorne transmission are described in Chapter 2.

The Van Doorne CVT has been used mainly in small and medium vehicles. There was an initial limitation on their power handling capability but this is gradually being overcome and such CVTs are now being implemented in larger vehicles. The response of the motoring press towards the new CVT vehicles has been good and their share of the small and medium car market has gradually increased since their introduction. Currently over one million Van Doorne based CVTs have been fitted to passenger cars, (VDT, 1994). Autocar & Motor (1992) reported that 6% of Ford Fiesta sales were cars fitted with the CTX transmission and that this figure was increasing. However, it must be recognised that the CTX is the only automatic transmission available in this particular vehicle.

Hendriks (1993) describes the vehicle performance and powertrain control of a 3.3 L Chrysler Voyager fitted with a 250 Nm capacity CVT. As in previous work in this field the use of the transmission to place the engine on an ideal operating line is discussed. Significant in this paper are experimental test results which show a 17 % decrease in fuel consumption over the ECE drive cycle when compared with the four speed automatic version of the vehicle. The same system with identical calibration also shows an improvement of one second in the 0 - 100 km/h acceleration time. Different control strategies enable powertrain operation in any of a sport, normal or economy mode.

Both Nissan and Subaru have marketed versions of the Van Doorne variable speed unit incorporated into transmissions having electro-hydraulic control of secondary pressures and electronic control of a magnetic powder clutch. A solenoid valve is used to control the hydraulic pump line pressure (which is usually applied directly to the secondary actuator). Control of the primary pressure is hydromechanical. The Subaru system is discussed by Narumi and Suzuki (1990), Sakai (1988) and Kasai and Morimoto (1988). It is clear from the complexity of the rules governing the operation of the clutch that a great deal of effort has been spent in the optimisation of its control strategy. The correct amount of torque being transmitted by the clutch in different circumstances is vital to a good vehicle drivability characteristic. For the control of the variable speed unit, Narumi and Suzuki first relate the level of the secondary pressure to the amount of torque which is to be handled by the transmission. Having set the engine throttle, and the secondary pressure, the remaining task is to set the transmission primary pressure. Particular care is taken in the determination of the primary pressure since it is this which controls the ratio and therefore has great effect on the perceived vehicle drivability. The derivative of the pulley ratio with respect to time is considered. If this value becomes too large, it indicates that the control strategy would cause an initial deceleration in the vehicle before a higher but uneven acceleration. At the other extreme, a small rate of change of ratio with respect to time would result in insufficient acceleration being achieved. The values of the target pulley ratio and the throttle opening angle are used in the determination of the primary pulley pressure. The resulting strategy is designed to operate the engine along an ideal operating line.

The experimental work presented in Chapter 3 involves testing of both an hydraulically controlled Ford CTX transmission and an electrohydraulically controlled Nissan N.CVT transmission. The observed operating envelopes and driving characteristics of these transmissions are discussed in more detail towards the end of that chapter.

1.3.5 Automatic control of transmissions

The task of controlling an automotive transmission can be considered to fall into two areas. Firstly there is the strategic function of determining the most appropriate response of the powertrain to the driver's demands. Secondly there are the tasks associated with achieving this response.

The first task is concerned with interpreting the accelerator pedal signal level and its rate of change. The strategy may adapt to the driving style and also be influenced by other vehicle and powertrain sensors. Finally, a choice must be made about the amount of power demanded from the engine and the ratio at which to operate the transmission. The demanded rates of change of these variables during transients must also be determined.

In order to achieve control of the engine power developed, both the engine torque and the engine speed must be governed. The amount of fuel injected per engine cycle is the main factor which determines the engine torque. This quantity is regulated by the fuel injection pump control system. The engine speed is a function of the vehicle speed and the transmission ratio when engaged. Therefore the required ratio must be achieved so that the engine runs at close to the demanded speed. In the case of the push belt CVT, it is the primary and secondary actuator pressures which must be controlled in order to define the transmission ratio and its rate of change. In conventional automatic transmissions, both the choices of discrete ratio and the conditions at which ratio shifts are to be made must be determined.

Early controllers for both stepped ratio and continuously variable transmissions were implemented hydraulically. Input signals were used from the accelerator pedal, selector lever position, engine speed and vehicle speed sensors. With the general trend towards the use of electronics and microprocessors in the control of vehicle systems, controllers which have been dependent upon hydraulics alone have been superseded. Hydraulics has remained for the actuation of clutches, whilst electronics is being used in making the choice of ratio and for the modulation of hydraulic clutch pressures or electromagnetic clutch actuation. Electronics used in this way have enabled the production of more flexible and refined strategies for all types of transmission.

Push belt CVT

Both the Van Doorne hydromechanical and the Van Doorne electrohydraulic controllers tested as part of the experimental work described in Chapter 3 were designed to place the powertrain operating point inside a pre-defined envelope on a vehicle speed - engine speed variogram (Figure 1.1). Demanded engine speed was a function of vehicle speed and accelerator pedal position. Demanded engine torque was a nearly linear function of accelerator pedal position. Inherent in the variogram approach and control structure were the strategies for both steady state and transient performance. Several algorithms designed to dampen and smooth the ratio shifting action were embedded into the strategy. Due to the non-linear nature of the transmission ratio control, the closed loop controller gains appeared to be scheduled with the transmission operating conditions. The Nissan N.CVT transmission controller operation also appeared to be based upon the philosophy of a vehicle speed - engine speed variogram control strategy similar to that shown in Figure 1.1 and described above.

The Van Doorne strategies were found to be generally good in terms of drivability. However, there are significant drawbacks associated with the use of vehicle speed in the generation of the engine speed demand and not considering the engine operating point in the torque speed domain as prominently as in the variogram. One outcome was that the engine speed was often set at a rather higher than necessary level for the power being developed and a lower torque used. The high speed, low torque area of an engine speed map is often the poorest for emissions and economy. The Nissan N.CVT powertrain operation suffered in the same way, albeit to a lesser degree. More detail is given in Chapter 3 on the steady state and transient performance of each of the above controllers for the Van Doorne transmission.

Stepped ratio automatic transmissions with torque converters

Improvements have been made to shift quality in stepped ratio transmissions through the use of engine torque reduction during shifts and the application of modern electronic techniques in controlling clutch pressures. Hojo et al, (1992) describe the application of modern control theory to Toyota's five speed automatic transmission. The five ratios are produced from two gear sets in series and it is necessary to shift each gear of the two gear sets synchronously. The basic concept of the strategy lies in the setting of target values for the speeds of the sun gears of the two units. A feedback system is then constructed so that the engagement pressures of the two clutches can be controlled such that the speeds of the sun gears follow the target values. The hardware used to implement the strategy consisted of the usual sensors, solenoid valves and two processors, one controlling the engine and communicating with the second, used for the transmission itself.

Torque converters are usually implemented in conventional automatic transmissions as the starting device. These allow the multiplication of torque when the input and output speeds are different. Unfortunately, the use of a torque converter introduces an area of inefficiency into the powertrain. As the difference between input and output speeds decreases, the efficiency increases. The use of a converter lockup clutch can improve the efficiency by synchronising the input and output speeds under certain suitable conditions. Electronic control strategies usually make use of engine load and transmission output speed measurements in determining the operation of the lockup clutch. Computer aided design tools have enabled optimisation of torque converter designs and operation. Kondo et al, (1990) describe the implementation of such a unit in a four speed transmission. Simulation of the oil flow within the unit enabled sudden changes of oil flow velocity, and the associated losses, to be avoided by improved design. The converter lockup clutch operation was determined electronically using speed and engine throttle signals.

Shift control strategies

Conventional automatic transmission shift control strategies which were inflexible and unable to adapt to driver and system requirements in their hydraulic controller implementations, have become greatly improved through the use of electronics. Original, hydraulically implemented, fixed shift strategies were set up by choosing a compromise between fuel economy and drivability requirements. Now, electrohydraulically implemented control systems adapt the transmission shift strategy according to measured powertrain variables and driving style. Yamaguchi et al, (1993) describe the implementation of a shift control strategy which uses fuzzy logic. A shift strategy, optimised for economy, is developed by considering the fuel consumptions in each of the gear ratios. A second strategy is developed for optimised drivability. This is done by choosing shift points so that the disturbance in force at the driving wheels during the shift is minimised. At large throttle openings it is not possible to match the power delivery from the engine in two adjacent transmission ratios and so the engine is allowed to reach rated speed during vehicle acceleration before shifts are initiated. As part of their work, Yamaguchi et al studied the behaviour of drivers in terms of their use of the accelerator, brake and steering wheel over both an expressway and a winding uphill road. A fuzzy controller was then developed which was able to recognise the driving environment from the way in which the vehicle was being driven. From this the controller was able to adapt the shift strategy in the appropriate direction. The resulting control strategy produced an improved transmission operation. A commonly recognised problem with shift strategies is symptomised by the transmission upshifting just before a slight bend due to the driver decreasing the accelerator demand, followed by the transmission downshifting again after the bend. The occurrence of this problem was greatly reduced by the implementation of the fuzzy logic shift schedule.

Stepped ratio automated transmissions with dry friction clutches

Inefficiencies associated with torque converters have motivated interest in the possibility of automating a conventional manual transmission and dry clutch. Such a system would not only have higher overall efficiency than a conventional stepped ratio automatic, but would also be likely to share many similar components making it less expensive to manufacture. Since driver effort would not be involved, the number of ratios could be increased leading to further efficiency gains. Watanabe et al (1984) applied an automatic control system to a mechanical clutch and five speed transmission. Both the clutch and transmission were standard production units. Operation was performed by actuators controlled by a central processor. The shift control strategy design for such a transmission raises essentially the same considerations as those relevant in the case of conventional stepped ratio automatic transmissions. However, simple automation of the conventional manual transmission and clutch does present a major challenge in the area of drivability. This is due in particular to the interruption of power which occurs during clutch disengagement. The problem is compounded by the fact that the driver may have no warning of an impending shift and that shifts can often quickly follow an increase in demand from the driver. This has been overcome in systems where there are two clutches but such systems can lose the advantage of full commonality with existing manual systems (Scott, 1983).

1.4 Control methodologies

Electronic systems are now standard in automotive engineering. Their applications include fuel injection and engine management systems, both for Diesel and spark ignition engines, supervisory systems to interact between the driver and the powertrain, (Yamaguchi et al, 1993), and safety systems such as anti-lock braking. The electronic hardware currently available has enabled manufacturers to move towards the use of both modern state space methods and intelligent control in their quest for improved powertrain control. This has led to cleaner, more efficient and more drivable vehicles.

The development of control theory and the application of the latest control methods to practical engineering problems is a vast and on-going process. Over the last twenty years one of the main growth areas has been that of robust multivariable feedback control and in the approach to problems caused by unknown or highly non-linear plant. The challenges involved and the alternative approaches are well documented, (Soeterboek, 1992, Lunze, 1988) At the same time, progress in another quite different area has involved a group of approaches collectively known as artificial intelligence. This group, which includes both the fuzzy logic and neural network approaches to multivariable control, is characterised by systems which have some ability to be trained or actively learn from real or simulated data. Due to this property, they can be applied in decision making systems, (White and Sofge, 1992, Pedrycz, 1993).

Modern state space approaches to robust multivariable feedback control and various decision, rule based and artificial intelligence methods are discussed in the following sections. Following this, there are comments on the use of the different approaches in automotive applications today. The relevance and suitability of the different methods to the objectives outlined in Section 1.1 are discussed.

1.4.1 Alternatives for powertrain control

The primary objective of this research work (that of designing an optimised controller for an engine and CVT) is one which may require the use of methods previously applied to the control of other non-linear multivariable systems. This section is used for a brief review of alternative methods of control for multivariable systems.

State space method

The application and benefits of applying modern control theory to automotive engine control are discussed by Tabe et al (1987) in their paper. Kamei et al (1987) also use state space methods in the design of a controller for an automotive engine. Consideration of the complete vehicle powertrain system in state space terms is essential for the application of some modern adaptive control techniques, which are described below.

Neural networks

Recently neural networks have been used increasingly for the modelling of non-linear systems. Their use is now being extended into areas of system control. Bacon et al (1992) discuss the replacement of various functions within a modern electronic engine control system with trained neural networks. Benefits such as ease of calibration and reduction of control system strategy are also mentioned. Since it is possible to construct a network with any desired number of inputs and outputs, this makes neural networks particularly suitable for the control of non-linear multivariable systems.

Fuzzy logic

Due to drivers' varying behaviour when driving, it may be necessary to adapt the response of the vehicle powertrain depending upon the levels and rates of change of the inputs received from the driver's controls. This could cause the system to behave more or less sensitively to changes of input signal levels. Fuzzy control has been applied to the shift scheduling strategy of an automatic transmission by Yamaguchi et al (1993). Many other applications of fuzzy control exist. For example, Abate and Dosio (1990) discuss its use with reference to engine idle speed control. Research and current methods in the fields of fuzzy logic and control in uncertainty may be relevant to the design of a suitable controller for a vehicle powertrain incorporating a CVT.

The need for adaptive control

As discussed above, some type of controller adaptability to the driving style seems desirable. Adaptive control has usually been applied to systems with the aim of producing a consistent performance. Here, its use is intended to modify system performance in different circumstances. It was envisaged that the control action would be aimed at generally raising the engine speed when the driving style was more transient or busy. This would give a more responsive feel to the vehicle in such conditions. The idea of a controller which adjusts its own parameters to the process is also appealing and extremely valuable in the cases of unknown, highly non-linear, or time varying processes. All of the control methods mentioned in this section can be configured so that they have an adaptive capacity. However, there has been continually increasing interest, over the last thirty or more years, in the broad field of adaptive control, and some methods of control have been specifically developed for their adaptive capability.

Some predictive controllers belong to the class of model based adaptive controllers. They have been applied successfully to both single input single output and multivariable control problems. Their performance can be comparable to Linear Quadratic or Pole Placement controllers but their implementation and tuning is often much easier. However in contrast to either of the above methods, predictive controllers may be applied to non-linear problems. There are many designs of predictive controllers some of which contain adaptive features. In all designs of predictive control, the future controller output sequence is calculated so that the predicted output of the process is close to the desired process output. The desired process output is called the reference trajectory and may be an arbitrary sequence or the response from a dynamic reference model. The process is continually repeated using the latest measured information which takes into account disturbances. The length of time ahead for which the predictions are made is known as the prediction horizon. This is a finite length for predictive control whereas for LQ control it decreases as time elapses. In practice LQ controllers often have an infinite prediction horizon making them similar to predictive controllers. In this case the only differences are that LQ controllers cannot take into account restrictions on the available control output and also cannot make use of non-linear plant models. In both LQ and predictive controllers a function is used to measure how well the output follows the reference trajectory. The control sequence is determined by minimising a function of the difference between the output and reference trajectories over the prediction horizon.

The development of an accurate reference model of the Diesel CVT automotive powertrain is fraught with difficulties due to key variables such as vehicle mass and road gradient being unknown and complex or impractical to measure or predict. Application of the state space approaches to the CVT powertrain control problem would certainly be hampered by the lack of a good reference model. In contrast to the LQ and predictive model based methods, both the fuzzy logic and neural approaches to multivariable control do not require any kind of dynamic reference model. In their application to the CVT powertrain control problem, the artificial intelligence methods are therefore at a distinct advantage.

1.4.2 The chosen approach to the design of the control strategy

The continually developing field of control theory and its application in engineering has been discussed briefly in the section above. Various alternative approaches have been discussed. So far the discussion has centred on the issues associated with the engine torque and speed control, for example the injected fuel quantity control signals, the transmission control pressures, the plant feedback signals, key variables and the practicalities of a system reference model. However, a further major issue to consider is the interaction of the driver with the system, at the other end, or side of the controller strategy. As discussed in Section 1.3.5, there is clearly a need for accurate interpretation of the driver's requirements from the inputs he or she supplies to the controller. Here it is also important to find the correct compromise between the goals of low vehicle emissions, high economy and good drivability. The fuzzy logic and neural network control approaches are considered advantageous in their ability to blend together operating rules or desired system behaviour into a realistic control action and in this way interface between the driver and the powertrain.

Due to the apparent advantages of the artificial intelligence approaches over alternative methods in their application to the CVT powertrain control problem, the decision was taken to investigate these methods further. This choice was made in the light of the issues already discussed and for the reason that the fuzzy and neural approaches were considered most appropriate for the tasks of decision making during powertrain transients and for the implementation of knowledge based control. The remainder of this section is used for a more detailed discussion of the artificial intelligence methods and the particular way in which they could be appropriately applied to the Diesel CVT powertrain.

Fuzzy Controllers

The idea of fuzzy sets, upon which fuzzy controllers are based, appeared first in about 1965. Zadeh (1965) published a number of papers at this time explaining their conception and properties. The concept of fuzzy sets seeks to provide a mathematical interpretation of situations which were previously only describable in terms of linguistics/semantics. Whereas with conventional set theory, a Boolean model is used to determine the state of belonging to a set, fuzzy logic defines a grade of belonging to a set. Members of a fuzzy set may have any state of intermediate belonging to a set between total membership and total non - membership. A membership function is a formula relating the member to its grade of membership.

Fuzzy sets may be used to represent various conditions of the measured inputs and/or plant feedbacks into and outputs from a control strategy. Controller operation can then be described initially in semantic terms. The control strategy may be implemented by means of a number of output actions dependent upon certain input conditions. Each of the possible input condition scenarios is described in this way, and by this means the output actions are blended together as the input conditions change from a strong match with one defined configuration to a strong match with another.

An early application of fuzzy control was in the adjustment of the fuel rate, the kiln speed, the burning and back zone temperatures and the exhaust oxygen from a cement kiln (Larsen, 1979). Human operators were questioned to determine their learned response in terms of control actions to meet each of the possible input situations. A set of linguistic rules was then written for the operation of the kiln. Fuzzy primary terms such as drastically low and slightly high were used for the measured variables and terms such as negative and very positive for the control variables. Rules representing the operating conditions were then translated into fuzzy conditional statements linking the input terms to the control terms.

The following years saw many further applications of fuzzy control in both domestic and industrial applications. Generally the concept was applied in areas where a great deal of information and experience had previously been gathered from running a process. Sensor cost was not usually a problem since high accuracy was not required due to the fuzzification process. Unit cost in applications warranting fuzzy control was usually high compared with sensors, due to implementation only in the 'top of the range' models. Development time was considered lower than when using alternative 'classical' methods.

Applications of fuzzy control may be classed according to the types of controller inputs and outputs. At one end of the spectrum are the numerical input, numerical output closed loop controllers of which there are many examples. A final output control action is a result of the numerical inputs and a number of rules and fuzzy functions. The controller may make use of previously developed look-up tables. Alternatively, applications exist in which the controller action is only used for information and guidance and it is a human operator who makes the final decision about the control action. Clearly the implications for stability and safety vary greatly at these two extremes.

Design aspects of fuzzy controllers

Important issues which need addressing in the design of a fuzzy controller are concerned with the generation of the rule set, the input/output algorithms and desired dynamic response. Four crucial aspects are the completeness of the rules, their consistency and interaction and finally the robustness of the controller. Taking each of these in turn:

There must be an appropriate output control action for any possible combination of the inputs.

It is important that the rules are consistent and for example two control rules with almost the same conditions do not suggest very different control actions.

When the conditions of one rule are perfectly met, other rules will be partially activated. The additional control output must not cause a diverse effect.

The effects of disturbance caused by noise on the inputs must be acceptable.

The dynamic properties of a fuzzy controller are a function of the scaling factors used on the inputs and control actions and the shapes of the membership functions. Appropriate values are usually found in simulation using a simple model of the plant. Fine tuning often takes place on the plant at the commissioning stage. It is sometimes possible to assess the stability of a fuzzy controller. Kickert (1975) showed that a fuzzy controller can sometimes be modelled using describing functions. Using such a model with a model of the plant, a frequency domain stability analysis can then be carried out. It is not always possible to do such an analysis, in which case, the controller must be tested in open loop operation for confidence in the quality of control to be gained.

Further features of fuzzy controllers recently to have been developed include context-invoked rules (which come into play when certain input conditions are met), zooming (the controller action becomes more detailed as a particular point in the operating envelope is homed in upon), hierarchical and hybrid structures of controllers, and the use of fuzzy control in supervisory control over other types of controllers having adjustable parameters.

Neural Network based controllers

Neural networks are inspired by the working of neurons found in the structure of the brain. Generally, neural networks have a structure of interconnected layers of neurons beginning with an input layer and ending with an output layer. Each neuron is represented as a (usually non-linear) mathematical function such as a sigmoid and is connected to every neuron in the adjacent layers. Signals arriving at a neuron from the previous layer are combined by multiplication with weighting functions before application to the mathematical function. Signals pass in this way from the input to the output layer of the network.

Networks are usually trained by exposure to training data and by the use of an algorithm which adjusts the weights and bias values associated with each neuron in an iterative fashion until errors are minimised over the entire data set. Once trained, the inputs of a network can be stimulated with input signals and the outputs give signals appropriate to the levels of the inputs.

Neural networks have been used in many applications concerning recognition such as speech or visual data processing. A major advantage they have here over other methods is their inherent noise rejection capability. They have also been used in control, (White and Sofge 1992).

It is clear from their operation that neural networks could be used to implement many other types of controllers - even if purely by training them on data collected from simulated operation of other controllers. However, due to consideration of the non-linear nature of CVT powertrain operation particularly near the edges of the operating envelope and the limited ability of neural networks to map sharp control discontinuities, it would seem most appropriate to use neural networks within a framework of more strongly defined rules for boundary controller operation. This control framework could be provided by a rule based approach.

Neuro-fuzzy controllers

Neural networks are notable for their ability to learn from example. They are also simple and efficient in their implementation and operation. Fuzzy functions have the ability to represent uncertain knowledge in a mathematical structure. Where it is possible to combine these two architectures, a very powerful method of knowledge based control arises.

Choice of controller structure

In reaching the objectives outlined in Section 1.1, it was expected that the issues of transient powertrain control would be dominant in terms of their impact on the design and types of control strategies implemented. Consideration of both drivability aspects and the dynamics of the powertrain itself leads to certain controller requirements including non-linear operation, adaptability and the ability to implement appropriate and distinctive actions in certain recognisable situations.

The approach of the research into alternative controller designs was described above. For practical reasons it was decided that the controller architecture would be of an hierarchical structure.
It was envisaged that there would be two basic levels. Firstly and at the higher level, there would be a supervisory controller responsible for the scheduling of the engine operating point depending upon the driver input, time and other powertrain feedbacks. At the second and lower level, there would be a powertrain controller for the closed loop control of the powertrain. This would schedule the fuel injection system demand, control the transmission primary pressure in order to achieve the demanded engine speed and schedule the transmission secondary pressure according to the ratio and engine torque demand. It was considered that any algorithms required in the powertrain controller for closed loop control of the primary pressure would be based upon previous work by Guebeli (1993), or on algorithms similar to those used by VDT in their production of an experimental electrohydraulic control system for the CTX transmission.

The decision to use an hierarchical approach to the controller structure was made because neither the engine fuel injection system controller or the transmission electrohydraulic system had been designed for use as part of a distributed intelligent controller network. It was easier to develop a supervisory controller structure, which communicated demands of engine torque and engine speed down the structure to the low level engine and transmission controllers. Alternative strategies could then be developed and tested after implementation in the controller structure.

Although the hierarchical structure was imposed, it was appreciated that an alternative Controller Area Network (CAN) structure could in the long term offer benefits of greater reliability and more fail-safe operation. Distributed CAN systems are being used increasingly in the automotive industry because of these advantages. Chauhan (1993) reviews the current state of automotive electronic systems architecture and discounts centralised architectures due to problems with space, heat dissipation, wiring and cost of replacement among others. Due to the general move of the automotive electronics industry towards distributed control systems, it was realised that, for future implementation, any control strategy designed in the course of powertrain project needed to be suitable for implementation in a distributed architecture.

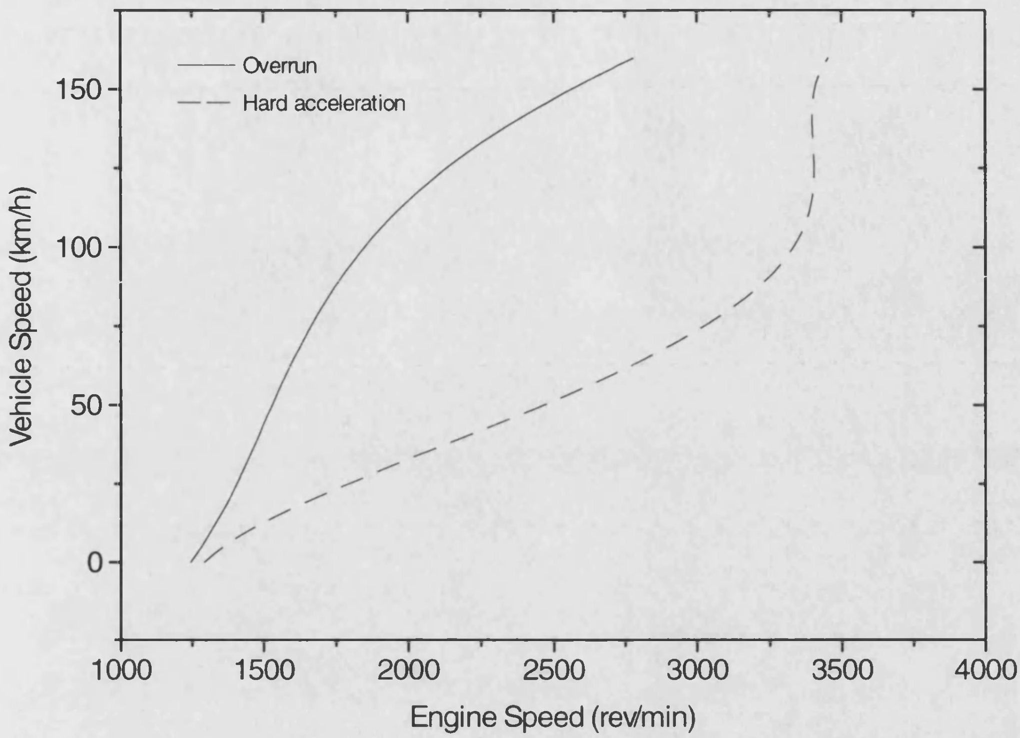

Figure 1.1 Characteristic CTX vehicle speed engine speed operating envelope

2. DESCRIPTIONS OF THE POWERTRAIN, TEST RIG AND VEHICLE

2.1 The Powertrain

2.1.1 Engine

The engine chosen for this work was the Ford 1.8L Direct Injection (DI) Diesel engine. At the time of the decision it was in a pre-production form but was sufficiently developed for the purposes of the project. The choice of Diesel as opposed to petrol was discussed in Section 1 and was made for reasons of efficiency. It was also considered that the narrower speed range of the Diesel engine would be beneficial in conjunction with a CVT. Over recent years there has been growing interest in the Direct Injection version of the Diesel engine due to its inherent ability to produce higher efficiencies than the Indirect Injection (IDI) Diesel engine. Turbocharging and intercooling were used to increase the efficiency and power to weight ratio of the engine unit.

The Lucas EPIC (Electronic Pumping Injection Control) system was used on the engine for the purposes of fuel injection and exhaust gas recirculation (EGR) control. The system is comprised of the rotary fuel injection pump, ECU (electronic control unit) and the EGR control valve. Software was available which enabled monitoring and recording of both pump and engine variables on a laptop computer. The EPIC system, developed over the last decade, was one of the most modern production engine control systems available at the outset of the work described here. The system was optimised to enable low hydrocarbon emissions through the use of high injection pressures, and the use of EGR to lower combustion temperatures and thereby reduce NOx. Clearly there were further developments in the fuel injection and control equipment which took place after the commencement of the work presented here. However, in order to draw valid comparisons about improvements given by newly developed control strategies, the level of development of the powertrain was kept constant from the outset of this work.

To enable compatibility with the transmission it was necessary to derate the engine from a maximum torque production of 180 Nm to one of 130 Nm. In order to produce a similarly shaped torque curve on the derated engine, this meant a reduction in rated engine power from 65 kW to 50 kW. The power of the engine was still appropriate for the medium passenger car application. Figure 2.1 shows the original and derated engine torque curves.

2.1.2 Transmission

Figure 2.2 shows a cut away view of the CTX transmission developed by Ford in the mid 80's. The variable speed unit is a Van Doorne push belt design described in Hendriks et al (1988). The viewpoint is from the engine side of the transmission. The bell housing and input shaft can be seen on the right. Behind this are the clutches and epicyclic unit which transmit the power to the belt drive, shown at the back left. The final drive and output shafts are located lower centre and the hydraulic controller is shown at the bottom.

The main components of the CTX transmission are also shown in schematic form in Figure 2.3. The engine drives the carrier of an epicyclic gear set at the CTX input. The purpose of the epicyclic gear is to enable a forward/reverse gear change for the vehicle. Clutches are used to facilitate either the forward or reverse directions. When the forward clutch is engaged, it connects the epicyclic carrier to the primary pulley of the belt drive. This locks up the epicyclic to transmit drive, since the epicyclic sun is permanently linked to the primary pulley. The reverse motion is enabled when the annulus of the epicyclic gear set is locked to the CTX casing by the reverse clutch. The planet gears rotate on the carrier and turn the sun gear in the opposite direction.

Power is transmitted from the primary V-pulley to the secondary V-pulley by means of the push belt. The belt is made up of about three hundred segments which are guided around the pulleys by ten steel bands. The steel bands are in tension whilst the segments on the side of the belt transmitting the power are in compression. Transmission ratio is varied by changing the path of the belt around the pulleys. This is done by altering the hydraulic pressure to the primary cylinder causing one of the primary V-pulley halves to change position axially. Belt tension is set by the main system pressure which acts on the secondary pulley. The output from the secondary pulley drives a differential gear set via a reduction gear. The differential output shafts drive the front wheels of the vehicle.

The oil pump which supplies pressure to the clutches and hydraulic actuators via the hydraulic control unit is located adjacent to the primary pulley. It is driven directly by the engine via a shaft concentric within the shaft supporting the primary pulley. The hydraulic controller is located in the sump at the bottom of the transmission. This consists of a complex arrangement of six interconnected hydraulic valve assemblies housed in a manifold. The functions of the unit are to match belt tension to engine torque, to match transmission ratio to the driving conditions, to match clutch torque to engine torque and to operate the clutch smoothly when moving off from rest. These four functions are effected by control of the primary and secondary cylinder pressures and the forward and reverse clutch pressures.

Figure 2.3 shows the inputs to the controller from the transmission. A slider on the primary V-pulley gives a measurement of the pulley position. This enables mechanical closed loop position control of the transmission ratio. There are also inputs from the transmission selector lever position, the accelerator pedal position, the primary V-pulley speed, and the engine speed.

Hydraulic/electronic prototype

For the work described here, an electrohydraulically controlled prototype version of the CTX transmission was used. This was essentially the same as the conventional hydromechanically controlled CTX but with the addition of two proportional solenoid valves which were used to electronically control the primary and secondary actuator pressures. The parts of the hydraulic circuit used to control the clutch pressure, and hence engagement remained as in the hydromechanical version of the CTX. The electrohydraulically controlled version of the CTX was known as the CTXE.

Prototype control

The original powertrain installed into the vehicle and onto the test rig is controlled by the EPIC fuel injection system and the Van Doorne electronic CTXE controller. The CTXE controller is positioned in the control structure between the driver's accelerator pedal and the transmission's primary and secondary pressure proportional solenoid valves. The accelerator pedal signal is also used as a direct input to the EPIC fuel injection equipment controller. Driver demands in terms of accelerator pedal position are used by the CTXE controller to schedule both the secondary pressure level (to enable torque transmission) and the transmission ratio.

2.2 The Test Rig

2.2.1 General layout

The powertrain is installed onto a test rig for the purposes of testing and developing the control software and for the provision of data for use in model validation. In addition, emulations of vehicle legislative emissions tests can be completed together with in depth analysis of engine emissions production.

The general layout of the test area is shown in Figure 2.4. It comprises of a test cell and separate control room. In the test cell, one central frame is used to house the engine, transmission and dynamometer. Torque transducers are installed in the shafts and couplings connecting the engine to the transmission and the transmission to the dynamometer. Area in the test cell adjacent to the rig itself is used for the associated systems, namely the emissions measuring equipment and the dynamometer hydraulic power pack. The control room is used to house the remainder of the emission measuring equipment in addition to the rig control and data acquisition computers and associated instrumentation.

2.2.2 Engine installation

The engine can be seen in Figure 2.5. Conventional mounts are used to support it on the test rig and a shaft connected the output drive to a torque transducer. An external system provides cooling water to the engine, the flow rate of which was regulated by a control valve. Software was developed to enable computer control of the engine coolant temperature, within the capability of the system, by reference either to a static setpoint or to a temperature profile with respect to time from a computer file. This facility was developed mainly for the purpose of performing legislative vehicle emissions tests, where a characteristic profile was previously found for the rate of increase of engine temperature with time.

Since the engine was intercooled, it was also important to try and represent a true characteristic of the intercooler operation and effectiveness on the test rig. Intercooler effectiveness is measured by looking at the reduction in the temperature of the air as it passed through the intercooler when compared with the temperature of the ambient air. In the vehicle the intercooler was, in fact, an air to air heat exchanger, the effectiveness of which increased with increasing vehicle speed. For the rig installation, a water to air heat exchanger is used in an arrangement which is shown in Figure 2.6. Computer control of the two butterfly valve positions enables the intercooler effectiveness to be scheduled with vehicle speed and the engine inlet air charge temperature to be controlled.

<u>EPIC fuel injection system</u>

The rig installation of the EPIC control system differs in a few minor aspects from the standard production vehicle installation. The standard control software is used but with reduced maximum fuel deliveries as mentioned in Section 2.1.1 in order to protect the transmission. Additional proprietary units are used with the fuel injection system to enable measurement and recording of injection pump and engine variable values. The wiring harness is modified to enable accelerator demand to be generated by either a manual demand box or from a supervisory control computer.

2.2.3 Transmission installation

A prototype electrohydraulically controlled transmission is installed on the test rig as shown in Figure 2.4. A spring damper plate, designed to reduce torsional oscillations created by the firing of the Diesel engine, is positioned on the input shaft to the transmission. The input shaft/engine torque transducer is situated prior to this in the driveline. Due to the normal transmission drive being passed out to the two front wheels of the vehicle, it was necessary to modify the output side of the transmission. This was done by fitting a 'solid' differential so that there was in fact only one transmission output drive which passed to the dynamometer via the output torque transducer.

Transmission controller

The transmission controller supplied by VDT was initially installed in its original form. The accelerator pedal signal was used as an input to both the VDT controller and the EPIC fuel injection system. The signal was used in the former for ratio control and for the setting of a secondary pressure level appropriate to the amount of torque developed by the engine. The EPIC system scheduled the engine torque according to the values of the accelerator pedal and engine speed signals. The VDT controller also included an alternative facility for the external control of both primary speed and secondary pressure. There was also a proprietary unit which was used to enable the monitoring and measurement of transmission variables during powertrain and controller testing.

2.2.4 Dynamometer

The dynamometer comprised a fixed inertia in the form of a steel disk and a separate hydraulic loading system. It was developed at the University prior to the work described here and its operation is explained by Dorey and Guebeli (1990). Software for control of the dynamometer enabled its operation in any one of three modes. The first of these was speed control. Here the speed of the fixed inertia and hence the transmission output speed was maintained at a demanded level. Deviation occurred only during transient changes and when the capability of the hydraulics was exceeded. The second operating mode was termed torque control. This was performed by maintaining the demanded torque at the transmission output shaft by loading or driving of the fixed inertia. The final operating mode, which was of most use, was the vehicle emulation mode. This was essentially a combination of the first two modes and enabled both the static and dynamic frictional drag terms of the vehicle to be emulated. A Loughborough Sound Images DSP control card in a host computer was used to enable the necessary software speed for control of the system. The control system was specified some years ago and there are several PC based input output control systems capable of the task today.

2.2.5 Data Acquisition system

The data acquisition system used for the rig work could be classified in terms of the acquisition speed and the number of measurement channels available. A slow acquisition rate of just under 2 Hz was used for all of the variables measured. The variables were measured either indirectly from the proprietary unit signals or directly using transducers on the engine, transmission and dynamometer. A list of all the measurements which were available is given in Table 2.1. The slow acquisition was performed using PC based software developed at the University in conjunction with Data Translation DT2812 data acquisition cards. The Lucas EPIC data acquisition software was also used simultaneously during some of the tests, running on a separate machine in order to record various fuel injection system variables.

Faster data acquisition (at 25 Hz) was performed using the same machine as for the slow acquisition and two further computers. The first system which ran both acquisition rates simultaneously used a Data Translation DAS58 data acquisition card and software developed at the University. The two additional systems each used one DT2812 card and Global Lab software. Although there was the capability for some data acquisition using the emissions measuring equipment and the fuel injection control system, the acquisition system described above was used in preference for all the data presented, including the variables recorded from these two systems. The main advantage in this approach was that as many variables as possible were recorded against the same time reference.

2.2.6 Powertrain controller hardware

For the purposes of implementing the control strategies resulting from the work presented here, a separate PC was used in conjunction with Data Translation PC24 and PC74 input and output cards.

2.3 The Test Vehicle

A 1992 year model Ford Orion car was used as the experimental vehicle for the project. This was a medium sized passenger car. Details of the load characteristic associated with this vehicle are described in detail in Section 4.4.

2.3.1 Engine and transmission installation

The engine was mounted in the vehicle in a configuration as close as was possible to that used for the production installation of the 1.8 litre IDI Diesel engine. There were, however, two main differences. Firstly, the original position of the turbocharger made it impossible to bolt the transmission housing onto the engine endplate. To rectify this problem, the transmission casting was machined slightly and the compressor was rotated by a small amount. Secondly, the type of vehicle body did not make possible the use of torque roll axis engine mounts. In addition a mounting point had to be fabricated for the transmission. The resulting engine and transmission mounts were not ideal in isolating the vehicle structure from noise and vibration.

2.3.2 Data acquisition system

The data acquisition system used in the vehicle was essentially a smaller version of that used on the rig in that a smaller number of powertrain variables were recorded. Both the DAS58 and DT2812 cards were again used in the same way as described in Section 2.2.5. Both the faster and slower speeds of data acquisition were possible. Some variables such as torques were not available from the vehicle powertrain. It was possible to select different combinations of variables to record during different tests. This counteracted the limitation of the maximum number of channels possible to record simultaneously on the vehicle data acquisition system.

2.3.3 Powertrain controller hardware

The controller hardware was installed on the vehicle in exactly the same configuration as that used on the test rig. The flexibility of the system allowed fast switching between alternative control strategies.

Time (s)	Total HC ppmC3H8
Bath pedal (0-10)	Particulates (g/sec)
Primary pressure feedback (bar g)	Opacity %
Engine speed (rev/min)	Exhaust manifold temperature
Exhaust pressure (bar g)	Temperature before catalyst
Pressure before catalyst (bar g)	Temperature at start of catalyst
CTXE speed dem (rev/min)	Mid-catalyst temperature
EPIC pedal signal (decimal)	Temperature at end of catalyst
CTXE secondary current (A)	Temperature before front box
Secondary pressure demand (bar g)	Temperature at smokemeter
Engine speed demand (rev/min)	Water temperature into Engine
Optimum speed demand (rev/min)	CTXE sump temperature
Fuel demand (decimal)	Temperature of fuel into EPIC
Fuel flow (kg/hr)	Temperature of fuel out of EPIC
Clutch pressure (bar g)	Temperature before Compressor
Air flow (corona) (kg/hr)	Temperature after compressor
Primary pulley speed (rev/min)	Temperature intercooler bypass
Secondary pulley speed (rev/min)	Temperature intercooler (out)
Primary current (A)	Temperature intercooler (mixed)
Secondary pressure (bar g)	Temperature inlet man
Engine torque (Nm)	Engine Sump temperature
Load torque (Nm)	Cell ambient temperature
Percentage CO2 (at inlet manifold)	Water out of engine temperature
CO ppm	Engine speed (rev/min)
Fast FID HC ppm	Dyno speed (rev/min)
NOx ppm	turbo speed (rev/min)
Percentage of O2	

Table 2.1 Measured powertrain and control variables available on the rig

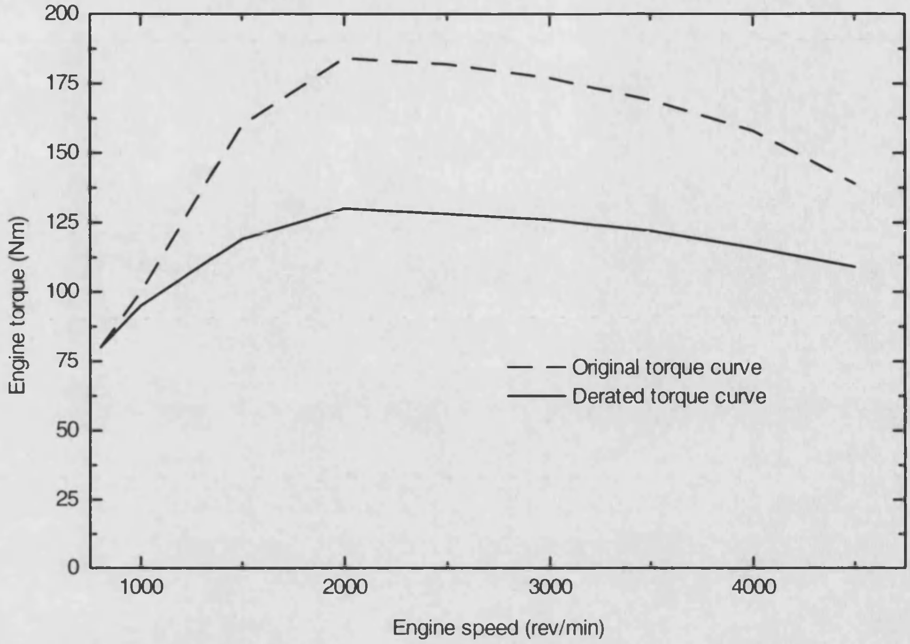

Figure 2.1 Original and derated engine torque curves

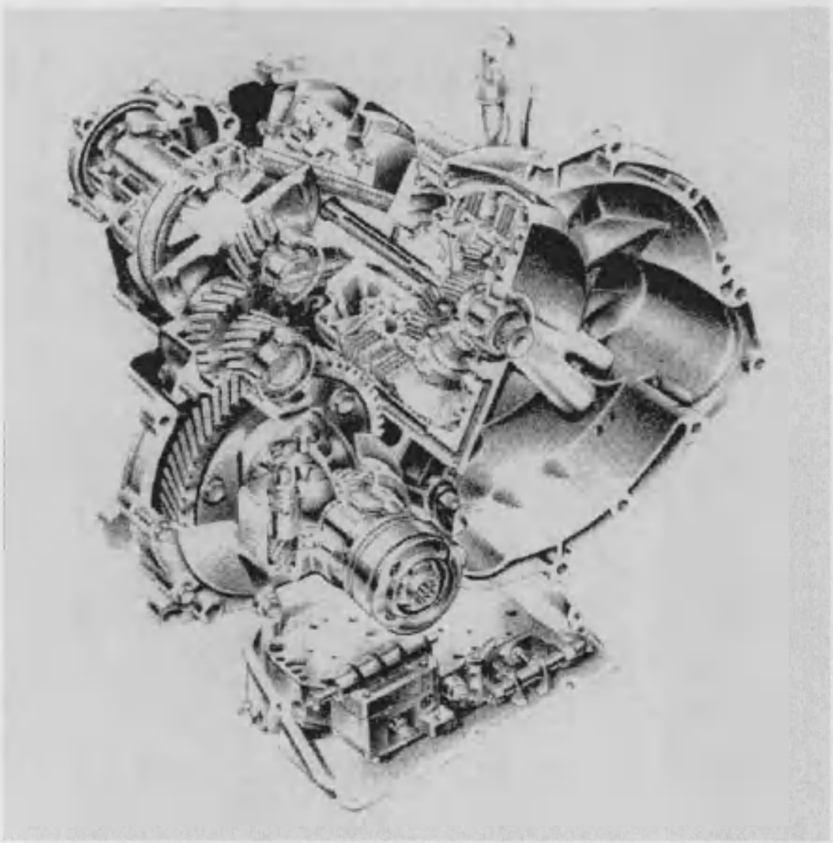

Figure 2.2 The Ford CTX transmission

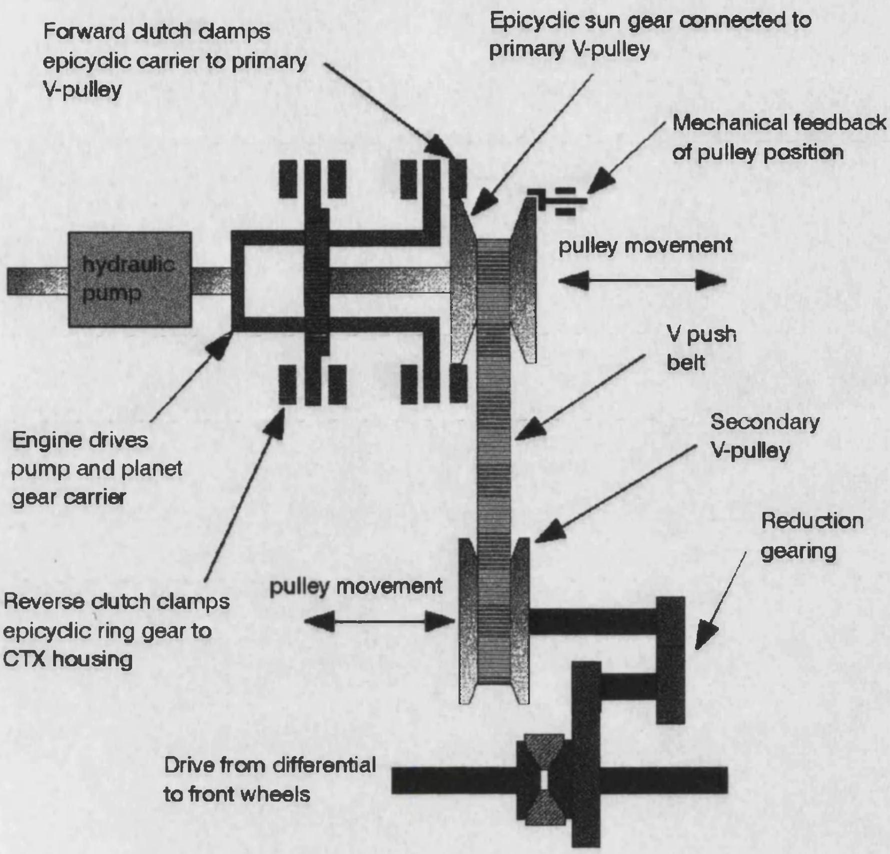

Figure 2.3 Schematic drawing of the Ford CTX transmission

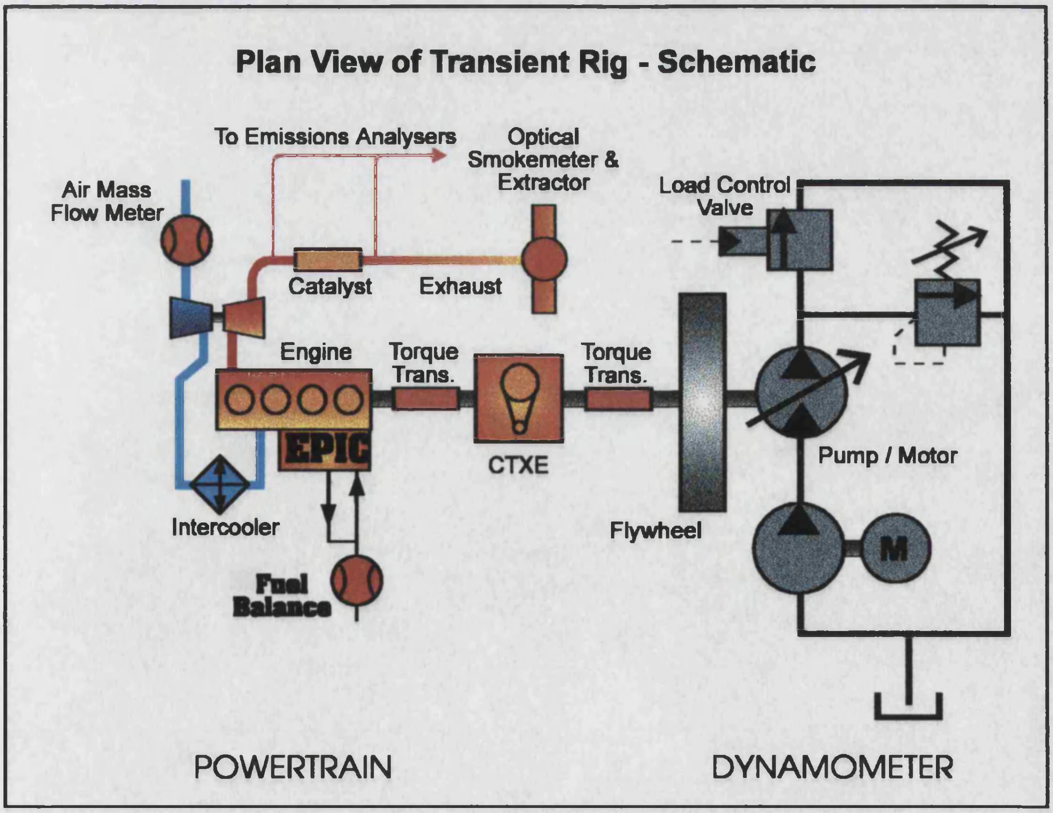

Figure 2.4 General layout of the test rig (Used courtesy of Brace, 1995)

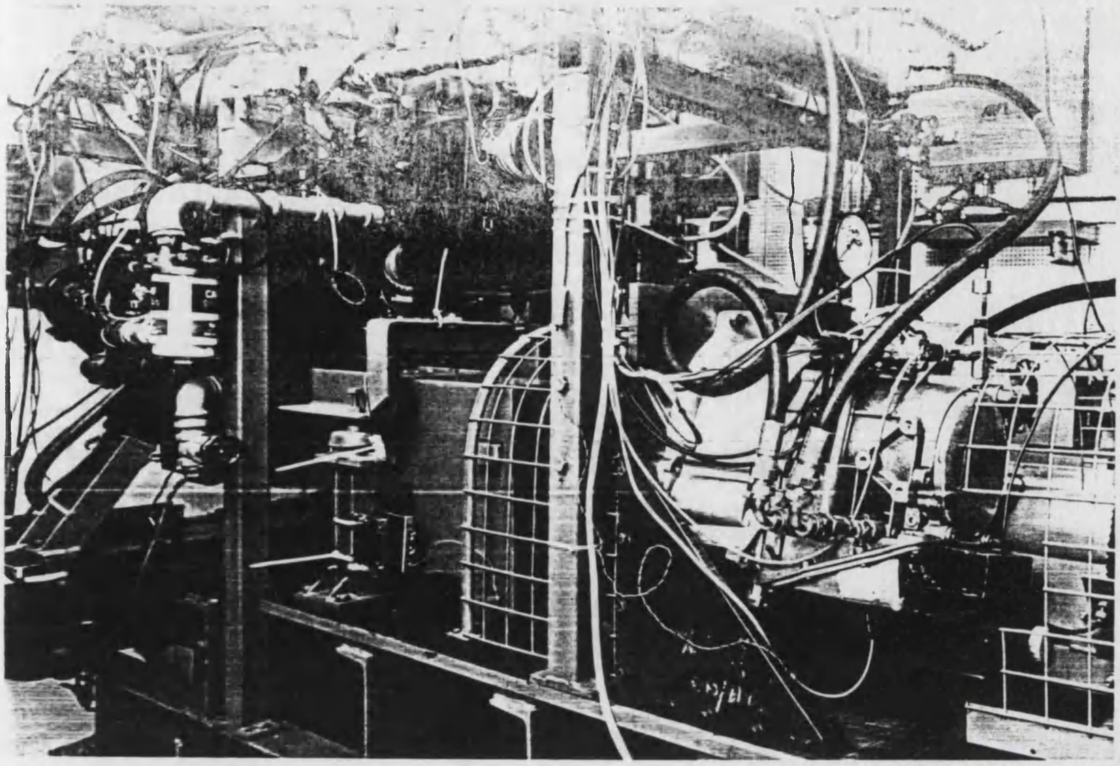

Figure 2.5 Photograph of the test rig

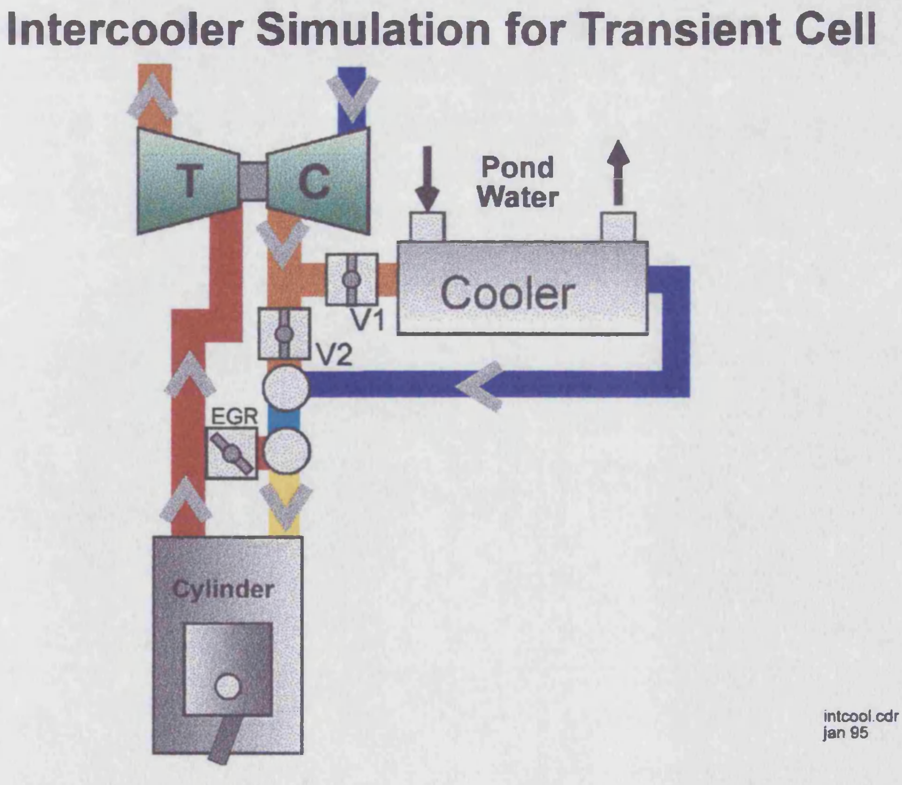

Figure 2.6 Control of engine intake air temperature on the rig (Used courtesy of Brace, 1995)

3. VEHICLE DRIVABILITY REQUIREMENTS

3.1 Introduction to the study

Targeting the goals of low emissions and high economy for passenger cars is likely to be successful only if drivability can be maintained if not improved. Whilst many manufacturers sell vehicles in the market place, those which offer vehicles with both high economy and good drivability will, all other things being equal, do best. Drivability is a measure of how well the vehicle and particularly the powertrain responds to the driver's inputs. This is clearly very subjective and depends upon such things as powertrain predictability, driver confidence and comfort. Research and development in the field of vehicle powertrains must therefore take into account drivers' perceptions of vehicle drivability as well as addressing the issues of vehicle economy and emissions.

The approach taken towards vehicle drivability is discussed in the following sections. It resulted in recommendations which were used in the design of the alternative supervisory controllers for the Diesel continuously variable powertrain. The results of a final appraisal of the test vehicle with the alternative control strategies are described in Chapter 8.

3.1.1 Objective

The objective of the work described in this chapter was to determine the important powertrain control features required to produce a vehicle with good drivability. From these, the principal requirements of a controller strategy for the Diesel CVT powertrain were to be defined. These requirements were considered essential for use in the design and evaluation of various controller strategies. Assessment of the quality of operation of powertrains is influenced directly by subjective perception of vehicle characteristics and therefore final vehicle drivability requirements were considered throughout these stages.

In order to achieve the objective, it was necessary to appraise a group of CVT vehicles and to relate subjectively obtained drivability assessments to the results of objectively recorded measurements taken whilst driving each of the vehicles through a series of tests.

The powertrain project vehicle was included in this appraisal. At the time, the powertrain consisted of an early set up which had been installed for the purpose of providing initial 'baseline' comparative information and for early investigations of the characteristics of a Diesel CVT powertrain. Strategies and methods of control used in the various vehicles were also investigated as part of the objective work.

3.1.2 Description of the vehicles

The vehicles used were a production Nissan Micra 1.3L N-CVT (petrol engine and electronically and hydraulically controlled continuously variable transmission), a production Ford Orion 1.6L LX CTX (petrol engine and hydraulically controlled continuously variable transmission) and the powertrain project Ford Orion with a 1.8L IDI TCi Diesel engine and a standard CTX hydraulically controlled continuously variable transmission.

3.2 Test procedures

The program of experimental testing was completed on the three vehicles at the Ford Motor Company's test facilities at Dunton in May 1993. As mentioned above, the work was divided into subjective and objective studies, the vehicles being fitted with instrumentation and data acquisition equipment to enable the latter.

The subjective appraisal involved a group of drivers comprising personnel from each of the companies involved in the integrated powertrain project. The drivers were asked to assess the drivability of the three vehicles fitted with continuously variable transmissions.

The following studies are therefore divided into subjective and objective sections. In the discussions and conclusions which follow, the findings of both sections are cross referenced and related to the perceived drivability requirements and expectations (listed in Table 3.1).

3.2.1 Subjective appraisals

Each vehicle was assessed on each of the aspects listed in Table 3.1 by each of the team of drivers. A ratings index was used (shown in Table 3.2). Questionnaires, completed at the time of driving the vehicles, also allowed for overall comment. The questionnaires were designed in conjunction with the project collaborators.

The types of driving possible for the vehicle appraisals were limited and different from those normally experienced during real driving. For example no driving on gradients was included. Driving the vehicles in an environment away from the influences of usual highway traffic may have had an impact on the appraisals. For example, assessment of vehicle response on entering a highway is clearly more difficult without the pressure of other vehicles. In addition to these limitations it is also accepted that the team of drivers, all qualified engineers, did not represent a true cross section of possible drivers.

3.2.2 Objective work

The objective vehicle test work consisted of a series of tests as outlined in Table 3.3. The tests were designed to link the subjective appraisals with measured data. Data were recorded on digital and analogue channels. The equipment used on the Nissan Micra and the Ford Orion (petrol) was supplied by Ford. The data obtained from the project vehicle was produced using instrumentation supplied by both the School of Mechanical Engineering instrumentation department and the Ford

Motor Company. Table 3.4 gives details of the variables recorded by each of the two data acquisition systems used. The data recorded were processed using a spreadsheet and plotting package in order to produce the graphs shown in the figures presented in this chapter. The following values, presented in the plotted data, were calculated from the measured variables. The vehicle power was calculated from the vehicle drag characteristic, vehicle speed and acceleration. From this the engine torque was inferred by dividing the vehicle power by the engine speed. In this calculation no assumed transmission losses were taken into account so it is likely that the true engine torque would be a fraction higher than the values presented. A check was made on the engine torque during each test by also calculating it independently using engine speed, pedal position and a knowledge of the torque speed characteristic for given pedal positions. There was generally good agreement between the two calculations of torque. Small differences may have been due to transmission losses.

Test descriptions

Each of the tests outlined in Table 3.3 is described in more detail below:

Test 1 - Constant speed driving in DRIVE

The aim of this test was to drive the vehicle at various constant speeds with the transmission set to DRIVE. The steady state values of ratio could then be determined and information gained about the relationship between the engine and vehicle speeds and loads.

Test 2 - Constant speed driving in LOW

The aims of this test were the same as for test 1. The transmission was in the LOW setting.

Test 3 - Tip-in response/smoothness (acceleration to maximum speed) in DRIVE

Here the test started with the vehicle driven at a constant speed. The accelerator was then depressed to a stopped position at either a quarter, half or fully down. The response of the vehicle and powertrain to this action was then assessed in terms of smoothness and rates of change of speeds and ratios.

Test 4 - Tip-in response/smoothness (acceleration to maximum speed) in LOW

The aims of this test were the same as for test 3. The transmission was in the LOW setting.

Test 5 - Deceleration smoothness (Deceleration from 100 km/h to idle in DRIVE)

For this test, the vehicle was accelerated to a constant speed and then allowed to decelerate to rest. The way the engine speed was controlled and the rate of vehicle deceleration were of particular interest in this test.

Test 6 - Deceleration smoothness (Deceleration from 100 km/h to idle in LOW)

The aims of this test were the same as for test 5. The transmission was in the LOW setting. This setting is particularly designed to produce more engine braking effect on the vehicle.

Test 7 - Acceleration from rest to maximum speed in DRIVE (wide open throttle ramped over 1 second)

The aim of this test was to investigate the response of the vehicle and transmission when undergoing hard acceleration from rest. The initial period involves the scheduled clutch engagement and the test enables the effects of this to be seen on the overall smoothness.

Test 8 - Acceleration from rest to maximum speed in LOW (wide open throttle ramped over 1 second)

The aim of this test was the same as for test 7. The transmission was in the LOW setting.

Test 9 - Acceleration versus pedal position (from idle to maximum speed) in DRIVE

In this test the pedal was depressed a set amount with the vehicle at rest causing the vehicle to accelerate to a terminal speed. The aim of the test was to measure the characteristic of change in vehicle and transmission response against pedal position.

Test 10 - On/off/on acceleration in DRIVE

This test was an attempt to excite oscillations in the driveline causing a second order type response in the longitudinal acceleration of the vehicle. The speed of decay of any induced oscillation could yield further information about the dynamics of the transmission.

Test 11 - On/off/on acceleration in LOW

The aims of this test were the same as for test 10. The transmission was in the LOW setting.

3.3 Discussion

Table 3.5 shows the mean values achieved by each vehicle in each of the categories of the three sections of the assessment. Tables 3.6, 3.7 and 3.8 list the names of the completed and processed tests for each of the vehicles. These tables enable Figures 3.1 to 3.39 showing the graphical representation of the test results to be matched to the actual type of test performed. The results filenames in Tables 3.6 and 3.7 are of the general form 'nSmRp' where 'n' is the test number, 'm' is the set number and 'p' is the run number. Results files in Table 3.8 have been produced from data from both acquisition systems. The general form of the file name is as before but with 'TOT' replacing the 'nS'. An asterisk next to the filename indicates that an associated figure is included in Figures 3.1 to 3.39. The full drivability report (Deacon, 1994) includes all of the figures listed in these tables.

In considering the results, it should be noted that the calibration of the hydraulically controlled transmission used in the Diesel Orion was not changed from the original set up (intended for the 1.6 litre petrol engine). At low power deliveries, this led to the Diesel engine operating at a higher speed than perhaps was necessary to achieve the required power. At full load operation, the rated engine speed was never reached. This limited the maximum power available in the Diesel Orion.

In order to draw conclusions from the subjective and objective studies it was necessary to relate each subjective attribute to an objective test, if this was possible. Table 3.9 shows where the relationships exist between the subjective attributes and the objective tests:

3.3.1 Nissan Micra NCVT objective tests - (Table 3.6, Figures 3.1 to 3.12)

Test 1 - Constant speed driving in DRIVE

The constant speed tests show a variety of constant vehicle speeds. The positions at which the ratio is held at each speed can be seen. Test 1S1-5R1, Figure 3.1 did not involve hard accelerations and it can be seen from the vehicle speed versus engine speed graph that the controller governs the engine speed to between 1650 and 1800 rev/min over a range of road speeds. For the constant speed tests at higher speeds (test 1S6-7R2), Figure 3.2, harder acceleration was necessary. This caused the engine speed to be pushed up to around 3000 rev/min in order to deliver the necessary power.

Test 2 - Constant speed driving in LOW

In the constant speed tests here, Figure 3.3, a different ratio profile across the vehicle speed range was noted. The vehicle speed versus engine speed graph approximates to a diagonal line from 1500 rev/min at 0 km/h to 3500 rev/min at 60 km/h, rather than the more vertical line seen when operating the vehicle with the transmission in DRIVE. As anticipated, this profile caused more engine braking effect.

Test 3 - Tip-in response/smoothness (acceleration to maximum speed) in DRIVE

The vehicle gave smooth responses to measured increases of pedal position. The response was immediate and the vehicle acceleration produced fell off gradually with increasing vehicle speed. The magnitude of the initial acceleration depended upon the increase in pedal displacement. The response of the engine and transmission was fairly smooth with no obvious hesitations or sudden changes in operating point. The changes in engine speed depended upon both the vehicle speed before the pedal movement and the increase in demand. For small increases of pedal demand at low initial vehicle speed, test 13S35R2, Figure 3.4, the engine speed was observed to increase at first before decreasing as the rate of vehicle acceleration fell, the vehicle having almost reached its new steady state speed. At low initial vehicle speeds combined with larger pedal movements, test 13S39R2, Figure 3.5, the engine speed increased rapidly initially and then continued to increase more slowly as the vehicle approached its new steady state speed. At higher initial vehicle speeds the engine speed increase depended upon the size of the pedal increase.

Test 4 - Tip-in response/smoothness (acceleration to maximum speed) in LOW

The main differences between the response of the vehicle in tests 3 and 4 were due to the ratio profile exhibited by the transmission when in the LOW setting. This was seen and described in test 2. In test 4, Figures 3.6 and 3.7, the engine speeds were higher before the pedal movements than in test 3 and consequently for small pedal increases at low initial vehicle speeds the engine speed did not generally fall again as the vehicle reached its new steady state speed.

Test 5 - Deceleration smoothness (Deceleration from 100 km/h to idle in DRIVE)

This test, Figure 3.8, shows decelerations from 70 km/h to rest with the transmission in the DRIVE position. The vehicle speed versus engine speed graph shows the hard acceleration characteristic of high engine speed followed by the downward shift in engine speed towards the overrun condition. The engine holds a steady 1650 rev/min from 70 km/h down to 20 km/h. At this point there is a sudden change in the engine speed to about 1200 rev/min together with a corresponding change in the transmission ratio. After this short lived increase in the transmission ratio, it then continued to decrease. The effect of this part of the controller strategy was to cause the vehicle to decelerate at a lower rate at speeds below 20 km/h.

Test 6 - Deceleration smoothness (Deceleration from 100 km/h to idle in LOW)

In the LOW position case, Figure 3.9, the acceleration and deceleration lines on the vehicle speed versus engine speed graph are very close together. This characteristic was mentioned under test 2. Deceleration occurred at a greater rate than in test 5 for speeds above around 20 km/h. At this speed there is a change in the rate of deceleration and for vehicle speeds below 20 km/h the rate of deceleration is similar to that observed in test 5.

Tests 7 and 8 - Acceleration from rest to maximum speed in DRIVE and LOW (wide open throttle ramped over 1 s)

These tests, Figures 3.10 and 3.11 were performed by ramping the throttle from closed to fully open over one second. The acceleration performance was not affected by whether the transmission was set in DRIVE or LOW. During hard acceleration the engine was running at high speed and the transmission ratio changed as the vehicle accelerated. The engine torque speed map shows the high power point at which the engine operated during these hard accelerations. As was shown in the earlier tests, the overrun condition was affected by the transmission setting.

Test 9 - Acceleration versus pedal position (from idle to maximum speed) in DRIVE

In these tests, Figure 3.12, the gradual change in vehicle and engine response to set increases in pedal position can be seen over the range from small step inputs to maximum changes in pedal displacement. The trends in the responses of the engine speed caused by changes in the transmission ratio are easily observable. For small pedal increases the engine speed initially rises smoothly before falling to a new value as the vehicle speed approaches its new steady state value. The response to large pedal increases is different, the engine speed rising rapidly but smoothly and staying close to the peak power point as the vehicle is accelerated.

Test 10 and 11 - On/off/on acceleration in DRIVE and LOW

A small number of these tests were performed at a range of speeds in an attempt to cause the driveline to oscillate. It was not found possible to induce such oscillations and so these tests were curtailed.

3.3.2 Ford Orion (petrol) CTX objective tests - (Table 3.7, Figures 3.13 to 3.25)

Test 1 - Constant speed driving in DRIVE

The constant speed tests (test 1S1-5R1), Figure 3.13, show a variety of vehicle speeds. The positions at which the ratio is held at each speed can also be seen. This test did not involve full accelerations and it can be seen from the vehicle speed versus engine speed graph that the controller governs the engine speed to between 1700 rev/min and 2100 rev/min over a range of road speeds, only exceeding 2100 rev/min during the accelerations.

Test 2 - Constant speed driving in LOW

The low transmission setting is intended to create a greater engine braking effect (to be used when driving long descents). A different ratio profile across the vehicle speed range was noted. In test 2S12-7R1, Figure 3.14, the vehicle speed versus engine speed graph approximates to a diagonal line from 1500 rev/min at 20 km/h to 3500 rev/min at 60 km/h, rather than the more vertical line seen when operating the vehicle with the transmission in DRIVE.

Test 3 - Tip-in response/smoothness (acceleration to maximum speed) in DRIVE

In the tip-in response/smoothness tests, Figures 3.15 to 3.17, the vehicle gave smooth responses to measured increases of pedal position. The response was fast and the vehicle acceleration produced fell off gradually with increasing vehicle speed. The magnitude of the initial acceleration depended upon the increase in pedal displacement. The response of the engine and transmission was fairly smooth with no obvious hesitations or sudden changes in operating point. However in test 3S24R2, Figure 3.16, the engine speed rose in a series of stages as the clutch took up the drive. The changes in engine speed depended upon both the vehicle speed before the pedal movement and the increase in demand. Unfortunately some problems with the engine speed signal were experienced at higher speeds leading to the loss of the signal for the some parts of the tests. However for small increases of pedal demand at low initial vehicle speed, the engine speed was observed to increase at first before decreasing slightly as the rate of vehicle acceleration fell, and then rising again as the vehicle approached its new steady state speed (in test 3S24R1), Figure 3.15. At low initial vehicle speeds combined with larger pedal movements (test 3S27R1-2), Figure 3.17, the engine speed increased rapidly initially and then continued to increase more slowly as the vehicle approached its new steady state speed. For higher initial vehicle speeds the size of the engine speed increase depended upon the size of the increase in pedal position.

Test 4 - Tip-in response/smoothness (acceleration to maximum speed) in LOW

The main differences between the response of the vehicle in tests 3 and 4 were due to the ratio profile exhibited by the transmission when in the LOW setting. This was seen and described in test 2. Here, Figures 3.18 and 3.19, the engine speeds were higher before the pedal movements than in test 3 and consequently for small pedal increases at low initial vehicle speeds the engine speed did not fall as much as when in DRIVE as the vehicle reached its new steady state speed. Some small deviations from a smooth engine speed curve are notable in tests 4S36R1 and 4S39R1-2.

Test 5 - Deceleration smoothness (Deceleration from 100 km/h to idle in DRIVE)

This test, Figure 3.20, shows decelerations from 70 km/h to rest with the transmission in the DRIVE position. The vehicle speed versus engine speed graph shows the hard acceleration characteristic of high engine speed followed by the shift in engine speed towards the overrun condition. The engine holds a steady 1750 rev/min from 70 km/h down to 20 km/h. At this point the engine speed decreases to the idle setting as the transmission clutch disengages. The vehicle decelerates at a uniform rate down to about 30 km/h. At about this point the deceleration rate increases gradually before decreasing again as the vehicle gradually comes to rest. It was noted that the point of disengagement of the transmission clutch varied somewhat and that the vehicle took some time to come to rest if the brakes were not applied.

Test 6 - Deceleration smoothness (Deceleration from 100 km/h to idle in LOW)

In the LOW position case, Figure 3.21, test 6S52R1, the acceleration and deceleration lines on the vehicle speed versus engine speed graph are closer together than in the DRIVE position case. This characteristic is similar to that mentioned under test 2. Deceleration occurred at a greater rate than in test 5 for speeds down to around 10 km/h. At this speed the deceleration ceased and the vehicle continued to move at 10 km/h for the remainder of the test, the transmission clutch not disengaging.

Tests 7 and 8 - Acceleration from rest to maximum speed in DRIVE and LOW (wide open throttle ramped over 1 s)

These tests, Figures 3.22 and 3.23, were performed by ramping the throttle from closed to fully open over one second. The acceleration performance was not affected by whether the transmission was set in DRIVE or LOW. During hard acceleration the engine was running at high speed (test 7S57R1-2) and the transmission ratio changed as the vehicle accelerated. The engine torque speed map shows the high power point at which the engine operated during these hard accelerations. As was shown in the earlier tests, the overrun condition was affected by the transmission setting. In test 8S62R1-2 the engine speed can be seen to rise to 1800 rev/min and flatten out before continuing to rise. This is thought to be the clutch engagement point.

Test 9 - Acceleration versus pedal position (from idle to maximum speed) in DRIVE

In these tests, Figures 3.24 and 3.25, the gradual change in vehicle response to set increases in pedal position can be seen over the range from small step inputs to maximum changes in pedal displacement. The trends in the responses of the engine speed caused by changes in the transmission ratio are easily observable. For small pedal increases (test 9S68R1-2), the engine speed initially rises before falling and then rising again to a new value as the vehicle speed approaches its new steady state value. The response to large pedal increases is different, the engine speed rising rapidly to 1900 rev/min, pausing and then continuing to rise rapidly to 2400 rev/min (test 9S70R1-2) before flattening out and then rising more gradually as the vehicle is accelerated. Some irregularities in the engine speed rate of change can be seen in these tests.

Test 10 and 11 - On/off/on acceleration in DRIVE and LOW

A small number of these tests were performed at a range of speeds in an attempt to cause the driveline to oscillate. It was not found possible to induce such oscillations and so these tests were curtailed.

3.3.3 Project Ford Orion (Diesel) CTX objective tests - (Table 3.8, Figures 3.26 to 3.39)

Test 1 - Constant speed driving in DRIVE

The constant speed tests, Figures 3.26 and 3.27, show a variety of constant vehicle speeds. The positions at which the ratio is held at each speed can also be seen. This test did not involve full accelerations and it can be seen from the vehicle speed versus engine speed graph that the controller governs the steady state engine speed to about 1700 rev/min over a range of road speeds. For the constant speed tests at higher speeds, harder acceleration was necessary. This caused the engine speed to be pushed up to around 3000 rev/min in order to achieve the necessary power.

Test 2 - Constant speed driving in LOW

Here in test TOT12R1, Figure 3.28, a different ratio profile across the vehicle speed range was noted. The vehicle speed versus engine speed graph approximates to a diagonal line from 1500 rev/min at 10 km/h to 3500 rev/min at 70 km/h, rather than the more vertical line seen when operating the vehicle with the transmission in DRIVE. This characteristic produces more engine braking effect as intended.

Test 3 - Tip-in response/smoothness (acceleration to maximum speed) in DRIVE

The vehicle gave smooth responses to measured increases of pedal position. The response was fairly quick and the vehicle acceleration produced fell off gradually with increasing vehicle speed. The magnitude of the initial acceleration depended upon the increase in pedal displacement. The response of the engine and transmission was also fairly smooth with no sudden changes in operating point. Engine speed rose in two stages as also observed with the petrol Orion in test 3. This characteristic being produced by the take up of drive in the clutch. The changes in engine speed depended upon both the vehicle speed before the pedal movement and the increase in demand. For small increases of pedal demand at low initial vehicle speed (test TOT23R2), Figure 3.29, the engine speed was observed to increase rapidly in two stages before decreasing slightly as the rate of vehicle acceleration fell, the vehicle having almost reached its new steady state speed. At low initial vehicle speeds combined with larger pedal movements (test TOT27R1), Figure 3.30, the engine speed increased rapidly initially and was held at around 2000 rev/min for a time before continuing to increase more slowly as the vehicle approached its new steady state speed. At higher initial vehicle speeds and small increases in pedal position (test TOT28R1), Figure 3.31, the engine speed increased more gradually to a new higher final level. For larger pedal increases at high initial vehicle speeds (test TOT32R1), Figure 3.32, the engine speed increased significantly as the vehicle accelerated.

Test 4 - Tip-in response/smoothness (acceleration to maximum speed) in LOW

The main differences between the response of the vehicle in tests 3 and 4 were due to the ratio profile exhibited by the transmission when in the LOW setting. This was seen and described in test 2. Here, Figure 3.33, the engine speeds were higher before the pedal movements than in test 3 and consequently for small pedal increases at low initial vehicle speeds the engine speed did not fall again as the vehicle reached its new steady state speed. It was noted that towards the end of some of these tests the engine speed actually rose when the pedal demand was removed (test TOT39R1). This was thought to be due to the setting up of the transmission.

Test 5 - Deceleration smoothness (Deceleration from 100 km/h to idle in DRIVE)

This test, Figure 3.34, shows decelerations from 70 km/h to rest with the transmission in the DRIVE position. The vehicle speed versus engine speed graph shows the hard acceleration characteristic of high engine speed followed by the shift in engine speed towards the overrun condition. The engine is governed to about 1700 rev/min from 70 km/h down to 30 km/h. At about this point the rate of deceleration gradually increases and then decreases again as the vehicle slows to rest. As with the petrol Orion the point of disengagement of the clutch is not definite and the vehicle was observed to continue for some time at low speed before the clutch disengaged.

Test 6 - Deceleration smoothness (Deceleration from 100 km/h to idle in LOW)

In the LOW position case, Figure 3.35, the acceleration and deceleration lines on the vehicle speed versus engine speed graph are closer together than in the DRIVE position. This characteristic was mentioned under test 2. Deceleration occurred at a greater and more uniform rate than in test 5 for speeds above around 10 km/h. At that point the rate of deceleration decreased and the vehicle continued to travel at 10 km/h until the brakes were applied.

Tests 7 and 8 - Acceleration from rest to maximum speed in DRIVE and LOW (wide open throttle ramped over 1 s)

These tests, Figures 3.36 and 3.37, were performed by ramping the throttle from closed to fully open over one second. The acceleration performance was not affected by whether the transmission was set in DRIVE or LOW. Initially during hard acceleration the engine speed rose rapidly before climbing more gradually as the vehicle accelerated. The engine torque speed map shows the line along which the engine operated during these hard accelerations. As was shown in the earlier tests, the overrun condition was affected by the transmission setting.

Test 9 - Acceleration versus pedal position (from idle to maximum speed) in DRIVE

In these tests, Figures 3.38 and 3.39, the gradual change in vehicle response to set increases in pedal position can be seen over the range from small step inputs to maximum changes in pedal displacement. The trends in the responses of the engine speed caused by changes in the transmission ratio are easily observable. For small pedal increases (test TOT68R1) the engine speed initially rises in two stages before falling slightly to a new value as the vehicle speed approaches its new steady state value. The response to large pedal increases is different. In test TOT70R1 the engine speed rising rapidly to around 2000 rev/min before climbing further as the vehicle is accelerated.

Test 10 and 11 - On/off/on acceleration in DRIVE and LOW

A small number of these tests were performed at a range of speeds in an attempt to cause the driveline to oscillate. It was not found possible to induce such oscillations and so these tests were curtailed.

3.4 Comparison of subjective appraisals with objective tests

The results of the subjective appraisal are presented in Table 3.5. It is worth noting here that there was no attempt made during this work to take into account the different relative importance, to the driver, of the drivability attributes, performance feel attributes or NVH aspects. Due to this, each aspect was considered individually and no calculation of overall weighted score was made.

Drivability attributes

Considering first the vehicle drivability attributes, it can be seen that the Micra and petrol Orion both score highly on the driveaway smoothness. The Diesel Orion scores slightly lower in the same category. It was noted during test 9 on each vehicle that smooth responses in vehicle and engine speeds were usually seen. The engine speed changes in the Micra were the most smooth, but this quality may have been somewhat lost due the small size of the car compared with the Orions. The responses were good in both the Micra and the petrol Orion and not as good in the Diesel Orion. The Diesel Orion response was slower and may have been due to the characteristics of the linkage connecting the accelerator pedal to both the fuel injection pump and the hydraulic transmission input.

In the kick down shift behaviour test, the petrol Orion and the Micra scored at almost the same level. The Micra seemed to have the advantage of smoother engine speed changes (seen in tests 3 and 4) and perhaps its size gave it a livelier response than the petrol Orion. The Diesel Orion again scored at a slightly lower level, its speed of response due to the characteristic of the accelerator linkage probably being the reason.

The tip in/back out test resulted in fairly high scores for the petrol Orion and the Micra, the Micra having the higher. The Diesel Orion scored somewhat lower, probably due to its slower response time to pedal movements. In this test, the characteristics of the accelerator pedal probably have great influence since a higher pedal gain at the low end of the operating range can make the system appear more responsive.

In the overrun/braking to rest the Micra scored a lot higher than either of the Orions. This result can be compared with test 5 of the objective studies. The higher score achieved by the Micra could have been due to the way the vehicle came to rest after the reduced deceleration rate at lower speeds in DRIVE. In the same tests, the Orions tended to decelerate more rapidly as the speed decreased, but then actually continue to creep forward rather than come to rest. Calibration of the hydraulic transmission to suit the Diesel engine characteristics may have improved the Diesel Orion score.

All three vehicles had similar scores in the traffic crawl test. Larger cars probably have an advantage here due to less pitching being caused by the take up of drive. The belt CVT seems to have an inherently smooth operation, and the type of controller did not seem to have a large influence on the results.

In the launch feel test the Diesel Orion fared worst. This was probably due to the slower response to accelerator pedal movements (already seen in the above tests). In both the Orion objective tests (test 9), the engine speed is raised in a couple of stages with a plateau between them. This characteristic (perhaps due to take up of drive by the hydraulic clutch) is not present in such a marked way in the Micra tests. The Micra scored highest and this was perhaps due to the smoothness of the engine speed changes and their perception by the driver.

The engagement of the drive using the selector lever was smoothest in the Micra and least smooth in the Diesel Orion. The Micra does not creep when in DRIVE and at idle. This benefited the Micra in the result of this test. Good design of the lever and linkage and setting up of the engine idle speed and transmission clutch obviously have an important part to play in the implementation of creep. Modification of the Diesel Orion may have adversely affected its performance in this test.

The overall drivability results were as shown with the Micra in the highest position followed by the petrol and then the Diesel Orion.

Performance feel attributes

The performance feel attributes were the next to be assessed. The scores for these tests are also shown in Table 3.5. The first of these, the accelerator pedal effort/smoothness, resulted in a high score for the petrol Orion. The design of the pedal and return spring, and the characteristic of pedal position against engine torque demand have great effect upon the outcome of this test. The Diesel Orion fared worst and this was probably due to an unfavourable coupling of the transmission and engine demands to the pedal linkage as discussed earlier.

In the full throttle overtaking/response entering highway, the Micra scored highest followed by the petrol and then the Diesel Orions. Absence of steps in the engine speed curves may have had a part to play here. These can be compared in test 7 and 8 of the objective drivability tests on each of the vehicles.

The 50 km/h tip-in overtaking manoeuvre test is designed to allow study of the vehicle and transmission response and their perception by the driver at a moderate speed. The Micra scored highest, followed by the two Orions. Again the rate of change of engine speed during the manoeuvre plays a significant part in the resulting scores from this test.

In the fun to drive impression and the overall performance feel the Micra scored highest, followed by the petrol and then the Diesel Orion. The relative size of the vehicles, the pedal position against engine torque characteristic and perhaps also the pedal spring stiffness and length of travel were all considered significant here.

<u>NVH aspects</u>

The final section of the subjective tests was concerned with noise and vibration harshness in the vehicles. The Micra scored highest in all but the 'engine presence during ratio change' category. The electromagnetic powder clutch may have accounted somewhat for the high scores in the idle noise categories. The Diesel Orion was lowest in all but one category. This was predictable and probably due to changes in the engine/gearbox mounts for the experimental installation. The petrol Orion scores were close to those of the Micra and highest in the case of the 'engine presence during ratio change' category.

3.5 Findings and implications for CVT powertrain control

The operation of the three transmissions was found to be similar, the differences being caused by the characteristics of the controllers. It seemed that the electronic control of the Micra CVT clutch was more refined than the hydraulic control of the Orion CVT clutches. This is supported by the Micra achieving the highest subjective appraisal scores of the three vehicles and the objective testing which showed that the Micra powertrain controller forced the engine to follow a smoother operating line than those seen in the Orion tests.

All vehicle testing was completed on a track of zero gradient. The effects of hills on engine and vehicle speeds were not investigated. Since these may be significant, future vehicle test work should include assessment of vehicle performance in these conditions.

The graph in Figure 1.1 shows the vehicle speed / engine speed operating envelope observed from the hydraulically controlled transmission installed in the Diesel Orion. The shapes of these curves are typical for the hydraulically controlled and the electronically controlled powertrains studied.

From the results of the subjective and objective work described in this report, the following considerations have been drawn. They are used as the basis to achieve good vehicle drivability characteristics through the design of an electronic controller for a continuously variable Diesel powertrain:

1 The vehicle and engine speed changes must be smooth both for small and large accelerator pedal changes.

2 An immediate vehicle response to accelerator pedal movements is needed. For example in the kickdown shift behaviour test the transmission ratio change must not be so fast in driving the engine to a new higher speed that the vehicle either fails to accelerate for some time or even decelerates.

3 At cruising speed the engine speed must take the form of a curve at the lower end of the envelope shown in Figure 1.1.

4 During acceleration the engine speed may rise smoothly within the envelope shown in Figure 1.1. For the case of full acceleration the engine speed may follow a curve of the form of the higher end of the envelope. This would require the engine to be held at a constant speed for a range of vehicle speeds. This type of engine behaviour may appear unusual to drivers of non-CVT vehicles, but no evidence was found during the subjective tests that drivers found this engine behaviour disturbing.

5 It is desirable to have no vehicle creep and for the clutch to disengage completely when the accelerator pedal is not being pressed and the engine is idling. This conclusion arose from

additional comments written on the subjective appraisal questionnaires, and the shift lever movement tests. However, due to the appraisal team not being a true representation of all drivers, this recommendation requires further support and investigation.

6 In the traffic crawl and tip in / back out situation at low speed, the vehicle response must be less sensitive to pedal movements. However, when the vehicle is being driven at moderate speeds the response must be more sensitive in order to give the driver confidence in the performance of the vehicle.

7 The Micra deceleration tests in DRIVE showed that it is desirable to have a greater deceleration at higher speeds and a lesser deceleration at lower speeds with the vehicle eventually coming to rest without the use of the brakes. From these results it is thought that the optimum deceleration curve would be one of a linear deceleration schedule, decreasing from a set value at top vehicle speed to zero deceleration as the vehicle comes to rest.

The work described in this chapter has given an insight into the way the characteristics of a CVT controller may affect driver perception of a vehicle. Following on from the work discussed here, the next stage was to consider the effects of different controller strategies on vehicle economy and emissions. This enabled controllers to be designed which took into account the findings of both the work described here in addition to issues of economy and emissions.

Drivability attributes
Drivability smoothness and response (forwards)
Drivability smoothness and response (backwards)
Kick down shift behaviour (response and smoothness)
Tip-in/back-out
Over-run/braking to rest
Traffic crawl
Launch feel (delays and hesitations)
Neutral/drive neutral/reverse engagement smoothness
Overall drivability
Performance feel attributes
Accelerator pedal effort/smoothness
Full throttle overtaking/response entering highway
50 km/h tip-in overtaking manoeuvre
Fun to drive impression
Overall performance feel
NVH attributes
Idle noise/vibration in neutral (vehicle stationary)
Idle noise/vibration in reverse (vehicle stationary)
Idle noise/vibration in drive (vehicle stationary)
Transmission drive noise
Reverse gear noise
Engine presence during ratio change
Overall NVH

Table 3.1 Perceived drivability requirements and expectations

<table>
<tr><th>Rating Index</th><th>Evaluation of vehicle component performance</th><th>Undesirable characteristics noted by</th><th>Status</th></tr>
<tr><td>1</td><td rowspan="3">Production reject - very poor performance</td><td>All drivers</td><td rowspan="4">Not Acceptable</td></tr>
<tr><td>2</td><td rowspan="3">Average driver</td></tr>
<tr><td>3</td></tr>
<tr><td>4</td><td>Production reject - driver complaint</td></tr>
<tr><td>5</td><td>Borderline</td><td rowspan="4">Critical driver</td><td rowspan="2">Borderline Acceptable</td></tr>
<tr><td>6</td><td>Barely acceptable</td></tr>
<tr><td>7</td><td>Fair</td><td rowspan="4">Acceptable</td></tr>
<tr><td>8</td><td>Good</td></tr>
<tr><td>9</td><td>Very good</td><td>Trained observer</td></tr>
<tr><td>10</td><td>Excellent</td><td>Not perceptible</td></tr>
</table>

Table 3.2 Ratings index used for completion of vehicle drivability assessment questionnaires

TEST	DESCRIPTION
1	Constant speed driving in DRIVE
2	Constant speed driving in LOW
3	Tip-in response/smoothness (acceleration to maximum speed) in DRIVE
4	Tip-in response/smoothness (acceleration to maximum speed) in LOW
5	Deceleration smoothness (Deceleration from 100 km/h to idle in DRIVE)
6	Deceleration smoothness (Deceleration from 100 km/h to idle in LOW)
7	Acceleration from rest to maximum speed in DRIVE (wide open throttle ramped over 1 s)
8	Acceleration from rest to maximum speed in LOW (wide open throttle ramped over 1 s)
9	Acceleration versus pedal position (from idle to maximum speed) in DRIVE
10	On/off/on acceleration in DRIVE
11	On/off/on acceleration in LOW

Table 3.3 Objective vehicle tests

Variables recorded on the Bath data acquisition system	Variables recorded on the Ford data acquisition system
Time	Time
Pedal position	Pedal position
Vehicle speed	Vehicle speed
Vehicle acceleration	Vehicle acceleration
Diesel engine speed	Petrol engine speed
Engine boost pressure	
Forward clutch pressure	
Reverse clutch pressure	
Transmission primary pressure	
Transmission secondary pressure	
Transmission selector position	
Primary pulley axial position	
Engine coolant temperature	
Engine oil temperature	
Ambient air temperature	
Exhaust temperature	
Inlet air temperature	
Fuel temperature	
Gearbox oil temperature	
Intercooler air temperature	
Primary pulley speed	
Secondary pulley speed	

Table 3.4 Variables recorded by each of the data acquisition systems

	Mean	values of	scores
	Ford Orion (Petrol)	**Ford Orion (Diesel)**	**Nissan Micra**
Drivability attributes			
Drivability smoothness and response (forwards)	8.04	7.63	8.21
Drivability smoothness and response (backwards)	8.33	7.5	8.25
Kick down shift behaviour (response and smoothness)	7.58	6.63	7.88
Tip-in/back-out	7.42	6.42	7.83
Over-run/braking to rest	7.13	5.96	8.5
Traffic crawl	7.58	7.04	7.08
Launch feel (delays and hesitations)	6.83	6.21	7.17
Neutral/drive neutral/reverse engagement smoothness	7.5	7.21	9.08
Overall drivability	7.83	6.88	8.42
Performance feel attributes			
Accelerator pedal effort/smoothness	8.42	6.83	7.63
Full throttle overtaking/response entering highway	7.17	6.54	7.96
50 km/h tip-in overtaking manoeuvre	6.83	6.54	7.75
Fun to drive impression	7.21	5.54	8.33
Overall performance feel	7.33	5.88	8.17
NVH attributes			
Idle noise/vibration in neutral (vehicle stationary)	8.29	3.08	8.88
Idle noise/vibration in reverse (vehicle stationary)	6.67	2.46	7.25
Idle noise/vibration in drive (vehicle stationary)	7.96	3	8.67
Transmission drive noise	7.96	7.08	8.63
Reverse gear noise	6.83	7.29	7
Engine presence during ratio change	6.96	5.67	6.67
Overall NVH	7.75	4.13	8.38

Table 3.5 Vehicle drive appraisal: mean values of all twelve questionnaires completed

Test 1 Constant Speed Driving in DRIVE			
1S1-5R1.XLS *			
	1S6-7R2.XLS *		
Test 2 Constant Speed Driving in LOW			
	2S12-8R2.XLS *		
Test 3 Tip-in response/smoothness (acceleration to max speed) in DRIVE			
13S35R1.XLS	13S35R2.XLS *		
13S36R1.XLS			
	13S39R2.XLS *		
	13S40R2.XLS		
	13S43R2.XLS		
	13S44R2.XLS		
13S45R1.XLS	13S45R2.XLS		
13S46R1.XLS		13S46R3.XLS	
Test 4 Tip-in response/smoothness (acceleration to max speed) in LOW			
12S23R1.XLS *	12S23R2.XLS		
12S24R1.XLS	12S24R2.XLS		
	12S27R2.XLS *		
	12S28R2.XLS		
	12S31R2.XLS		
	12S32R2.XLS		
12S33R1.XLS		12S33R3.XLS	
12S34R1.XLS		12S34R3.XLS	
Test 5 Deceleration Smoothness (Deceleration from 100 kph to idle in DRIVE)			
	5S47R2.XLS *		
5S48R1.XLS			
Test 6 Deceleration Smoothness (Deceleration from 100 kph to idle in LOW)			
	6S52R2.XLS *		
6S53R1.XLS			
Test 7 Acceleration from Rest to Max Speed (WOT ramped over 1 sec) DRIVE			
7S57R1.XLS	7S57R2.XLS *		
Test 8 Acceleration from Rest to Max Speed (WOT ramped over 1 sec) LOW			
8S62R1.XLS	8S62R2.XLS *		
Test 9 Acceleration v's Pedal Posn (from idle to max speed) 70mm max travel DRIVE			
9S67R1.XLS			
9S68R1.XLS *	9S68R2.XLS		
Test 10 On/Off/On Acceleration DRIVE			
10S78-1R.XLS			
Test 11 On/Off/On Acceleration LOW			
Calibration Tests			
15S1R1.XLS	15S1R2.XLS	15S2R1.XLS	16S1R1.XLS

Table 3.6 Nissan Micra processed drivability tests

Test 1 Constant Speed Driving in DRIVE			
1S1-5R1.XLS *	1S1-5R2.XLS		
Test 2 Constant Speed Driving in LOW			
2S12-7R1.XLS *	2S12-7R2.XLS		
Test 3 Tip-in response/smoothness (acceleration to max speed) in DRIVE			
3S23R1-2.XLS			
3S24R1.XLS *	3S24R2.XLS *		
3S27R1-2.XLS *			
3S28R1-2.XLS			
3S31R1-2.XLS			
3S32R1-2.XLS			
3S33R1.XLS	3S33R2.XLS		
3S34R1.XLS		3S34R3.XLS	
Test 4 Tip-in response/smoothness (acceleration to max speed) in LOW			
4S35R1.XLS			
4S36R1.XLS *	4S36R2.XLS		
4S39R1-2.XLS *			
4S40R1-2.XLS			
4S43R1-2.XLS			
4S44R1-2.XLS			
4S45R1.XLS		4S45R3.XLS	
4S46R1.XLS		4S46R3.XLS	
Test 5 Deceleration Smoothness (Deceleration from 100 kph to idle in DRIVE)			
5S47R1.XLS *	5S47R2.XLS		
Test 6 Deceleration Smoothness (Deceleration from 100 kph to idle in LOW)			
6S52R1.XLS *	6S52R2.XLS		
Test 7 Acceleration from Rest to Max Speed (WOT ramped over 1 sec) DRIVE			
7S57R1-2.XLS *			
Test 8 Acceleration from Rest to Max Speed (WOT ramped over 1 sec) LOW			
8S62R1-2.XLS *			
Test 9 Acceleration v's Pedal Posn (from idle to max speed) 70mm max travel DRIVE			
9S67R1&3.XLS			
9S68R1-2.XLS *			
9S69R1-2.XLS			
9S70R1-2.XLS *			
9S71R1-2.XLS			
9S72R1-2.XLS			
Test 10 On/Off/On Acceleration DRIVE			
Test 11 On/Off/On Acceleration LOW			
Calibration Tests			
15S1R1.XLS	15S2R1.XLS	16S1R1.XLS	16S1R2.XLS
17S1R1.XLS			

Table 3.7 Ford Orion (Petrol) processed drivability tests

Test 1 Constant Speed Driving in DRIVE			
TOT01R1.XLS *			
	TOT06R2.XLS *		
Test 2 Constant Speed Driving in LOW			
TOT12R1.XLS *			
	TOT19R2.XLS		
Test 3 Tip-in response/smoothness (acceleration to max speed) in DRIVE			
TOT23R1.XLS	TOT23R2.XLS *		
TOT27R1.XLS *	TOT27R2.XLS		
TOT28R1.XLS *	TOT28R2.XLS		
TOT31R1.XLS	TOT31R2.XLS		
TOT32R1.XLS *	TOT32R2.XLS		TOT32R4.XLS
TOT33R1.XLS	TOT33R2.XLS		
TOT34R1.XLS			
Test 4 Tip-in response/smoothness (acceleration to max speed) in LOW			
TOT35R1.XLS	TOT35R2.XLS		
TOT39R1.XLS *	TOT39R2.XLS		
TOT43R1.XLS	TOT43R2.XLS		
TOT44R1.XLS	TOT44R2.XLS		
TOT45R1.XLS	TOT45R2.XLS		TOT45R4.XLS
TOT46R1.XLS			
Test 5 Deceleration Smoothness (Deceleration from 100 kph to idle in DRIVE)			
TOT47R1.XLS *	TOT47R2.XLS		
Test 6 Deceleration Smoothness (Deceleration from 100 kph to idle in LOW)			
TOT52R1.XLS *	TOT52R2.XLS		
Test 7 Acceleration from Rest to Max Speed (WOT ramped over 1 sec) DRIVE			
TOT57R1.XLS *	TOT57R2.XLS		
Test 8 Acceleration from Rest to Max Speed (WOT ramped over 1 sec) LOW			
TOT62R1.XLS *	TOT62R2.XLS		
Test 9 Acceleration v's Pedal Posn (from idle to max speed) 70mm max travel DRIVE			
TOT67R1.XLS		TOT67R3.XLS	
TOT68R1.XLS *	TOT68R2.XLS	TOT68R3.XLS	
TOT69R1.XLS	TOT69R2.XLS		
TOT70R1.XLS *	TOT70R2.XLS		
TOT71R1.XLS	TOT71R2.XLS		
TOT72R1.XLS	TOT72R2.XLS		
Test 10 On/Off/On Acceleration DRIVE			
Test 11 On/Off/On Acceleration LOW			

Table 3.8 Ford Orion (Diesel) processed drivability tests

Subjective attribute	Objective test (from Table 3.3)
Drivability attributes	
Drivability smoothness and response (forwards)	3, 4, 9
Drivability smoothness and response (backwards)	3, 4, 9
Kick down shift behaviour (response and smoothness)	3, 4, 7, 8
Tip-in/back-out	3, 4, 10, 11
Over-run/braking to rest	5, 6
Traffic crawl	3, 4
Launch feel (delays and hesitations)	7, 8
Neutral/drive neutral/reverse engagement smoothness	
Overall drivability	
Performance feel attributes	
Accelerator pedal effort/smoothness	1, 2
Full throttle overtaking/response entering highway	7, 8
50 km/h tip-in overtaking manoeuvre	3, 4
Fun to drive impression	3, 4, 7, 8, 9
Overall performance feel	
NVH attributes	
Idle noise/vibration in neutral (vehicle stationary)	
Idle noise/vibration in reverse (vehicle stationary)	
Idle noise/vibration in drive (vehicle stationary)	
Transmission drive noise	
Reverse gear noise	
Engine presence during ratio change	3, 4, 5, 6, 7, 8
Overall NVH	

Table 3.9 Relationship between subjective attributes and objective tests

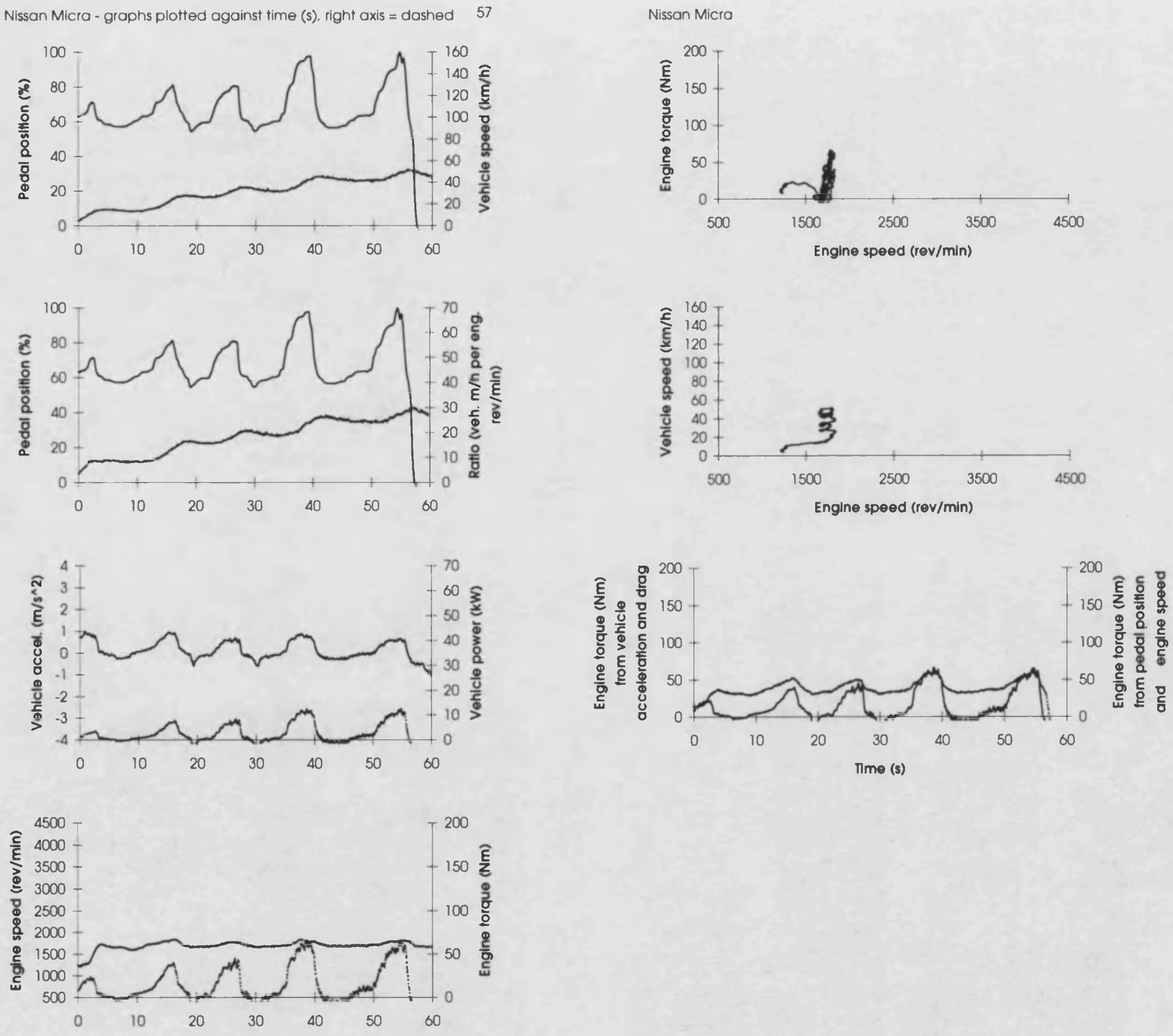

Figure 3.1 Test 1S1-5R1

Figure 3.1

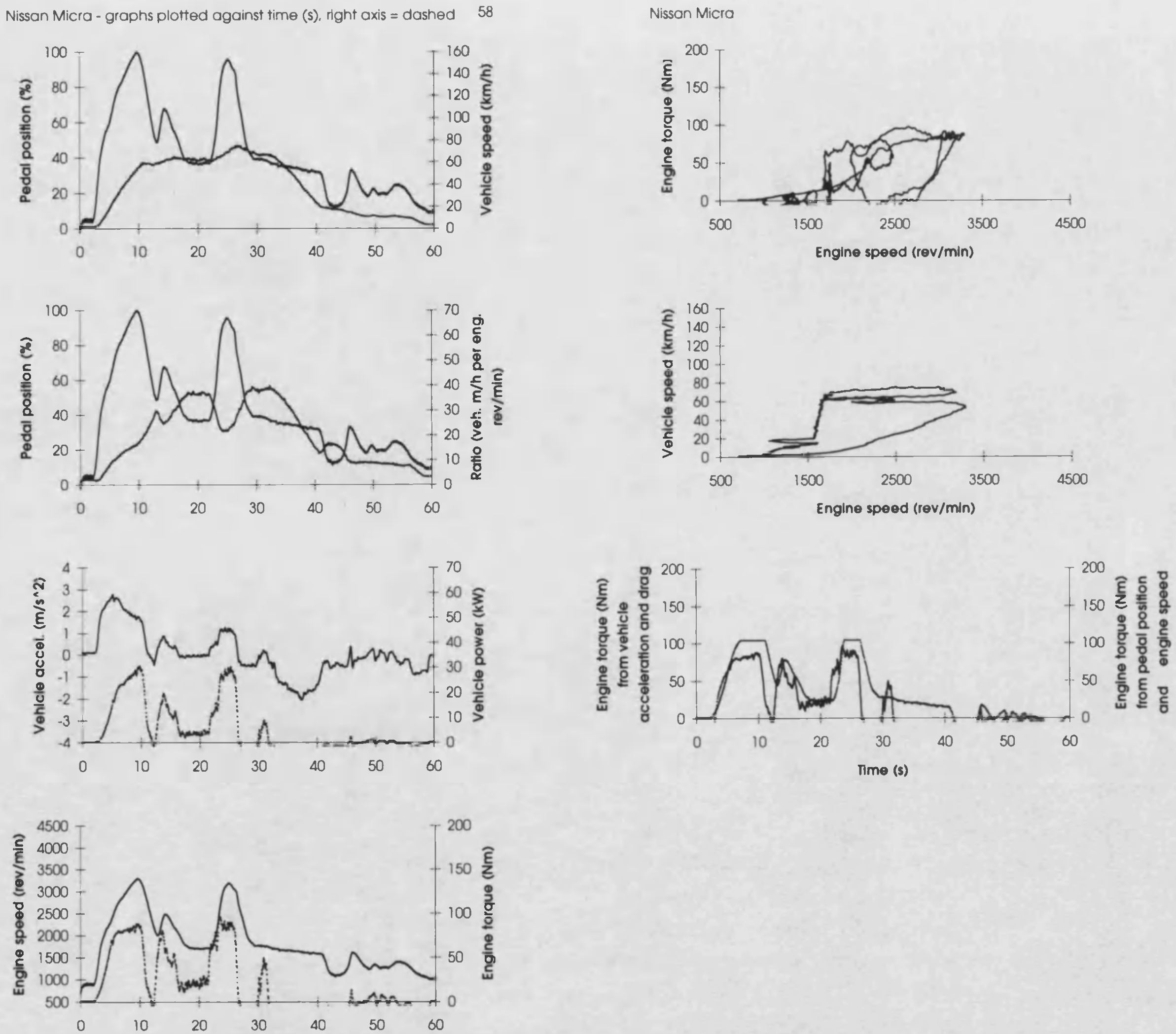

Figure 3.2 Test 1S6-7R2

Figure 3.2

Nissan Micra - graphs plotted against time (s), right axis = dashed line 59

Nissan Micra

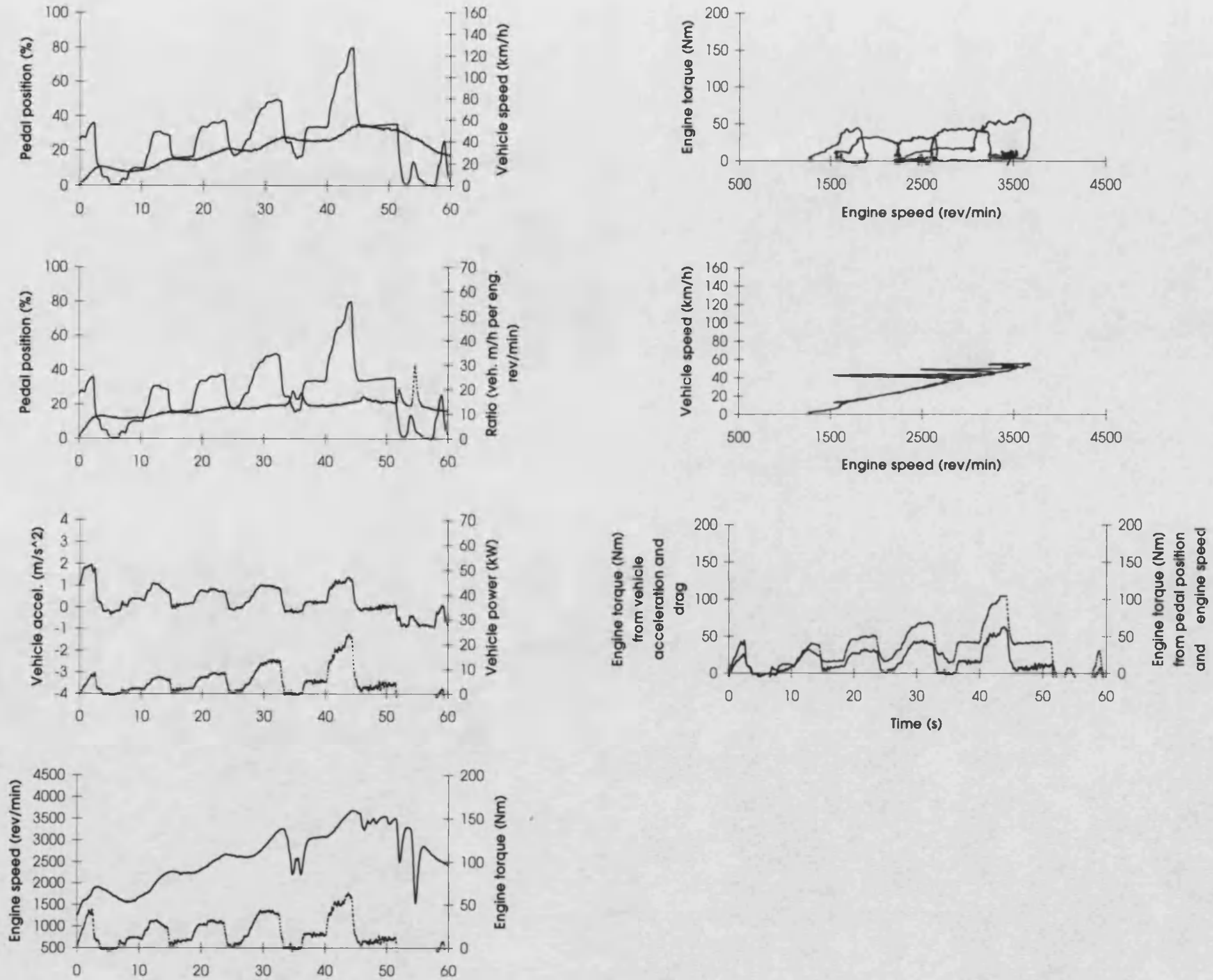

Figure 3.3 Test 2S12-8R2

Figure 3.3

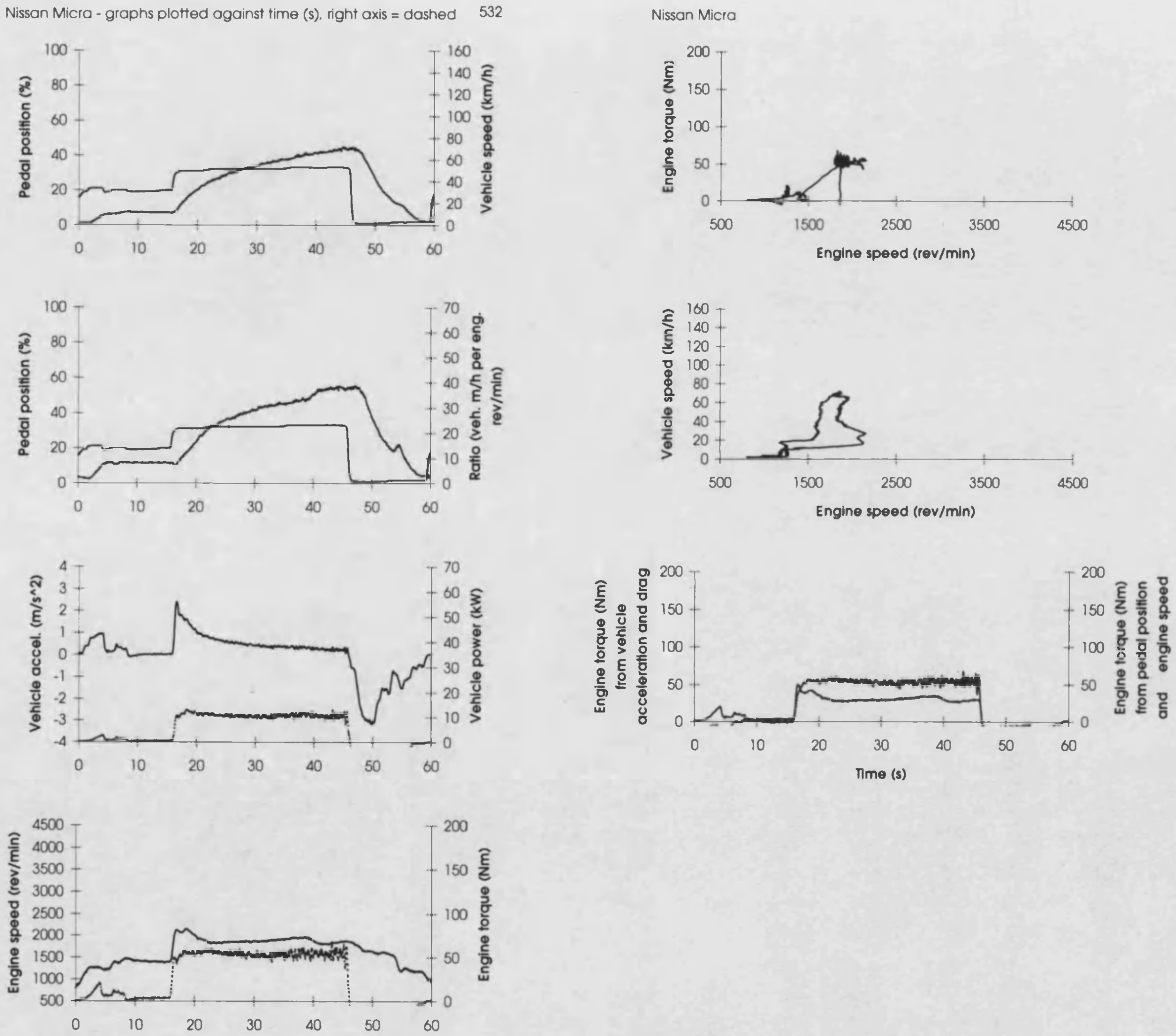

Figure 3.4 Test 13S35R2

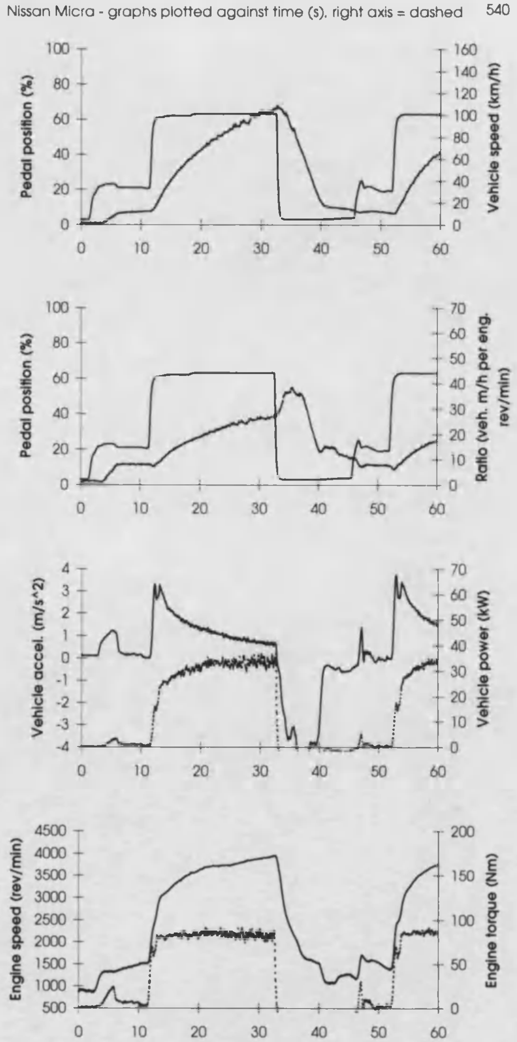

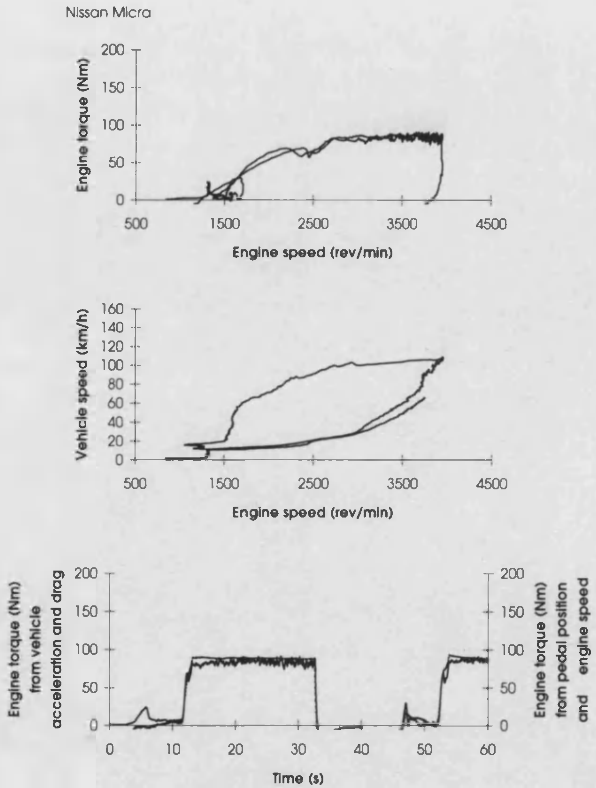

Figure 3.5 Test 13S39R2

Figure 3.5

Nissan Micra - graphs plotted against time (s), right axis = dashed 534

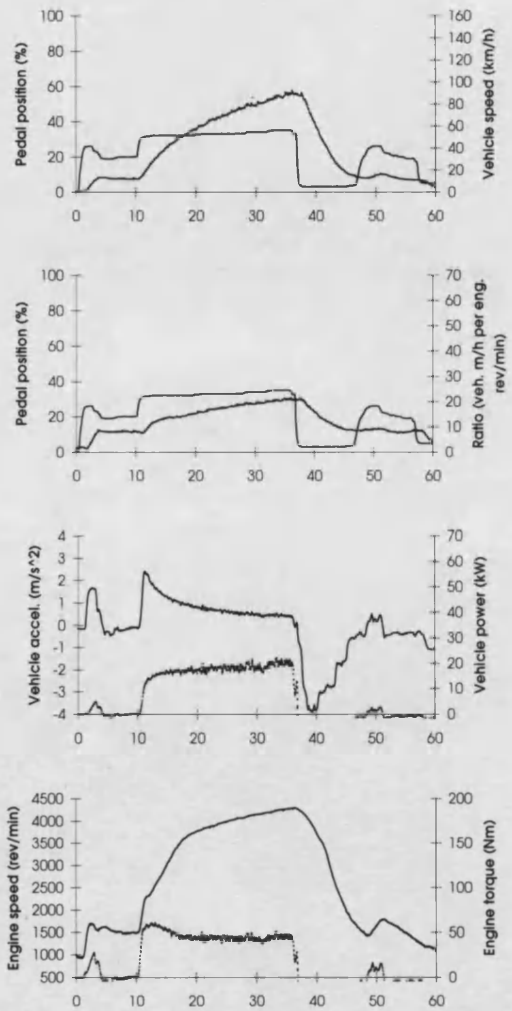

Nissan Micra

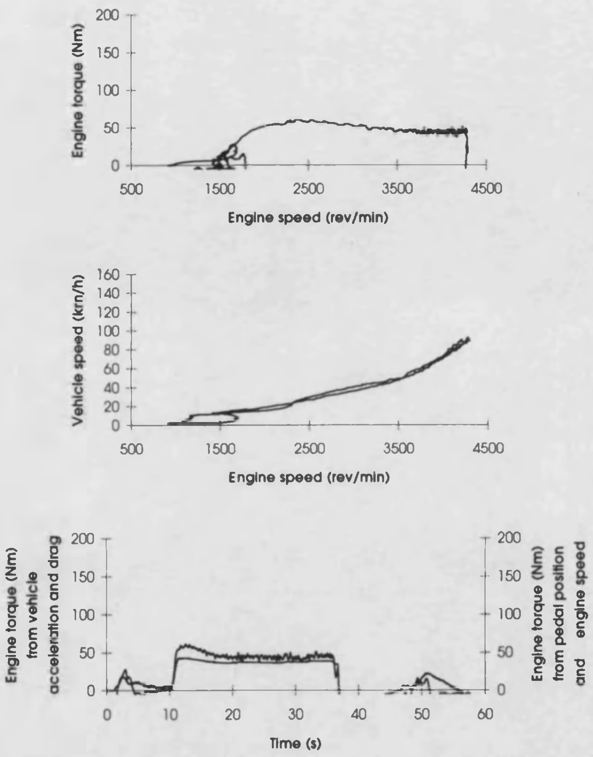

Figure 3.6 Test 12S23R1

Figure 3.6

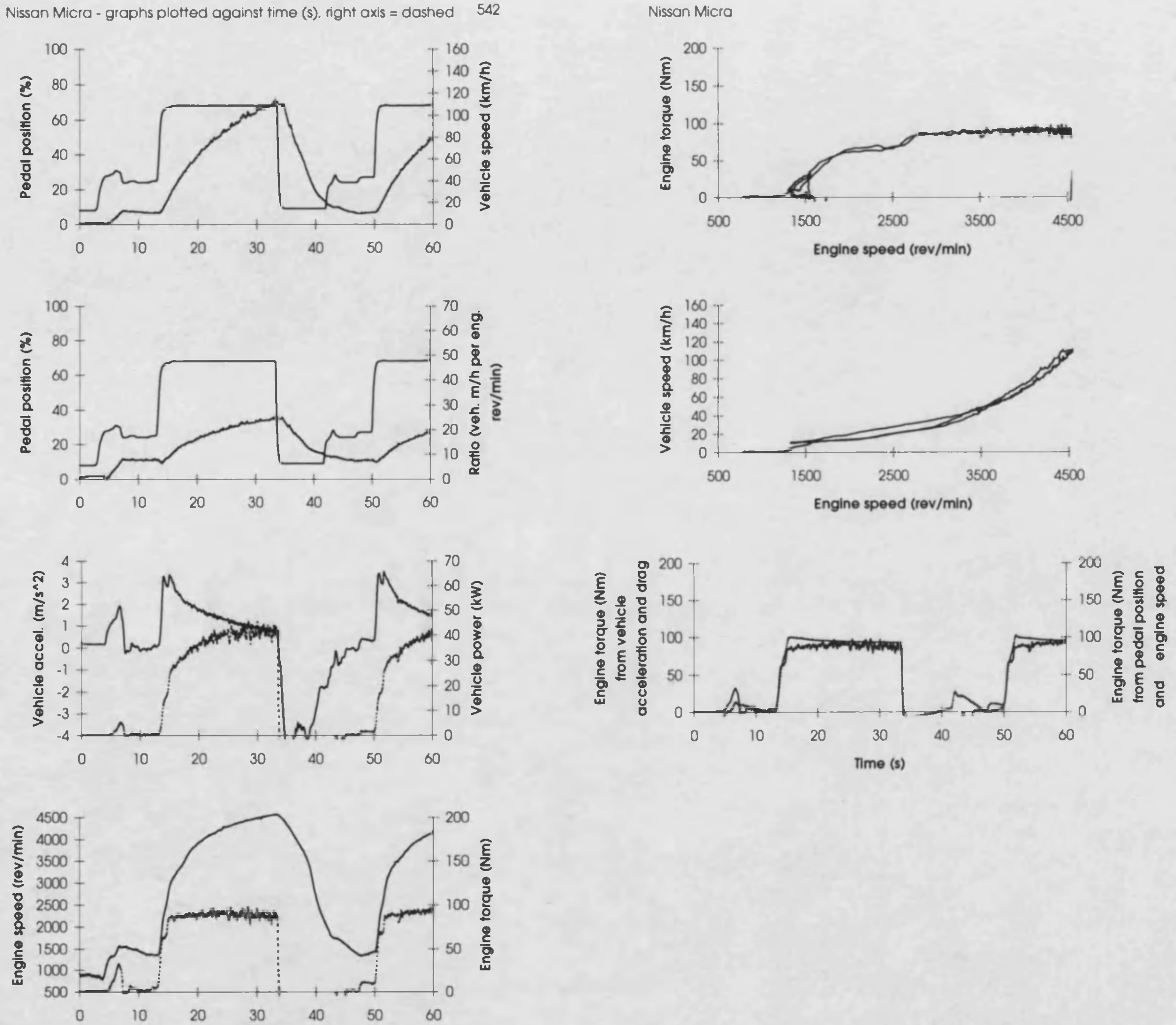

Figure 3.7 Test 12S27R2

Figure 3.7

Figure 3.8

Nissan Micra - graphs plotted against time (s), right axis = dashed 511

Nissan Micra

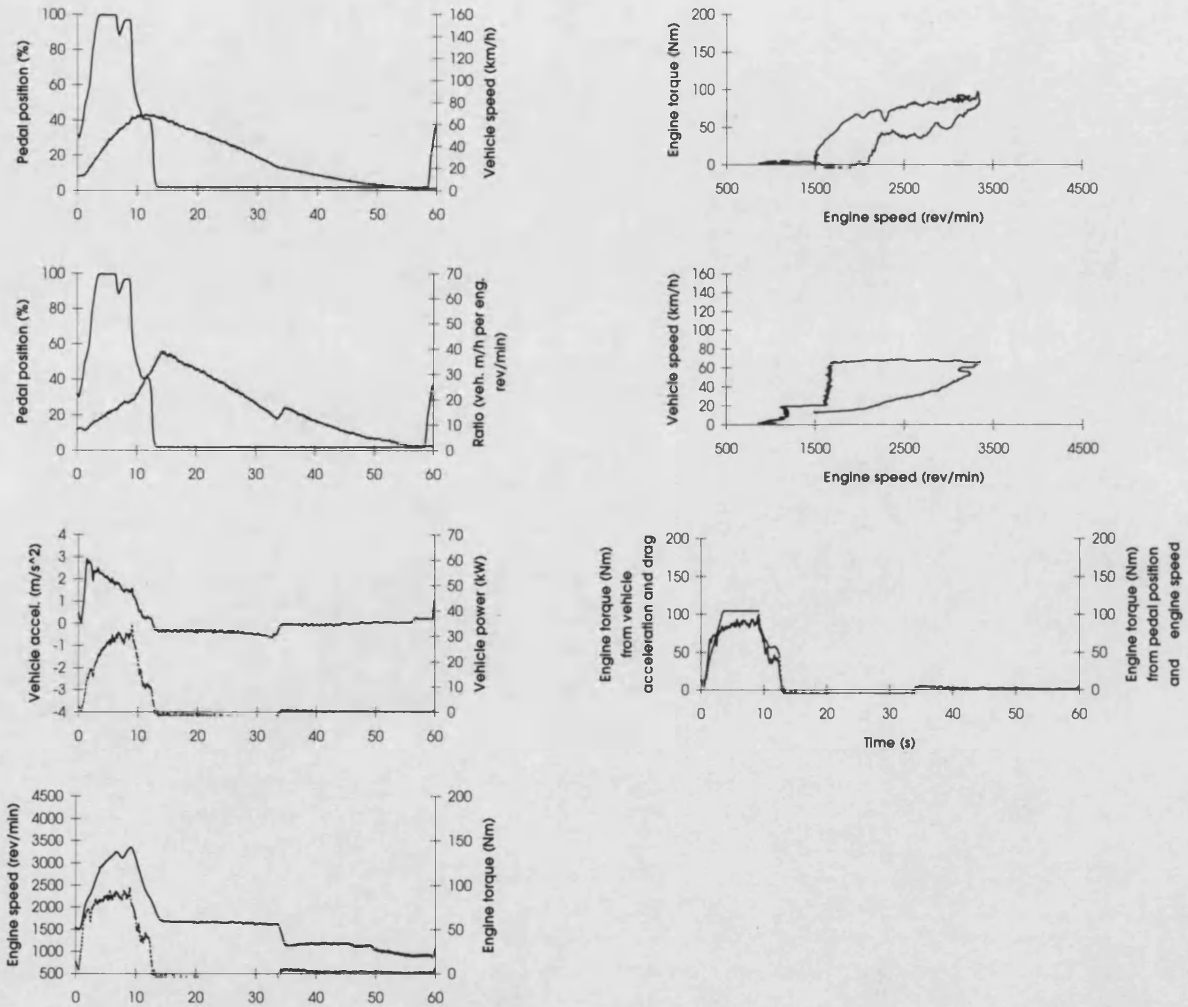

Figure 3.8 Test 5S47R2

Nissan Micra - graphs plotted against time (s), right axis = dashed 515

Nissan Micra

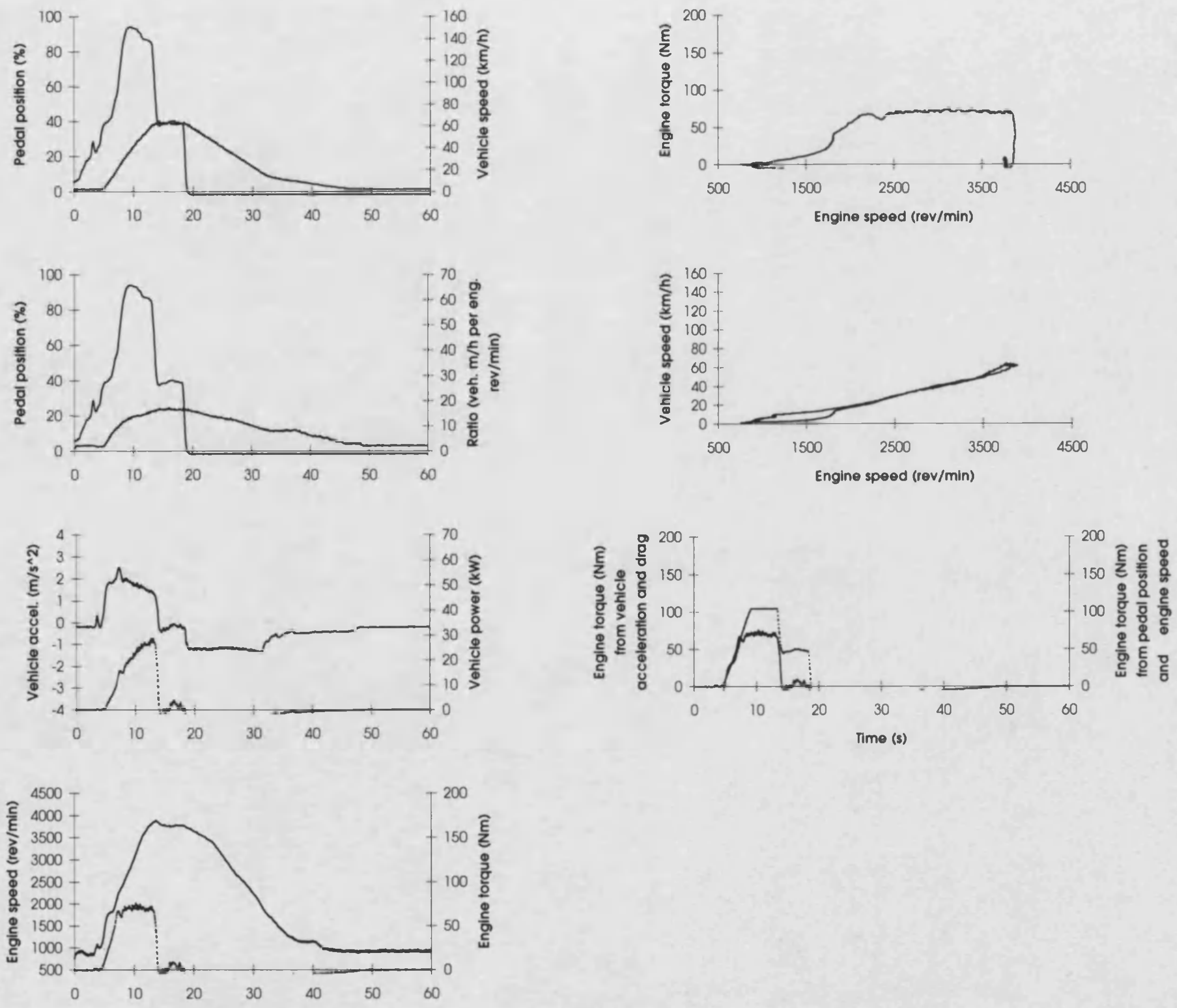

Figure 3.9 Test 6S52R2

Figure 3.9

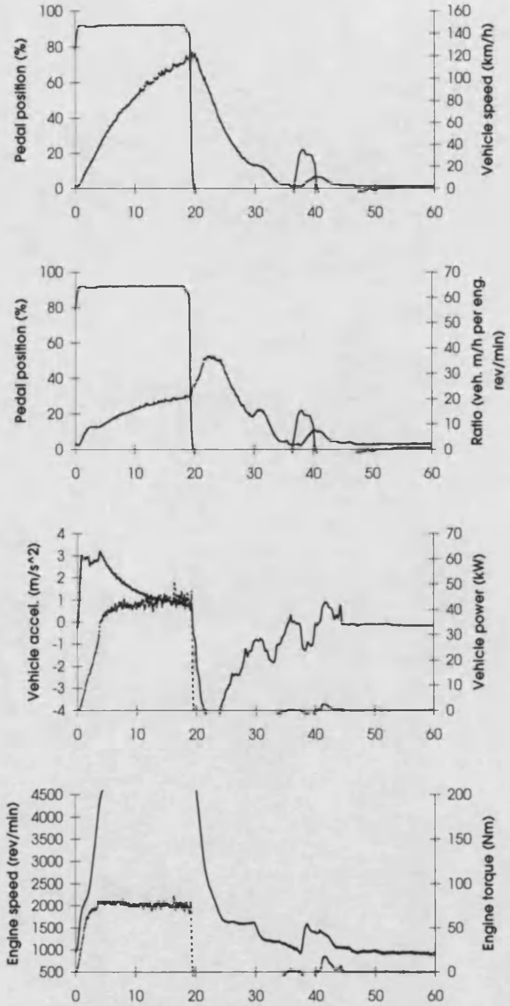

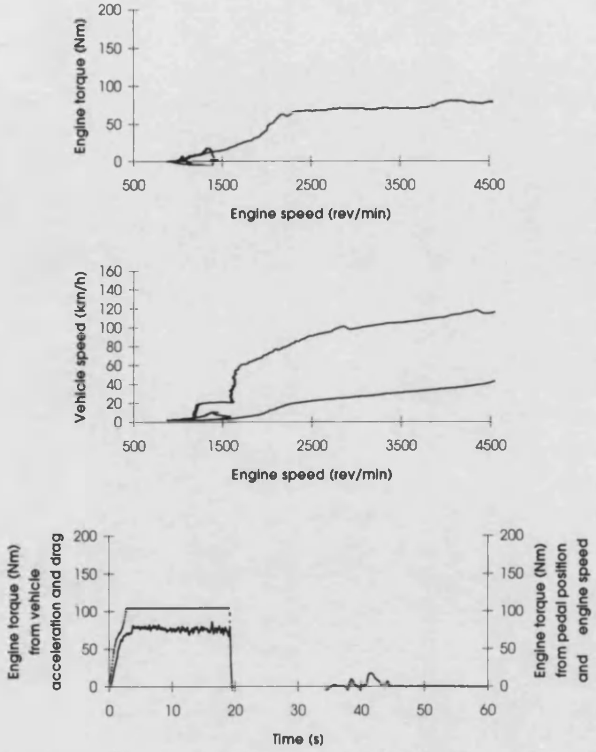

Figure 3.10 Test 7S57R2

Figure 3.10

Figure 3.11

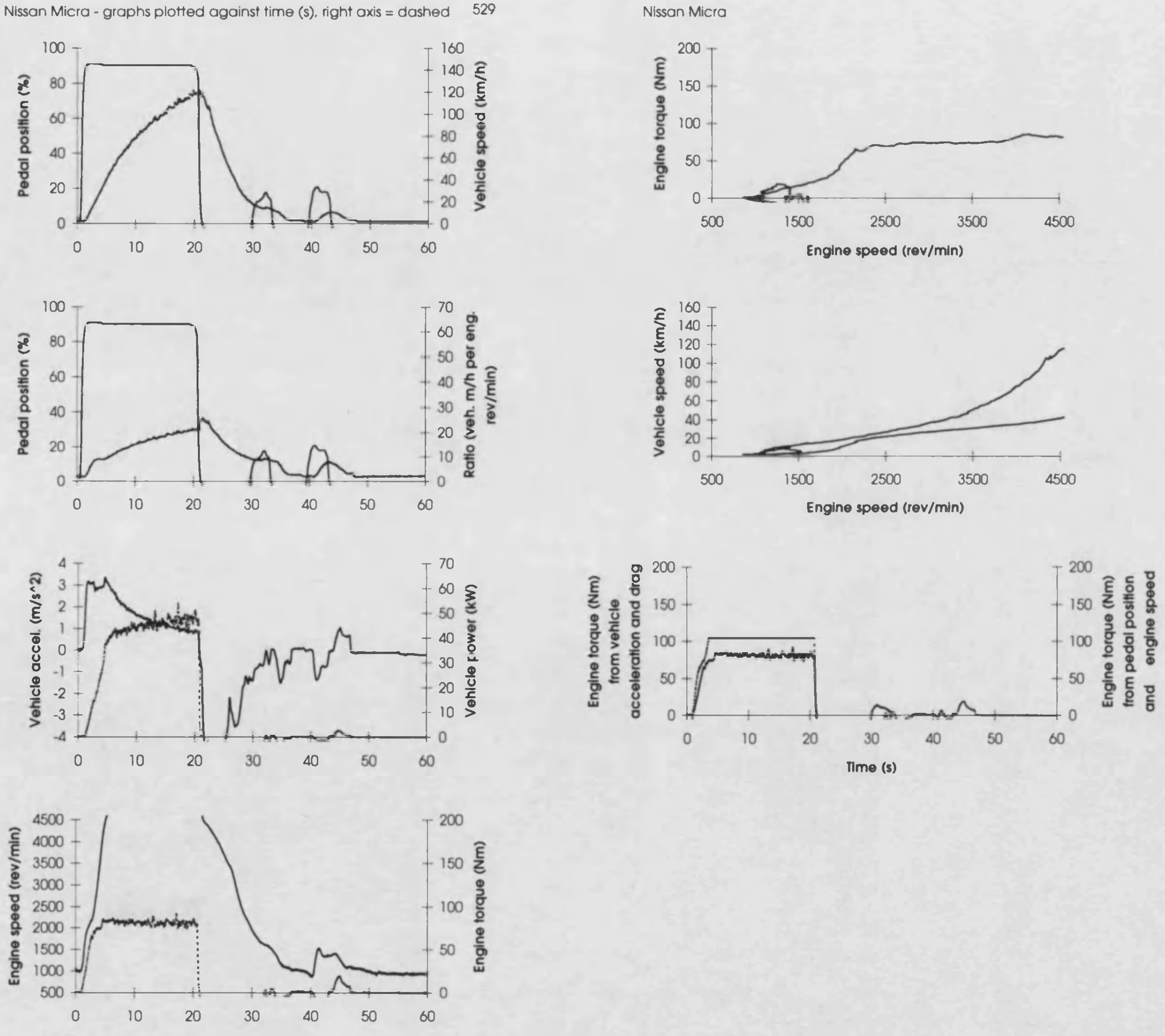

Figure 3.11 Test 8S62R2

Nissan Micra - graphs plotted against time (s), right axis = dashed 538

Nissan Micra

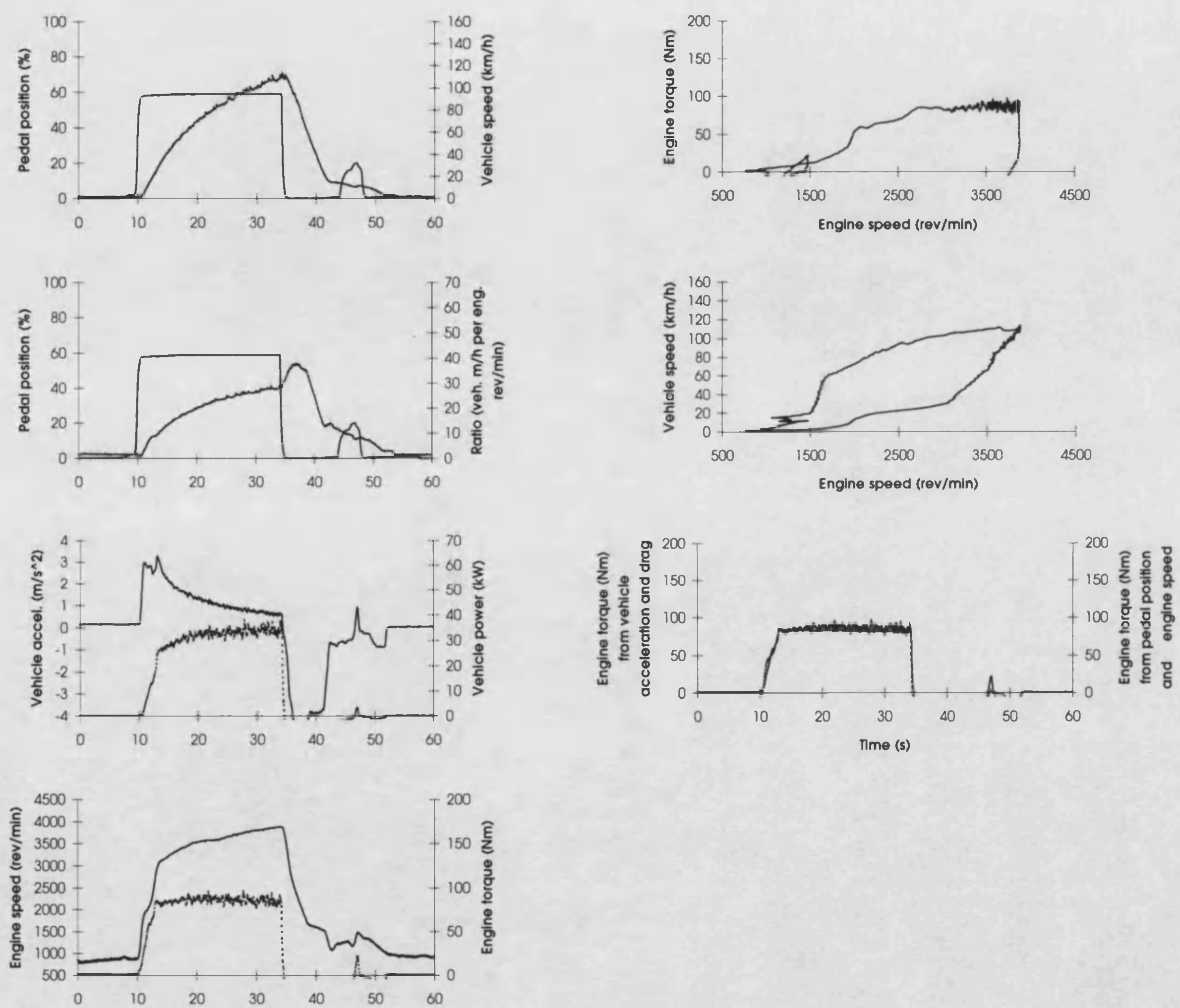

Figure 3.12

Figure 3.12 Test 9S68R1

Ford Orion (petrol) - graphs plotted against time (s), right axis = dashed
TEST613.TXT

Ford Orion (petrol)

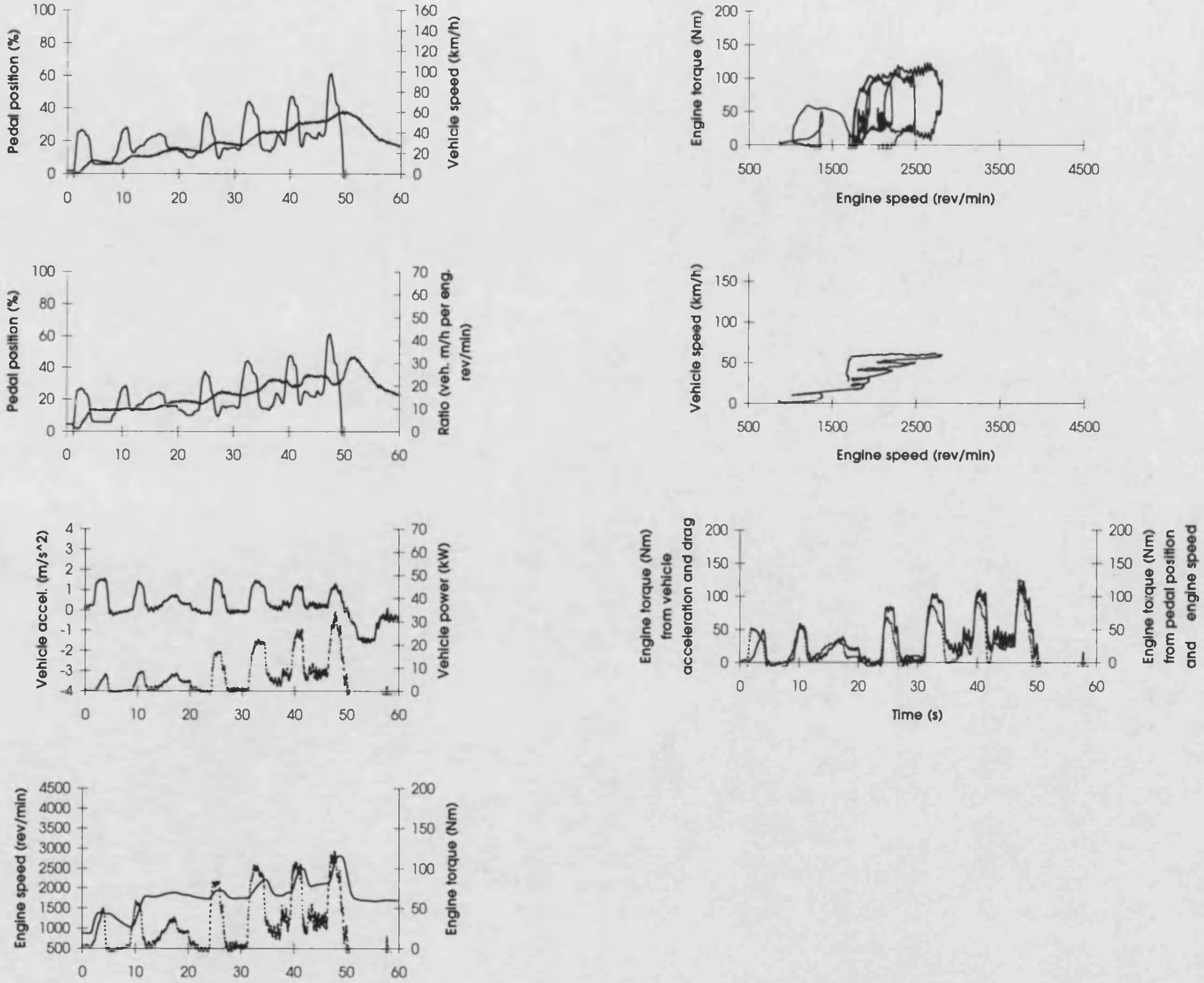

Figure 3.13 Test 1S1-5R1

Figure 3.13

Ford Orion (petrol) - graphs plotted against time (s), right axis = dashed
TEST615.TXT

Ford Orion (petrol)

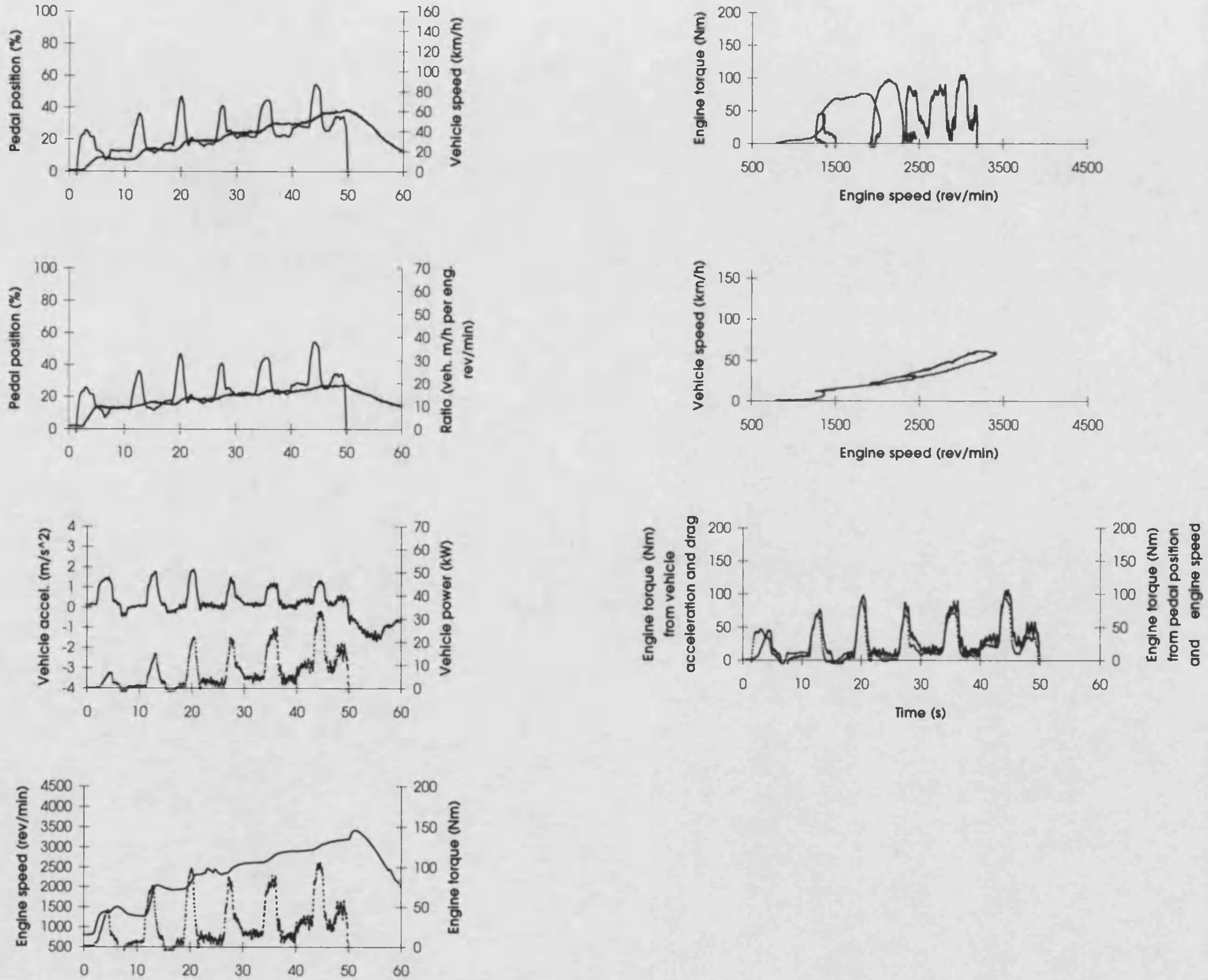

Figure 3.14 Test 2S12-7R1

Figure 3.14

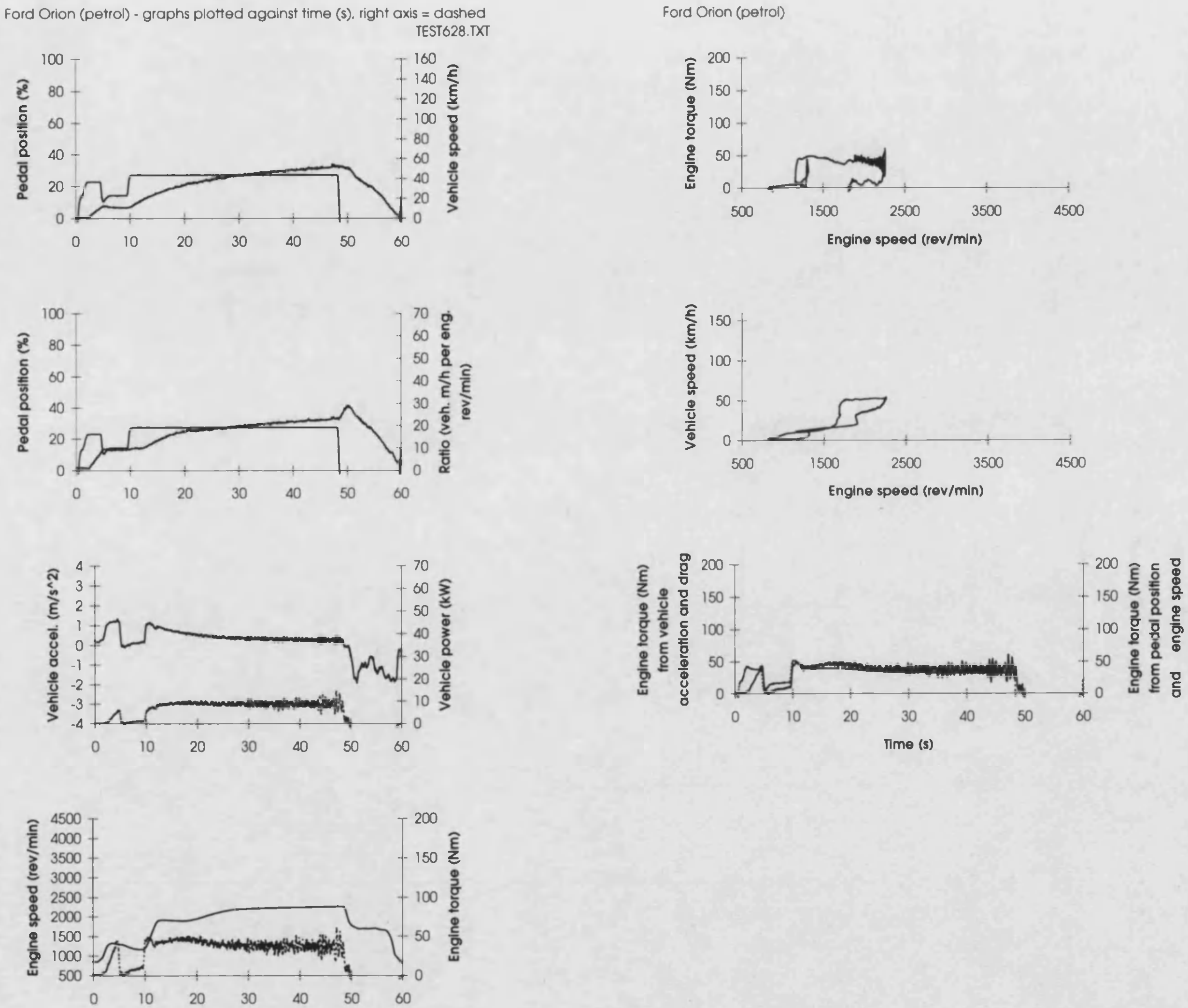

Figure 3.15 Test 3S24R1

Figure 3.15

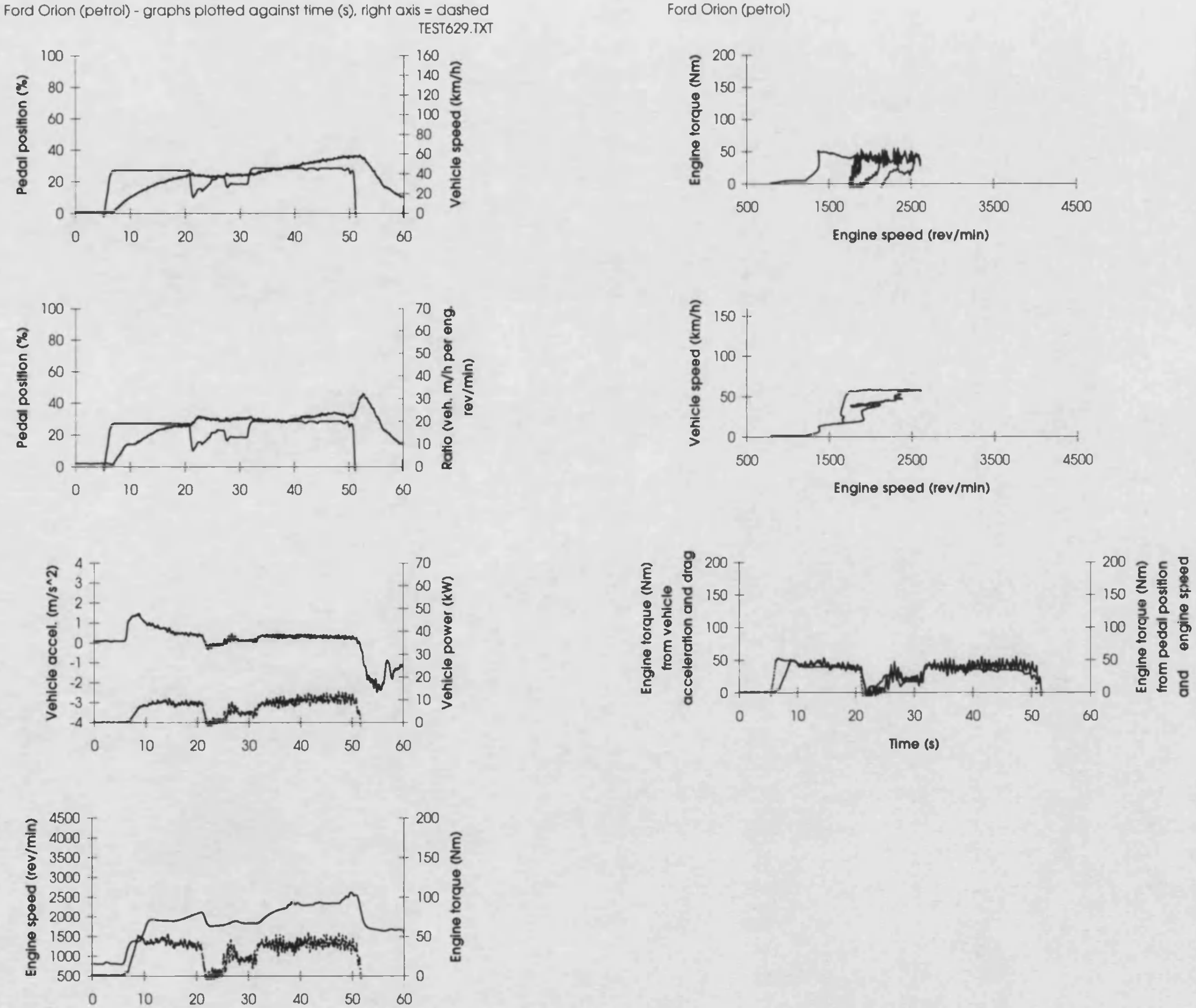

Figure 3.16 Test 3S24R2

Figure 3.16

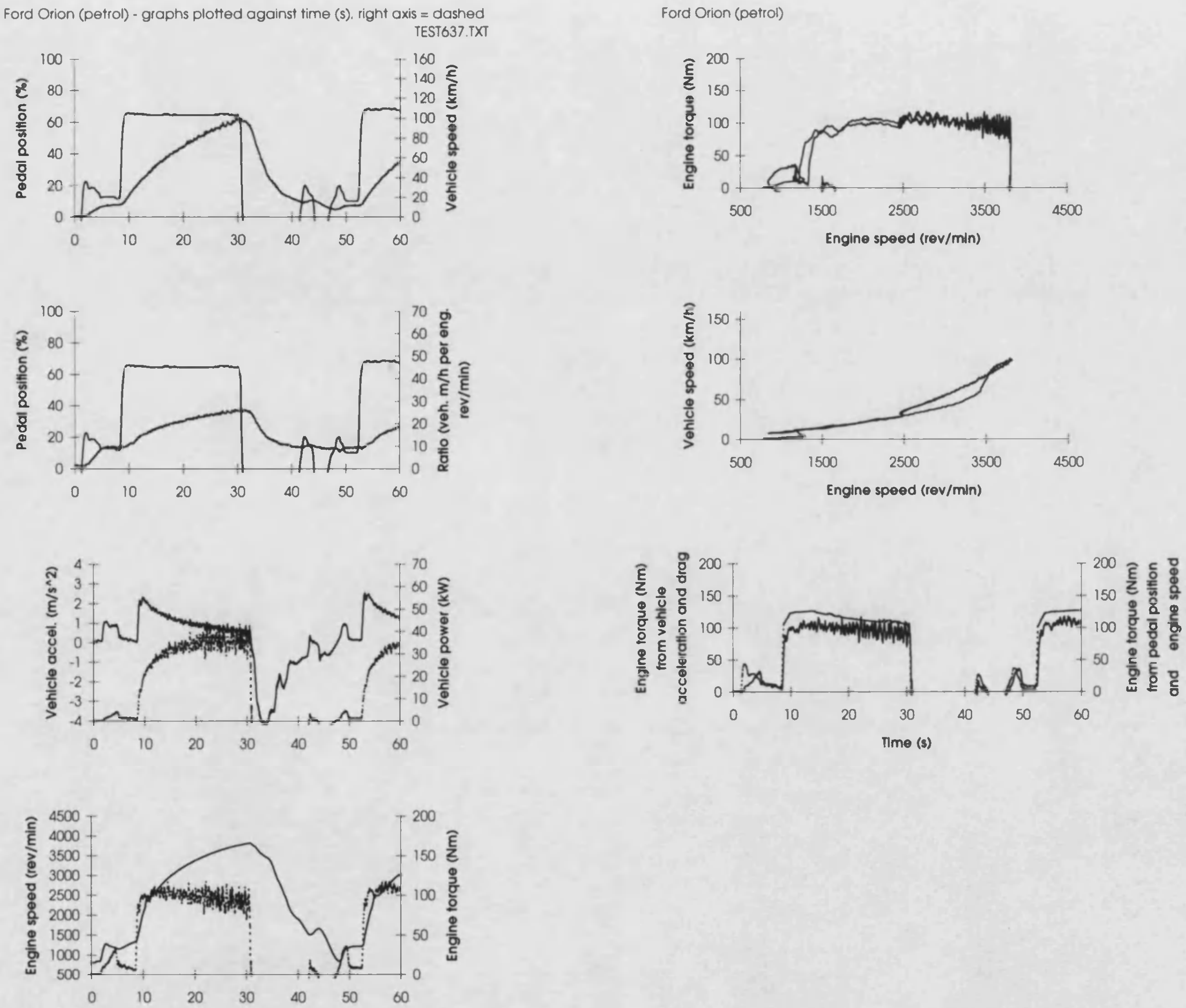

Figure 3.17 Test 3S27R1-2

Figure 3.17

Figure 3.18

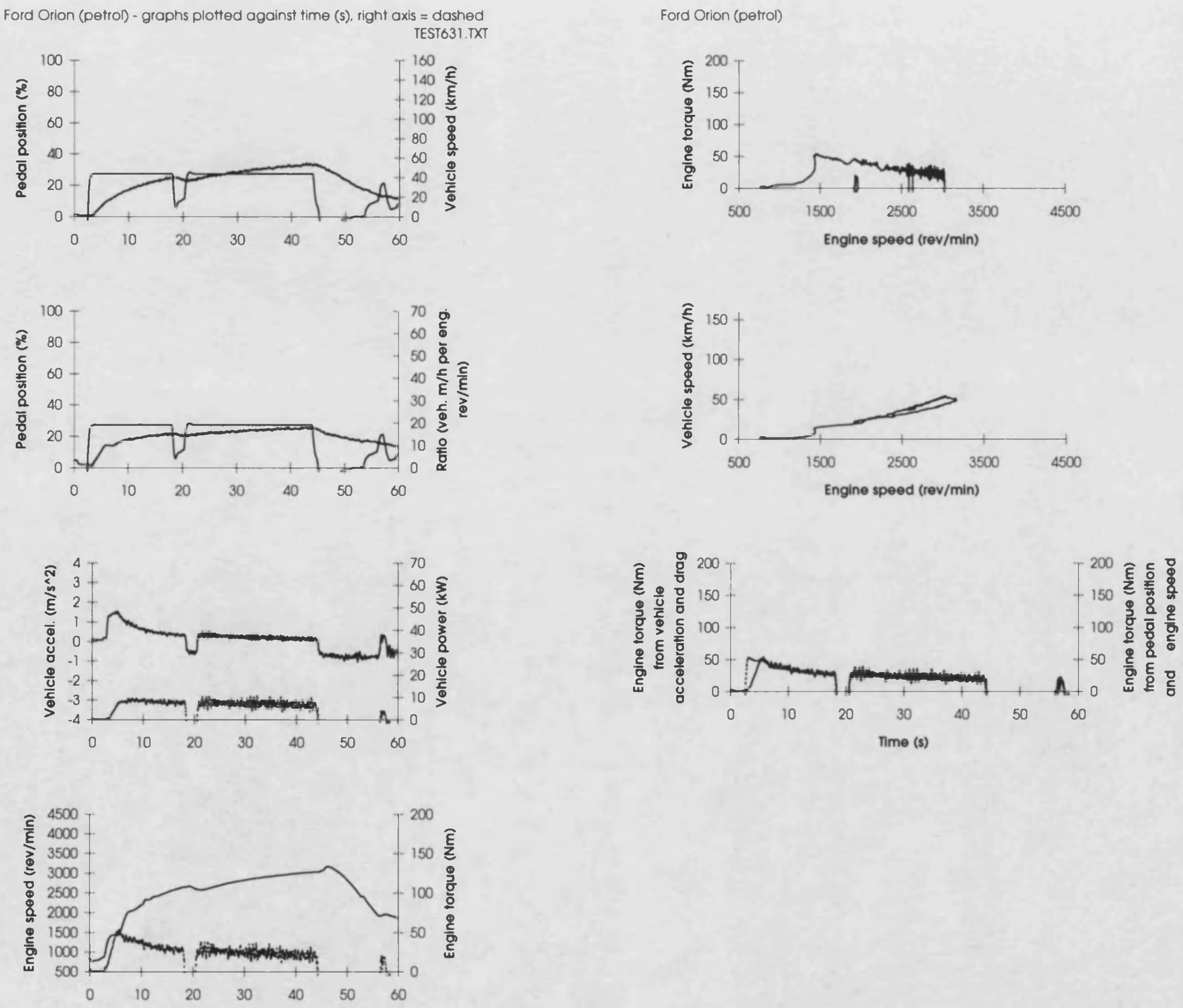

Figure 3.18 Test 4S36R1

Figure 3.19

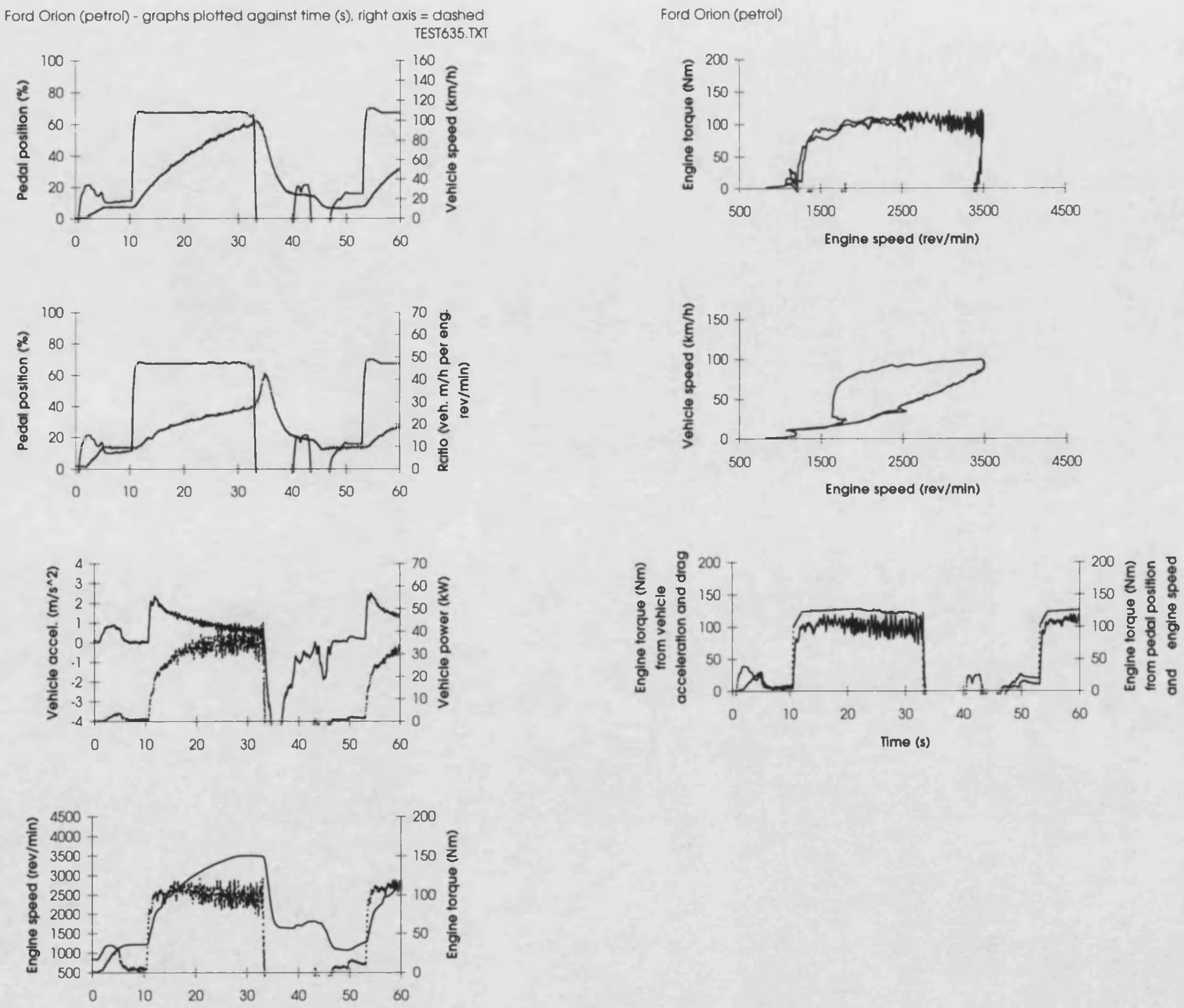

Figure 3.19 Test 4S39R1-2

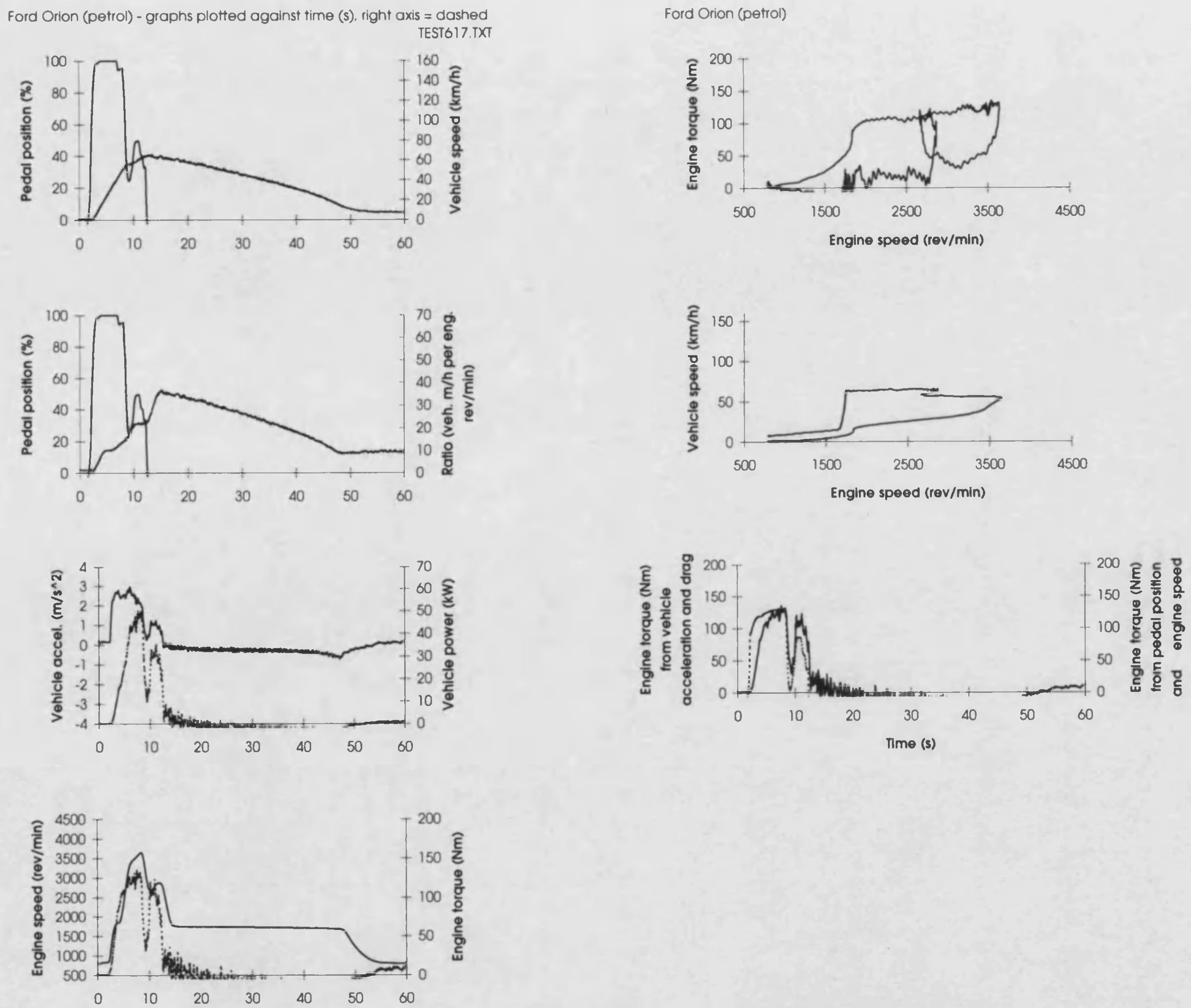

Figure 3.20 Test 5S47R1

Figure 3.20

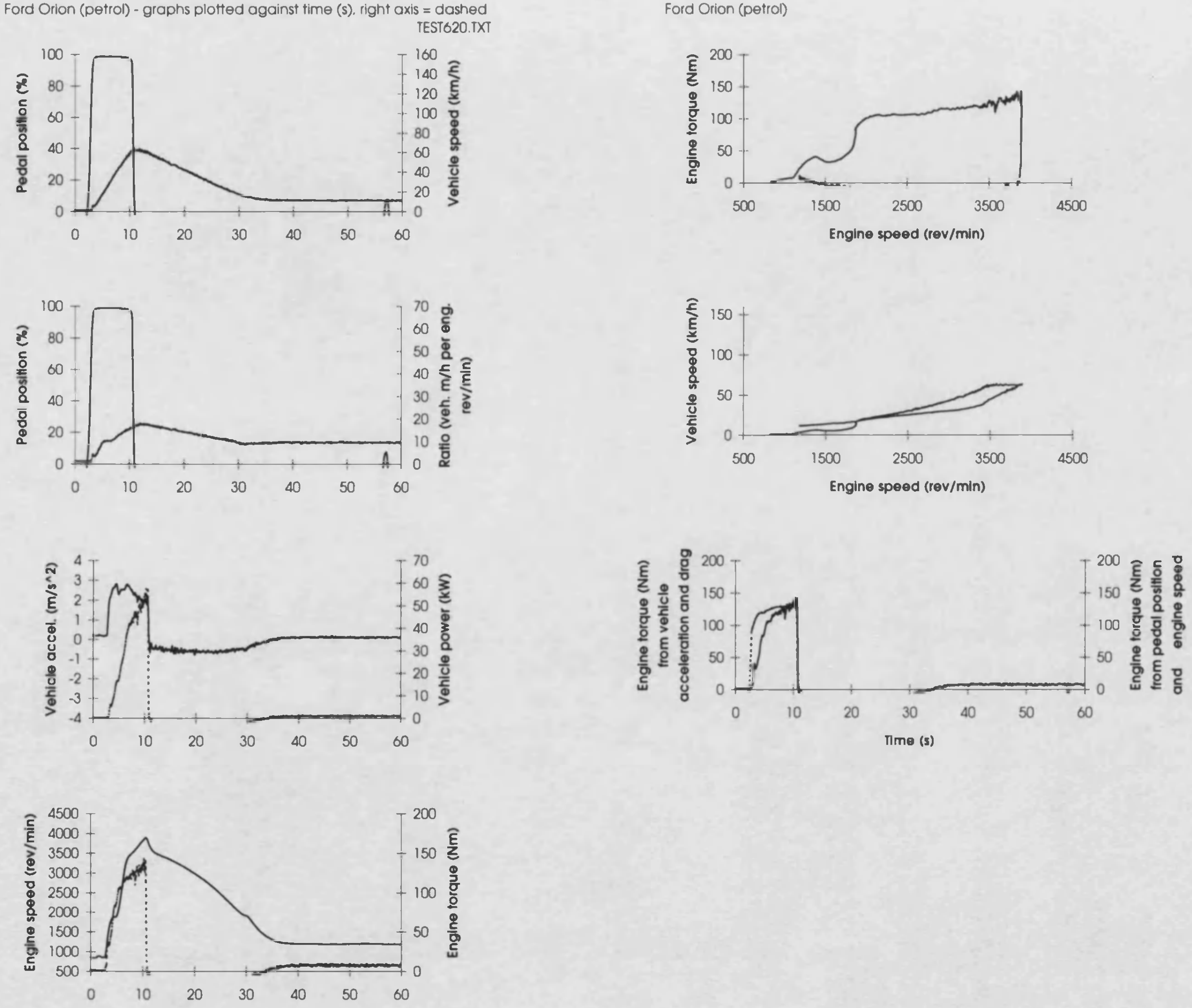

Figure 3.21 Test 6S52R1

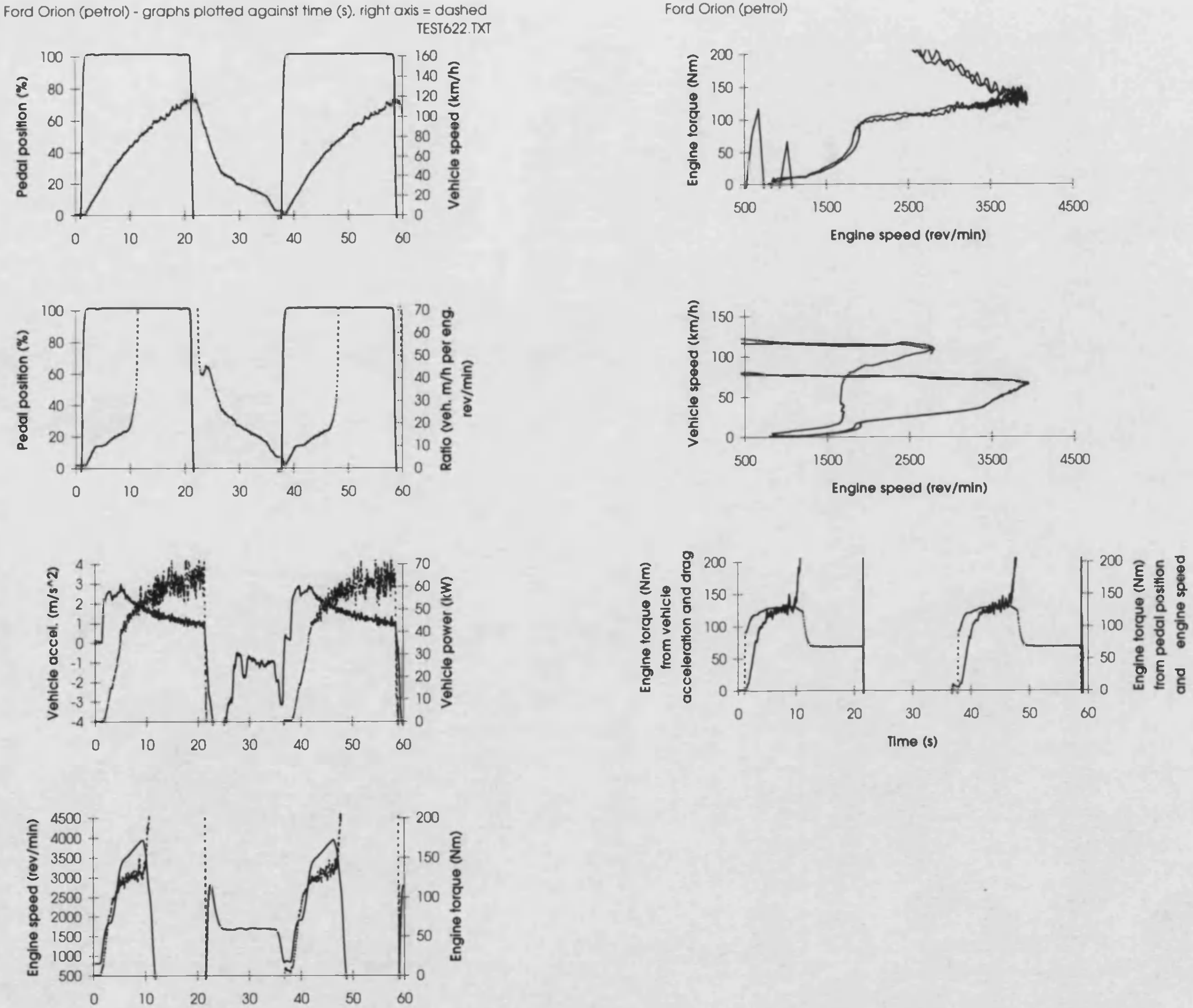

Figure 3.22 Test 7S57R1-2

Figure 3.22

Figure 3.23

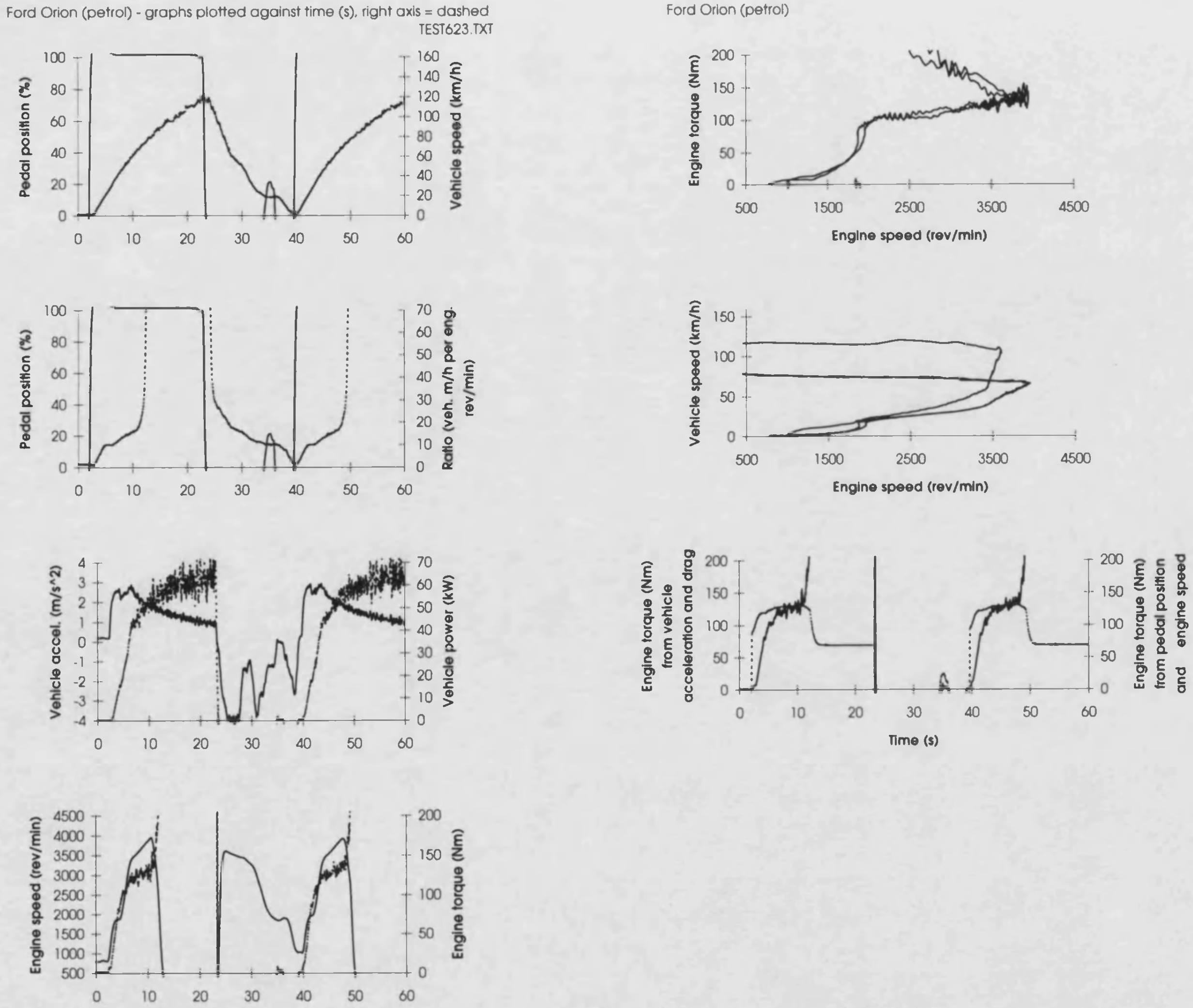

Figure 3.23 Test 8S62R1-2

Figure 3.24

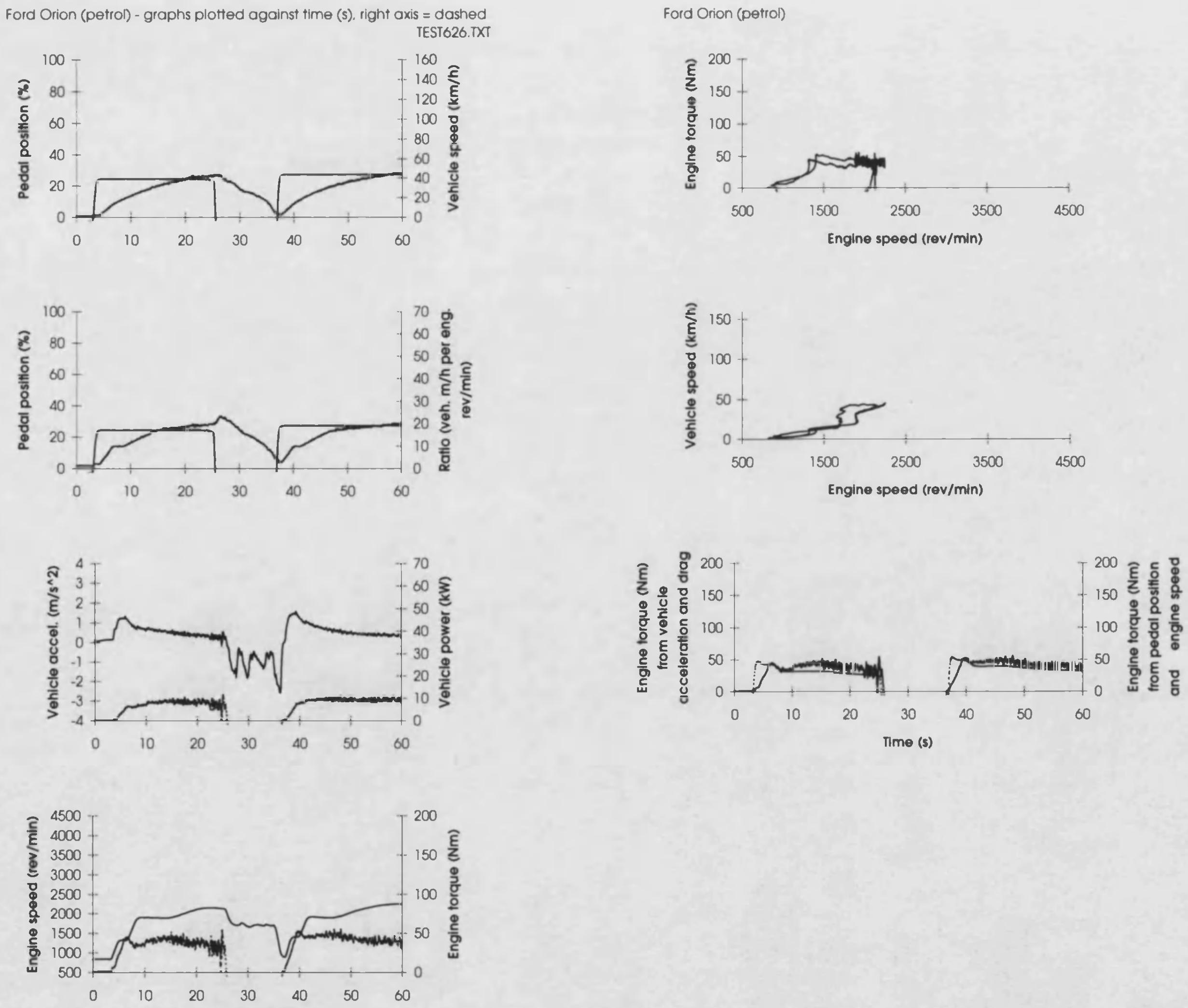

Figure 3.24 Test 9S68R1-2

Figure 3.25

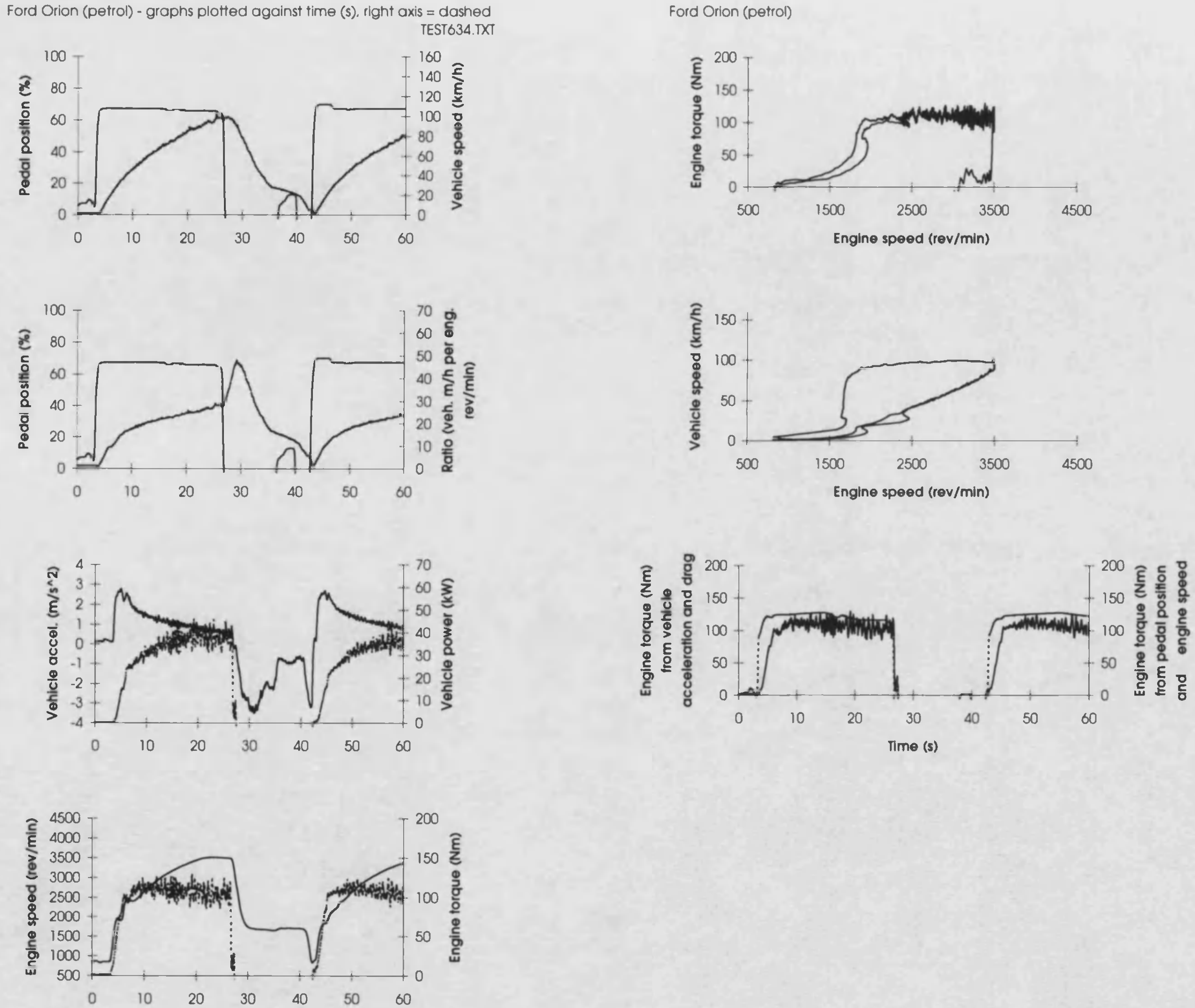

Figure 3.25 Test 9S70R1-2

Ford Orion (Diesel) - graphs plotted against time (s), right axis = dashed line

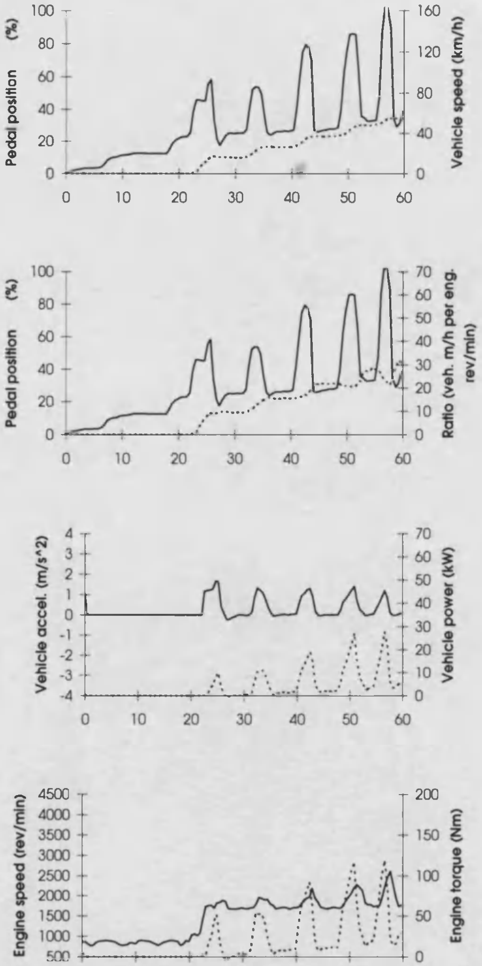

Ford Orion (Diesel)

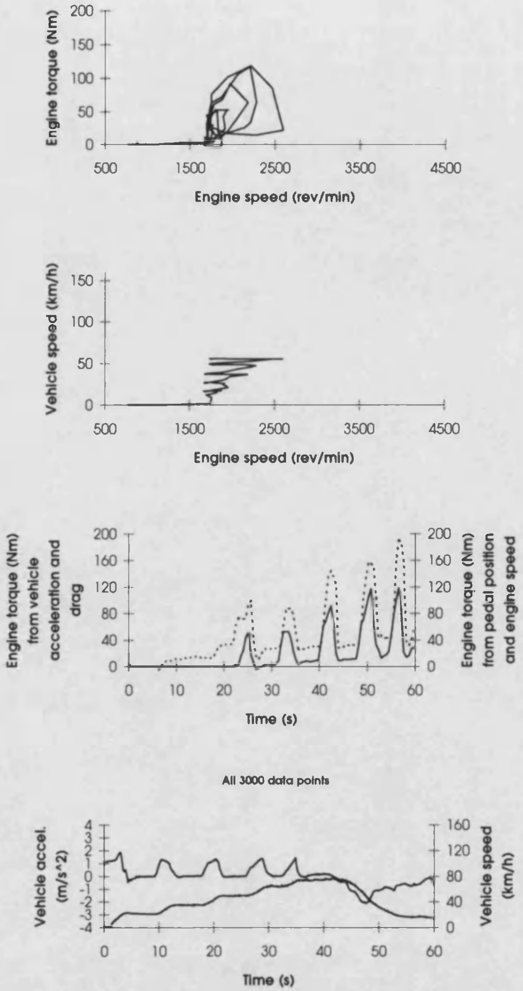

Figure 3.26 Test TOT01R1

Figure 3.26

Figure 3.27

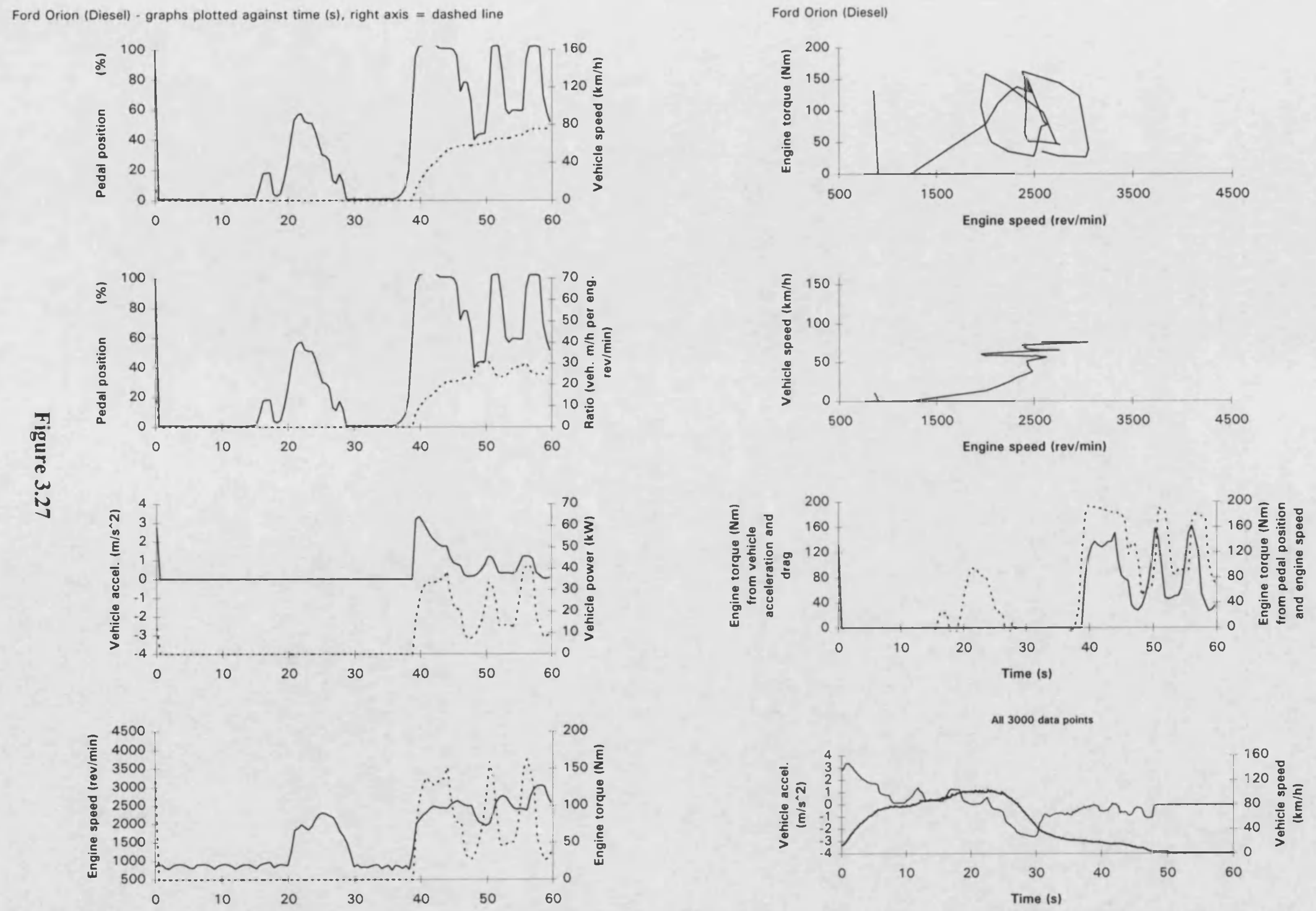

Figure 3.27 Test TOT06R2

Ford Orion (Diesel) - graphs plotted against time (s), right axis = dashed line

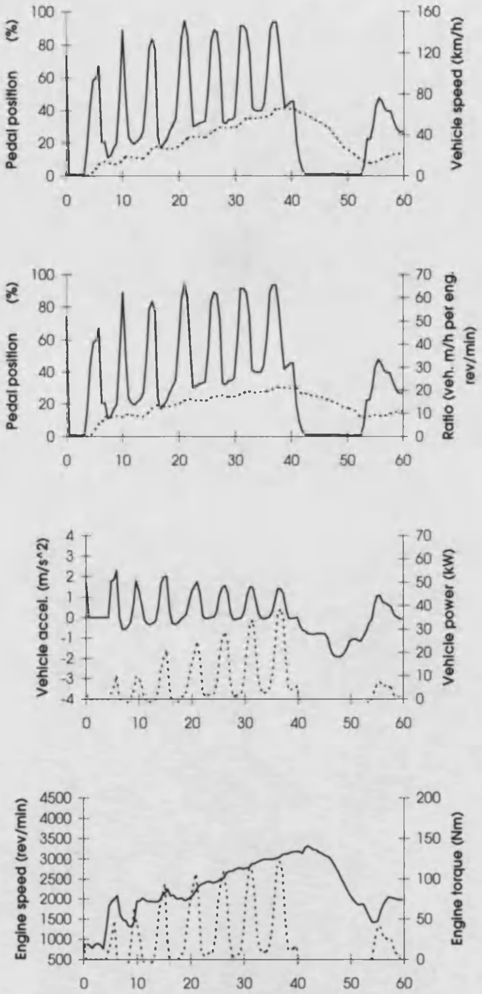

Ford Orion (Diesel)

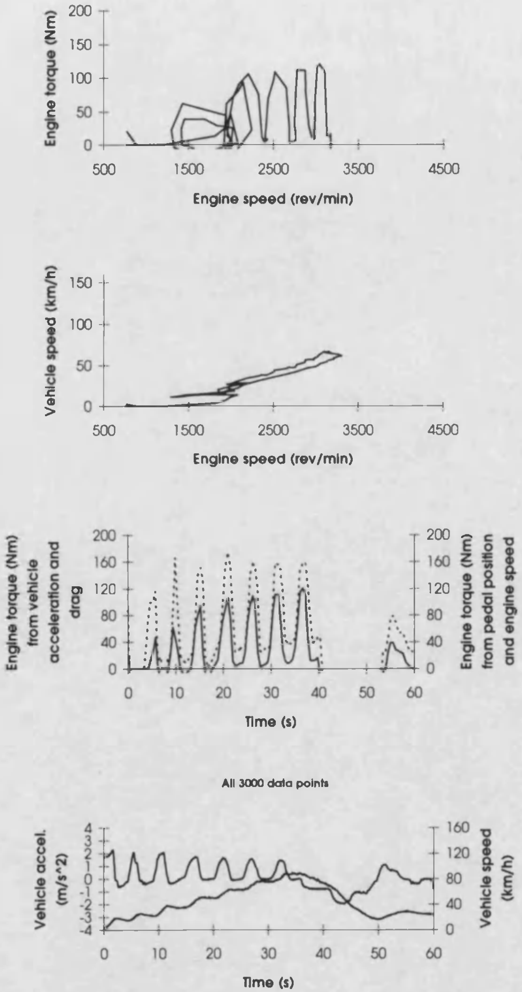

Figure 3.28 Test TOT12R1

Figure 3.28

Ford Orion (Diesel) - graphs plotted against time (s), right axis = dashed line

Ford Orion (Diesel)

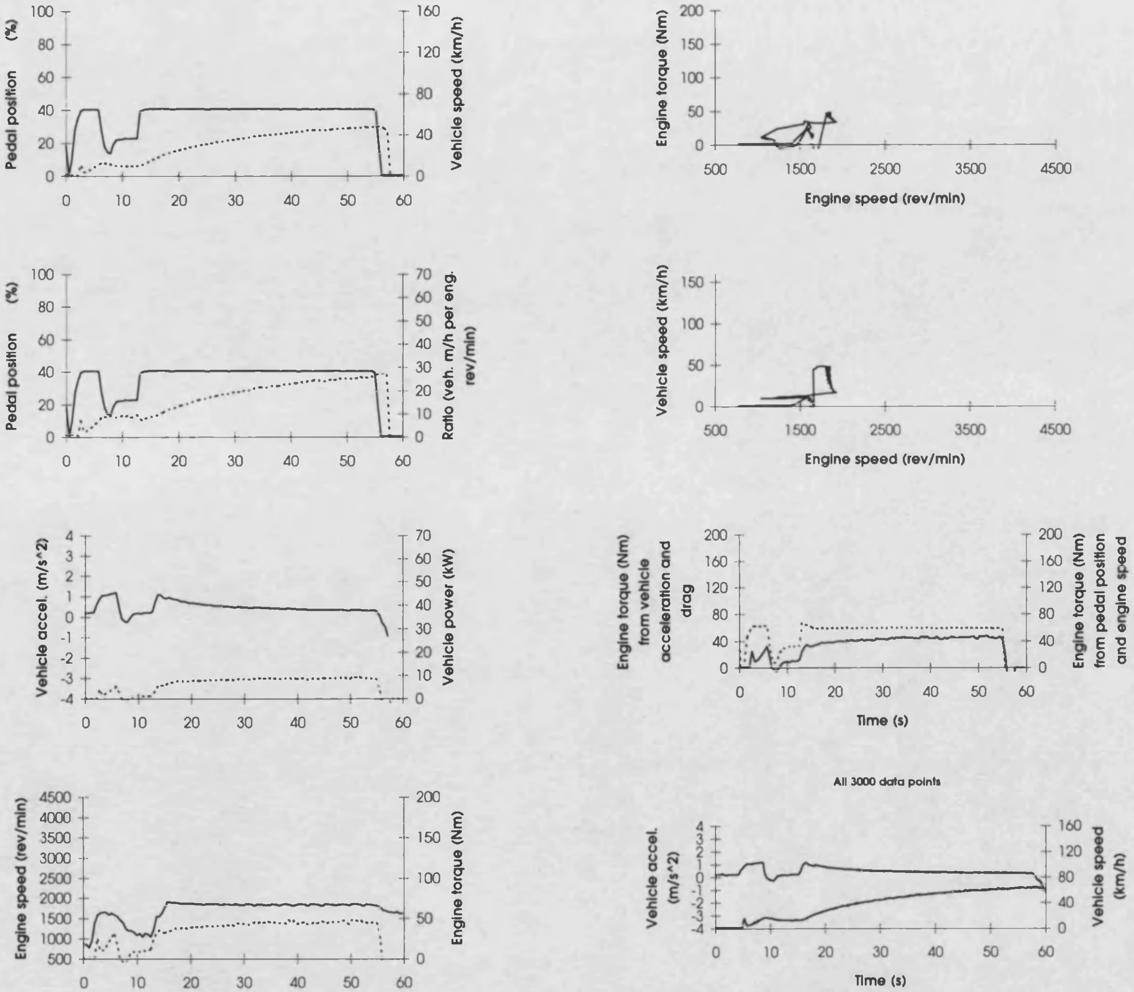

Figure 3.29 Test TOT23R2

Figure 3.29

Ford Orion (Diesel) - graphs plotted against time (s). right axis = dashed line

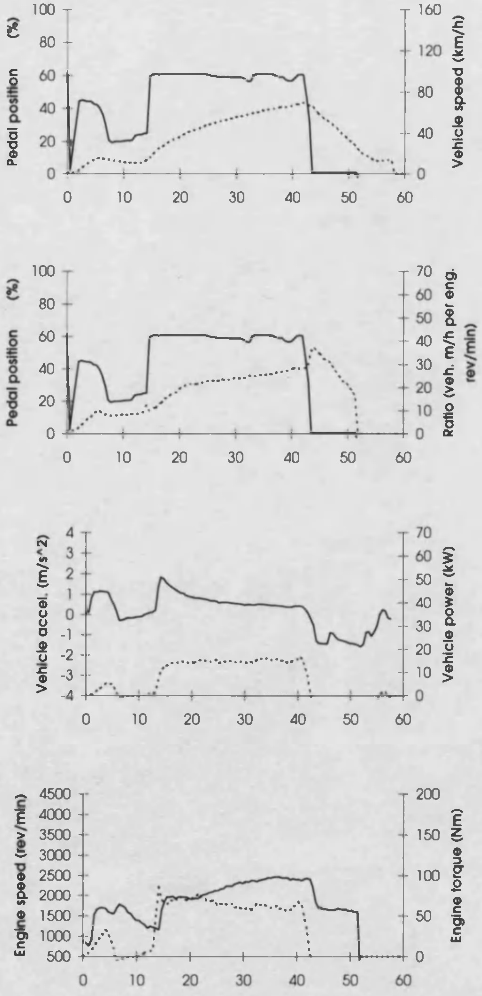

Ford Orion (Diesel)

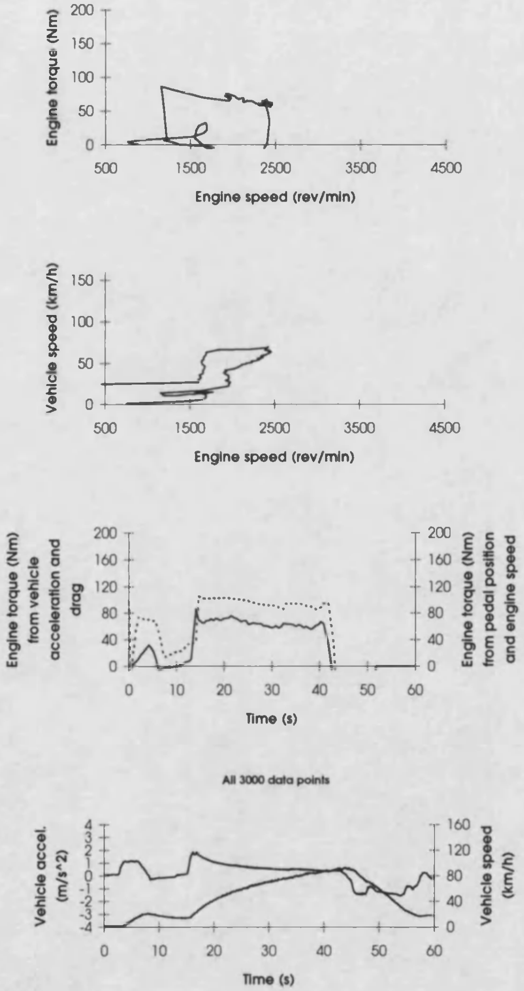

Figure 3.30 Test TOT27R1

Figure 3.30

Ford Orion (Diesel) - graphs plotted against time (s), right axis = dashed line

Ford Orion (Diesel)

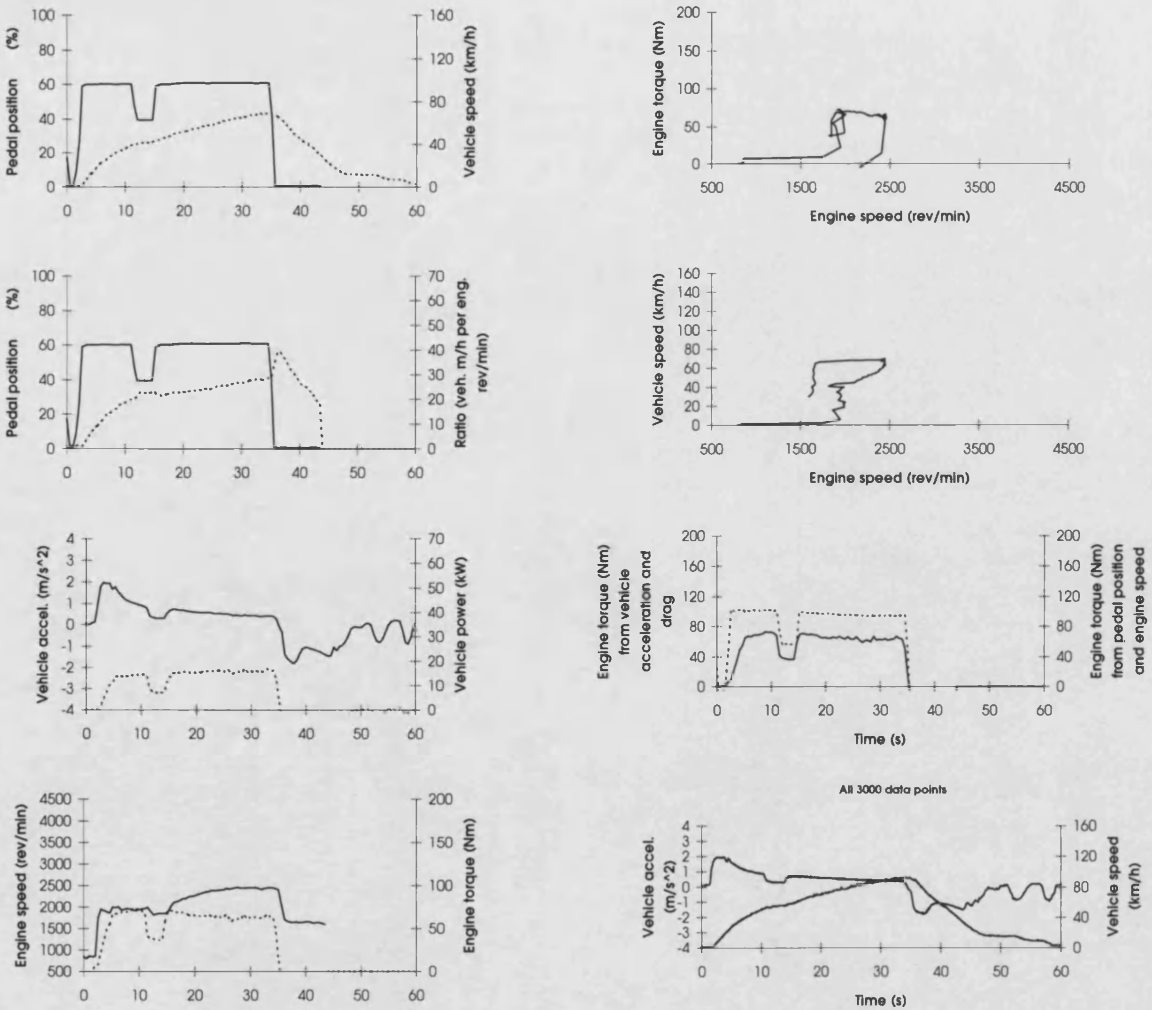

Figure 3.31 Test TOT28R1

Figure 3.31

Ford Orion (Diesel) - graphs plotted against time (s), right axis = dashed line

Ford Orion (Diesel)

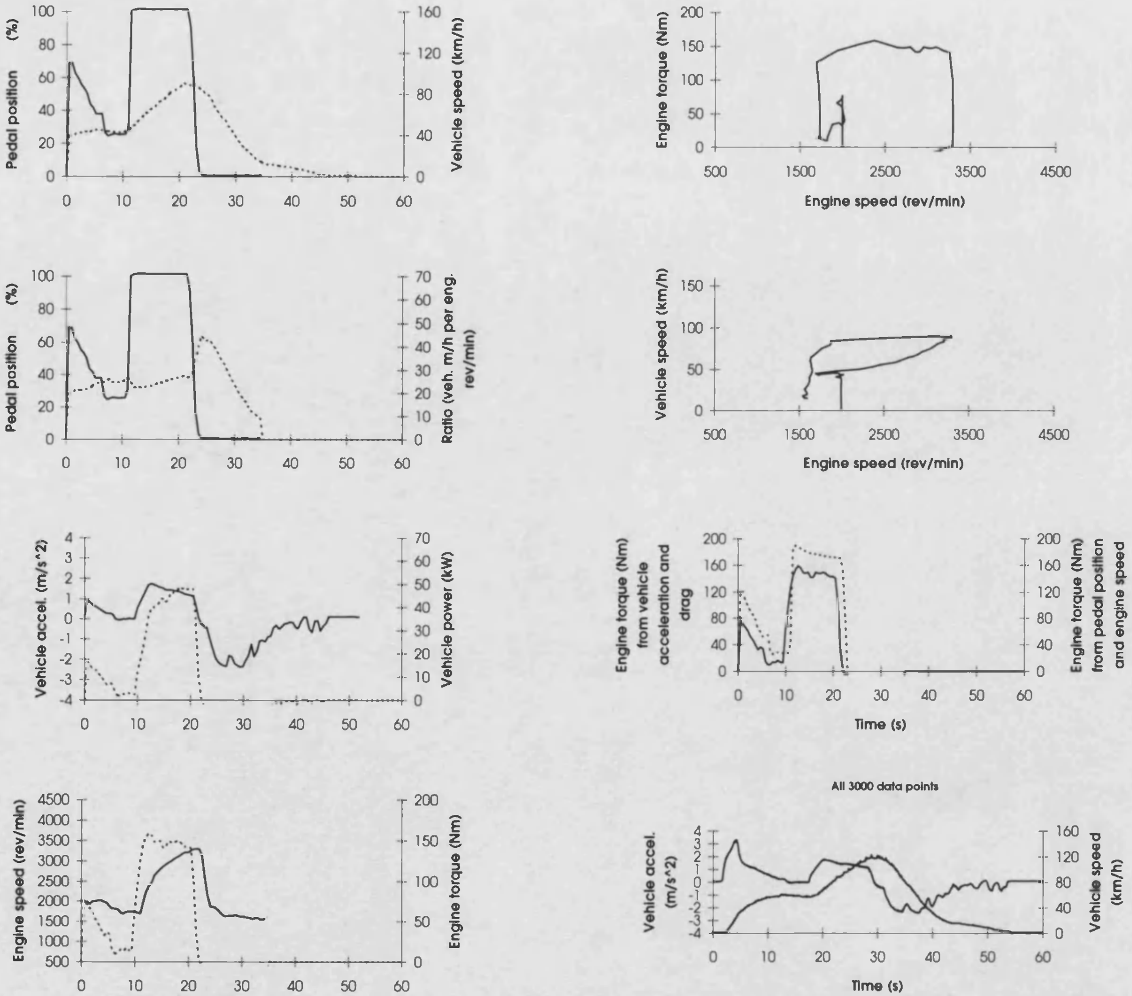

Figure 3.32 Test TOT32R1

Figure 3.32

Ford Orion (Diesel) - graphs plotted against time (s), right axis = dashed line

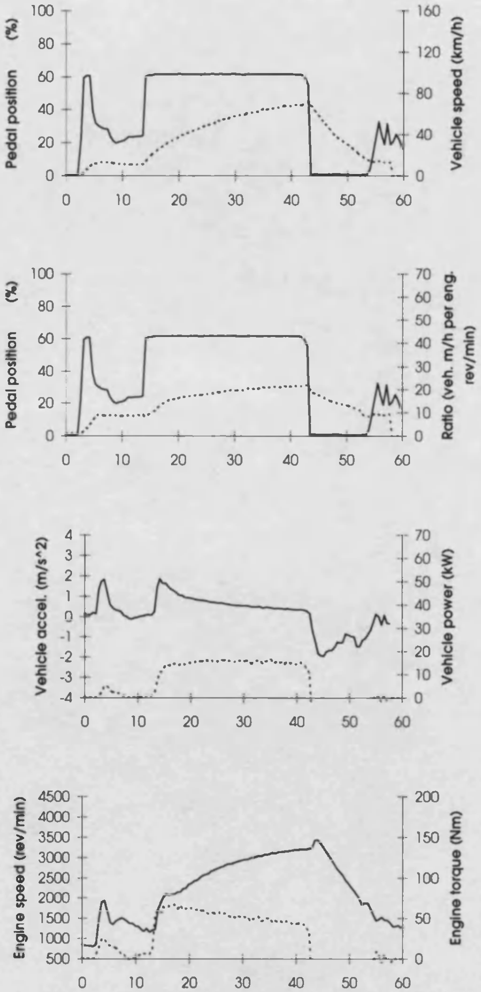

Ford Orion (Diesel)

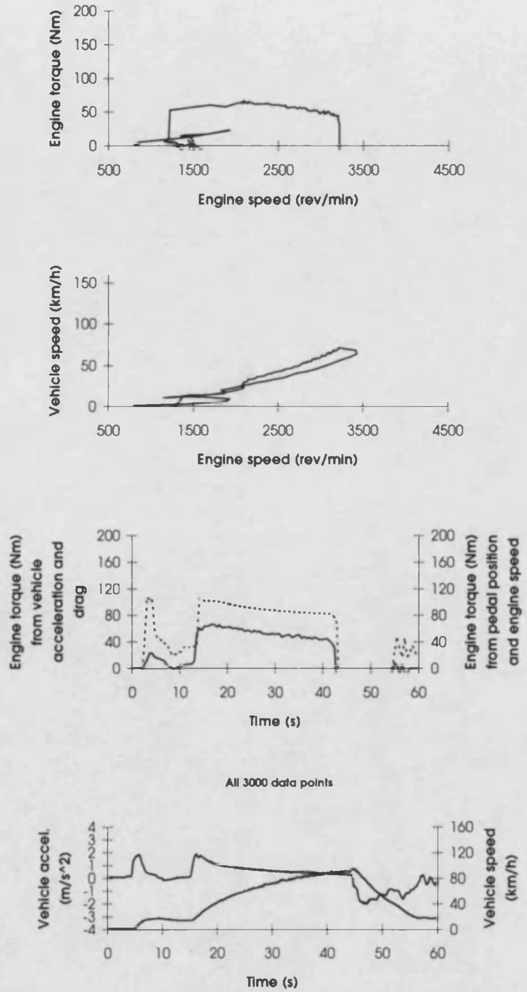

Figure 3.33 Test TOT39R1

Figure 3.33

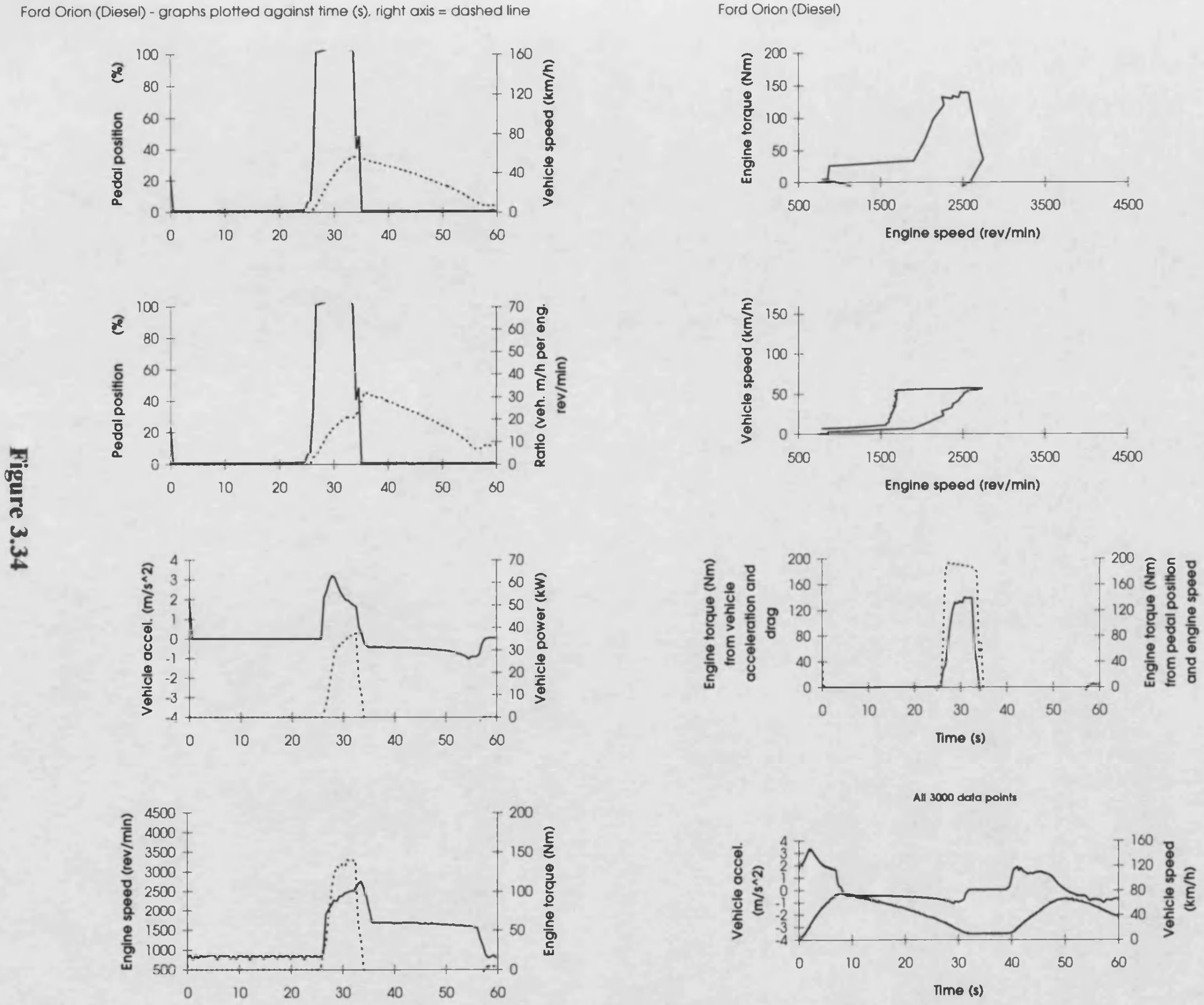

Figure 3.34 Test TOT47R1

Figure 3.34

Ford Orion (Diesel) - graphs plotted against time (s), right axis = dashed line

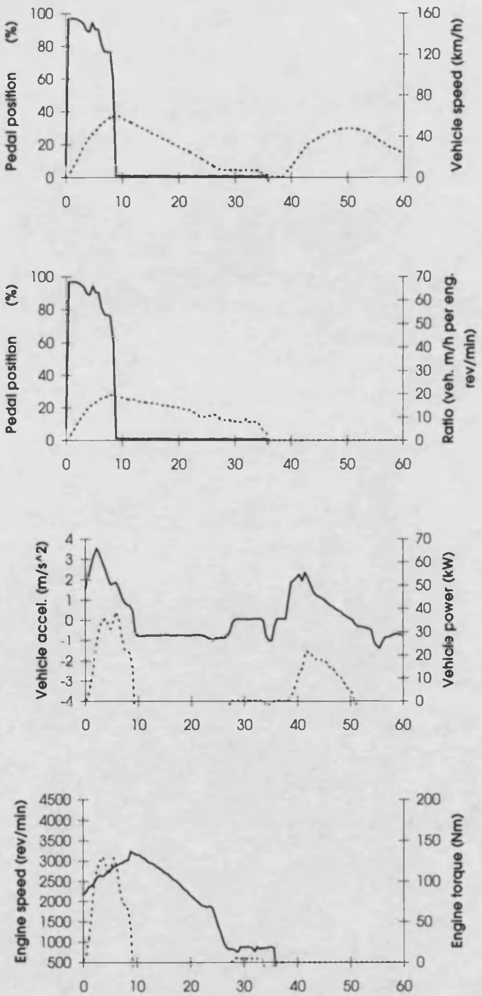

Ford Orion (Diesel)

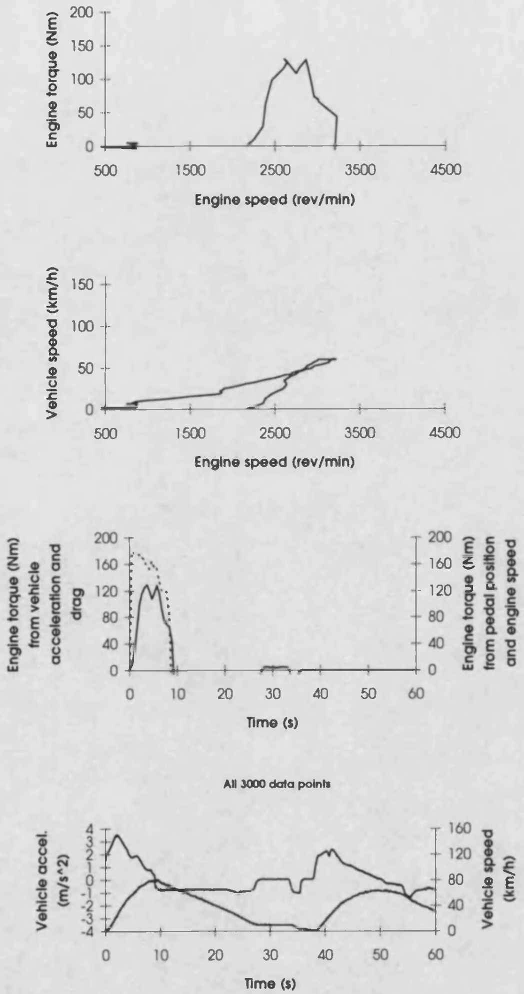

Figure 3.35 Test TOT52R1

Figure 3.35

Ford Orion (Diesel) - graphs plotted against time (s), right axis = dashed line

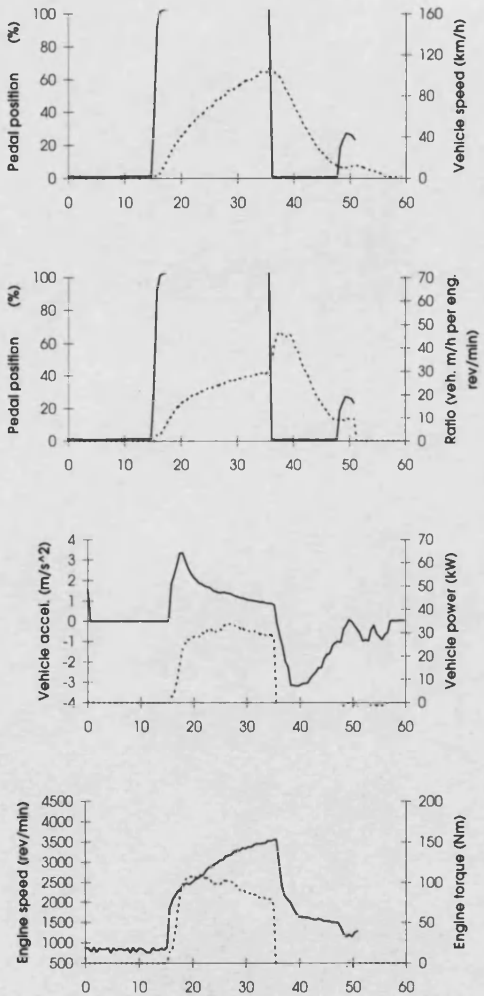

Ford Orion (Diesel)

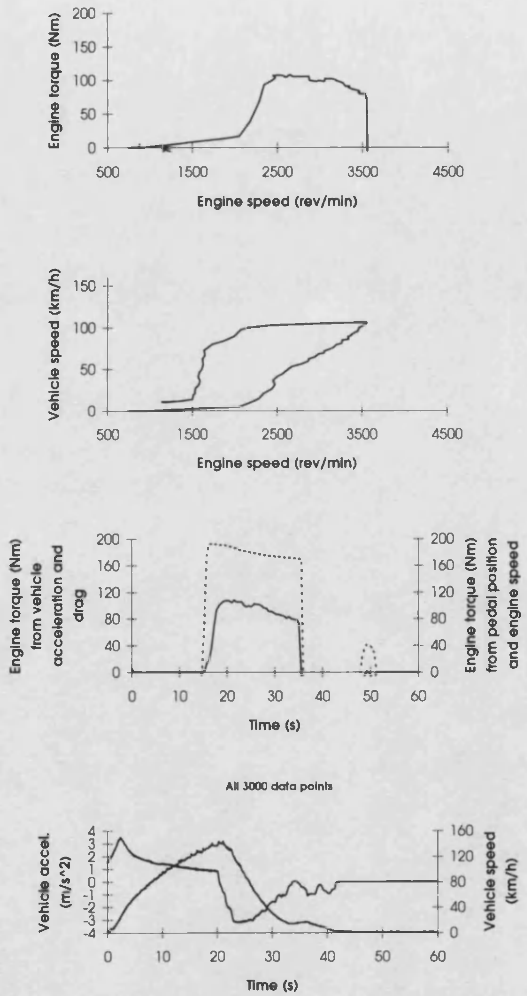

Figure 3.36 Test TOT57R1

Figure 3.36

Figure 3.37

Ford Orion (Diesel) - graphs plotted against time (s), right axis = dashed line

Ford Orion (Diesel)

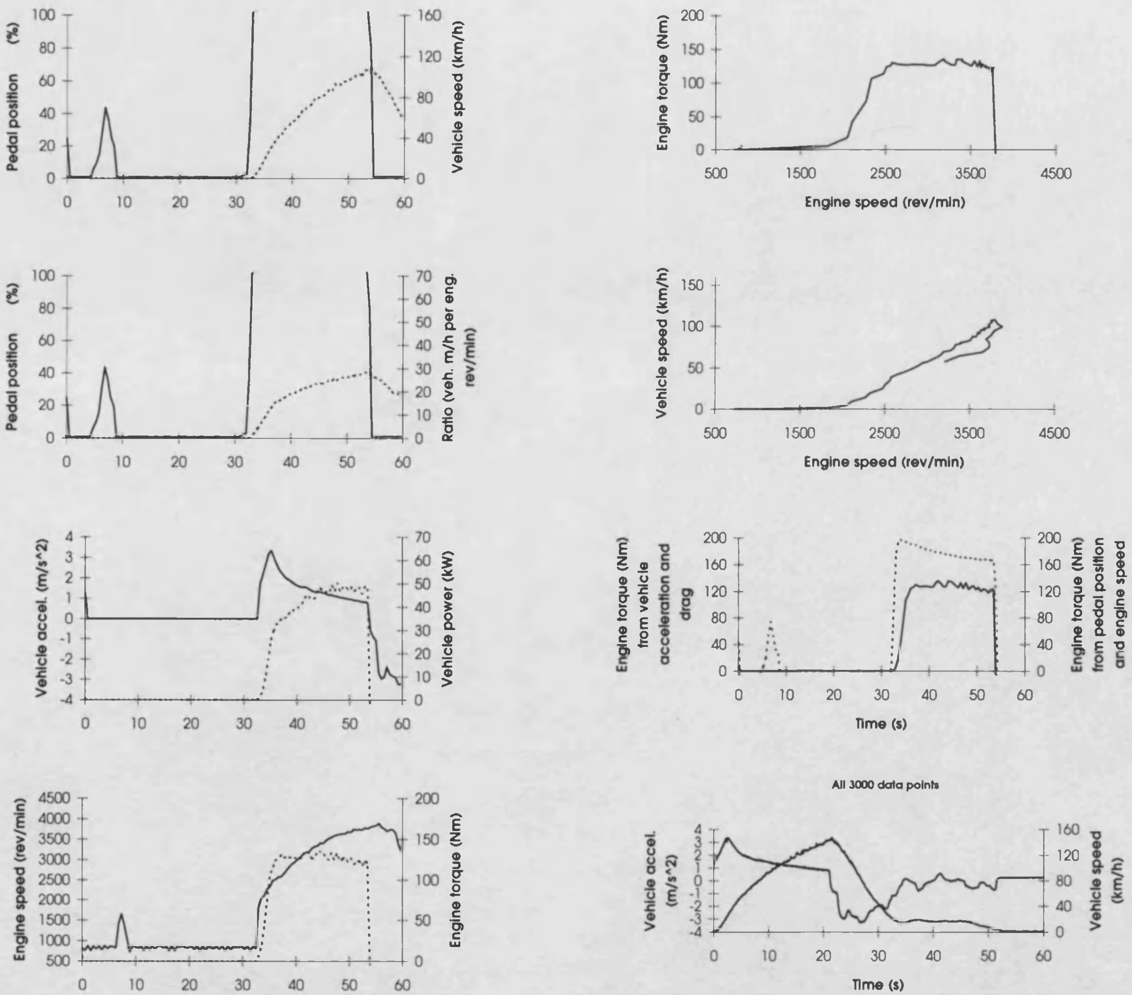

Figure 3.37 Test TOT62R1

Ford Orion (Diesel) - graphs plotted against time (s), right axis = dashed line

Ford Orion (Diesel)

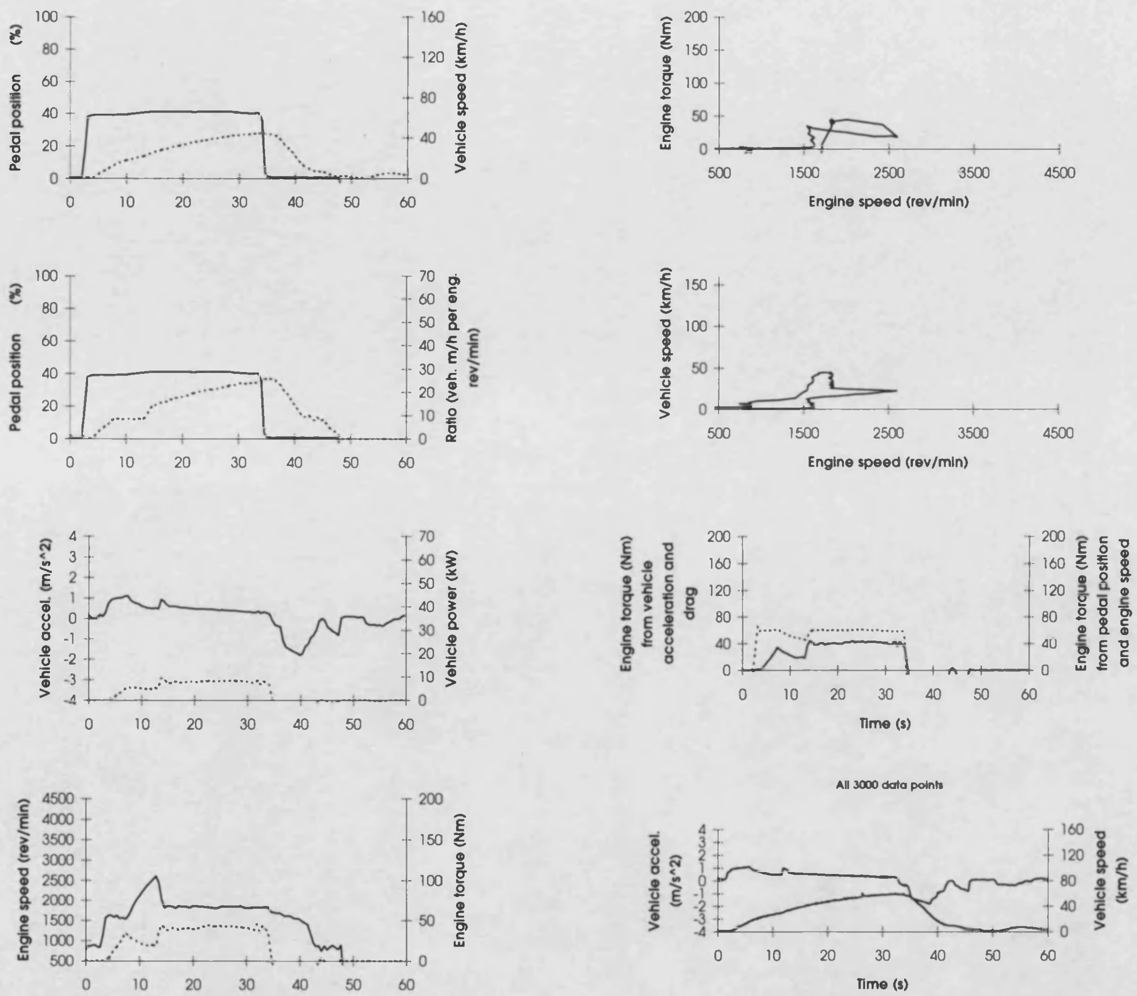

Figure 3.38 Test TOT68R1

Figure 3.38

Ford Orion (Diesel) - graphs plotted against time (s), right axis = dashed line

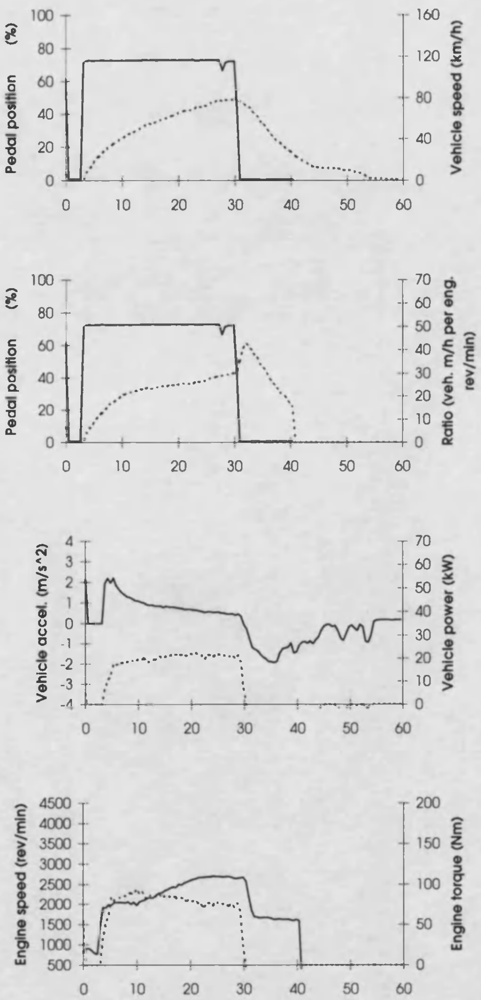

Ford Orion (Diesel)

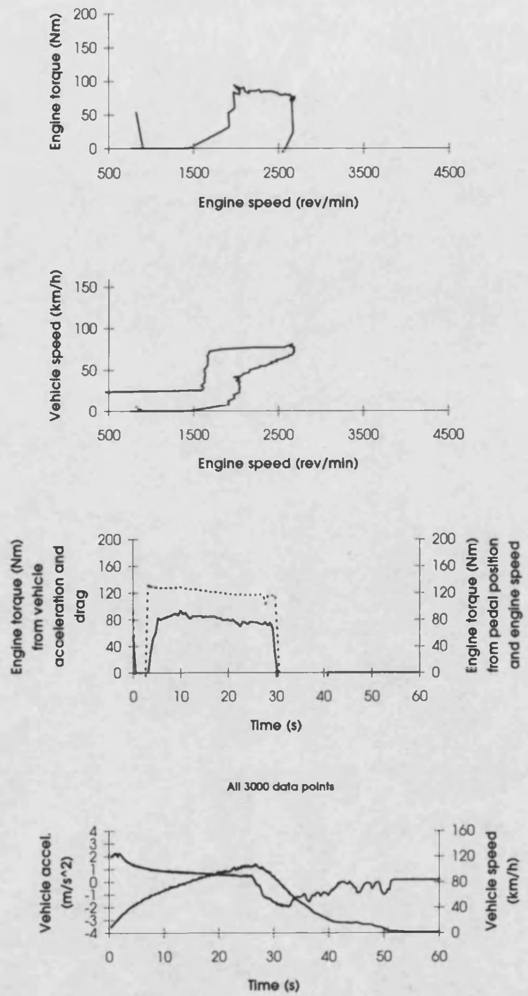

Figure 3.39 Test TOT70R1

Figure 3.39

4. COMPUTER SIMULATION OF THE POWERTRAIN

The powertrain comprising engine, transmission and vehicle was modelled using the Bath*fp* simulation software developed at the University and described in Richards et al (1990). This enabled the early development and comparison of controller strategies. The simulation work enabled investigations into both dynamic system performance and into vehicle emission formation during transient manoeuvres represented by the legislative test. It also made possible the observation of those variables not measurable on the vehicle or test rig. In contrast to experimental work, simulation tests were repeatable and could be used for the detection of small more subtle effects in the powertrain control and operation. Use of the Bath*fp* simulation software is described in more detail below.

The Bath*fp* simulation software

Figure 4.1 shows a sample screen from the Bath*fp* software. Here the powertrain circuit is displayed in the main area of the screen. Icons are used to represent component models, and these are linked together to generate the circuit. Icons can be linked directly or can be linked by line model icons representing electrical or hydraulic connections. The four buttons at the top of the window show the mode of operation of the software. The software is displayed in circuit drawing mode. In this mode the circuit checks for compatibility between icons by checking the units and types of inputs and outputs associated with the connected ports.

Once the circuit is completed the next stage is model selection. Each icon must be associated with a model coding already written in C or FORTRAN. Since one icon can represent many models, there are choices here. Many standard models are available as part of the Bath*fp* software. These include models of hydraulic and pneumatic components such as valves and pumps. Circuits can be created from existing icons and models or from new icons and models written by the user. Again before proceeding to the next stage the software checks for compatibility between models.

In the third mode parameters and initial conditions are defined after the package has automatically linked all of the individual model codes into an executable circuit simulation program. This stage is completed by clicking the mouse on each of the models and defining the values presented in the pop - up menus.

Finally in the fourth mode the simulation can be run. This is an interactive process. Component states may be observed before completion of the program and graphs may be drawn via the same type of components pop - up menus used in the third mode.

There are utilities which enable users to write and develop their own icons and models. Component models can range from simple instantaneous models to complex dynamic distributed parameter models. Empirical data may also be represented as a model. The use of the Bath*fp* simulation software requires the powertrain component models to be modular in form. Advantages of this approach are firstly that it makes writing and fault finding far easier since component models can be tested in isolation and secondly that models can be upgraded easily.

Bath*fp* makes use of the LSODA integrator. This performs the mathematical integration necessary for the dynamic models to run. LSODA uses both the Adams and the Gear algorithms described by Richards et al (1990). The advantage of this integrator over many others is that it can vary its time step according to the rate of change of the calculated variables. This means that more accuracy is available when needed but without sacrificing run times since time steps are bigger when less change is taking place in the system.

<u>The Bath*fp* powertrain models</u>

The powertrain was divided into individual or groups of components for modelling purposes. A model was created for each component group within the Diesel CVT powertrain. Clearly, there was some scope for choice in this process. However, the components were modelled in the degree of complexity necessary for adequate representation and sufficiently accurate interaction with the other models in the powertrain. Each model, supported by either a C or FORTRAN subroutine, was represented by an icon. Inputs and outputs to each model were transferred through the subroutine 'call' statement, represented by the icon ports. Figure 4.2 shows the icon for the flywheel model. Torque and speed signals are transferred into and out of the ports as shown. The models may be linked together at their ports assuming they are compatible. This feature enables many simple models to be built up into a much larger system model. In this way a system model of the complete Diesel CVT powertrain was created.

Figure 4.3 shows the complete Bath*fp* circuit of component models used to represent the powertrain, vehicle, associated hydraulics, controllers and driver. The remainder of this chapter is divided into sections, each dedicated to the description of the models representing one distinct area of the powertrain.

4.1 Engine and ancillaries

The engine model was represented by two program modules. The first was used to represent the dynamic response of the complete engine in a simplified way. It was decided to model the engine dynamics in this way for two reasons. Firstly the approach of minimising the model complexity throughout the powertrain was taken wherever possible. It was found in later model validation work that a simple model of the engine was sufficient in the overall powertrain model. Secondly, an over complex engine dynamic model, such as one including air flow and torque variations with respect to crank angle, would be inappropriate for use with simpler models in the remainder of the powertrain, and could lead to unnecessarily long computation times.

The engine torque was modelled using Equations (4.1) and (4.2). Equation (4.1) represents the limiting torque curve of the engine. Information was used, provided by Lucas Diesel Systems, which characterised the shape of torque versus speed plots of the engine for constant demands applied to the EPIC system. These data were combined with the motoring frictional loss of the engine to create Equation (4.2). This second equation includes one overall first order lag which represents the lag due to turbocharger speed changes in addition to less significant dynamic effects in, for example, the fuel injection pump hydraulics and the EPIC control software. The program module resulting from these equations required inputs of the demand to the fuel injection system and the engine speed and produced an output of the engine torque.

$$T_{max} = -33.879701 + 0.20533745\omega - 9.2749518e^{-5}\omega^2 + 1.7990256e^{-8}\omega^3 - 1.3226246e^{-12}\omega^4 \tag{4.1}$$

$$\frac{dT}{dt} = \frac{((-9.75 - 0.00395\omega) + ((T_{max} + (9.75 + 0.00395\omega))(d/10))) - T}{\tau_1} \tag{4.2}$$

The purpose of the second module in the engine model was to represent fuel consumption and emission formation. This part of the model was based upon the work described by Brace et al (1994). A neural network representation of the engine was used to predict emissions. The inputs to the model were coolant temperature, engine speed and engine torque. Outputs from the model were the instantaneous emission and fuel consumption levels which could be summed cumulatively over the length of a drivecycle or other vehicle simulation.

For the purpose of modelling the engine fuel consumption at idle, an engine speed controller was included in the model. This became operational only as the engine speed fell towards the chosen idle speed. The fuel injection system demand was then modulated and its level controlled depending upon the error between the engine speed and the chosen idle speed.

Flywheel

The flywheel model was used to form an essential link between the engine and spring damper plate models. It was modelled using Equation (4.3). This equation represented a torque difference calculation applied to an inertia resulting in a change in inertia speed. The value of the inertia was used to represent the total of the engine and flywheel inertia. The model inputs were the shaft torques on each side of the flywheel and the model output was the flywheel speed.

$$\frac{d\omega}{dt} = \frac{(T - T_L)}{J} \tag{4.3}$$

Spring Damper Plate

A spring damper plate model was produced using data provided by Ford. The model inputs were the shaft speeds either side of the spring damper plate. The resultant torques in each direction were calculated by the model, Equation (4.4). The damping produced by this model was found to be necessary in the overall powertrain model. Initial omission of the model resulted in oscillatory behaviour of the complete powertrain model.

$$T_{res} = k_1(\omega_2 - \omega_1) + k_2 r \tag{4.4}$$

Clutch

A model of the clutch was necessary to enable investigation of the powertrain behaviour during the starting and stopping of the vehicle. Additionally, it would not have been possible to simulate the vehicle being driven through the legislative drivecycle emissions test without the ability to simulate the vehicle at rest with the engine at idle.

The clutch, Section 2.1.2, which was of the wet multiplate type, was modelled as two separate inertias, one associated with the driving plates and the other with the driven plates. The model was designed to operate in one of several modes depending upon the relative speeds of the driving and driven plates and the axial forces between them due to the hydraulic clutch pressure. Modelling of the discontinuities between the different operating modes enabled the model to switch between them. The different modes are defined as follows:

Mode	Clutch Engagement	Input / Output Speeds
1	Engaged, not slipping	Speeds identical
2	Engaged, slipping	Input faster, speeds converging
3	Engaged, slipping	Input faster, speeds diverging
4	Engaged, slipping	Output faster, speeds converging
5	Engaged, slipping	Output faster, speeds diverging
6	Disengaged	Not relevant

The clutch may be engaged and the speeds of the two inertias are identical. If the speeds are not identical then either the driving or driven plates are rotating faster. In each of these two cases, the clutch pressure may or may not be sufficient to cause the speeds to converge. Finally the clutch may be disengaged completely. Equation (4.5), (Gemeinholzer, 1990), is the key equation used in the model and defines the maximum amount of torque which may be transmitted by the clutch before the conditions for slip are reached.

$$T_e = \frac{2C_f N_p A_c P_c (R_e^3 - R_i^3)}{3(R_e^2 - R_i^2)} \tag{4.5}$$

4.2 Transmission

Some aspects of the operation of the CTX and the electrohydraulically controlled CTXE transmissions are still to be fully explained. As yet, no model can be considered to describe completely the interaction between the belt and pulleys. The aim of modelling the transmission was to produce a model which could be used with the engine and vehicle models to give an accurate representation of the operation of the powertrain. It was also hoped that the model would be sufficiently developed to enable analysis of the behaviour of the powertrain, and for investigative work into areas such as efficiency.

The model of the transmission was based upon submodels originally developed by Guebeli (1993) and Micklem (1994). It can be divided into two areas. Firstly, there is the variable speed unit, which comprises the belt and pulleys. Secondly, there are the other submodels which make up the remainder of the transmission.

The modelling of the variable speed unit is based upon Micklem's (1990, 1991, 1993) work. Micklem developed a viscous shear stress model which defined the load-slip relationship between the belt and pulleys. Previous models based on a Coulomb friction approach had been shown to be less accurate in predicting belt slip. Micklem also developed a torque loss model which accounted for the necessary energy required to force the belt into and out of the pulleys.

The remaining models were the final drive and the models associated with the hydraulic circuit components. The hydraulic clutch, although being part of the transmission, was modelled separately, above. The final drive comprised two gear sets and the differential. The differential was not modelled since the work here was only concerned with straight line driving. The speed relationship and the efficiency of the final drive were modelled. The model for the efficiency was based upon an approximation developed by Van Dongen (1982).

Submodels were used to build the hydraulic circuit. Standard hydraulic models developed as part of the Bath*fp* package were used for this purpose. The hydraulic circuit of the prototype CTXE transmission differed from that of the CTX transmission. Some modifications and additions to the submodels developed by Guebeli (1993) and Micklem (1994) were therefore necessary. The final hydraulic circuit model represented all of the components shown in the hydraulic circuit diagram, Figure 4.4. The model parameters where chosen with reference to the transmission components manufacturers' information, or where this was not available, experimental data obtained from the test rig was used.

Table 4.1 gives details of the transmission components and computer models used to represent them. The important parameters associated with each of the models are listed together with their numerical values in Table 4.2.

4.3 Hydraulic controller strategy

The initial installation of the IDI Diesel engine and powertrain into the vehicle (Chapter 3) allowed data to be collected using the standard hydromechanically controlled CTX transmission. Since it was valuable to be able to collect data in this way and to use it to validate the computer models of the powertrain, it became necessary to develop a model of the VDT hydromechanical control strategy. Information supplied by VDT together with data collected from the vehicle enabled a model to be created. Rather than pursuing the detailed modelling of the full valve bank controlling the hydraulic circuit, the task of modelling the strategy was approached in an empirical way. Experimental values of engine speed, vehicle speed and pedal position were used to create the envelope shown in Figure 1.1. The two lines at high and low engine speed were then represented by the polynomial curves of Equations (4.6) and (4.7) respectively. The model was then completed by using the vehicle speed and pedal position (linearly between the two lines) to create an engine speed demand. This model of the hydraulic controller strategy required the use of a description of the lower level part of the VDT control strategy in order to achieve the demanded engine speed via transmission ratio control and to set the secondary pressure. Equation (4.8) was used to model the secondary pressure demand. The engine torque demand signal was taken from the driver pedal demand into the VDT controller for the purpose of substitution in Equation (4.8).

$$\omega = 793.409 + 7.8252v - 0.06598v^2 + 0.00048v^3 \tag{4.6}$$

$$\omega = 793.409 + 11.225107v + 0.4783328v^2 - 0.0054733097v^3 + 0.0000160835v^4 \tag{4.7}$$

$$Ps_{dem} = ((T/25) + 2)(\omega_p / \omega_s) + (T/11.4) - 2 \tag{4.8}$$

4.4 Driveline, vehicle and road

The output of the transmission model which was a speed signal was applied to a driveshaft model. This was similar to the spring damper plate model described in Section 4.1. The model was based upon Equation (4.4) and accepted inputs of speed at each end and produced torques at each end as outputs.

The vehicle model, which was connected to the driveshaft model, needed to take torque as an input and produce speed as an output to complete the line of powertrain submodels. This was done by use, in the model, of Equation (4.9). This equation relates the forces on the vehicle due to driving torque, rolling resistance and gradient and produces a value for vehicle acceleration. This is used together with the integration time interval to update the vehicle speed which is the model output required at the driveshaft model. The vehicle rolling resistance and drag terms used in Equation (4.9) were obtained experimentally by Ford from a vehicle towing test and so include all losses due to vehicle road interaction. It was, therefore, considered not necessary to model the complexities of the interaction of the tyres with the road surface.

$$a = [F_d - F_b - ((4.2 + 0.0756v + 0.2801v^2) / R_w) - W_v * \sin(Gr)] / M_v \qquad (4.9)$$

4.5 Validation

4.5.1 Vehicle work

Early validation work (Deacon et al, 1994) involved comparison of simulated basic powertrain variables with those measured from the test vehicle. It was important to establish the validity of the approaches to the modelling of the engine, transmission and vehicle before going on to develop powertrain control strategies using these models. The initial validation work included comparison of the variables listed in Table 4.3. Figures 4.5 to 4.7 show direct comparison of simulated and experimental powertrain responses to three different inputs. The model of the VDT hydraulic controller strategy was used for this work. In addition the clutch and spring damper plate were not included in the model, so this validation work was limited to the operation of the vehicle with a locked up clutch. Analysis of the figures shows good correlation in terms of the engine responses (speed and torque) and a fair comparison for the transmission in terms of ratio. At this point in the powertrain project, although there was still scope for further improvement, it was considered that the powertrain models were of sufficient quality to allow the development and assessment of alternative control strategies.

4.5.2 Steady state rig work

The steady state rig which comprised an engine and dynamometer (Charlton et al, 1992) made possible the production of detailed engine emission and fuel consumption maps for the 1.8 DI Diesel engine. These were used by Brace et al (1994) to create the neural network engine emissions model described in Section 4.1. Some of the data collected on the rig was not used to train the emissions model. Later use of this data enabled the validity of the model to be tested. The paper contains direct comparisons of this emissions data with the predicted emissions levels from the neural network. Figure 4.8, taken from the paper, shows the experimental and predicted levels of NOx emissions. The predicted levels compare well with the experimental values. Since the paper was written, further data has been collected and used to enhance the accuracy of the model.

4.5.3 Transient test rig work

Correct prediction of trends in powertrain behaviour was considered more important than the accuracy of the predicted variables in absolute terms. The reasoning behind this was that good comparative assessment of controller performance depends very much more on the accurate prediction of powertrain behaviour in response to controller inputs than on the numerical accuracy of results. The type of validation work undertaken was based upon this philosophy. Comparisons of simulated and experimental powertrain behaviour were examined, the path taken by the engine on the torque speed map being a primary focus of attention, whilst numerical differences in predicted and experimental results were of secondary importance. Confirmation of the predicted path of the engine on the torque speed map was produced by the test rig results presented in Chapter 8. These are compared with similar predicted results in Chapter 7 which used the powertrain models described in this chapter and the newly designed controller strategies, described in Chapters 5 and 6. The predicted and experimental results are presented in this order so that the control strategies may be explained first, and so that the overall structure of the thesis is coherent. The comparison of the predicted and experimental results is revisited briefly in Section 8.1.2.

The transient rig enabled validation work not possible using the vehicle. Firstly, actual measurement of torque was possible rather than inference from other variables as in the vehicle work. Secondly, it was possible to measure emissions produced by the powertrain with more flexibility than when using the vehicle on the chassis dynamometer. The second area of comparison, then, was that of the emissions produced during emulated and simulated drivecycle tests. In comparing the results presented in Chapters 7 and 8, it is important to note the rig results were produced with the catalyst installed whereas the effects of the catalyst were not accounted for in the predicted results. However, the trends in the predicted results produced by changes in the control strategy are verified by the experimental work.

Transmission component	Model details
Spring damper plate	Theoretical model originating from Bath*fp*
Hydraulic clutch	Theoretical model developed as part of this work
Variable speed unit (push belt and V-pulleys)	Model developed by Micklem (1994) and Guebeli (1993)
Reduction gearing	Model developed by Guebeli (1993) and based upon work by Van Dongen (1982)
Differential	Not modelled
Hydraulic circuit	Theoretical and empirical models used originating from Bath*fp*

Table 4.1 Transmission components modelled

Transmission submodel	Submodel parameters	Parameter value
Spring damper plate	Rotational Spring Constant	2.000000e+02 N/rad
	Rotational Damping Constant	1.000000e+02 N/(rad/s)
Hydraulic clutch	shaft/clutch output inertia	1.000000e-02 kgm2
	coefficient of friction during engagement	1.200000e-01
	internal radius of clutch plates	6.300000e-02 m
	external radius of clutch plates	8.400000e-02 m
	area of clutch actuator	3.010000e-03 m^2
	number of clutch surfaces	8
Variable speed unit (push belt and V-pulleys)	Primary actuator area	1.9792e-02 m2
	Secondary actuator area	9.7193e-03 m2
	Maximum Power Transmission Efficiency	9.700000e-01
	90% Efficiency Torque Point	1.000000e+01 Nm
	Final Drive Inertia (Reduced to Output)	5.000000e-01 kgm2
	Minimum Oil Volume of Prim. Actuator	5.000000e-01 L
	Minimum Oil Volume of Sec. Actuator	5.000000e-01 L
	Primary Orifice Diameter	9.079000e+00 mm
	Secondary Orifice Diameter	1.009000e+01 mm
Driveshafts	Driveline Spring Constant	1.000000e+03 Nm/rad
	Driveline Damping Constant	4.000000e+02 Nms/rad
Vehicle	Car Mass	1.360000e+03 kg
	Aerodynamic Drag Coefficient	3.500000e-01
	Cross Section	1.951600e+00 m2
	Air Density	1.202000e+00 kg/m3
	Dynamic Wheel Radius	2.809000e-01 m
Reduction gearing	Final drive reduction ratio	5.047000e+00
Hydraulic circuit	pump displacement	9.720000e+00 cc/rev
	relief valve flow/pressure gradient	6.000000e+02 (L/min)/bar

Table 4.2 Transmission submodel parameters

Vehicle pedal
Engine speed
Engine torque by inference
Transmission ratio
Vehicle speed
Vehicle acceleration

Table 4.3 Measured powertrain variables included in the initial model validation work

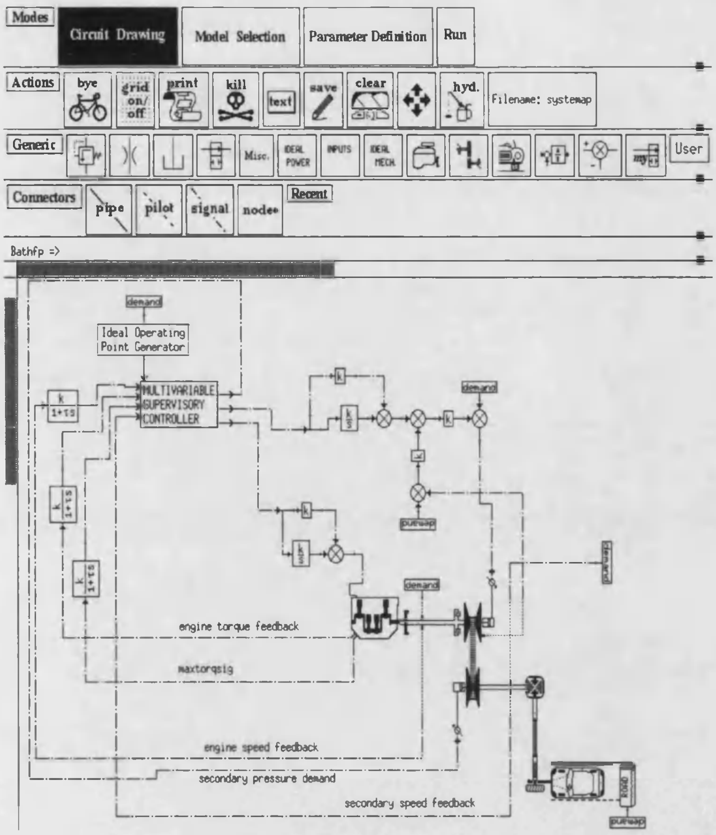

Figure 4.1 A sample screen from the Bath***fp*** simulation package

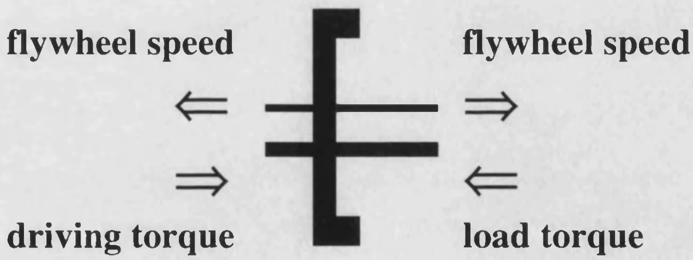

Figure 4.2 The icon used to represent the flywheel model in the Bath***fp*** simulation environment

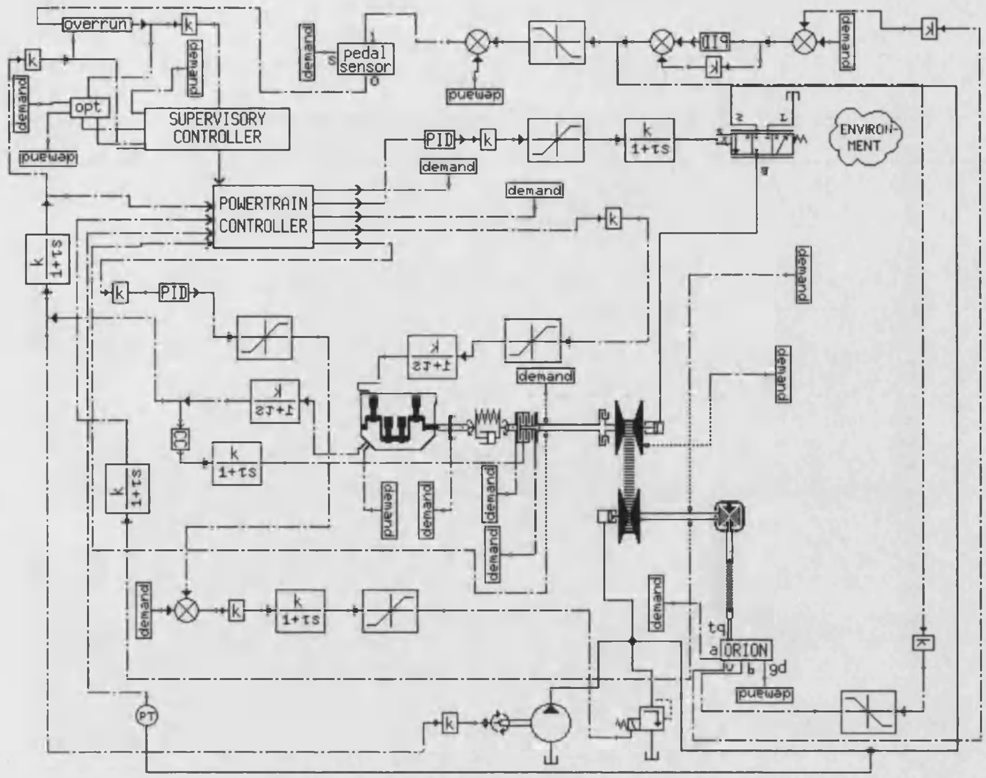

Figure 4.3 The Bath*fp* circuit used for the predictive work

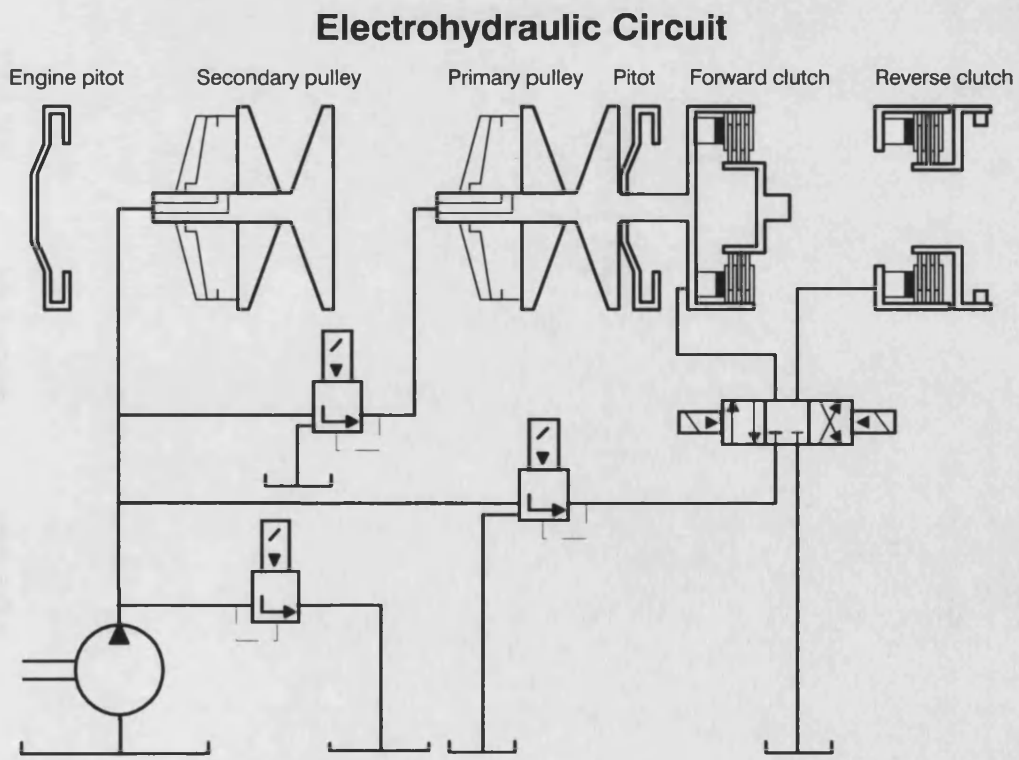

Figure 4.4 The hydraulic circuit included in the transmission model

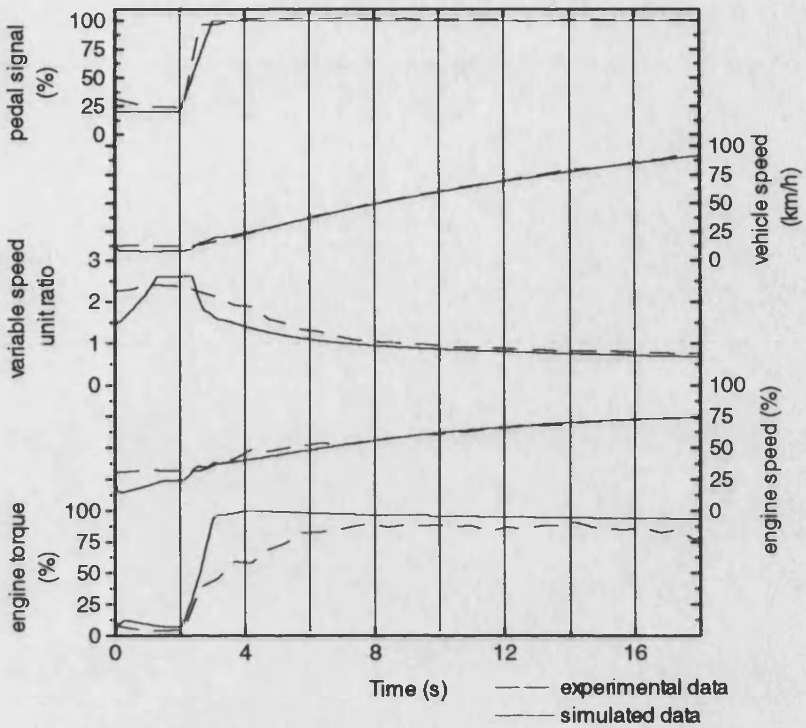

Figure 4.5 Comparison of simulated and vehicle experimental data using the hydromechanically controlled CTX transmission

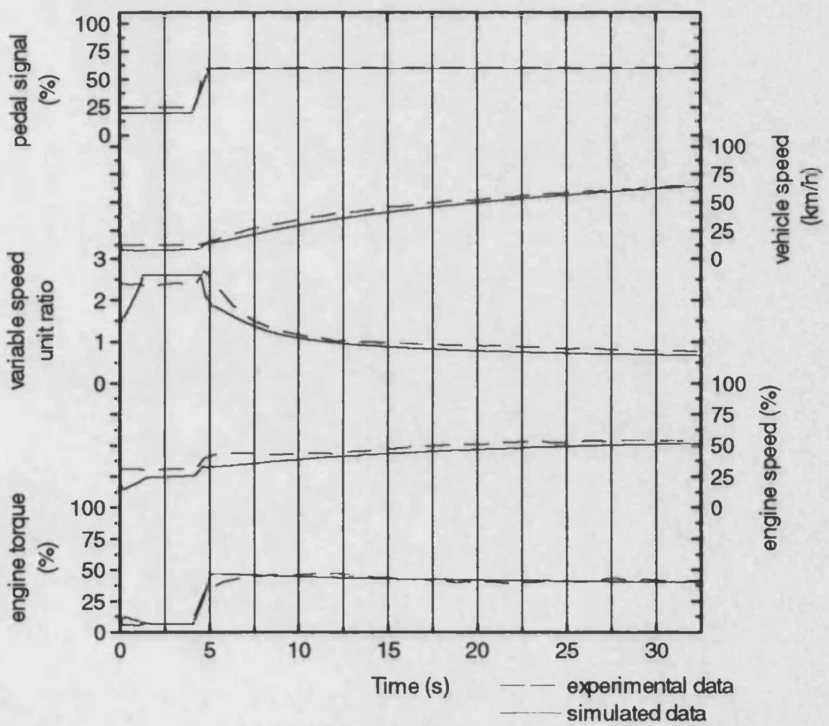

Figure 4.6 Comparison of simulated and vehicle experimental data using the hydromechanically controlled CTX transmission

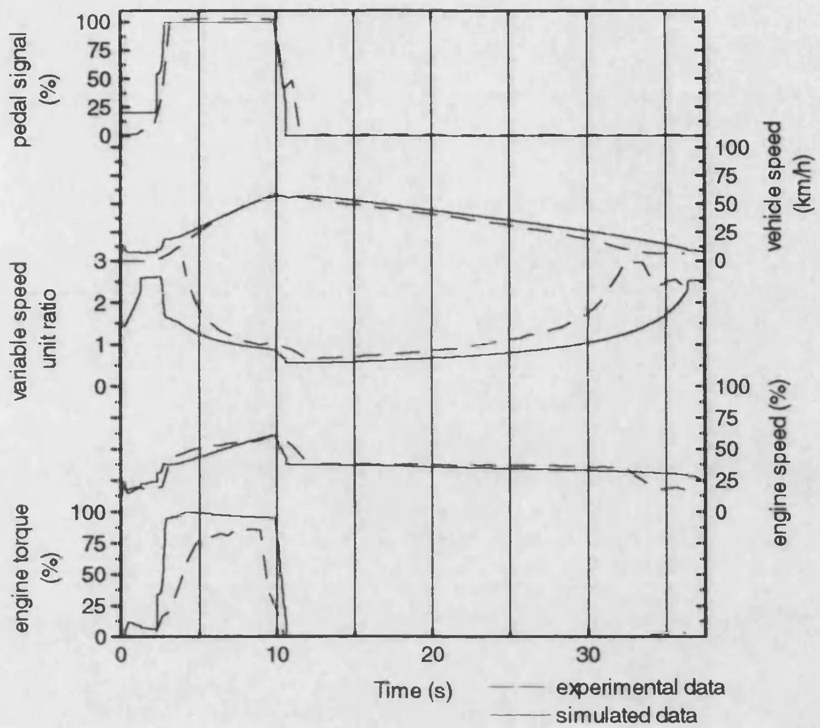

Figure 4.7 Comparison of simulated and vehicle experimental data using the hydromechanically controlled CTX transmission

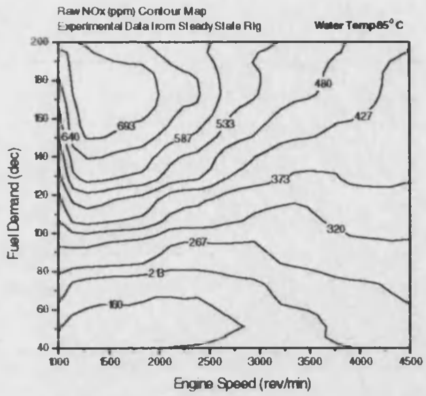

Experimental data

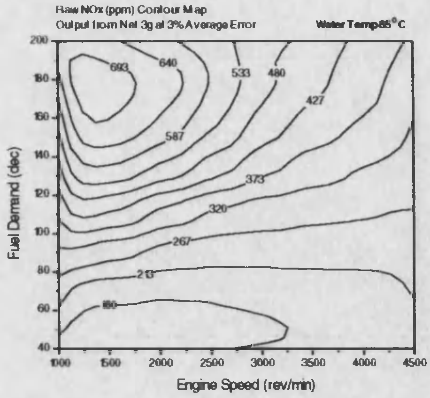

Neural network predicted data

Figure 4.8 Comparison of measured and Neural Network predicted levels of NOx emissions (courtesy of Brace et al, 1994)

5. TRANSIENT POWERTRAIN CONTROL - DESIGN CONSIDERATIONS

In this chapter, the approach to transient powertrain control is considered. Firstly, the discussion concentrates on the requirements of a powertrain controller both in terms of vehicle drivability and in terms of economy and emissions. Secondly, the architecture and design of various controller strategies are considered. For the controller objectives in terms of vehicle drivability, account of both the drivability study findings, and the dynamic characteristics of the powertrain are taken. Economy and emissions considerations are influenced by the characteristics of the engine and transmission.

5.1 Requirements of good vehicle drivability

Good vehicle drivability is characterised by the driver having ease of control of the vehicle and confidence in both predictable and desirable system responses to his or her demands. It is very much dominated by the performance of the powertrain and vehicle in transient conditions. In steady state powertrain operation, drivability performance is not particularly discernible, and powertrain operation can be optimised more for emissions and economy. The categories of drivability and performance feel attributes listed in Table 3.1, and discussed in Chapter 3, comprehensively cover the breadth of the issue.

5.1.1 Implementation of drivability study findings

From the initial drivability study described in Chapter 3 observations and recommendations were made (Section 3.5) regarding the design of a controller for a powertrain incorporating a CVT.

These considerations have been taken into account in the design of the alternative controller strategies which follow. In the case of the rule based controllers, specific rules were written for use during transient operation on the basis of the recommendations made. Maps or look up tables used within controller strategies were also considered with respect to these recommendations, and the control algorithms were written such that controller operation would follow the guidelines set out. There are clearly situations during normal driving which require large deviations of the engine from any ideal operating line during the transient. The particular compromise between different emissions may lead to an ideal line for emissions which is not necessarily good, in terms of drivability. For example, an ideal line using high torques and low engine speeds could result in there being little excess torque available at the steady state engine speed when the driver demands an increase in power. This could result in the vehicle having a sluggish, unresponsive feel.

5.2 Emissions and economy considerations

The legislated emissions for vehicles with Diesel engines are hydrocarbons, particulates, NOx and carbon monoxide. Smoke is also of interest and likely to be of increasing importance. Carbon dioxide production, although not currently legislated, is directly related to the fuel economy of the vehicle. Appendix A gives the current legislative limits for these emissions together with future projected limits. Significant reductions in the emissions from todays engines are required if they are to meet future legislation. Carbon monoxide emissions are less of a problem for Diesel engines because of the excess air present for combustion. The emissions of NOx and particulates are usually of most concern. The effect of EGR is to reduce NOx emissions at the expense of increasing particulates. To reduce both simultaneously requires a substantial improvement in the engine combustion.

5.2.1 Ideal operating points and lines

The concept of an engine economy line has been widely discussed (Stockton, 1984, Yang et al, 1985). Such a line is formed by joining together points of increasing engine power on an engine torque speed map. Each point represents the most economic torque speed combination which will produce the specified power. The line starts at zero torque and engine idling speed and finishes at the maximum power, which for automotive Diesel engines is usually at full load and rated speed.

The idea used in the classic case of the economy line for minimum brake specific fuel consumption can be extended to lines optimised for each of the engine emissions of concern. For example a line optimised for low NOx emissions can be generated by joining together points of increasing engine power, each point being at the torque speed combination for lowest emission of the pollutant at the particular power. Ideal lines for economy and for each of the emissions of concern are shown in Figures 5.1 to 5.5. The lines shown in these figures are based upon steady state engine conditions for the particular engine used for the project rig work. In reality the positions of the lines vary with changing engine conditions such as coolant temperature and turbocharger boost pressure. Ideal lines may also vary from engine to engine due to production variance but this effect is not considered as part of this work.

The ideal lines for economy and emissions, based upon steady state engine conditions, are distributed over a large part of the torque speed map. Clearly the ideal line for economy is not ideal for NOx emissions, for example. Because of this, a compromise must be made between the economy and each of the emissions so that an operating line can be generated for use in practice. The compromise between the various ideal lines must be made by considering the level of concern associated with each of the particular pollutants and the proximity of the legislative limit to the experimental value produced when testing the particular engine vehicle combination. There is no legislation currently applied to the economy of passenger cars. However economy is of interest to the customer and so appropriate consideration must be applied to the economy line when generating the compromised operating line. In practice the compromised operating line may be generated by applying numerical weightings to each point of each alternative line for the power concerned and repeating this process for points of increasing power. Figure 5.6 shows an ideal line produced in such a way by combination of the ideal lines of Figures 5.1 to 5.5. This line was used in some of the early predictive work. For further optimisation, the weightings may be scheduled with the measured temperatures of the engine coolant and the catalyst. One way in which this could improve the overall emissions is by giving a higher weighting to the hydrocarbons line when the catalyst is cold.

5.2.2 Producing the ideal operating point

The ideal operating point is generated by a set of algorithms contained within the operating point optimiser, Brace et al (1996). The optimiser takes, as one of its inputs, a positive power demand, produced by the supervisory controller and uses this to generate an ideal engine operating point in terms of engine torque and speed. This is done by interpolation along a pre-determined line produced by the operating line optimiser.

The operating line consists of eleven torque speed points at sequential 5 kW intervals from 0 to 50 kW. For each of the points from 5 kW to 45 kW inclusive, the algorithm finds the engine speed at which a weighted sum of the predicted emissions is a minimum. Emissions are predicted using a version of the neural network engine emissions model. The weightings of the different emissions can be set manually or modified as a result of on line calculations and may include measurements such as engine and catalyst temperatures.

On the overrun, negative powers are demanded from the powertrain. Ideal operating points for negative demanded powers are generated elsewhere in the controller. In this situation, little or no fuel is injected, and so emissions are at a minimum. Transmission ratio is used to control engine speed and the amount of engine braking effect upon the vehicle.

The sections above have described the generation of the ideal operating point. However, since vehicle drivability is sometimes of greater importance than emissions and economy (for example, during highly transient conditions), a balance must be found between the use of the ideal operating point and use of the best operating point to give the driver's desired powertrain response. The following section is used to consider this balance.

5.2.3 Operational considerations for a multivariable drivetrain controller

Requirements of the complete control system are twofold. Firstly, the controller must enable use of the chosen ideal operating point in the steady state. In transient conditions, deviation from this point must be by the minimum amount necessary to achieve acceptable vehicle response. Secondly, the controller must give the driver a good sense of control over the vehicle powertrain. Vehicle drivability may be impaired by too close adherence of the engine to an ideal line.

Consideration of the dynamics of the powertrain must also come into play when discussing operation of a drivetrain controller. On a direct injection Diesel engine, subject to the maximum slew rates in the Diesel injection pump software and hardware (which are usually relatively fast), torque changes may be made very quickly, the main delay often being only the time between the demanded change and the time of the next injection. On the other hand, engine speed changes may not be made so quickly. They are constrained by the maximum slew rates of the transmission ratio, the need not to impair the vehicle feel by sharp acceleration or deceleration and the high inertia of the engine and flywheel.

5.3 Compromising performance and emissions/economy

As was mentioned above, large deviation from the ideal operating line is sometimes necessary in order to achieve good drivability. There are, however, other issues which may cause or require deviation during steady state driving if drivability and performance are not to be compromised.

Firstly, operating at a low engine speed and near to the limiting torque curve during steady state can cause the driver to have a poor perception of the vehicle response when he or she demands a large increase in vehicle speed. This is because there is a lack of extra torque available at the current engine speed. The torque is needed to accelerate the vehicle immediately and to accelerate the engine to a faster speed where more power can be produced.

Secondly, the ratio range of the CVT severely limits the lowest operating speed of the engine at the higher vehicle speeds. For example at 100 km/h it would be possible to generate the required power for steady driving of the vehicle along a flat road by having the engine operating at 1400 rev/min and about 90 Nm whereas the transmission ratio limit requires a minimum engine speed of 2130 rev/min. This effect of ratio limitation can result in poorer economy at high vehicle speeds. Vehicle drivability may also be adversely affected in that the driver may perceive the engine speed to be higher than desired. This may make driving at high vehicle speeds seem less relaxed than if a lower ratio was available.

5.3.1 Path finding on the torque speed map

Several options are available for moving between steady state points on the engine torque speed map. If the vehicle is at constant speed and the powertrain is operating in steady state then clearly, any movement of the engine on the map must be in a direction such as to maintain power if the vehicle is not to decelerate. A movement along a constant power line in either direction will cause no change in the speed of the vehicle, however an increase of engine power will eventually cause the vehicle to accelerate. Looking again at the case of movement along a constant power line, a tiny change in the engine speed must be caused by a change in the torque balance between the engine combustion torque and the engine load torque. The engine load is composed of the vehicle load and the engine internal friction and pumping losses. The engine load cannot therefore change until either the engine speed or the vehicle load changes. Hence the only way to initiate a change in operating point is to change the torque produced by the engine. Once this is done, the increase or decrease in power can be used to increase or decrease either the engine or the vehicle speed. If the transmission ratio is changed at the correct rate, this increase or decrease in power can be achieved whilst operating the engine along an ideal operating line.

5.3.2 Implications of the transmission efficiency

Transmission efficiency is clearly an important factor in the level of vehicle emissions and economy achieved. Work by Guebeli (1993) and Micklem (1992) showed that the CTX efficiency was a function of secondary pressure. Too high a secondary pressure would result in large parasitic losses in the transmission hydraulic pump whilst too low a pressure would result in gross slippage of the belt with a loss in transmission efficiency. Guebeli (1992) showed that there was an optimum belt slip level at which the overall transmission efficiency would be at a maximum.

For the purposes of the work described here, a prototype electrohydraulically controlled transmission had been supplied by VDT. Since lowering the secondary pressure had potential risks to transmission life, it was decided that the approach to the transmission efficiency issue would be first to ascertain whether the efficiency varied with load, speed and ratio before any changes were made to the secondary pressure control strategy. To this end, a process of mapping the transmission efficiency was completed using the transient test rig. Secondary speed was kept constant, representing a constant vehicle speed. Ratio and torque were varied together such that the secondary speed was maintained and at each of these points the efficiency was calculated from the measured transmission input and output speeds and torques. This process was repeated at different values of secondary speed. The results showed that efficiency varied with load, speed and ratio.

Variation in the transmission efficiency across the torque versus ratio map at constant vehicle speed and load may have resulted in the modification of the engine ideal operating line whatever the relative weightings of emissions and economy used in its generation. Since the transmission efficiency was found to be a function of torque and ratio at different constant vehicle speed load points, it was necessary to include the effects of the transmission in the engine operating line optimiser. This was done by modification of the logical steps used in the optimiser as described below.

Firstly a neural network was trained to represent data on transmission efficiency collected from the rig. The structure of the network is shown in Figure 5.7. The network consisted of a three input, one output arrangement with one hidden layer containing thirty neurons. Since the data collected showed the shape of the efficiency map of the transmission was not complex, a neural network approach to representing the data was considered appropriate. Neural networks, Sections 1.4.1 and 1.4.2, are able to represent smooth continuous functions accurately and demand little computational load.

Secondly the algorithm in the optimiser was modified to take into account transmission efficiency in the generation of the ideal line. In generating each 'ideal' point on the ideal line the optimising process included a test of one point of equivalent engine power at a higher torque and a lower speed than the 'ideal' point and one point of equivalent engine power at a lower torque and a higher speed than the 'ideal' point. If either of the points adjacent to the 'ideal' point was actually found to be better, the 'ideal' point was adjusted in the direction of that point. In this way the ideal line was kept constantly up to date. To take into account transmission efficiency, the emissions and economy values at the 'ideal' point and each of the adjacent points were multiplied by the relative transmission efficiencies.

Before this modification, the line was adjusted simply if the weighted emission and economy total of a point adjacent to the line became better than the value associated with the line itself. Now the values associated with the adjacent points and the point on the line were subject to multiplication by the transmission efficiency. The early version of the operating optimiser produced an engine power output equal to that demanded in terms of power. This meant that the power at the vehicle wheels was subject to the transmission efficiency and so the pedal feel characteristic was also subject to that efficiency. With these modifications to the optimiser, engine demands were multiplied by the inverse of the predicted transmission efficiency so that a demand at the accelerator pedal related directly to the amount of power being delivered at the road wheels.

5.4 Controller architecture

The decision was taken to design the controller architecture in a centralised hierarchical manner for two reasons. Firstly, the advantages of this type of arrangement were considered more relevant than the disadvantages. These were discussed in Section 1.4.2. Secondly, the hardware supplied by both Lucas and VDT gave rise to a supervisory controller being more suitable than one of a distributed nature in this case. The controller architecture, shown in Figure 5.8, is therefore divided into two distinct areas, firstly the supervisory controller and secondly the powertrain controller. A logical boundary existed between the two areas and each had its own tasks. The five alternative designs of supervisory controller each contained the software responsible for the choice of engine operating point in terms of torque and speed during transient conditions. In determining the final steady state operating point following a transient, the various alternative supervisory controllers referenced the operating line optimiser which was described in Section 5.2.2. Other inputs used by the strategies included the pedal position, a measure of time, and various plant feedbacks.

All five alternative designs of supervisory controller were evaluated. The different approaches were pursued initially because they were all viable options and each was believed to have different strengths in the areas of low emission control, good drivability and ease of controller set up and tuning. The supervisory controller strategies are described in detail in Chapter 6.

The outputs of the supervisory controller are passed to the inputs of the powertrain controller where direct control of the powertrain is performed. When the clutch is engaged, the engine speed is controlled via the transmission ratio. The ratio is controlled by modulating the transmission primary pressure via the primary solenoid current. The signal used to generate the solenoid current results from the error between the demanded and measured engine speeds. When the clutch is disengaged the engine idling speed is controlled by the EPIC fuel injection system and during clutch partial engagement the engine speed is a function of primary speed, clutch pressure and the EPIC demand signal.

The powertrain controller also sets the value of the EPIC fuel injection system demand signal in order to achieve the demanded engine torque. This is an open loop process. An algorithm is used which is based upon a model of the EPIC demand / engine torque characteristic. Measured engine speed is applied to this algorithm, together with the demanded engine torque. The transmission secondary pressure is likewise controlled by the powertrain controller. The secondary pressure affects the torque transmitting capacity of the variable speed unit. The demand is generated by an algorithm involving engine torque, speed and the ratio. The secondary pressure control loop is closed with a signal fed back from a pressure transducer.

The set up of the powertrain controller was kept constant whilst comparisons were made between the various supervisory controllers. However, the calibration was optimised at several stages through the experimental work and a different set up was found to be necessary for the vehicle compared with the test rig. These calibrations reflected differences in the hydraulics (due to manufacturing tolerances) between the vehicle and rig transmissions. The VDT controller is very similar to the powertrain controller in that it can be used to control engine speed externally via transmission ratio. Since the VDT controller gains were already set up at the beginning of this work and its performance was evaluated and seen to be satisfactory it was used in conjunction with the powertrain controller for the tasks of engine speed control and transmission secondary pressure control.

Within the architecture described, the various controller strategies designed, all take account of the findings of the drivability report as well as the emission/economy considerations through use of an 'ideal' operating line. In addition to these, general consideration has been taken of the dynamics of the powertrain and the desired operation of the engine especially during the extreme conditions of hard acceleration and vehicle overrun.

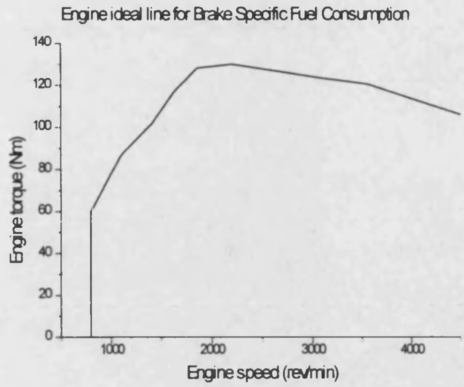

Figure 5.1

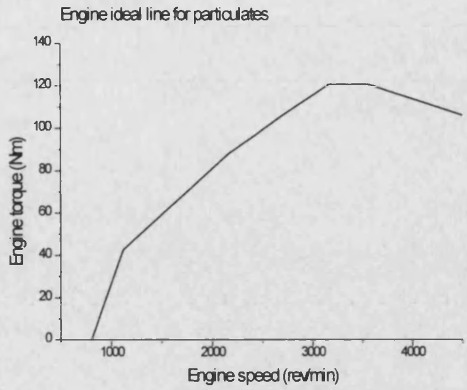

Figure 5.4

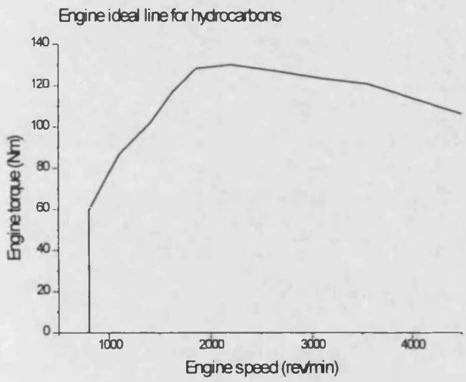

Figure 5.2

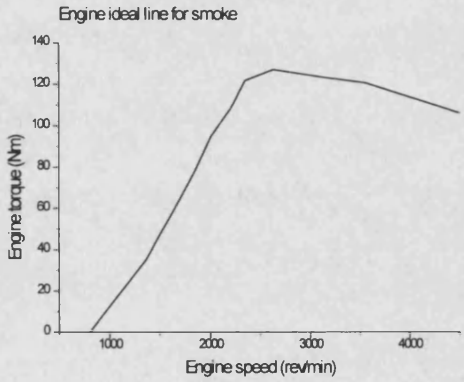

Figure 5.5

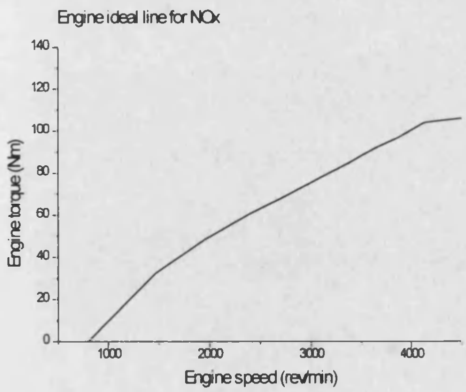

Figure 5.3

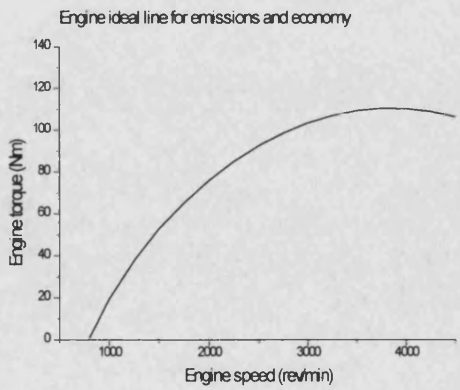

Figure 5.6 Ideal line produced by minimising the weighted sum of emissions: [HC(g/kWhr)]/12 + [NOx(g/kWhr)]/16 + [Particulates(g/kWhr)]/24 + ([BSFC(g/kWhr)]-150)/850

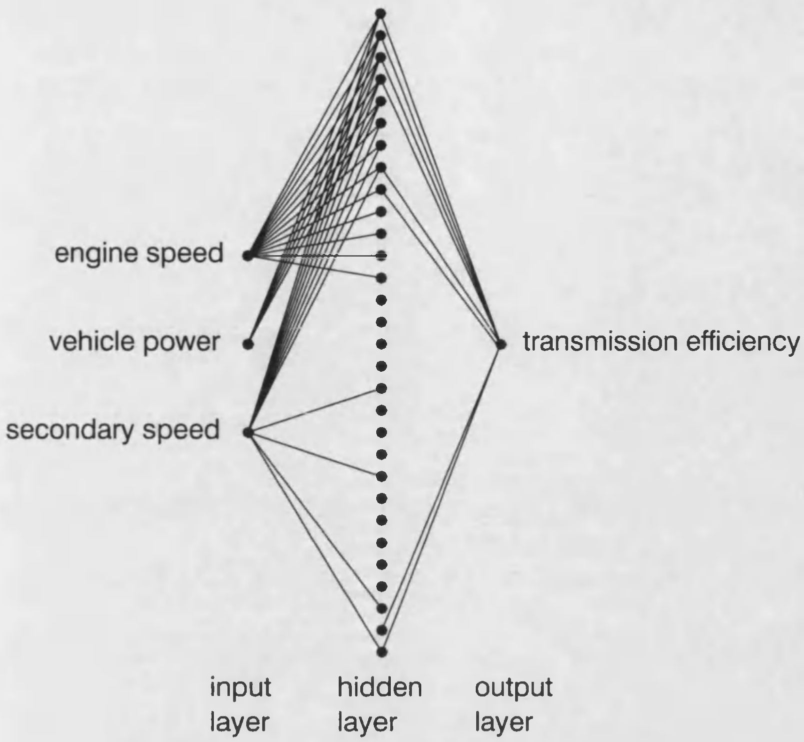

Figure 5.7 Neural network structure for transmission efficiency model

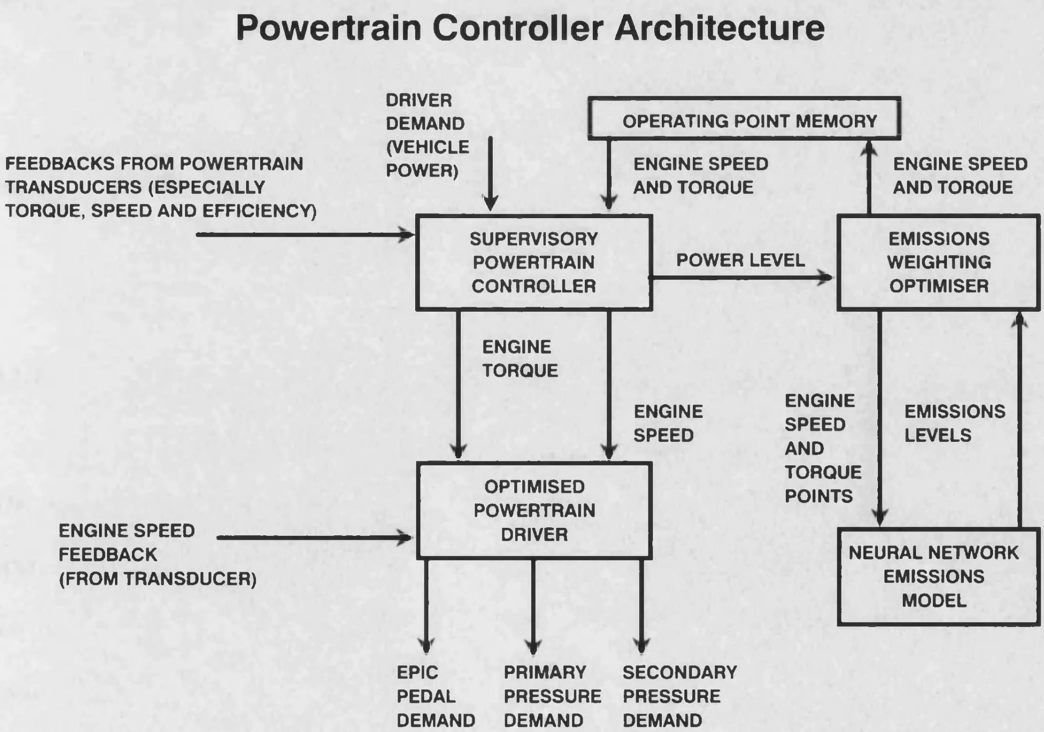

Figure 5.8 Chosen controller architecture

6. TRANSIENT POWERTRAIN CONTROL - IMPLEMENTATION

6.1 An intuitive approach to supervisory control (Rule based controller)

An intuitively motivated or rule based controller was the first of the five alternatives to be designed. The objective of moving upwards from one operating point on an ideal operating line to another ideal point higher up the same line was examined in detail. Various ways of achieving this were studied. Step increases in the torque and or engine speed demand resulted in system saturation and a loss of control of the relative rates of change of the two variables. Therefore it was important to schedule the rates of change of the two variables together. After initial simulations using stepped and ramped changes in the torque and speed demands, it was considered that a better system response would be one more typical of a first order system. In addition, results from the drivability work, and considerations of the complete powertrain supported the view that if the transient engine torque and speed changes could be forced to follow a first order characteristic this would be beneficial to the vehicle drivability. (The findings of the drivability study, Section 3.5 included a desire for smooth but responsive changes in the engine operating point). Therefore the rule based controller was designed around a demand scheduling algorithm based upon a first order lag approach to changing engine torque and speed demands.

6.1.1 Design and implementation

The design of the Rule based controller was based upon the principle of following the engine ideal operating point during steady state operation. It was accepted that during transients a deviation from the line would be necessary in order for the demanded power to be developed sufficiently quickly to ensure good vehicle drivability.

Figure 6.1 shows the structure of the Rule based controller. The pedal position is used by the operating point optimiser for the generation of the ideal engine torque and speed. These are used together with the pedal position and a measure of time by a module which selects the operating mode of the controller. The mode selector then passes control signals to a demand scheduling algorithm which produces the demanded engine torque and speed.

6.1.2 Modes of operation and use of time

The controller operation is governed by the mode selector. Table 6.1 shows how the mode is determined based upon the pedal position and time. The demand scheduling algorithm, based upon a first order lag approach, is defined by Equation (6.1). The time constants of the lags in this algorithm are varied according to the operating mode. In addition values for the pure delays are sometimes introduced into the process.

$$L_t = 1 - \exp(-(t - (t_0 + \delta)) / (\tau_2)) \tag{6.1}$$

The controller operation, and indeed drivetrain operation, were classified into six modes for the purpose of designing the control algorithms. These are shown in Table 6.1. Acceleration is divided according to severity into modes 1, 2 and 5. The overrun condition is covered by mode 3. Steady state and a delay prior to change of mode are covered by modes 0 and 4 respectively.

Acceleration is classified by being slow, moderate or hard. Slow acceleration is the closest condition to steady state and so it was decided to operate as closely as possible to the ideal operating line. Therefore the time constants for the torque and speed changes are kept equal and large. There are no time delays involved in the generation of the demands.

For moderate accelerations, the time constants for the torque and speed changes are equal and are a function of the accelerator movement as defined in Equation (6.2). There is also a pure delay after the mode is entered and before the speed demand starts to change. This enables the torque to be changed and initially used completely for vehicle acceleration response rather than to accelerate the engine.

$$L_t = 1 - \exp((-(t - (t_0 + \delta))) / (0.2((AP - AP_0) \ / \ 2.5))) \tag{6.2}$$

Hard accelerations are characterised by the accelerator pedal being at a level of at least 95% of its full scale value. In this situation the full torque available is required and so a very large torque is immediately demanded from the system resulting in saturation of the fuelling demand. This torque is used to accelerate both the engine and vehicle. The ultimate objective is to move the engine to full power and so the engine speed demand is increased exponentially to its rated value with a time constant of 0.2 seconds.

The values chosen for the classification modes of Table 6.1 and the time constant and delay values for the different situations were initially chosen through their use in the simulations of the system. It was expected that further tuning of these values would be necessary for use of the controller on the test rig and in the vehicle.

6.2 A fuzzy logic rule based open loop supervisory controller (Fuzzy controller)

The Rule based controller, Section 6.1, had the advantage of simplicity. Each particular mode operated in isolation and was therefore easy to tune. However the tuneable envelope of controller operation was very limited and it was thought that the necessity to switch from one operating mode to another may have led to discontinuity and poor drivability in operation. A logical step forward would have been to extend greatly the number of operating modes and carefully tune the controller response for each one. This approach would have been very labour intensive and would have led to long repetitive software and was not judged an ideal solution.

The fuzzy logic rule based approach was investigated because of three inherent advantages over the Rule Based controller method. Firstly its rigorous approach to the production of a rule base enables a relatively small number of conditions to describe adequately the ideal controller response over the entire operating envelope. Secondly it has the ability to blend the different rule outputs together and achieve smooth operation from one condition to another. Finally, tuning of the controller could be done by initial coarse adjustments greatly affecting the whole operating envelope and secondly by fine adjustments affecting only a smaller operating region.

A fuzzy logic controller was designed following the work and experience achieved from the rule based controller. The objectives of steady state and transient control were unchanged.

Figure 6.2 shows the Fuzzy controller architecture. The pedal position is available to the operating point optimiser which supplies the ideal operating point to the Fuzzy controller. The pedal position itself, together with its rate of change and a measurement of the immediate history of its rate of change, defined as its busyness and described in more detail later, are also inputs to the Fuzzy controller. The current torque and speed demand complete the inputs to the controller. The Fuzzy controller generates demanded values for the rate of change of engine torque and speed. These are applied to integrators, the outputs of which are the current values of the torque and speed demands.

6.2.1 Background development of fuzzy control

The development of fuzzy control and the increase in its use have been described in Sections 1.4.1 and 1.4.2. It was initially pursued as a potential solution because of the reasons stated. In addition to these, it was considered suitable because of the ease of construction of the controller from a linguistic rule set, and because of its applicability to non-linear systems and the implementation of non-linear control strategies.

6.2.2 Design and implementation

The fuzzy controller module at the centre of Figure 6.2 consisted of essentially three stages. Firstly fuzzification algorithms were used to convert the input signals into values associated with the fuzzy input terms. The values of the fuzzy input terms were then applied to the rules in the rule base. The outputs of the rule base, the values of the fuzzy output terms, were then passed through a defuzzification process to produce the fuzzy controller module output signals. The fuzzification and defuzzification processes were essentially non-linear or linear mapping functions. The rule base was a set of linguistic rules which were interpreted mathematically.

The fuzzy controller module inputs consisted of the accelerator busyness function, a measure of the rate of change of the accelerator pedal signal, minus the last acquired value, the ideal engine speed demand, the ideal engine torque demand, the actual engine speed demand, the actual engine torque demand and the actual pedal demand. The fuzzy controller had five inputs each of which was associated with two fuzzy terms, either small or large and positive or negative. In the case of the engine speed and torque demands, the differences between the ideal values and the actual values were calculated and applied as two of the controller inputs. The controller fuzzification process is described by Equations (6.3) and (6.4).

The initial stage of fuzzification, Equations (6.3), is used to scale the measured variables so that they are at appropriate levels for use in the process defining the fuzzy terms. It was decided to scale the variables such that all of the inputs, I_1 to I_5 ranged from zero to one hundred. This ensured that all of the inputs had equal dominance at this stage. This was important, since in the design of fuzzy logic controllers, it is in the rule base that the dominance of particular inputs should be defined and not at any earlier step.

$$
\begin{aligned}
I_1 &= 10A_b \\
I_2 &= 5((AP_n - AP_{n-1}) + 10) \\
I_3 &= ((N_{ideal} - N_{dem}) + 3700) / 74 \\
I_4 &= ((T_{ideal} - T_{dem}) + 130) / 2.6 \\
I_5 &= 10AP_n
\end{aligned}
\tag{6.3}
$$

Having scaled the controller inputs, the next stage of fuzzification is to define the fuzzy terms associated with each of the inputs. This is done in Equations (6.4). The fuzzy terms are 'high' and 'low' and are calculated for each of the inputs, I_1 to I_5. HI and LO are the variables used to define the fuzzy terms 'high' and 'low'. They fall in the range of -1 to +1. If the value of HI is +1 then the input I is as high as is possible. Similarly if the value of LO is -1 then the input is as low as is possible. Between these two extremes, HI and LO define the 'highness' and 'lowness' of the input.

These, Equations (6.4), can be used to alter the relative impact of each of the inputs upon the controller strategy. There is, in effect, a gain and an offset associated with each of the fuzzy terms for each input. By adjusting each of these values the control action of the strategy can be tuned to give the desired response. The simulation environment was used for the initial development and set up of the controller and further tuning was performed using the test rig and in the vehicle.

$$
\begin{aligned}
&HI_1 = -0.4 + 0.014 I_1 \\
&\text{if}(I_2 \geq 50)\, HI_2 = 1 \\
&\text{if}(I_2 < 50)\, HI_2 = 0 \\
&HI_3 = -1 + 0.02 I_3 \\
&HI_4 = -1 + 0.02 I_4 \\
&HI_5 = -9 + 0.1 I_5 \\
&LO_1 = 1 - 0.014 I_1 \\
&\text{if}\,(I_2 \geq 50)\, LO_2 = 0 \\
&\text{if}\,(I_2 < 50)\, LO_2 = 1 \\
&LO_3 = 1 - 0.02 I_3 \\
&LO_4 = 1 - 0.02 I_4 \\
&LO_5 = 1 - 0.01 I_5
\end{aligned}
\tag{6.4}
$$

The Fuzzy rule set is shown in Table 6.2. The rules were generated by consideration of the recommendations of the drivability work described in Chapter 3 and using the experience gained with the Rule Based controller. Separate rules were generated for the control of the rate of change of the engine speed demand and the rate of change of the engine torque demand. This enabled independent tuning of the controller for each of the outputs which was found to be valuable in the rig and vehicle situations. Production of the rule base was through consideration of each combination of the fuzzy terms on the five inputs. The appropriate fuzzy output terms were chosen for each rule. Equation (6.5) gives the details of the implementation of Fuzzy rule 6.

Equations defining the outputs of the fuzzy rules (an example)

$$\begin{aligned}
&R_{06} = LO_1 \\
&\text{if } (R_{06} > HI_2)\ R_{06} = HI_2 \\
&\text{if } (R_{06} > LO_4)\ R_{06} = LO_4 \\
&\text{if } (R_{06} > LO_5)\ R_{06} = LO_5
\end{aligned} \tag{6.5}$$

Of the rules shown in Table 6.2, many were repeated. This had the effect of reinforcing a particularly important rule. Rules were repeated because of the fact that some inputs were not relevant to the rule and had ANY entered instead of a fuzzy input term. The output from each fuzzy rule was multiplied by one of four gains depending upon the semantics of the rule. This was the first stage of the defuzzification process and the four gains were the values associated with the fuzzy output terms. The fuzzy output terms ranged from large positive through small positive and small negative to large negative. The final fuzzy controller module output of rate of change of torque demand is defined by Equation (6.6) which sums the effects of all of the rules, each multiplied by the appropriate fuzzy output term gain. This was the second stage of the defuzzification process. This was then used to modify the torque demand as described by Equation (6.7). The rate of change of speed demand is defined by equations of the same form as Equations (6.6) and (6.7).

$$\Delta T = k_T \sum R_n k_n \tag{6.6}$$

$$T_{dem_n} = T_{dem_{n-1}} + \Delta T \tag{6.7}$$

It was possible to tune the controller very coarsely by making changes to the rule base. However the rule base was considered to be correct at a fairly early stage in the simulation work. The main scope for tuning the controller was through adjustment of the gains and offsets associated with both the fuzzification process (as described above) and the defuzzification process, Equations (6.6).

6.3 Control of vehicle acceleration using a fuzzy logic approach (Fuzzy acceleration controller)

The Fuzzy controller, Section 6.2, was considered both robust, by the extensiveness of the rule base, and flexible in its ability to be tuned to control non-linear systems. However, the driver is controlling vehicle speed and does this through demanding delivered power levels which control the rate of change of vehicle speed. It was considered that using the drivers' accelerator pedal to give more direct control over vehicle acceleration would be beneficial to vehicle drivability. Initial tests using the Fuzzy controller had been promising and so therefore it was decided to pursue this approach by extending the Fuzzy controller to give control of vehicle acceleration. It was considered that the effect of including control of acceleration would be to improve vehicle drivability, but this would be at the expense of operating the engine further from the ideal operating line. Therefore although the primary objectives of low emissions/high economy and drivability were unchanged, in this controller the emphasis was moved away from the low emissions/high economy objective towards the drivability objective.

Figure 6.3 shows the Fuzzy Acceleration controller architecture. This is very similar to that of the Fuzzy controller. The main difference in the structure is the addition of a module called the vehicle acceleration predictor. This predicts the desired vehicle acceleration depending upon pedal position and vehicle speed. The calculated value is compared with the current vehicle acceleration and the error used as an additional input to the Fuzzy controller module. This extra input affects the Fuzzy controller module outputs through the design of the fuzzy acceleration rule base. The strategy, programmed through the rule base, was designed both to control the vehicle acceleration during transients and to operate the engine as closely as possible to the ideal operating line.

6.3.1 Design and implementation

The design and implementation of the fuzzy acceleration controller were similar to that of the original fuzzy controller except for the addition of the acceleration feedback signal, a time input and the extra rules in the rule base. The extension to the rule base dealt with the approach and strategy taken depending upon the relative different levels of acceleration feedback. Acceleration feedback was easy to arrange in system simulation, and results are discussed and presented in Chapter 7.

The major challenge presented by this approach was that of designing an algorithm for the demanded vehicle acceleration. The Equations (6.8) describe the approach used.

$$\begin{aligned} \alpha_1 &= AP_n / 2 \\ \alpha_2 &= 3.3 - 4.5 \exp(-v / 60) \end{aligned} \qquad (6.8)$$

α_1 is a variable which represents that part of the vehicle acceleration demand based upon the accelerator pedal position. As can be seen, the calculation of α_1 is very simple and includes only the one factor. However the power available from the powertrain for vehicle acceleration becomes less as the vehicle speed increases. α_2 is used to compensate for this effect. The resulting acceleration demand is the difference between α_1 and α_2. Other terms were eventually included in this algorithm during the development of the controller. These accounted for the engine power losses, the engine acceleration and the vehicle drag and acceleration. Section 7.1 includes further discussion of the development of this algorithm, and its effect on the controller strategy.

6.3.2 Inclusion in the fuzzy controller

The fuzzy acceleration rule set is shown in Table 6.3. Rules 4 to 7, 12 and 13 are used to implement control of the vehicle acceleration. Acceleration control is achieved by a combination of engine torque and engine speed control. Increasing engine torque clearly increases the acceleration of the engine and/or the vehicle. However, good control of the ratio can be used to make fine adjustments to the amount of torque used to accelerate the engine inertia and hence that remaining to accelerate the vehicle.

The rule base for this controller is somewhat shorter than that used in the original Fuzzy Logic controller. This is due to the accelerator busyness and the accelerator movement/direction inputs not having any initial relevance in the rule base. The effects of both inputs were excluded from the rule base at this point because they were seen to conflict with those produced by the acceleration control algorithm.

Equations (6.9) describe the fuzzification algorithms applied to the relevant inputs. Equations (6.10) describe the generation of the fuzzy terms.

$$\begin{aligned} I_6 &= 10t_s \\ I_7 &= 5(a_{err} + 10) \end{aligned} \tag{6.9}$$

$$\begin{aligned} HI_6 &= 0.01 I_6 \\ HI_7 &= 0.01 I_7 \\ LO_6 &= 1 - 0.01 I_6 \\ LO_7 &= 1 - 0.01 I_7 \end{aligned} \tag{6.10}$$

Further discussion concerning results and the effectiveness of this approach is to be found in Chapter 7.

6.4 Transient shaping controller

The transient shaping controller was motivated by the desire to keep the engine more strictly on the ideal operating line than perhaps was possible with the fuzzy logic controller. Inherent in the fuzzy logic approach was that there was no predetermined path for the engine during a transient. The design of this controller seeks to address this issue by controlling the shape of the path taken on the torque speed map by the engine during a transient. Priority during steady state operation and during slow transients was given to the low emissions/high economy objective. Clearly there was a still a need to move away from the ideal line in the highly transient situation. To enable this the torque and speed demands were trimmed to enable movement of the drivetrain along transient operating paths away from the ideal emissions/economy line. This trimming or 'shaping' of the operating path during powertrain transients gave rise to the name of this approach.

6.4.1 Design and implementation

Figure 6.4 shows the architecture of the Transient Shaping controller. It should be noted that the ideal operating line optimiser is used twice by the strategy. In the first instance, however, the optimiser is modified to take engine speed as an input rather than demanded power. A value of torque which corresponds to the point at which this value of engine speed intersects the ideal line is calculated. In the second instance, the optimiser is used conventionally to predict the ideal torque speed point for the demanded power. In addition the measured engine speed is used as an input to the controller, in effect, closing an outer loop on the engine speed control. The structure can be divided roughly into two parts, the first concerned with the torque demand and the second with the speed demand. There are links between the two parts which are active in a transient but are zero during steady state operation.

In the steady state, the first optimiser is used to convert measured engine speed into the ideal torque for that particular engine speed. This gives one component of the torque demand, shown as torque demand 1. When the system is in steady state, the second component of the torque demand, torque demand 2, is zero and so torque demand 1 becomes the (total) torque demand. On the speed control side of the controller, the rate of change of speed demand is zero and so the integrator holds a constant output speed demand which is where the engine is operating. This steady state part of the strategy ensures operation on the ideal line due to the measurement of engine speed and its use in the upper optimiser.

The remainder of the structure, which is used to demand the extra torque and to determine the rate of change of speed demand to move the engine operating point during powertrain transients, is now described. The torque component of the transient engine operating path is shaped by the addition of torque demand 2 and the rate of change of speed demand becomes a non-zero value. These tasks are performed by the functions represented by networks 1 and 2. The pedal position is fed into the second instance of the operating point predictor to make available the instantaneous ideal speed and torque. These are compared with the signal levels for the steady state torque and speed demand and a torque error and speed error generated respectively. The torque error is used with the pedal position in network 1 to generate torque demand 2, and the speed error and pedal position are used in network 2 to generate the rate of change of speed demand. Figures 6.5 and 6.6 show graphical representations of the functions in networks 1 and 2 respectively. The functions were generated by considering the desired function outputs in extreme and steady state operation and by shaping a function between these points. This process, described in the next section, was not dissimilar to that used to generate the rule bases for all of the other newly designed controllers. The functions were initially represented by neural network functions in the controller code. However generation of the neural network functions was labour intensive and more flexibility was gained by replacing them with interpolation routines for the purpose of controller tuning. Equations (6.11) and (6.12) show the way in which the steady state and transient components of the torque and speed demands are combined. The global gains associated with the rate of change of speed demand surface are modified to take into account the accelerator pedal busyness, Section 6.7, as shown in Equation (6.12).

$$T_{dem1lag} = T_{dem1lag} + 0.01((T_{dem1} - T_{dem1lag}) / 5)$$

$$T_{dem_n} = T_{dem1lag} + T_g T_{dem2} \tag{6.11}$$

$$N_{dem} = N_{dem} + 0.01 N_{slew} k_{slew}$$

$$\text{if } (N_{slew} < 0)$$
$$N_{dem} = N_{dem} + 0.01 N_{slew} k_{slew} (10 - A_b) / 5 \tag{6.12}$$

6.4.2 Generation of the shaping functions

Torque shaping function

Figure 6.5 shows the torque shaping function used during powertrain transients. It has as its inputs pedal position and torque error, torque error being the difference between the ideal torque generated from the pedal position and the torque demand 1 resulting from the current engine speed. Its output is torque demand 2.

Steady state

Clearly for steady state operation, the torque error will be zero. Therefore for operation along the ideal line in steady state, torque demand 2 must be zero also. This condition must occur for all but extreme pedal positions.

Accelerator pedal at zero

The zero pedal position represents the overrun condition and must result in the torque demand 2 being large and negative whatever the torque error. This is important to ensure that no fuel is entering the engine. Torque demand 2 must more than cancel the effect of torque demand 1 in this situation.

Accelerator pedal at maximum

The full pedal position represents the kickdown condition and must always result in a large value of torque demand 2. This will drive the engine fuel system into saturation ensuring that full engine torque is available.

Overrun with non-zero accelerator pedal

Negative torque errors indicate that the engine power is higher than that demanded. This is similar to the overrun condition but may occur at non-zero values of the accelerator pedal position. This condition must also result in large negative values of torque demand 2 and is the reason for the lower plateau in Figure 6.5.

Small to large acceleration demand

The remaining surface for positive values of torque error was set up initially in simulation using a neural network function and then in the vehicle using an interpolation function. This part of the shaping function was used during small, moderate and large accelerations and was tuned in the vehicle for good drivability.

Rate of change of speed shaping function

The rate of change of speed demand was generated using the function depicted in Figure 6.6. The surface describes a neural network which takes accelerator pedal position and speed error as its inputs and produces the rate of change of speed demand as its output. The speed error is the difference between the instantaneous speed demand produced by the lower optimiser using the pedal position and the current speed demand.

Steady state

In steady state operation the speed error will be zero and the rate of change of speed demand should also be zero whatever the value of the pedal position. This gives rise to the horizontal line through the surface at the value of speed error equal to zero.

Transient conditions of increasing power

Positive speed errors indicate that the power in the system is increasing and the rates of change of speed demand are positive, their value increasing both with increasing speed error and increasing pedal position.

Transient conditions of decreasing power

Negative speed errors indicate that there is a transient reduction in power. Again the system responds more rapidly at higher negative values of speed error and large negative values of pedal position. This is so that if a large power is currently being delivered and a large reduction in power is demanded, the system moves quickly into the overrun condition. In practice, the extreme edges of the surface would be reached rarely and then only momentarily during the transient.

6.5 Hydraulic controller

The Hydraulic controller described here is an emulation of the Van Doorne developed powertrain controller which took the form of the hydromechanical controller in the CTX and an electrohydraulic controller in the CTXE. Figure 6.7 shows the structure of the Hydraulic controller. It was generated using a simplified experimentally validated computer model of the original VDT hydromechanical CTX controller. It is also similar in operation to VDT's electronic CTXE controller (Deacon, 1994). It is described here as an option since it was intended that it be used as a 'baseline' comparison with the newly designed controller strategies. The controller performed two functions. Firstly, the engine speed demand was generated by an algorithm taking pedal position and the vehicle speed as its inputs. Secondly the engine torque demand was generated using pedal position. There was no reference to any ideal operating line, and it seemed that the main emphasis of the controller design was on ensuring good vehicle drivability.

The first function of Figure 6.7 is shown graphically in Figure 6.8. When the pedal is off, the overrun line is followed. When the pedal is fully on, the hard acceleration line is followed. The engine speed is generated as a linear function of pedal position for values in between the two extremes. The engine torque demand was a near to linear function of the pedal position. The curves used in both algorithms were generated by polynomial curve fitting functions.

6.6 Powertrain control

6.6.1 Torque scheduling to EPIC

The 'production release' EPIC software was designed for manual vehicles. There was a built in pedal characteristic which determined the engine torque demand dependent upon engine speed and pedal position. Essentially, this feature provided torque backup - i.e. with falling engine speed and constant pedal, torque increased, - and was designed to give good manual vehicle drivability and performance feel. This characteristic, however, was not desirable as part of the supervisory controller since it would have interfered with the achieved engine torque. Therefore one of the key functions of the powertrain controller was to provide an inverse mapping of this function, thereby ensuring that the torque produced by the engine was the same as that demanded by the supervisory controller.

6.6.2 Scheduling of the CTX line pressure

The secondary pressure which was at the same level as the transmission hydraulic pump line pressure was set by an algorithm which took into account the engine torque and the transmission ratio. Equation (4.8) describes the relationship used to demand secondary pressure taking these inputs into account. This algorithm was generated using information and recommendations from VDT concerning pressures necessary to enable torque transmission without gross belt slippage. The relationship shows that as engine torque increases so must the secondary pressure. The secondary pressure also increases as the ratio of primary speed to secondary speed increases.

Micklem (1994) and Guebeli (1993) showed that large reductions in secondary pressure are possible due to the mechanism of torque transfer between the belt and pulleys of the variable speed unit. These reductions enable significant improvements to be made in transmission efficiency. However, it was important to ensure that the life of the transmission would be sufficient for the work presented here and therefore investigations into lowering the secondary pressure were restricted to the simulation environment, Chapter 7.

6.6.3 Engine speed control via ratio control

Upon clutch engagement, the engine speed can be controlled by the transmission ratio. The ratio is itself controlled by a flow control valve which allows hydraulic oil to flow into or out of the primary pulley actuator. Electronic modulation of this valve from a control strategy, then, is the means by which the engine speed is controlled. The loop is closed by measuring primary speed and using it as a feedback. The powertrain controller must use appropriate action to compensate for varying speeds, transmission ratios, torque throughputs and errors between demanded and actual primary speeds.

The structure of the Van Doorne electronic controller is shown in Figure 6.9. Its design was based upon classical techniques and analysis of transmission response at several points within the operating envelope. The controller has three terms, the gains of which are scheduled with measured powertrain variables. The Van Doorne controller could be used either as a stand alone controller, or the supervisory module could be disabled, making it possible to use the lower level controller to externally demand primary speed and/or secondary pressure.

Rig test work using the Van Doorne transmission controller with its facility for external demand of primary speed showed that it was capable of moving the transmission ratio to the value necessary to achieve the demanded primary speed with negligible overshoot. Following this work, described in Chapter 8, it was decided to use the lower level part of the Van Doorne controller rather than duplicating it with a very similar low level controller.

Consideration of the powertrain operation changing between the conditions of the vehicle accelerating and the vehicle decelerating showed that there was a need to match the engine speed demanded to the actual engine speed at the point of change over between the two operating conditions. If this was not done, some hysteresis in the system operation would result, leading to a lack of immediate response to changing driver inputs. Equation (6.13) was used in the Transient Shaping controller to govern the condition of changing from the overrun to vehicle acceleration. The conditions of the equation are met immediately after there is an increase in demand from the driver following the powertrain being in overrun. The engine speed will be greater than the demand because the demand has been decreasing during the overrun period. Since the pedal signal has just been increased, the engine speed will be less than the target ideal value (unless the pedal signal increase was extremely small). The slew rate of the engine speed demand will be positive since a pedal increase has just occurred. In this situation, instead of a delay in response until the engine speed demand increases to the actual engine speed under the usual algorithms, the demand is immediately increased in stepwise fashion to a value slightly greater than the actual engine speed.

$$\begin{aligned} &\text{if } ((\omega > N_{dem}) \text{ and } (\omega < N_{ideal}) \text{ and } (N_{slew} > 0)) \\ &N_{dem} = \omega + 0.01\, N_{slew}\, k_{slew} \end{aligned} \tag{6.13}$$

Equation (6.14) was used for the same reasons in the event of a change from vehicle acceleration to the overrun condition. Similar equations were implemented in the other alternative controller strategies.

$$\begin{aligned} &\text{if } ((\omega < N_{dem}) \text{ and } (\omega > N_{ideal}) \text{ and } (N_{slew} < 0)) \\ &N_{dem} = \omega + 0.01\, N_{slew}\, k_{slew} \end{aligned} \tag{6.14}$$

6.7 Pedal sensitivity and busyness

The driver uses the accelerator pedal to control vehicle speed. However, on the vast majority of vehicles, the accelerator pedal position is not interpreted as a speed demand by the system, nor is it anywhere nearly linear with vehicle speed. On vehicles with manual transmissions, where the engine speed is a function of vehicle speed and the gear selected, the accelerator pedal position relates to fueling and therefore torque produced at the current engine speed / vehicle speed operating point. On such vehicles the driver has more control of the transmission than on vehicles with automatic transmissions. He or she can change gear to raise the engine speed and deliver more power in an attempt to move the vehicle speed to the desired level more quickly.

The driver of a vehicle with a fully automatic transmission has only the accelerator pedal with which to interact with the powertrain. Therefore in an automatic vehicle, choice of engine torque and speed is a function of the control strategy rather than as in a manual vehicle where they are a function of the drivers inputs of selected gear ratio and pedal position. Powertrain control system interpretation of the accelerator pedal position must be different in an automatic vehicle compared with that of a manual vehicle, because a full knowledge of driver intention must be gained from just the one input.

Consideration of manual transmission and conventional automatic transmission vehicles at three operating conditions supports the argument that the pedal position should be treated as a powertrain power demand. Firstly, at a 30 to 40 mph steady cruise on a road with no gradient, typically both vehicles would be driven in the lowest ratio with the pedal at somewhere between 5 and 30% of its full depression. Typically, little power is required at such an operating point and the pedal is depressed only slightly. Secondly, during a hard acceleration, at moderate speed, the pedal position would be near full depression and the engine speed near maximum. In the automatic vehicle a ratio would have been selected to move the engine near to maximum speed to deliver full power, and in the manual vehicle, it is likely that the driver would have chosen a gear ratio such that the engine was similarly near to maximum speed. In this condition, near full power is being delivered by the engine, and the pedal position is close to full depression. Thirdly, in the overrun condition, the pedal position would be at zero depression, and in the manual vehicle, a gear selected such that the engine would be absorbing power to give an 'engine braking' effect and slow the vehicle. Conventional automatics are sometimes criticised for the lack of engine braking, but sometimes there is an additional selector position which can be used by the driver to force the transmission into a higher ratio to increase the engine speed and therefore the engine braking effect. In this third condition, zero pedal deflection equates to the delivery of zero power from the engine, and usually the absorption of power by engine braking.

Due to the reasons presented in the above discussion, the pedal position signal was initially interpreted as a linear power demand by each of the new control strategies. Zero on the pedal signal was interpreted as a demand of zero power - effectively zero torque at a demanded engine speed of idle speed. In the overrun condition, if the vehicle speed was high and the transmission ratio was not sufficient to enable the demanded primary speed, then algorithms ensured the transmission ratio was pushed into overdrive and the engine speed slowed as much as possible until the vehicle slowed sufficiently for the engine speed to reach idle speed (and the clutch to disengage).

One of the main problems of this approach to pedal position interpretation was that a minimum demand of zero power gave no engine braking to the vehicle in the overrun situation. It became clear from this that it was sometimes necessary to demand negative powers at zero pedal as in Equation (6.15), Figure 6.10. The offset of -13 kW used in this equation was a prediction of the amount of power required to motor the engine at full speed. The prediction was made using data collected from the test rig which showed the torque produced at constant fuelling across the speed range. The maximum engine power available was 50 kW and so the gain of 63 was required to ensure a full power demand at maximum pedal position.

$$P_{dem} = -13 + 63\, AP_n / 10 \tag{6.15}$$

However, when considering the feel of a vehicle with a fixed gear ratio in the overrun situation, it is apparent that more engine braking is felt at higher engine speeds. This is due to the engine motoring torque which increases with speed due to the increases in internal friction and pumping work. Based upon this and the reasons discussed above, it was decided that a suitable power demand may be produced by combining the accelerator pedal signal and the engine speed signals as shown in Figure 6.11 and described by Equations (6.16).

$$P_{intercept} = (-9.75 - (0.00395\,\omega)) * \omega * 2\pi / 60000;$$

$$P_{gradient} = (50 - P_{intercept}) / 10; \qquad (6.16)$$

$$P_{dem} = P_{intercept} + AP_n * P_{gradient}$$

Further investigations could be made in this area. The accelerator pedal signal could be considered as a torque demand and some other algorithm used, perhaps involving vehicle speed to produce an engine speed demand. This approach might lead to full power only being available at certain vehicle speed conditions in addition to more engine operation away from the ideal line. It is notable from the original VDT strategy that engine speed demand is a function of vehicle speed. This was probably done for drivability reasons. With a full accelerator pedal signal, this enables the engine speed to continue to increase throughout the vehicle acceleration which may contribute to a vehicle with a more 'manual transmission' feel.

Perhaps at the centre of these issues is the expectation of the driver in terms of system responses for different accelerator pedal displacements in different situations. Many drivers who are used to manual vehicles, find CVT powertrain behaviour unusual if not disturbing (Deacon, 1994). These views may cause pressure in the industry to try to make CVT vehicles feel more like manual vehicles. It would be interesting to gauge the acceptance of manual vehicles if CVTs were the norm. There is one perhaps unchangeable characteristic difference which may always prevent the two feeling similar. Full pedal in a CVT (or conventional automatic) vehicle will always cause a kickdown response, the engine to be raised to close to rated speed and full power to be delivered. With full pedal in a manual vehicle, however, power is limited by engine speed, and whilst the engine may be forced to operate up on the torque curve, its speed cannot be increased over that caused by the vehicle acceleration unless the driver changes gear.

If it is assumed that pedal position can be related to power demand, there is still the issue of whether or not the relationship should be linear to be resolved. Pedal sensitivity can be used to affect the drivers' perception of the vehicle. Evidence of this is presented in Chapter 8. Producing a characteristic which makes the pedal more sensitive at the beginning of its travel and less sensitive at the end gives the vehicle a more lively and responsive feel, perhaps making it more 'fun' to drive. Doing the opposite gives the vehicle a quite sluggish feel. Drivers seem to adjust to the characteristic and learn what to demand to produce the vehicle response which they desire. With more time spent with the same pedal to power characteristic, the effects of any non-linear characteristics on the driver seem to decrease. Evidence of this was found when undertaking the vehicle appraisal work described in Chapter 7.

The powertrain itself can also be made to feel more or less responsive by altering maximum engine slew rate gains associated with the rule based, fuzzy logic and transient shaping controllers. These changes, although clearly affecting emissions because of the different times spent away from the ideal operating line during a transient, may be used in conjunction with the pedal sensitivity to produce the desired vehicle feel.

Finally it was possible to set up an algorithm which enabled each of the newly designed control systems to adapt to either more or less sensitive settings. This algorithm produced a value which was termed the accelerator pedal 'busyness'. This was made possible by measuring the rate of change of the pedal position. The algorithm used is shown and discussed below. If the busyness was high, the system moved towards a more sensitive setting, if it was low, the system became less sensitive. The rates of change were set up for demonstration and it is appreciated that further work would be necessary to optimise them for open road use. It was thought very important that any on line changing of the system response did not cause surprise to the driver, giving him or her either far more or far less response than he or she would expect in a given situation.

6.7.1 Affect on drivability, emissions/economy

Making the system more responsive is likely to have a detrimental effect on the emissions and the economy, even if it improves the drivability. Some vehicles have been produced with automatic transmissions which have sport, normal and economy settings (Hendriks, 1993). However, systems with manually adjustable sensitivity must pass the legislative emissions tests in all of the possible settings. It is important that a system with adaptive sensitivity could pass the emissions legislative tests in all settings if it were possible for the driver to consciously change the sensitivity.

6.7.2 Gain scheduling and implementation

The algorithm which was used to generate a measure of the pedal busyness, A_b, is described by Equation (6.17). It relates to the passage of time, t, and the measured accelerator pedal signal on the current iteration, AP_n and the last controller iteration, AP_{n-1}. Changing the two gains, currently set at 0.01 and 0.015, can be used to cause the pedal busyness to slew more rapidly between its maximum and minimum settings. Further development of the algorithm could perhaps involve the level of the pedal signal itself since during the kickdown situation it may be appropriate to keep the busyness high rather than let it fall due to lack of continued movement.

$$
\begin{array}{l}
\text{if}\,(t \geq (F_{A_b} + 0.05)) \\
\quad \{ \\
\quad F_{A_b} = F_{A_b} + 0.05 \\
\quad \text{if}\,(AP_n > 0.5) \\
\quad A_b = A_b + (0.01 * (1 + \text{fabs}(AP_n - AP_{n-1}))^3) - 0.015 \\
\quad \} \\
\text{if}\,(A_b < 0)\, A_b = 0 \\
\text{if}\,(A_b > 10)\, A_b = 10
\end{array}
\qquad (6.17)
$$

Rule Based Controller

Operating Mode	Pedal Change	Description
0	< 1 %	**No transient** - outputs remain at steady state
1	> half remaining movement (increase)	**Moderate acceleration** - outputs are moved exponentially towards the ideal speed and torque. The time constant is a function of accelerator movement. There is a pure delay before the speed demand change to enable torque response.
2	< half remaining movement (increase)	**Slow acceleration** - outputs are moved together exponentially so that the ideal operating line is followed. The time constant is one second.
3	> 1 % (decrease)	**Overrun** - the torque is decreased immediately to the ideal operating line value. The speed demand is dropped off exponentially, the time constant depending upon an accelerator busyness function.
4	follows mode change	**Delay** - a pedal change occurred in the last 0.05 seconds and will be ignored until that time has elapsed.
5	position > 95 %	**Hard acceleration** - a large torque is demanded to ensure operation on the engine torque curve. The speed demand is increased exponentially with a time constant of 0.2 seconds.

Table 6.1 Operating modes of the rule based controller

RULE	AB	AC0-1	IS0-ES	IT0-ET	AC0	DES	DET	COMMENTS: EXTREMES - DESCRIPTION
1	S	P	ANY	ANY	L	-	LP	KICKDOWN
2	S	P	ANY	ANY	L	-	LP	KICKDOWN
3	S	P	P	ANY	L	LP	-	KICKDOWN
4	S	P	N	ANY	L	SN	-	KICKDOWN
5	S	P	ANY	P	S	-	SP	TORQUE UNDER
6	S	P	ANY	N	S	-	SN	TORQUE OVER
7	S	P	P	ANY	S	SP	-	SPEED UNDER
8	S	P	N	ANY	S	SN	-	SPEED OVER
9	L	P	ANY	ANY	L	-	LP	KICKDOWN
10	L	P	ANY	ANY	L	-	LP	KICKDOWN
11	L	P	P	ANY	L	LP	-	KICKDOWN
12	L	P	N	ANY	L	SN	-	KICKDOWN
13	L	P	ANY	P	S	-	SP	TORQUE UNDER
14	L	P	ANY	N	S	-	SN	TORQUE OVER
15	L	P	P	ANY	S	SP	-	SPEED UNDER
16	L	P	N	ANY	S	SN	-	SPEED OVER
17	S	N	ANY	ANY	L	-	LP	KICKDOWN
18	S	N	ANY	ANY	L	-	LP	KICKDOWN
19	S	N	P	ANY	L	SP	-	KICKDOWN
20	S	N	N	ANY	L	SN	-	KICKDOWN
21	S	N	ANY	P	S	-	SP	TORQUE UNDER
22	S	N	ANY	N	S	-	LN	TORQUE OVER (OVERRUN)
23	S	N	P	ANY	S	SP	-	SPEED UNDER
24	S	N	N	ANY	S	LN	-	SPEED OVER (O'RUN NONBUSY)
25	L	N	ANY	ANY	L	-	LP	KICKDOWN
26	L	N	ANY	ANY	L	-	LP	KICKDOWN
27	L	N	P	ANY	L	SP	-	KICKDOWN
28	L	N	N	ANY	L	SN	-	KICKDOWN
29	L	N	ANY	P	S	-	SP	TORQUE UNDER
30	L	N	ANY	N	S	-	LN	TORQUE OVER (OVERRUN)
31	L	N	P	ANY	S	SP	-	SPEED UNDER
32	L	N	N	ANY	S	SN	-	SPEED OVER (O'RUN BUSY)

Key: S=SMALL L=LARGE P=POSITIVE N=NEGATIVE

INPUTS: AB = accelerator business function
AC0-1 = accelerator movement/direction
IS0 = instantaneous engine speed demand
IT0 = instantaneous engine torque demand
ES = engine speed demand
ET = engine torque demand
AC0 = instantaneous pedal demand

OUTPUTS: DES = engine speed demand slew rate,
DET = engine torque demand slew rate

Ranges

Inputs	1	AB	0 to +10 signal	2 state	}		{(0 to 100) to (0 to 1)
	2	AC0 -1	-10 to +10 signal	2 state	}	0	{straight lines either
	3	IS0-ES	-3700 to +3700 rev/min	2 state	}	to	{0,0 to 100,1 or
	4	IT0-ET	-130 to +130 Nm	2 state	}	100	{0,1 to 100,0
	5	AC0	0 to +10 signal	2 state	}		{
Outputs	1	DES	-1000 to +1000 rev/min/s	4 state	}	areas of rectangles, height 0 to 1	
	2	DET	-1300 to +1300 Nm/s	4 state	}	width of base constant - linear defuzzification	

Table 6.2 Fuzzy logic controller rule set

RULE	AB	AC0-1	IS0-ES	IT0-ET	AC0	TI	ACC	DES	DET	COMMENTS: EXTREMES - DESCRIPTION
1	**L/S**	**P/N**	**P/N**	**P/N**	**L/S**	**L/S**	**LPN**	**LPN**	**LPN**	
2	-	-	-	-	**L**	-	-	-	**LP**	KICKDOWN
3	-	-	**P**	-	**L**	**L**	-	**SP**	-	KICKDOWN
4	-	-	**N**	-	**L**	**L**	-	**SN**	-	KICKDOWN
5	-	-	**P**	-	**L**	**S**	**N**	**LP**	-	KICKDOWN
6	-	-	**N**	-	**L**	**S**	**N**	**SN**	-	KICKDOWN TIME SMALL
7	-	-	**P**	-	**L**	**S**	**P**	**SN**	-	KICKDOWN TIME SMALL
8	-	-	**N**	-	**L**	**S**	**P**	**LN**	-	KICKDOWN TIME SMALL
9										
10	-	-	**P**	-	**S**	**L**	-	**SP**	-	TIME LARGE SPEED UNDER
11	-	-	**N**	-	**S**	**L**	-	**SN**	-	TIME LARGE SPEED OVER
12	-	-	-	**P**	**S**	-	-	-	**SP**	TIME ANY TORQUE UNDER
13	-	-	-	**N**	**S**	-	-	-	**SN**	TIME ANY TORQUE OVER
14	-	-	-	-	**S**	**S**	**N**	**SP**	-	TIME SMALL ACCEL OVER
15	-	-	-	-	**S**	**S**	**P**	**SN**	-	TIME SMALL ACCEL UNDER
16										

Key: S=SMALL L=LARGE P=POSITIVE N=NEGATIVE

INPUTS:
AB = accelerator business function
AC0-1 = accelerator movement/direction
IS0 = instantaneous engine speed demand
IT0 = instantaneous engine torque demand
ES = engine speed demand
ET = engine torque demand
AC0 = instantaneous pedal demand
TI = time from last significant movement
ACC = vehicle acceleration error

Inputs							
	1	AB	0 to +10 signal	2 state	}		{(0 to 100) to (0 to 1)
	2	AC0 -1	-10 to +10 signal	2 state	}	0	{straight lines either
	3	IS0-ES	-3700 to +3700 rev/min	2 state	}	to	{0,0 to 100,1 or
	4	IT0-ET	-130 to +130 Nm	2 state	}	100	{0,1 to 100,0
	5	AC0	0 to +10 signal	2 state	}		{
	6	TI	0 to 10 seconds	2 state			
	7	ACC	-10 to +10 m/s^2	2 state			

OUTPUTS:
DES = engine speed demand slew rate,
DET = engine torque demand slew rate

Outputs						
	1	DES	-1000 to +1000 rev/min/s	4 state	}	areas of rectangles, height 0 to 1
	2	DET	-1300 to +1300 Nm/s	4 state	}	width of base constant - linear defuzzification

Table 6.3 Fuzzy logic acceleration controller rule set

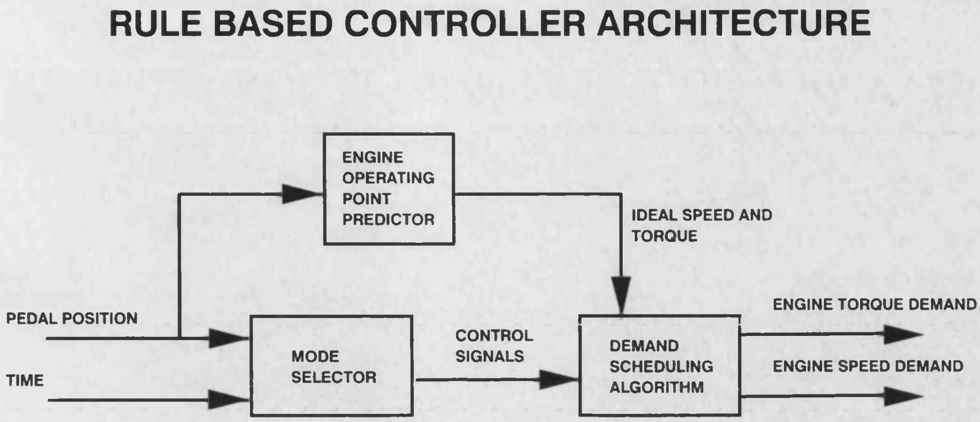

Figure 6.1 Rule based controller structure

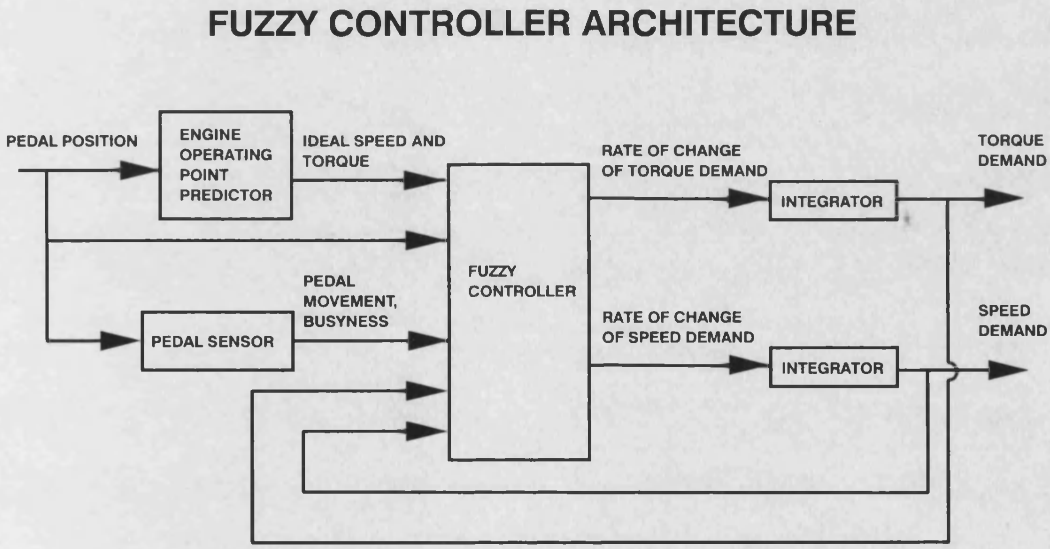

Figure 6.2 Fuzzy logic controller structure

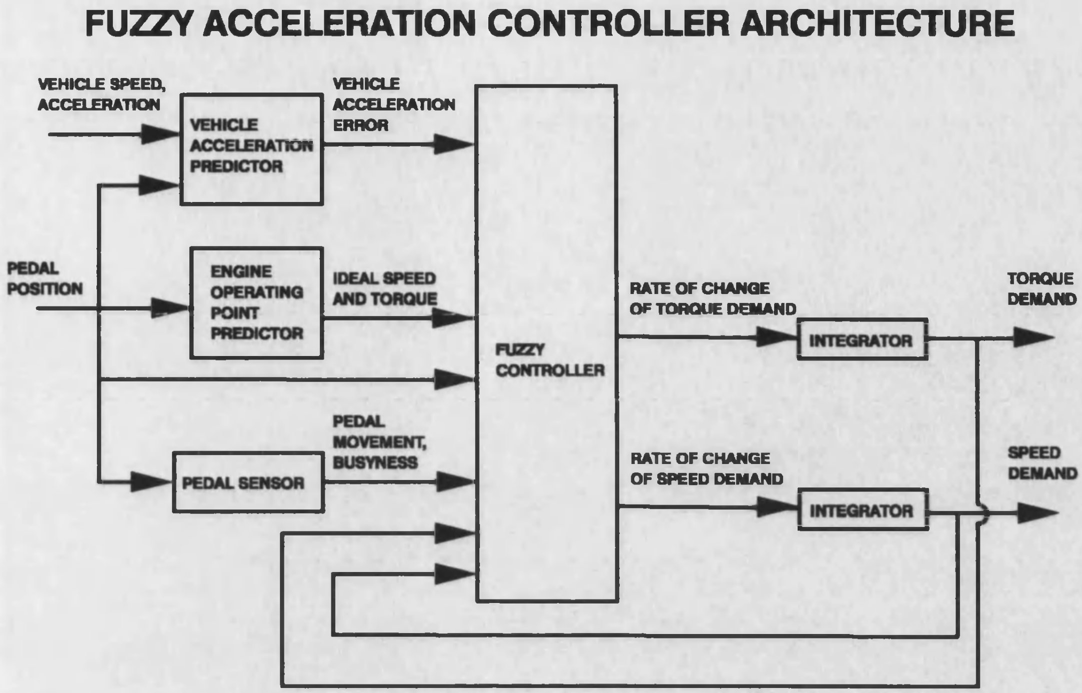

Figure 6.3 Fuzzy acceleration controller structure

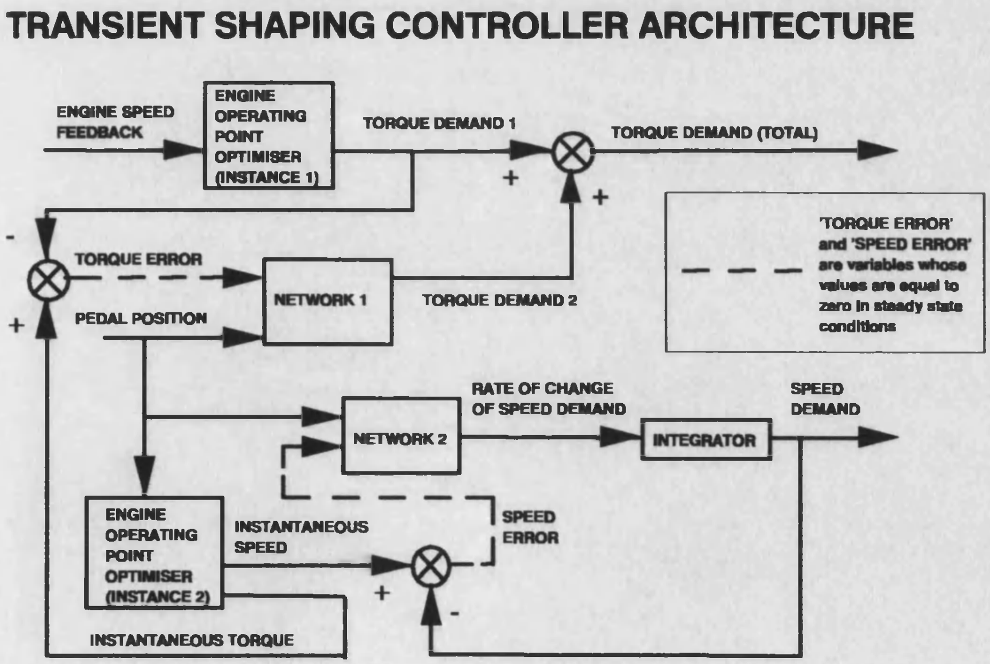

Figure 6.4 Transient shaping controller structure

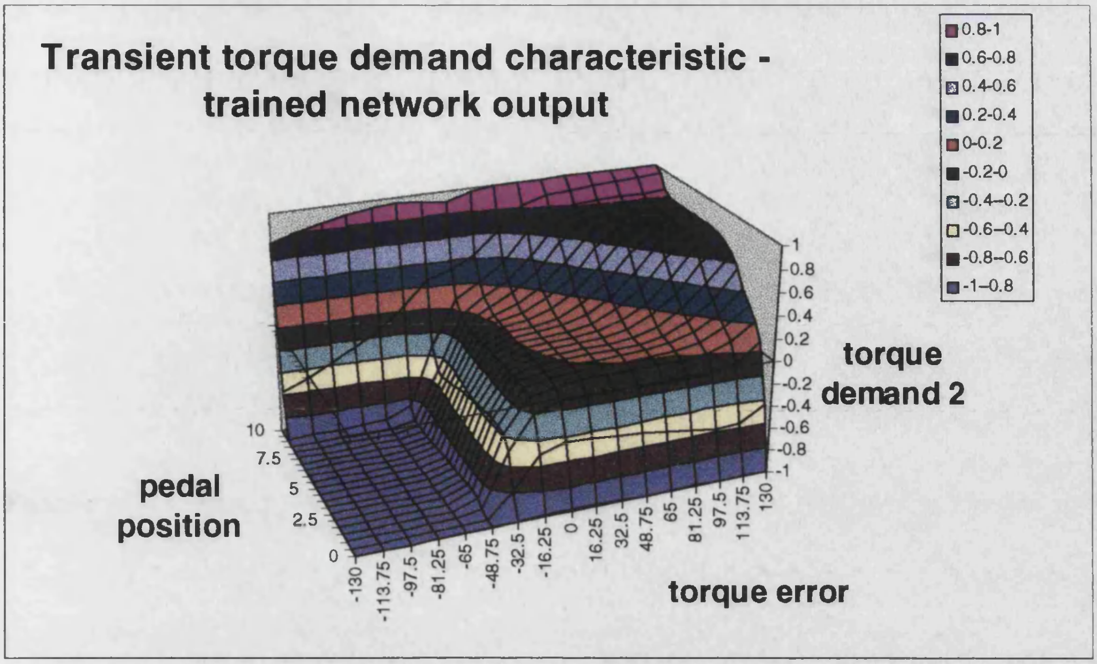

Figure 6.5 Transient shaping torque trimming network

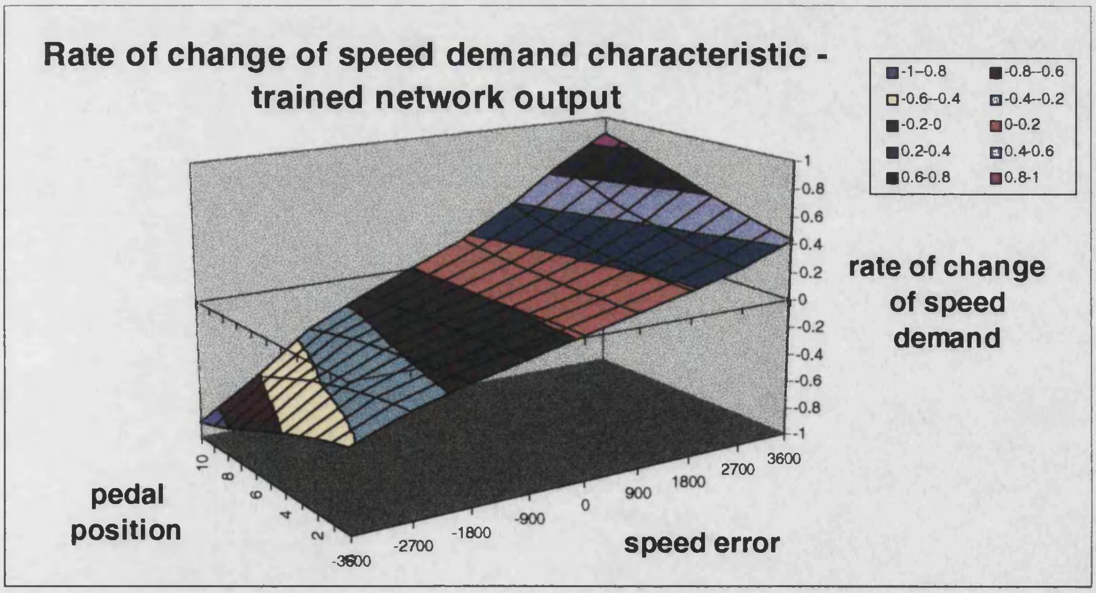

Figure 6.6 Transient shaping speed rate of change network

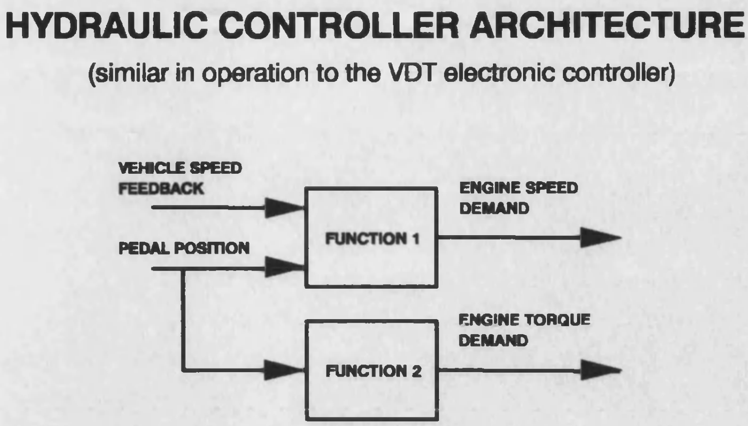

Figure 6.7 Hydraulic controller structure

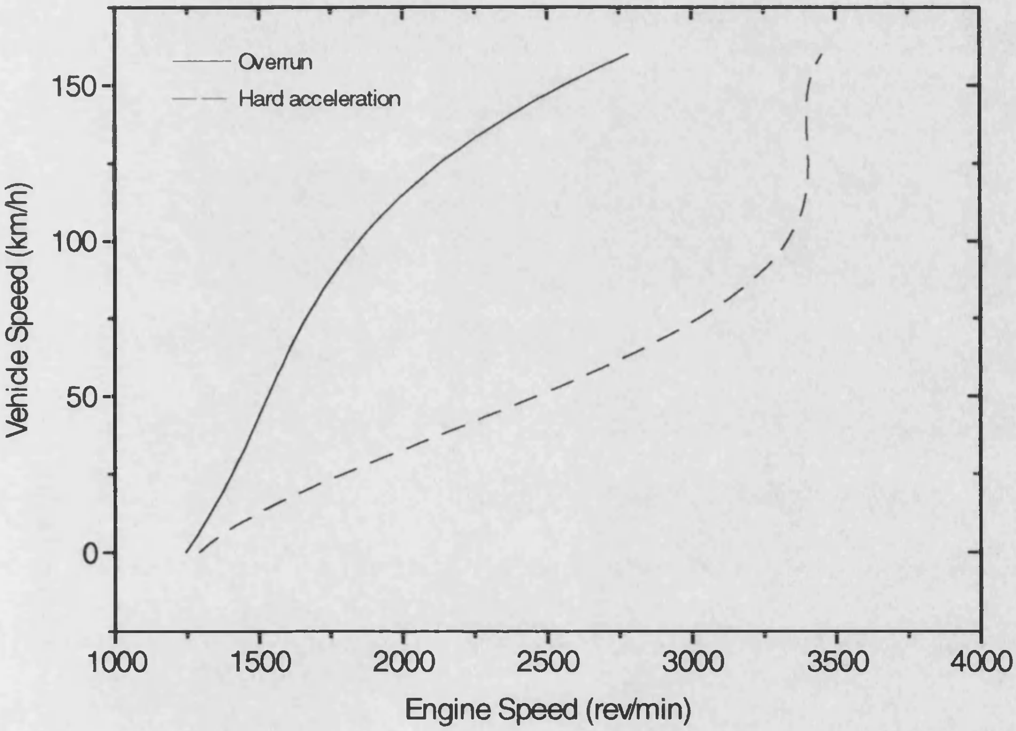

Figure 6.8 Hydraulic controller governor lines

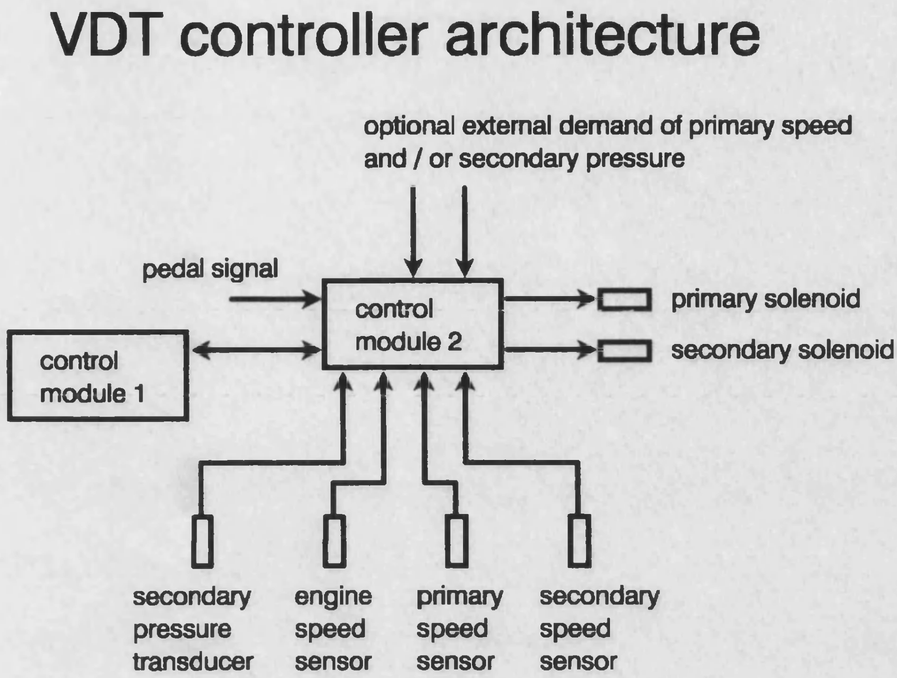

Figure 6.9 VDT controller structure

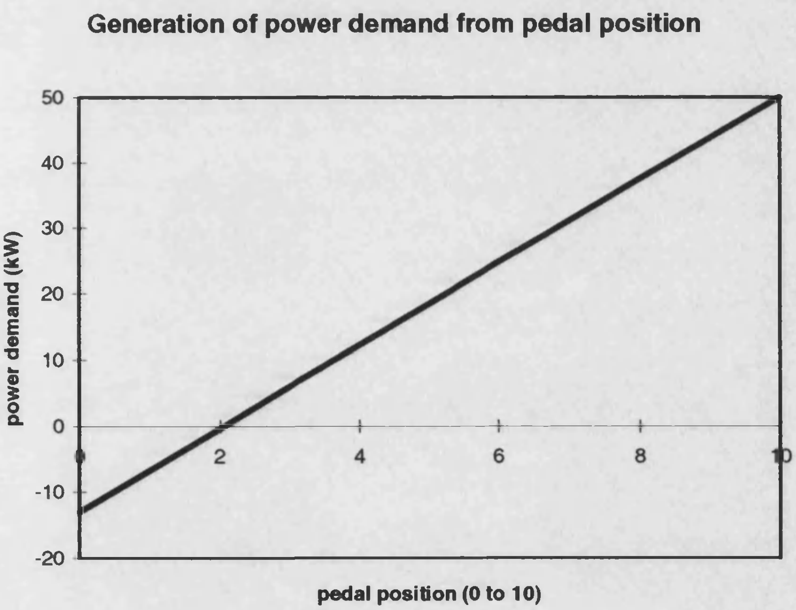

Figure 6.10 Generation of power demand from pedal position

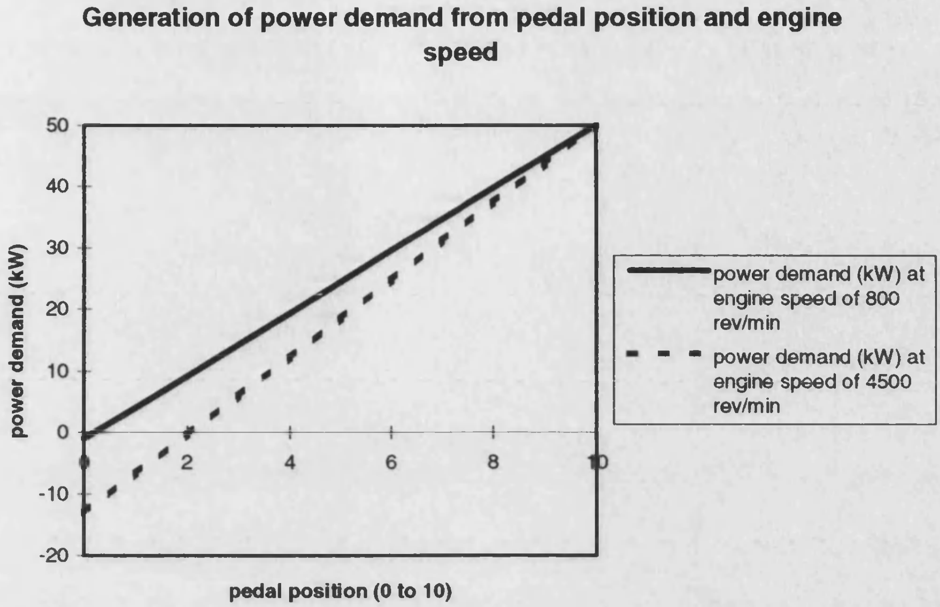

Figure 6.11 Generation of power demand from pedal position and engine speed

7. DISCUSSION OF SIMULATION RESULTS

The simulation environment proved to be the ideal place for the design, development and initial testing of alternative controller strategies. After initial predictive studies, three of the five alternative designs were considered suitable for further development. These were fully implemented and refined further on the test rig and in the vehicle. The remaining two, which had been shown in simulation to be viable options, were not fully implemented due to the reasons discussed below. The powertrain model also enabled the comparison of the emissions performance of the alternative strategies over the simulated legislative European emissions drivecycle.

In addition to controller development and comparison, the powertrain model enabled easy investigation of issues which would have been difficult or impossible to study using the test rig or vehicle, for example the effect of ratio range on drivecycle emissions levels.

7.1 Controller and powertrain performance

In this section, the general performance and viability of each of the alternative controllers is considered. The different characteristics of the designs are discussed and judged against set criteria, shown in Table 7.1. The choice of the controller strategies to be implemented on the test rig and in the vehicle is considered below.

7.1.1 Rule based controller

The Rule based controller had advantages of being simple in terms of operation. It also met the criterion of enabling the engine to operate at steady state on an ideal operating line. However the way in which the software was written was not flexible. It was considered that the switching from one operating mode to another during powertrain transients could lead to unpredictability, abruptness of operation and lack of refinement. To tune and refine this controller further, it would have been necessary to increase greatly the number of operating modes. Calibration of the modes for various degrees of acceleration would have been extremely labour intensive, and the software which was initially simple, would have grown enormously as would the potential for near undetectable software errors. However, this controller was the first to be designed, and was extremely useful as both a benchmark comparison and a learning tool in the design of the subsequent alternatives.

Although it was not practical to develop this strategy further due to the reasons discussed above, this controller was tested very briefly on the rig and in the vehicle. The ease of implementation made testing of this controller worthwhile because of the experience gained and because it was the first strategy to be sufficiently developed to enable this.

7.1.2 Fuzzy controller

Figure 7.1 shows the predicted path followed by the engine in the torque speed domain as the result of a step increase in the accelerator pedal position. The starting and finishing points are on the ideal operating line optimised for low NOx emissions. Figures 7.2 shows the responses of the engine and vehicle variables against time. The system starts from a position of near steady state on the ideal operating line and moves smoothly towards the higher power point on the engine ideal NOx line. The torque demand is increased at a rate such that the final level is demanded long before the final speed is demanded. The actual engine speed lags the demanded by a small amount.

The simulation studies allowed the initial tuning of the controller. At the outset of the predictive work the controller had had a very slow action. This was quickly rectified by increasing some of the gains associated with the fuzzification and defuzzification processes. The semantic rules governing the controller action, and their representation in the rule base appeared to be appropriate from an early stage in the work. During various simulated powertrain conditions and driver demands, both steady state and transient, the engine operating point was driven towards the appropriate parts of the torque speed map. The vehicle response was in accordance with the driver demand and there seemed to be no anomalies in the controller operation.

This initial work had shown the Fuzzy controller to be robust in operation, (operation was not subject to mode changes as in the Rule based controller), and easily tuneable. The controller action was appropriate in the various tested conditions and deemed suitable for practical application. Therefore it was decided to proceed with this strategy and implementations were completed on both the rig and vehicle systems. Further refinement was then possible with respect to economy, emissions and drivability.

7.1.3 Fuzzy acceleration controller

The Fuzzy acceleration controller has many of the qualities of the Fuzzy controller above. Since the rules which enable the Fuzzy acceleration controller implementation compromise somewhat the rules aimed at achieving good vehicle emissions and economy, it is possible to operate the system such that the engine is at a steady torque and speed but sometimes not at a point on the ideal operating line. This type of operation is shown in Figure 7.3. Here the predicted path of the engine during a transient acceleration and deceleration is plotted. The engine steady state points at the extreme points of the trace are not at the ideal operating points. The accelerator pedal demand changes are similar to those used in the Fuzzy controller test above and are shown in Figure 7.4. However, even though the engine is close to steady state, the vehicle is accelerating or decelerating, Figure 7.5. This action is caused by the acceleration control feature of the strategy which is aimed at improved vehicle drivability.

This compromise may be a worthwhile one in terms of the vehicle drivability benefits. There are, however, practical difficulties in both predicting and measuring vehicle acceleration. The task might be relatively easy if the vehicle was considered always to be on zero gradient road where the wind speed was also zero. However the effects of inclines, towing, wind and general deterioration of the vehicle's performance with age would tend to complicate any prediction which was made. Due to the difficulties of practical implementation discussed above, this controller was not taken beyond the simulation study stage.

7.1.4 Transient shaping controller

Figure 7.6 shows the predicted path of the engine on the torque speed map using the Transient shaping controller. The accelerator pedal demand was increased for several seconds and then decreased again as in the simulated tests of the Fuzzy controllers above. The points demanded during the transient are essentially functions of the trimming functions, Section 6.4.2. The controller may be tuned by altering the shapes of these surfaces.

From this early simulation work, it was immediately clear that the smoothness of the torque and speed trimming functions was extremely important. The zigzag type response shown in Figure 7.6 would not be acceptable in practice. As a result of this early work, the coarse look up tables which were used for the test shown, were replaced by neural networks which inherently gave smooth output changes in response to changing inputs.

Figure 7.7 shows a simulation test using the smooth trimming functions. The resulting engine path taken is much improved, and this result is therefore more promising. However, the use of neural networks did cause the tuning of the controller to become a rather long and tedious process. Therefore the networks were replaced by three dimensional map interpolation functions which solved the tuning difficulties and were also smooth enough to give good powertrain response during transients. The shapes of the surfaces used in the trimming map functions are shown in Figures 6.5 and 6.6.

Simulation studies showed this approach to give good adherence of the engine to the ideal operating line, and appropriate vehicle response to the driver's demand. This controller was tuned to a certain degree during the simulation work and was considered suitable for implementation where further refinement was possible.

7.1.5 Hydraulic controller

The software for this controller was written to mimic the operation of the hydromechanical CTX controller and the operation of the Van Doorne CTXE controller. This was done mainly for the purposes of simulation work, Chapter 4. The Van Doorne CTXE controller was used on the rig and in the vehicle applications and results are presented in Chapter 8.

Figure 7.8 shows the points demanded and visited by the engine on the engine torque speed map. Figures 7.9 and 7.10 show important powertrain and vehicle variables plotted against time. In this case since there is no reference to the operating point generator and so the points visited bear no relation to any 'ideal' operating line.

The hydraulic controller software was implemented on the test rig and in the vehicle. As intended, it behaved in a very similar way to the Van Doorne CTXE controller. However, for the test rig and vehicle work described in Chapter 8, the Van Doorne CTXE controller was used because of its greater refinement and because the hydraulic controller was designed purely to simulate the VDT controller.

7.2 Further efficiency considerations

The transmission efficiency work can be divided into two areas. Firstly, there are operating strategies which can be followed in order to optimise system performance through choice of transmission ratio and torque throughput. Secondly, the work described by Micklem (1994) and Guebeli (1993), can be implemented for improved transmission operation, in addition to the hardware optimisation of the transmission design itself. The work described below falls into the first area.

7.2.1 Transmission efficiency and its inclusion in the operating point optimiser

Transmission efficiency can clearly have a large impact on the complete powertrain system performance. Whether optimising for the best fuel economy or for low NOx emissions, larger than optimum transmission losses lead to a higher than necessary engine operating power and hence more fuel being used and more emissions being produced. The scale of potential savings which can be made by optimum choice of transmission ratio and torque throughput depends upon how much the efficiency varies across the operating envelope. This then, clearly required further investigation.

Micklem (1994) and Guebeli (1993) showed the predicted variation of transmission efficiency through use of the viscous shear model. For the purposes of the work described here it was desirable to map the transmission efficiency using the test rig.

For a fixed vehicle operating point in terms of speed, the powertrain variables are the engine speed and torque. Transmission ratio is inherently defined through the presence of both engine and vehicle speed. Vehicle load can be represented by considering vehicle power as one of the variables. This removes the need to specifically include engine torque since it is defined through the transmission efficiency. As a result of these considerations it was decided to map the transmission efficiency against engine speed and dynamometer power at fixed secondary pulley speeds.

Figure 7.11 shows the characteristic shape of the transmission efficiency map which is produced at a constant secondary pulley speed, whilst the engine speed and dynamometer power are varied. A neural network function was used for the purposes of smoothing the raw data in order to produce this figure. Figure 7.12 shows both the network generated surface and raw data points so that the validity of the smoothing function can be established. It is clear from this figure that there are areas of the generated surface for which there are no data points. This is due to those areas being unreachable in practice, for example full power at 1000 rev/min engine speed, and these areas should be ignored. The most prominent feature of the efficiency map is the valley of lowest efficiency at close to zero dynamometer power. Clearly as work done decreases, the magnitude of transmission losses will increase comparatively leading to this shape. The minimum efficiency points for each engine speed are not always at exactly zero kW on the dynamometer power axis. This may have been due to lack of resolution in measuring small transmission output torques. It was necessary to scale the transmission output torque transducer for the maximum possible output torques. The figure also shows that for most efficient operation of the transmission, it was best to operate the engine at as low a speed as was possible.

The process of designing and training of a neural network function to predict transmission efficiency was completed so that transmission efficiency could be taken into consideration by the operating point optimiser in the choice of the powertrain ideal operating point. The transmission efficiency prediction code was incorporated into the optimiser program and some comparisons of ideal operating lines were made. The NOx line was chosen principally for this investigation since it was the line of highest engine speeds with torques. Since Figures 7.11 and 7.12 point towards the use of lower engine speeds it was considered that the NOx line would be likely to undergo the greatest changes with inclusion of transmission efficiencies. Figure 7.13 shows the ideal operating line for low NOx emissions, with and without inclusion of the transmission efficiency. As can be seen there is very little difference between the positions of the two lines at engine speeds of above 1500 rev/min. Looking again at Figures 7.11 and 7.12, it is apparent that the efficiency rises steeply at low powers and settles out onto almost a plateau at medium and higher powers. Below 1500 rev/min, there is the greatest difference between the two lines. Part of this, then, is due to the incorporation of transmission efficiency. However, the optimiser code linearly interpolates in terms of speed for powers between each of the fixed power points on the ideal line. This is an approximation which may be exaggerating the differences between the two lines. Finally, however, in Figure 7.14 which shows the predicted clutch torque capability, it is clear that most of this region at less than 1500 rev/min is unreachable due to the constraints of the clutch operation. In addition to this, drivability considerations require that the engine operating line is one with a steady increase of delivered power with engine speed. For both of these reasons it was decided to complete the experimental investigations with the original engine operating lines.

7.3 Emission tests

Simulations of the European legislative drivecycle test were completed using the models of the powertrain and the alternative controller strategies. Analysis of emissions production in this way proved invaluable as a means of comparison of the alternative strategies. Table 7.2 shows a summary of the results of the drivecycle simulations and enables consideration of the relative quantities of emissions produced in the different tests.

7.3.1 The standard system

The legislation for the European emissions test states that the vehicle must have remained for several hours at 25 C prior to the test. This is termed a cold start. Cold starts and heat up during the simulated tests were performed by the use of a file of recorded engine coolant temperatures against time from a real emissions test on the vehicle dynamometer at Ford, Dunton. A comparative test was completed at a steady hot engine temperature of 85 C. Two alternative ideal operating lines were used in this work. They were the ideal line for NOx and the ideal line for fuel consumption and were chosen for the same reasons that they were chosen for the rig and vehicle experimental tests.

The first part of the table shows predicted emissions using the standard CTXE transmission. The first two tests show results using the Fuzzy logic controller and the ideal line for NOx. The results of the first test are marginally better. This is to be expected and is due to the engine being at operating temperature throughout the simulation. The results obtained show generally that there is improvement of NOx when using the NOx line and improvement of fuel consumption when using the BSFC line. The results using the transient shaping controller are generally better than those obtained using the fuzzy logic controller. This is especially true for the NOx or BSFC being optimised. The unoptimised emissions are also generally improved by the use of the transient shaping controller but this is less marked. The hydraulic controller (emulation of the VDT controller) produces the best NOx result overall but is worst for HC, particulates and fuel consumption. This would indicate perhaps that the VDT strategy coincidentally follows the NOx line (which is considered the better of the two lines for drivability), and does this more closely than either of the alternative strategies. The benefits of designing the transient shaping controller for close adherence to the ideal line would seem to have been shown by these results.

7.3.2 Optimising the clutch operating pressure

The second section of the table shows the benefits which can be achieved by improved control of the transmission clutch. This could be performed in reality by implementing electronic control of the clutch pressure. For these simulations it has been assumed that a higher clutch pressure can be achieved at lower engine speeds. This has then lowered the minimum usable engine speed and increased the amount of operation possible on the ideal operating lines at lower engine speeds. There is clearly a benefit shown in the NOx figures for the fuzzy logic controller with both operating lines. However the new clutch operating strategy produces a deterioration in the NOx figures using the transient shaping controller. The cause of this may be that use of the extra low portion of the ideal lines causes the powertrain behaviour to be more oscillatory. This would be especially true in the case of the transient shaping controller because of the engine speed feedback used in generation of torque demand one, Figure 6.4, Section 6.4.1.

The improved clutch operating strategy increases the fuel efficiency of the powertrain under control of both the fuzzy logic and transient shaping controllers when the BSFC line is in use. For the first time, fuel consumptions of less than four litres per hundred kilometres are predicted. The use of the improved clutch operating strategy with the BSFC ideal line produces benefits with all of the other emissions in each of the two tests except the NOx result using the transient shaping controller.

7.3.3 Lowering the secondary pressure

Work completed by Micklem (1994) and Guebeli (1993) showed that lowering the transmission secondary pressure produced efficiency benefits. The simulation results presented in this, the third section from the table, are from tests where the secondary pressure demand was generated using three quarters of the original demand from the VDT algorithm. This is not optimised and it is expected that further gains could be made by implementation of a secondary pressure optimisation strategy as discussed by Micklem and Guebeli. The new, lower secondary pressure levels produce savings in fuel consumption on all four tests, both those where optimisation was for BSFC and also in the tests which used the NOx ideal line. The same is also true of the values of NOx emissions predicted. Figure 7.15 shows the transmission variables in two tests, one with the lowered secondary pressure. It can be seen that although the variable values are different, there is not excessive belt slip in the simulated test with the reduced secondary pressure.

7.3.4 Improving the transmission ratio range

A set of simulations was run with a modified transmission model to investigate the effect of increasing the ratio range on the emissions and economy performance of the vehicle. The modification was performed by reducing the allowable secondary pulley minimum radius from 0.032 m to 0.016 m. The effect of this change on the emissions performance was to improve the NOx value in each of the tests where the NOx ideal line was being used. This improvement did not carry across to the fuel consumption figures in the tests which used the BSFC ideal line. This would indicate that the use of the lower part of the ideal line during the high vehicle speed part of the test, which was enabled by the extended ratio, is not, in this case, a major factor in the determination of the fuel economy figures.

7.3.5 Simulations with all three improvements

Individually the lowering of the secondary pressure seemed to produce the greatest benefit of the three changes. However, the forth section of the table shows the results of simulations which were completed with all three of the above changes implemented. Each of the different modifications has been shown to give varied amounts of improvement and by combining them, the improvements tend to accumulate. The best predicted results for both fuel consumption and NOx emissions were produced from these simulated tests.

7.3.6 Lowering the engine inertia

A brief investigation was carried out into the effect of engine inertia on the vehicle emissions and economy performance. This was performed using the transient shaping controller, the NOx ideal line and an engine inertia of one half the normal value. This reduction gave a definite improvement in the predicted NOx value for the drivecycle. At the same time, there was also an improvement in the fuel consumption. Reduction of the engine and flywheel inertia is in practice a trade off between the benefits shown here, improved drivability and the degradation of vehicle NVH due to increased engine vibration.

7.4 Summary

The simulation environment proved to be invaluable in the design and initial development of all of the alternative controller strategies. It made possible the impartial selection of the Fuzzy and Transient shaping controllers for further study and implementation. In addition to controller development, the powertrain model made possible many investigations, into issues such as powertrain efficiency. These would have been impractical, if not impossible, using the test rig or vehicle.

Criteria for Comparison of Controllers	
Using Simulation	
1	Simulation emissions/economy performance
2	Time to achieve ideal operating line after disturbance
3	Vehicle performance during acceleration and overrun
4	Ease of tuning
5	Robustness
Using Rig Test	
1	Rig emissions/economy performance
2	Time to achieve ideal operating line after disturbance
3	Vehicle performance during acceleration and overrun
4	Ease of tuning
5	Robustness
Using Vehicle Test	
1	Subjective vehicle drivability testing
2	Chassis rolls emissions/economy performance
3	Time to achieve ideal operating line after disturbance
4	Vehicle performance during acceleration and overrun
5	Ease of tuning
6	Robustness
General	
1	Portability to other powertrain/vehicle combinations
2	Number/type of transducers, cost hardware
3	Safety

Table 7.1 Controller selection criteria

Controller strategy	Cold/Hot start	Ideal line used	Vehicle distance km	HC g/km	NOx g/km	PM g/km	HC+NOx g/km	Fuel l/100km
Simulations using basic CTXE transmission								
Fuzzy logic	hot	NOx	11.21	0.135	0.494	0.134	0.628	4.068
Transient shaping	hot	NOx	11.23	0.141	0.475	0.138	0.615	4.144
Fuzzy logic	cold	NOx	11.21	0.139	0.494	0.140	0.634	4.174
Fuzzy logic	cold	BSFC	11.22	0.137	0.594	0.141	0.730	4.155
Transient shaping	cold	NOx	11.22	0.139	0.421	0.136	0.560	4.138
Transient shaping	cold	BSFC	11.22	0.133	0.491	0.132	0.624	4.079
Van Doorne	cold	n/a	11.22	0.147	0.410	0.141	0.557	4.197
Predicted % improvement using improved clutch model allowing improved ideal line and minimum engine speed								
Fuzzy logic	cold	NOx	-4.4	2.9	19.7	5.8	16.0	-0.4
Fuzzy logic	cold	BSFC	-4.5	3.1	19.9	6.9	16.7	3.9
Transient shaping	cold	NOx	-0.4	0.8	-6.3	-0.4	-4.5	0.3
Transient shaping	cold	BSFC	-0.1	1.2	-5.5	0.7	-4.1	3.5
*Predicted % improvement using lower secondary pressures (0.75 * VDT algorithm)*								
Fuzzy logic	cold	NOx	-0.2	4.4	19.6	7.5	16.2	3.6
Fuzzy logic	cold	BSFC	-0.1	3.1	17.5	6.4	14.8	2.5
Transient shaping	cold	NOx	0.0	1.3	4.1	2.1	3.4	1.6
Transient shaping	cold	BSFC	0.0	1.2	3.6	1.7	3.1	1.3
Predicted % improvement using increased transmission ratio range								
Fuzzy logic	cold	NOx	-0.3	-1.1	9.3	1.4	7.0	-0.5
Fuzzy logic	cold	BSFC	-0.1	-3.4	-7.4	-2.9	-6.6	-2.9
Transient shaping	cold	NOx	0.1	-0.2	2.0	0.5	1.5	0.1
Transient shaping	cold	BSFC	0.0	-3.6	-13.9	-4.2	-11.7	-2.7
Predicted % improvement using all three of the above improvements								
Fuzzy logic	cold	NOx	-5.2	3.3	26.2	7.5	21.2	-1.0
Fuzzy logic	cold	BSFC	-4.9	1.4	10.1	5.3	8.5	4.1
Transient shaping	cold	NOx	-1.8	3.3	4.2	3.7	4.0	3.3
Transient shaping	cold	BSFC	-1.8	5.3	-6.3	5.7	-3.9	9.9
Predicted % improvement with reduced engine inertia and using basic CTXE transmission								
Transient shaping	cold	NOx	-0.1	-0.1	18.6	3.9	14.5	1.0

Table 7.2 Predicted drivecycle emissions results

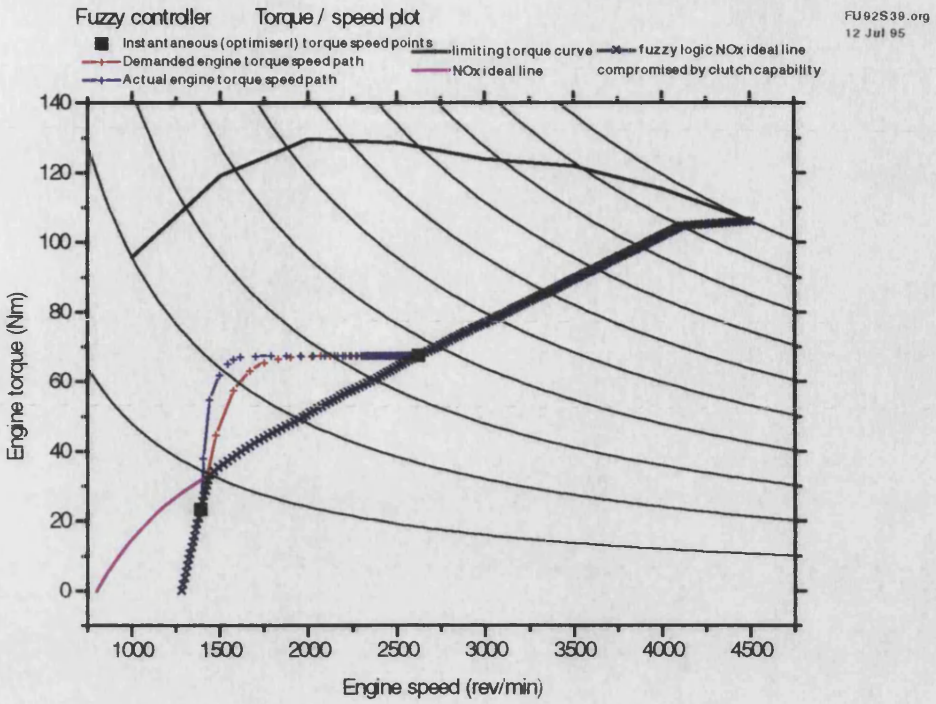

Figure 7.1 Fuzzy logic controller - predicted engine path followed during transient

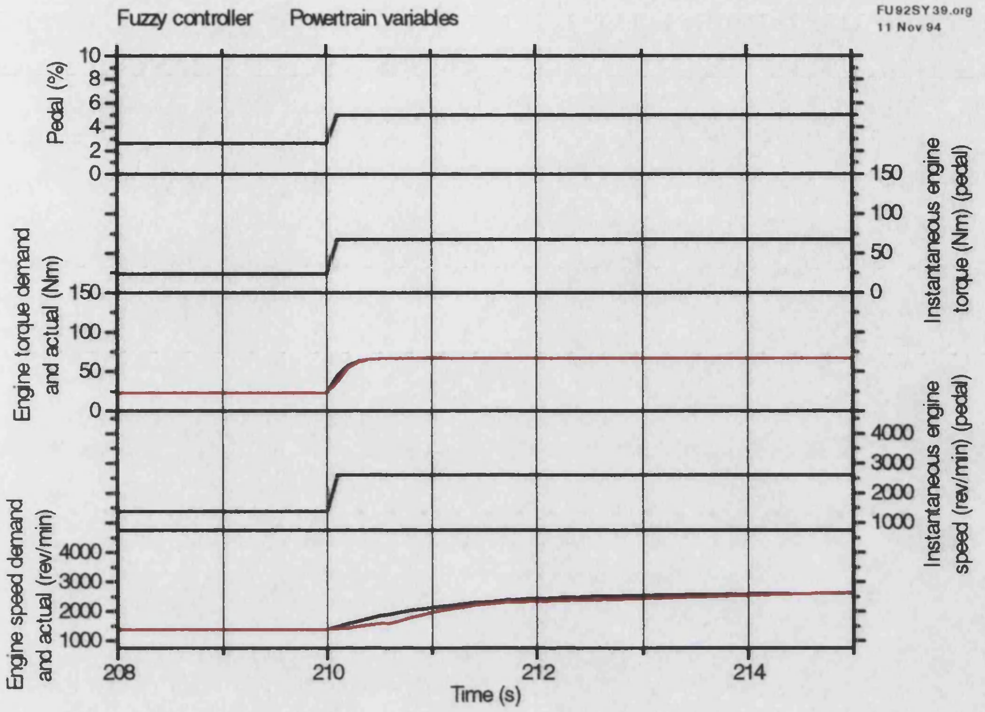

Figure 7.2 Fuzzy logic controller - predicted powertrain responses against time
Black = demand, Red = actual

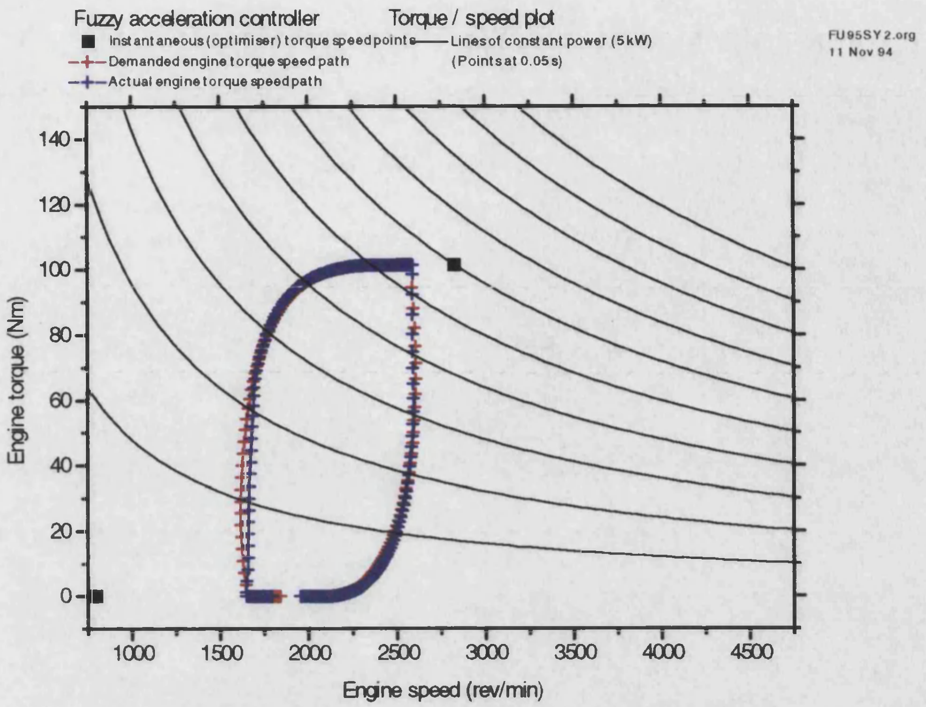

Figure 7.3 Initial fuzzy acceleration controller simulation results

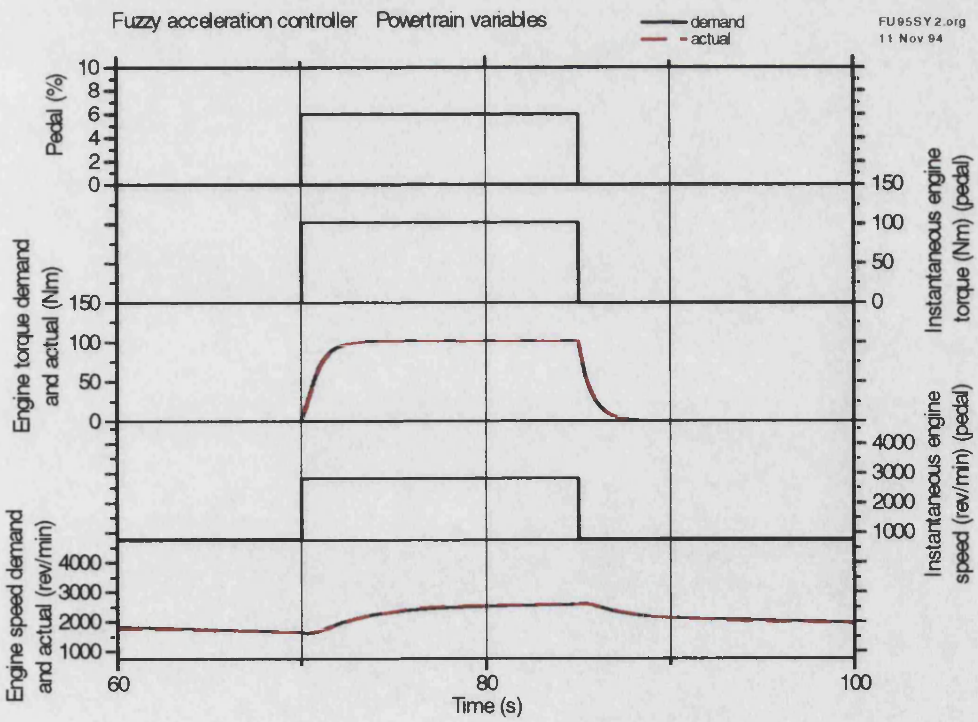

Figure 7.4 Initial fuzzy acceleration controller simulation results

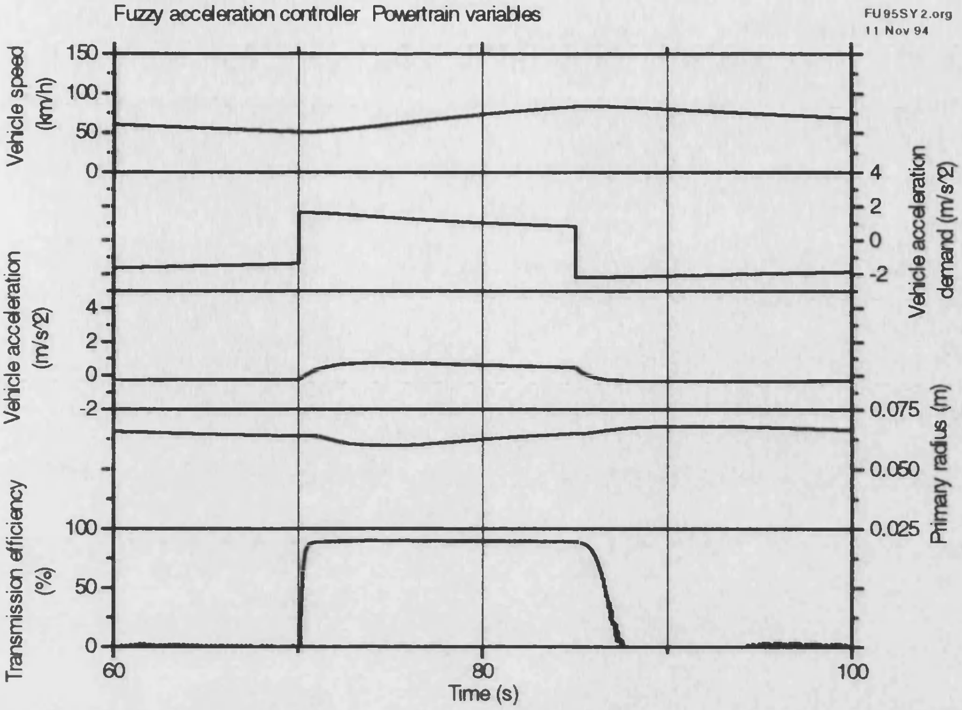

Figure 7.5 Initial fuzzy acceleration controller simulation results

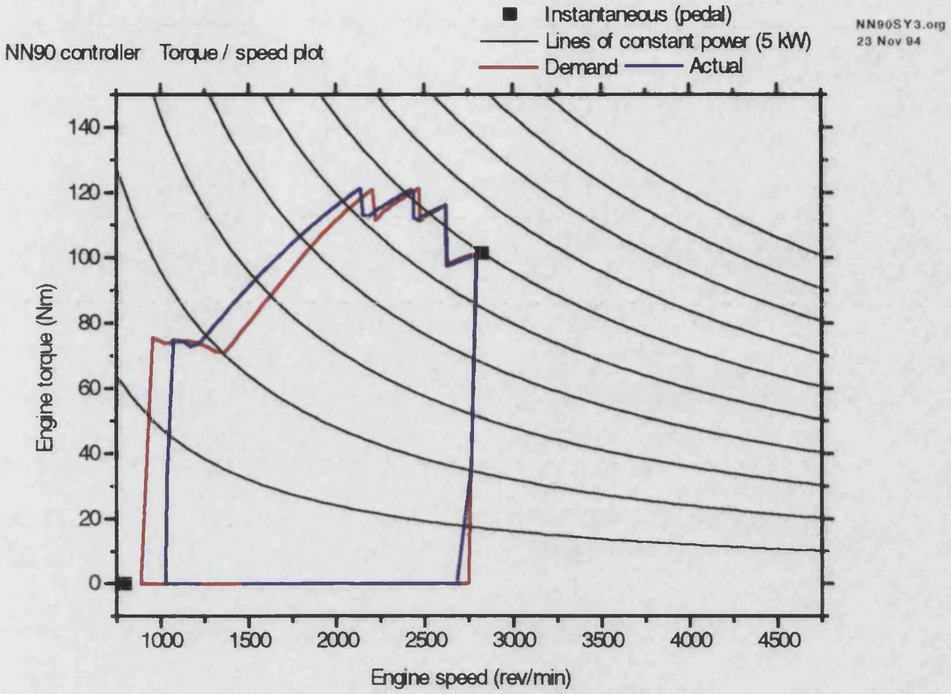

Figure 7.6 Initial transient shaping controller simulation results

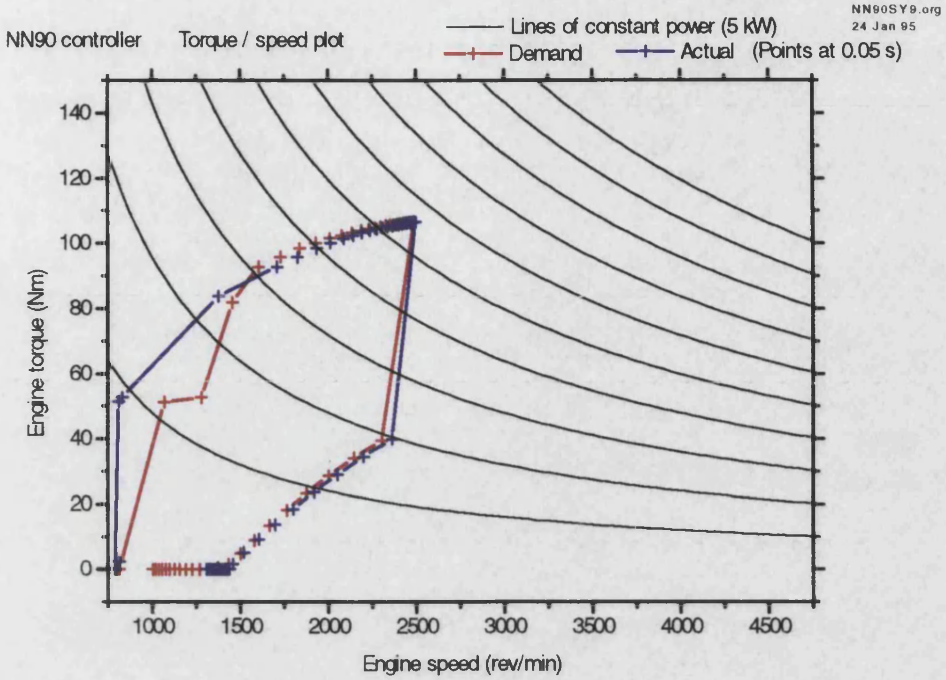

Figure 7.7 Transient shaping controller simulation results (using the smooth trimming functions)

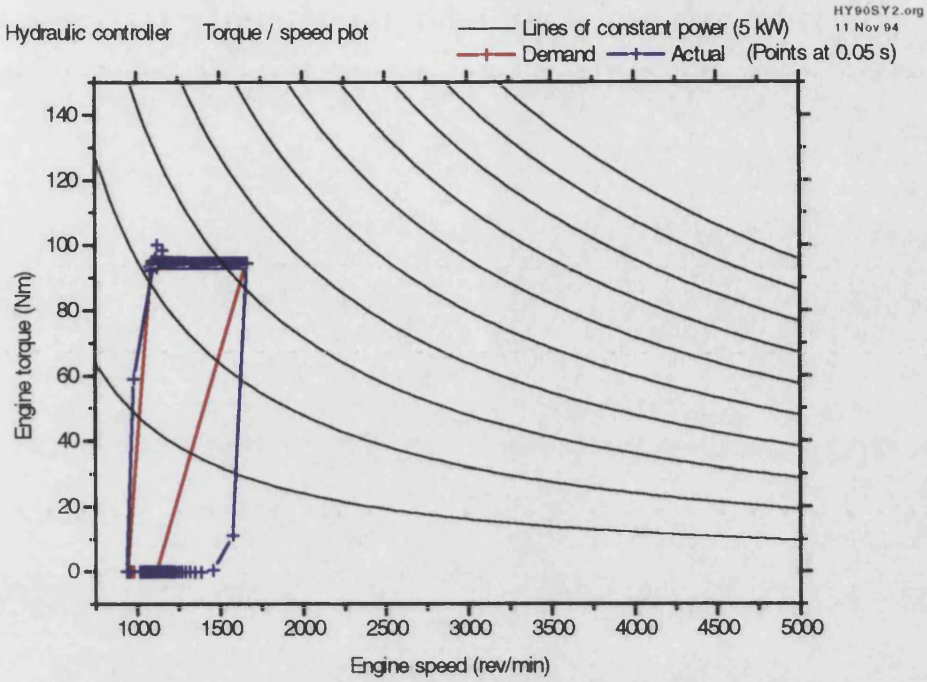

Figure 7.8 Initial hydraulic controller simulation results

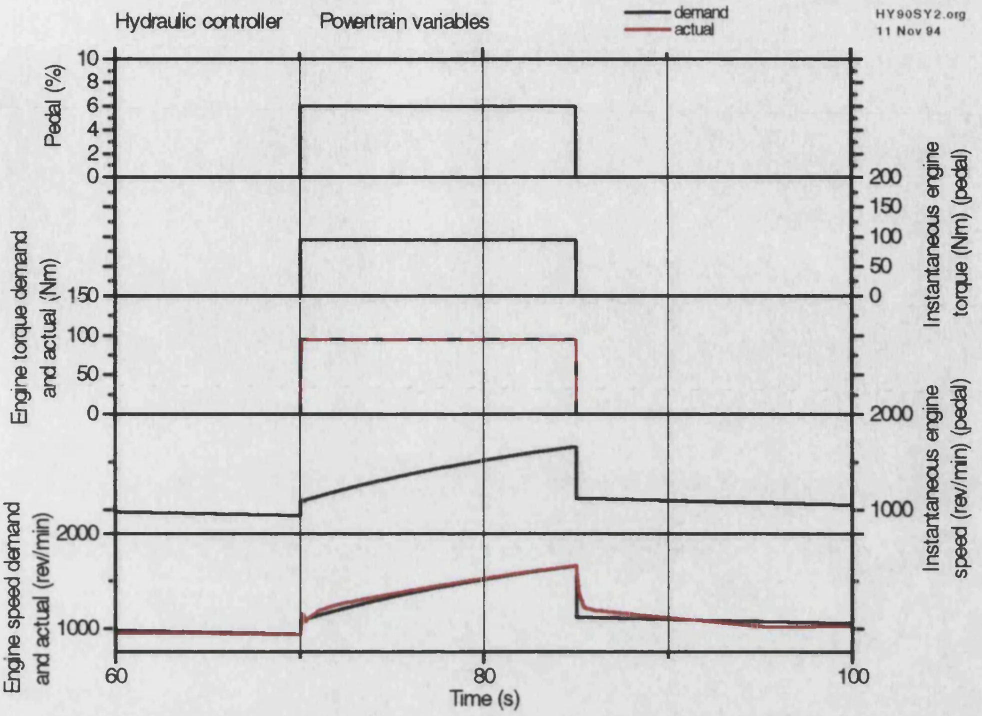

Figure 7.9 Initial hydraulic controller simulation results

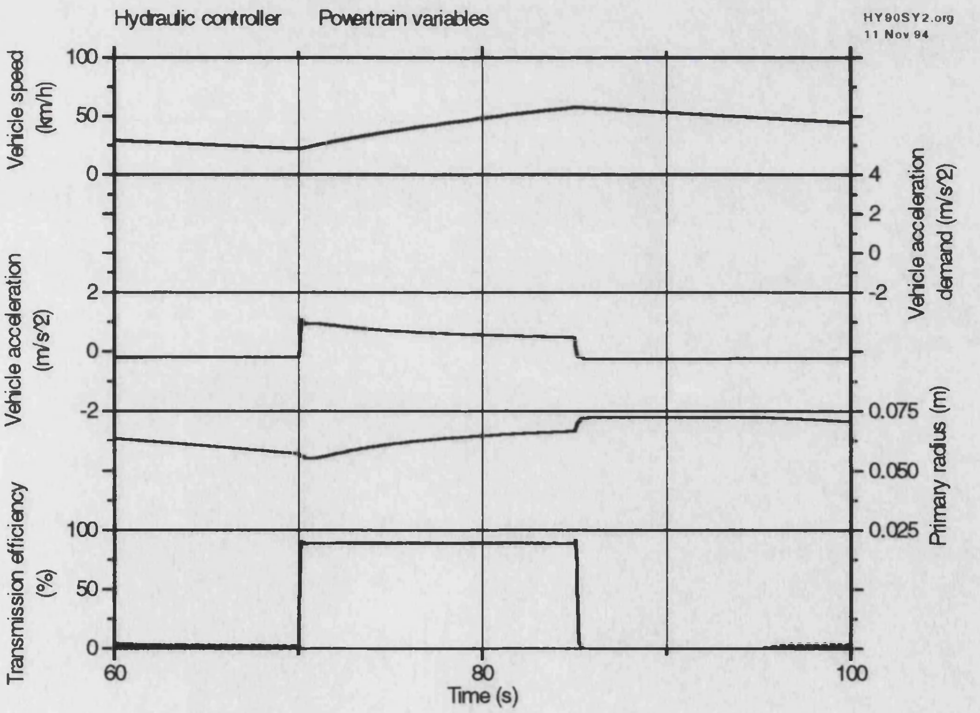

Figure 7.10 Initial hydraulic controller simulation results

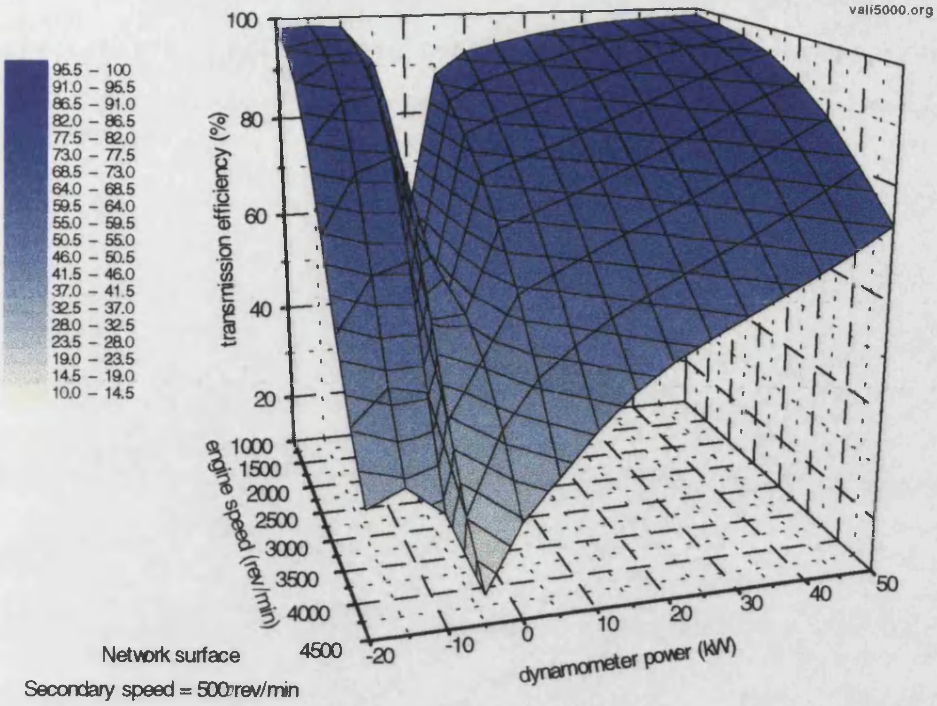

Figure 7.11 Neural network prediction of transmission efficiency

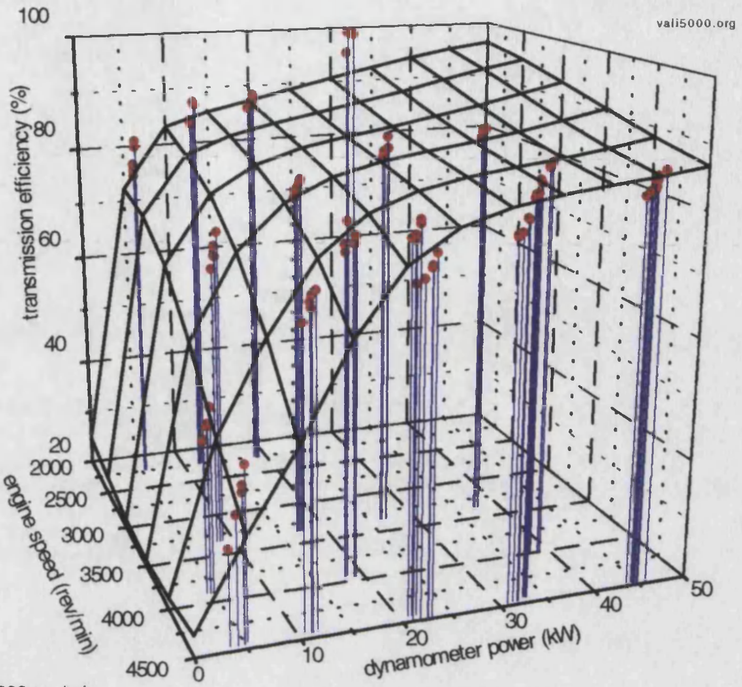

Network surface
Secondary speed = 5000 rev/min
Experimental data (secondary speed from 4000 to 5000 rev/min)

Figure 7.12 Neural network prediction of transmission efficiency with rig data

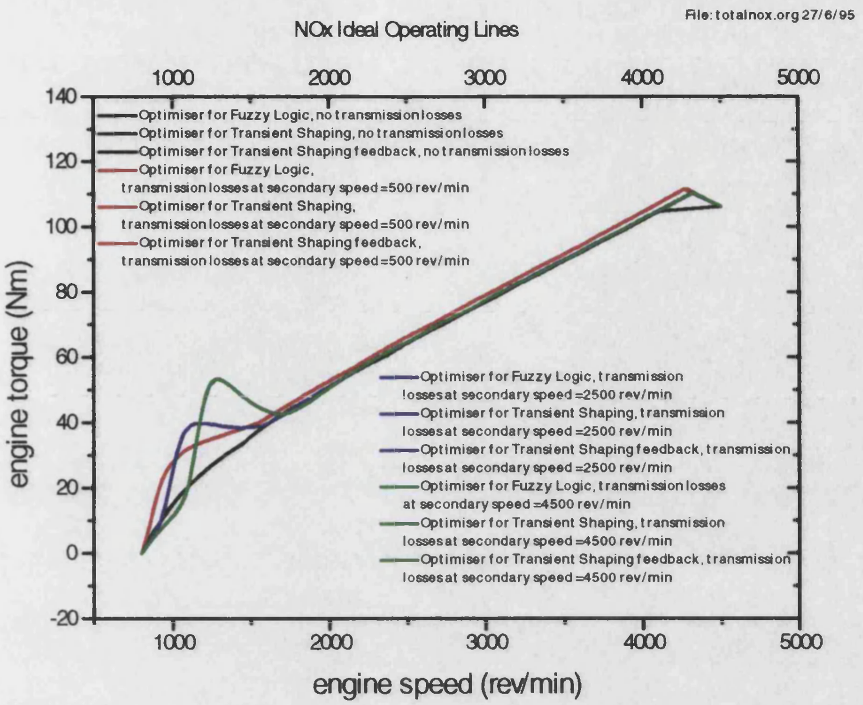

Figure 7.13 Transmission efficiency effect on ideal NOx operating line

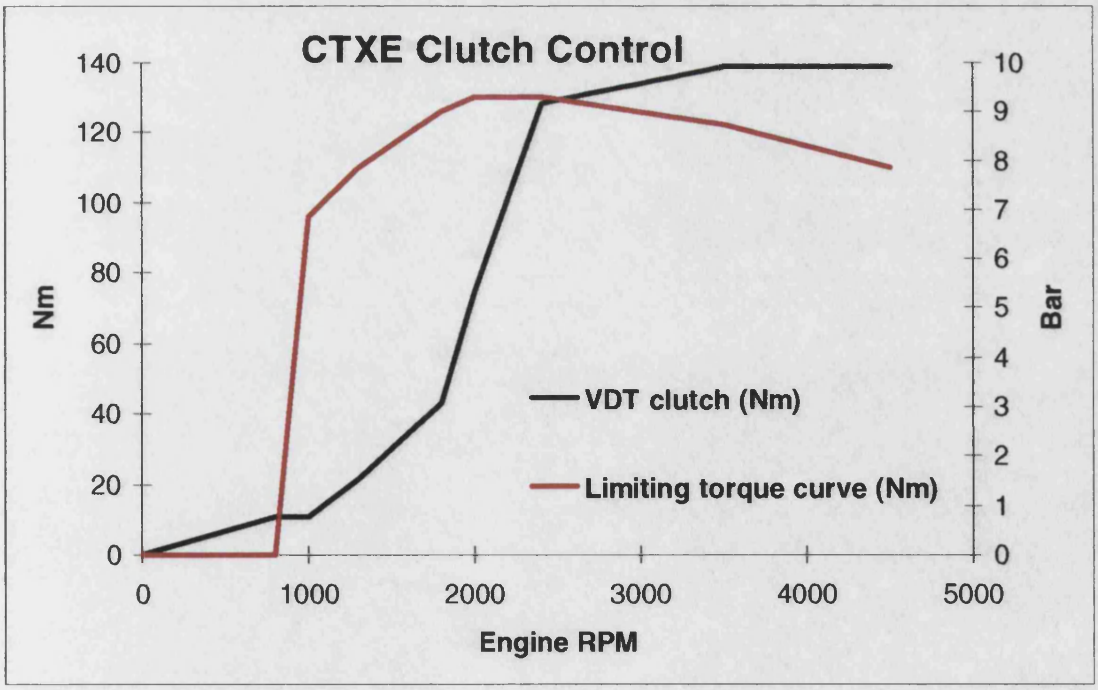

Figure 7.14 Prediction of clutch capability to transmit torque

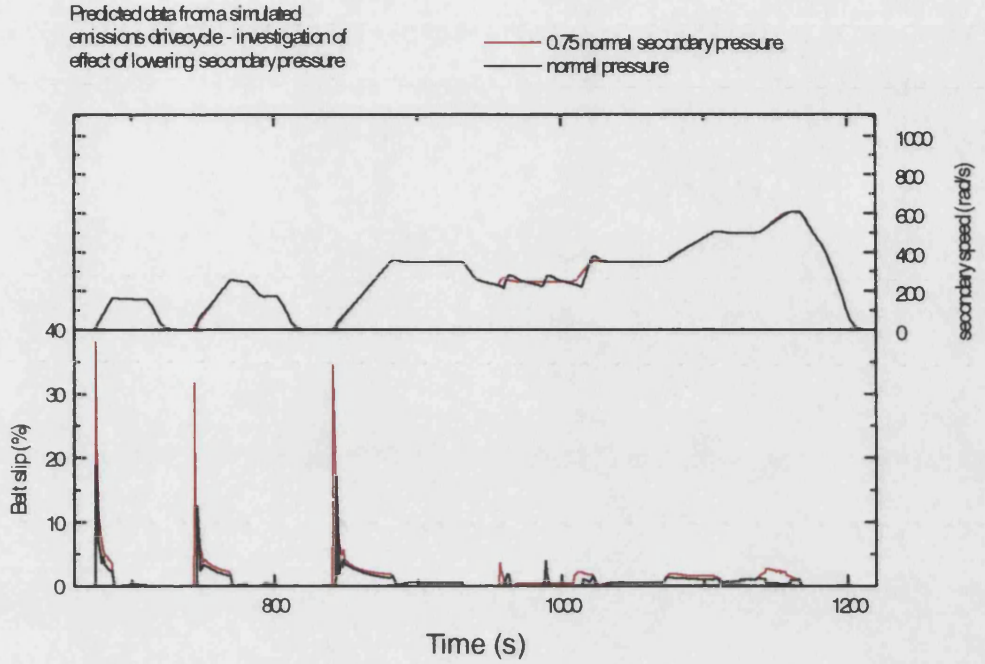

Figure 7.15 Predicted powertrain operation with lowered secondary pressure

8. DISCUSSION OF EXPERIMENTAL RESULTS

This chapter begins with a discussion of the issues connected with the practical implementation of the newly designed controllers. The interaction of the strategies with both the VDT and EPIC controllers and the generation of a powertrain demand from the accelerator pedal position is described. The development of algorithms for improved engine speed control and the prevention of clutch slip at low engine speeds are discussed prior to the presentation of some initial rig tests of the Fuzzy logic, Transient shaping and VDT controllers.

The second section of this chapter is used for the presentation of emissions test results. The European legislative emissions test was emulated on the test rig and performed on the vehicle using a chassis dynamometer. The two environments each enabled comparison of the three controller performances in terms of powertrain emissions.

The drivability work is the subject of this chapter's closing section. The two appraisals completed over the duration of the powertrain project are discussed. The results are presented and analysis follows.

8.1 Controller implementation

8.1.1 Practical issues

Mapping of VDT and EPIC controller algorithms

The controller architecture described in Section 5.4 utilises both the EPIC fuel injection control system and the VDT low level control module. It was necessary to map the operation of the EPIC and VDT controllers to ensure that the correct levels of demanded signals were fed to these two units when they were used in conjunction with the newly designed supervisory controllers.

Firstly in the case of the EPIC system for control of the engine torque, the engine was mapped at many steady state normal operating points across the speed and load range. The relevant variables recorded were the engine speed, the EPIC system demand signal and the engine torque developed. From the data, an algorithm was developed such that the correct EPIC demand signal could be generated by the supervisory controller for the desired torque at the current engine speed. There were, however, several disturbing influences on the mapped relationship. Firstly, the detailed mapping was carried out on a different test rig from that used for the comparison of the controller strategies. Secondly, it was not possible to guarantee that all of the relevant engine variables were always at the same values during normal operation as they had been during the mapping. For example, if the level of intercooling was slightly different from its value during the mapping, this could have a significant effect on the engine torque developed.

Secondly in the case of the VDT control module, it was necessary to ascertain the relationship between the demanded primary speed and the actual value of the primary speed. From work completed using the transient rig this relationship appeared to be independent of both the transmission ratio and the torque transmitted. Values of offset and gain between the demanded and actual steady state values were determined with fair accuracy. However, there did seem to be some unpredictable hysteresis present in the system and it was for this reason that the speed integral algorithm was developed, described below.

The mapping process was repeated for the vehicle application of the VDT control module, since the different transmission unit seemed to have a slightly different level of response to demanded primary speeds. However, since it was not possible to accurately measure the torque in the vehicle, the EPIC demand algorithm remained as it was developed using the rig.

Pedal algorithm for generation of power demand

For the reasons discussed in Section 6.7, the steady state power demand was generated as a function of both pedal position and engine speed. An initial algorithm was applied to the pedal input signal giving the ability to change the pedal sensitivity across the range of pedal positions. The output of this calculation was then combined with the engine speed signal to generate the demanded power as shown in Figure 6.11.

A disadvantage of including the engine speed feedback signal in the calculation of demanded power was that the demanded power could change at constant pedal position as a result of engine speed perturbations. As engine speed increases, demanded power decreases. Although this characteristic had no effect on steady state operation on the ideal operating line, it affected transient powertrain control and would probably have had an effect upon drivability. In order to remove this effect, the original relationship between pedal signal and power demand, as described by Equation (6.15) was used in some of the further work

Further study is required into the best way of generating a powertrain demand from the accelerator pedal position. The different methods described above were satisfactory for the work described here. However it was shown by the drivability study that the pedal algorithm had a significant impact on the driver perception of the vehicle drivability.

Use of integrator for improvement of engine speed control

Part of the lower level module of the VDT controller (Section 5.4 and Figure 5.8) was used in the engine speed control loop. Although this gave a reasonable response in transient conditions, it was unable to produce the steady state engine speed accuracy required. Figure 8.1 shows a test completed with the VDT controller alone attempting to control the engine speed.

It was decided to introduce an integral term into the speed control loop in order to improve the steady state accuracy of the engine speed control. The value of the term was kept low to minimise its effects upon the transient control of the engine speed. Figure 8.2 shows a test completed with the integral term included in the speed control loop. The target engine speed is now achieved, although the response is perhaps more oscillatory. Figure 8.3 shows a transient in which the integral term is clearly too great and the response is much more oscillatory.

From the work described in Chapter 3, it was concluded that engine speed changes have a definite impact on the driver and his or her perception of the vehicle drivability. Clearly then it is important then that the correct compromise is made between powertrain control in transient and steady state situations, since engine speed oscillation would have a negative impact on vehicle drivability.

In the experimental tests, the integral term described above was set to the maximum level possible without the engine speed becoming oscillatory. This enabled good steady state accuracy with a minimum degradation of the transient performance. Recorded tests such as those shown in Figures 8.1 to 8.3 were used to subjectively choose the appropriate integral term gain.

Use of an algorithm for preventing clutch slip

Figure 8.4 shows the clutch hydraulic pressure profile which was an inherent characteristic of the CTXE transmission. Although small adjustments to this may have been possible, the ideal position of having full electrohydraulic control of clutch pressure was outside of the scope of the work described here. This meant that that the maximum torque transmissible by the clutch was a function of hydraulic pump speed and hence engine speed. A prediction of this is shown in Figure 7.14. By comparing Figure 7.14 with the ideal engine operating lines in Figures 5.1 to 5.5, it is clear that some compromise must be made, since the clutch is not capable of transmitting many of the ideal operating line engine torques at low engine speeds. Figure 8.5 shows how two of the ideal operating lines are compromised in their lower speed sections.

It was discovered through investigation using the vehicle, that the predicted clutch torque transmission capability shown in Figure 7.14 was lower than in reality. As a result of this it was decided to develop a piece of software within the controller code which would continually move the engine operating point towards the true ideal line at low engine speeds until it detected the start of clutch slip. This was completed and enabled the full use of the clutch torque transmission capability and meant that the smallest change possible was made away from true ideal line operation at low engine speeds.

Choice of ideal operating lines

It was possible to find an optimum engine torque and speed point to produce a particular demanded engine power by taking into account any weighted combination of the engine emissions of unburned hydrocarbons, nitrogen oxides, particulates and smoke and engine brake specific fuel consumption. Loci of the optimum points as already discussed produce engine ideal operating lines. Figures 5.1 to 5.5 show the engine ideal operating lines produced by taking into account only one of each of the emissions and fuel consumption at any one time. The graph clearly shows that the differently optimised ideal lines are dispersed across a range of torque speed combinations. The two most different lines are the line for minimum NOx production and the line for minimum BSFC. The NOx line tends to be more in the high speed low load part of the map where cylinder pressures and temperatures are low and hence NOx production is at a minimum. The BSFC line follows the maximum torque curve of the engine more closely. At low engine speeds, engine friction is at a minimum and the line is a function of this and combustion quality considerations. For much of the work described in this Chapter it was decided to use only these two ideal operating lines. The use of the most extreme lines was considered to be the most testing in terms of the control strategies and hardware and was also thought to be likely to reveal the most useful information in the drivability work. The discussion in Chapter 9 covers the effects of engine operating lines on vehicle drivability. From the points made, it can be predicted that the NOx ideal operating line would give the better vehicle characteristics in terms of drivability and performance.

Pedal/controller busyness

The algorithm used to change the pedal busyness, Section 6.7.2, was used only for demonstration purposes. During the results presented here, the value of the pedal busyness was kept constant so that other powertrain and controller characteristics could be analysed without disturbance from this source.

8.1.2 Performance

Fuzzy logic controller rig test example

Figures 8.6 to 8.9 show a test of the Fuzzy logic controller completed on the rig. In this test the power demand was generated according to the linear algorithm involving accelerator pedal signal level. The pedal sensitivity and busyness algorithms, Section 6.7, were set to medium values and the speed integral term and the clutch slip algorithms were both switched off. The operating line optimiser was set to minimise NOx emissions.

Figures 8.6 and 8.7 show the time response of the powertrain to a step increase in accelerator pedal signal. During the first few seconds of the test, conditions are stabilised with the pedal at about one quarter of its full scale value. The engine and vehicle speeds are steady and the transmission clutch is not slipping. The raw measured torque signals do exhibit cyclic variations of significant amplitude although these are not matched by any such variation in the EPIC fuel signal. FFT filtering was used to reduce the noise on the measured torque signals. There are small steady state errors between the demanded and actual engine torques and speeds. Following the step increase in accelerator pedal signal, the demanded values of engine speed and torque start to change immediately. The demanded and actual values of engine torque move quickly towards the new ideal value with no overshoot. The settling time to the new torque value is less than two seconds. As before there is a small steady state error. The engine speed takes five or six seconds to reach a new steady state value, again with a small error. The actual value lags the demand slightly and there is no overshoot. The vehicle speed increases gradually following the pedal signal change. The acceleration is smooth and at a gentle rate.

The paths taken by the controller demand and the engine in the torque speed domain are shown in Figure 8.8. The initial and final ideal points on the low NOx operating line are clearly marked. The demand starts at the lower of these and moves immediately to the actual level of engine speed since this is higher and the new ideal point is in this direction. Section 6.6.3 gives the equations governing this action together with its purpose. The demand then continues to move toward the new ideal point, the torque being increased ahead of the speed. The actual path followed by the engine also follows this trend. This is shown using both the torque calculated from the EPIC fuel demand and the filtered value from the torque transducer. The initial and final engine operating points are only close to and not actually on the ideal line. The small steady state errors result from the hysteresis present in the operation of the VDT low level controller and from the approximations used in the mapping of the EPIC fuel demand to engine torque relationship.

Figure 8.9 shows the levels of production of NOx both with respect to time and to vehicle distance travelled. The trace showing NOx in g/km was generated by calculation of the amount of NOx produced and the dynamometer equivalent to the vehicle distance travelled in each data acquisition interval. The value measured was steady before the step increase in pedal. After the change, there is an increase in the NOx produced, the trace being affected by the transport delay in the movement of the gas to the analyser. The NOx emission level settles at a new value corresponding to the new engine operating point. There is a downward trend in the production of NOx per kilometre as the dynamometer speed increases.

Transient shaping controller rig test example

Figures 8.10 to 8.11 show a test which was similar to that described above. This time however, the Transient shaping controller was used. The vehicle pedal signal change was of a similar level of magnitude as above, the initial level being slightly different in order to achieve a similar initial dynamometer speed. The clutch slip algorithm was in fact active, but this had no effect during the portion of the test being analysed. The ideal line for low NOx emissions was used as before.

Stable conditions were achieved before the pedal increase, but with some steady state errors between the demanded and actual engine torques and speeds existing. As with the above test, the raw measured torque signals showed moderate cyclic variations, although the speed and fuel signals do not undergo similar changes. There are steady state errors between the demanded and actual values of engine speed and torque.

There is an immediate response to the increase in pedal position. The torque demand undergoes a large increase to a value greater than the ideal. This is due to the influence of the trimming torque function which is designed to provide sufficient additional torque to drive the powertrain through the transient, Section 6.4.2. The torque demand is held at this new higher level for some ten seconds before being gradually reduced to the new ideal level. The engine speed demand is gradually increased to the new ideal level over a period of about five seconds. The actual speed also increases gradually, and with no overshoot, due to the demand change and the extra torque available. There are final small steady state errors between the demanded and actual values of engine torques and speeds. The vehicle speed increase is gradual and immediate following the pedal signal change. Again the acceleration is smooth and the rate low.

The levels of NOx emissions measured during this test are shown in Figure 8.13. The levels with respect to time and vehicle distance both seemed stable prior to the accelerator pedal increase. Following this there is a definite rise in both traces, the level per kilometre decreasing slightly as the vehicle speed increases.

Figure 8.12 shows the paths followed by the controller and engine on the engine torque speed map. The target points on the ideal low NOx line are marked. The shape of the path taken by the controller during the transient is mimicked by the engine, the path of which is plotted using both the predicted torque from the fuel signal and the filtered torque transducer signal. This plot emphasises how quickly the torque is increased compared with the engine speed. This characteristic would clearly have an impact on the drivability and performance feel of the vehicle.

Van Doorne controller rig test example

Figures 8.14 to 8.17 show data recorded during a test of the VDT controller on the rig. The engine torque and speed changes following the step increase in pedal are shown in Figure 8.14. There is an immediate response of the powertrain to the increase in demand. The engine speed increase takes place over about five seconds and there is no overshoot. The engine torque increase is much faster and to a level in excess of the final level to which it then decreases. The equivalent of vehicle speed increases smoothly and at a gentle rate following the pedal increase.

Figure 8.17 shows the NOx emission levels. The levels with respect to time and vehicle distance increase markedly following the pedal increase, before falling gradually to new levels. The peaks of NOx production taking into account transport delays correspond with the pedal increase and the peak power delivery.

The traces followed on the torque speed plot are shown in Figure 8.16. Although no emissions optimum line is being actively followed, the VDT controller does tend towards steady state demands close to the ideal NOx line, certainly during this test in the low power area of the engine map. Paths were generated using both the EPIC fuel signal and the filtered torque transducer signal. The transient change is made up of two sections. Firstly there is a fast increase in torque whilst the engine speed is increased more gradually. Secondly the torque is reduced to a final level while the engine speed change is completed.

Discussion

The results presented above have shown that the differences in the alternative controller strategies have a significant impact on the shape of the path followed by the engine on the torque speed map during a transient. The trends which were apparent in the simulation studies have been confirmed by this experimental work. The differences between the stategies are expected to have an impact upon drivability, and can be seen to have an impact on the formation of emissions. Clearly, for an accurate comparison of these alternative strategies to be made, they must be subjected to identical tests both on the rig and chassis dynamometer in the case of emissions assessment and in the vehicle for the assessment of drivability.

8.2 Emissions tests

8.2.1 Rig emissions test results

The test rig, Chapter 2, was used to assess the emissions control potential of the different strategies over the legislative European emissions drivecycle. This was enabled by a drivecycle control program which was developed and run on a test rig computer. Dynamometer speed was compared with the drivecycle speed versus time file and the difference was used in an algorithm to calculate the accelerator pedal signal value. The same program also had the capability of controlling engine temperature and intercooler effectiveness with reference to files and thus enabled realistic cold start legislative tests to be performed.

Fuzzy logic controller

Figures 8.18 to 8.21 show some data which represent the European test performed by the powertrain on the rig under the supervision of the Fuzzy logic controller. The vehicle pedal signal, Figure 8.18, is fairly steady during each of the steady state vehicle speeds of the test. The engine torque seems to follow the demand fairly closely with perhaps some experimental error and offset. The demanded and actual engine speeds are coincidental almost all of the time that the clutch is engaged. The only major difference in actual and demanded speeds occurs towards the end of the test and is due to the overdrive ratio limit of the transmission. The low NOx ideal line was used in this test. If a more high load, low speed ideal line had been used, the transmission ratio limit would have caused greater difference between the demanded and actual engine speeds. In Figure 8.18, the characteristic shape of the test can be seen in the actual dynamometer speed. The errors between the actual and demanded speeds are considered negligible. Dynamometer load is also plotted.

Figure 8.19 shows some of the appropriate variables on a torque speed graph. The characteristic shape of the ideal NOx line is present in the output from the optimiser software. The demanded operating points coincide very well with the line most of the time. This gives an indication that this legislative test generally requires low power from the engine and that the transients are not very harsh. Both the actual and predicted operating torque speed points follow the shape of the line well although both are slightly low perhaps due to experimental error and inaccuracies.

The totalised emissions measured during this test are plotted in Figure 8.20. The NOx emissions increase gradually during the low speed section of the test before increasing more rapidly during the latter high speed section. The final value was 5.5 grams. The HC emissions increase more evenly throughout the test. More emissions seem to coincide with the accelerations, particularly away from rest. The final HC figure was 1.35 grams. The particulates increase very rapidly at the end of the test and are steadier, earlier on. Engine stalls at about 150 and 600 seconds seem to have unfairly increased the result. The final figure was 0.58 grams but this could be arguably corrected to nearer 0.5 grams. Finally the total fuel used was 450 grams. This increased at the greatest rate during the final part of the test.

Figure 8.21 shows the equivalent vehicle speeds and distance travelled. This totals 9.8 km. The total for the test should be 11.2 km. However, there are tolerances for the vehicle speed during the test which can also account for a different distance travelled at the end of the test. The emissions in grams per hour are also presented on this plot.

Transient shaping controller

A test similar to that described above was completed using the Transient shaping controller rather than the Fuzzy logic controller. All other conditions on the test rig were kept as constant as possible between the two tests. Figures 8.22 to 8.25 show the data representing the test results. The vehicle pedal signal, Figure 8.22, follows a similar trace to that of the Fuzzy logic controller test. It is, however, more oscillatory, suggesting that the transient shaping controller gives a more rapid or sensitive response to accelerator pedal movements. The torque traces show good correlation between the demanded and actual torques in the higher section of the range. At lower torques, there appears to be a steady state offset error, but this is coincident with the periods of idle, and therefore more due to torque transducer calibration than quality of engine torque control. The actual engine speed follows the demanded quite well particularly during the steady state sections of the test. The most notable exceptions appear to be during idle, hard engine acceleration, and deceleration of the vehicle where the engine speed is ratio limited. Figure 8.22 also shows the dynamometer speed and load.

The engine torque speed points are plotted in Figure 8.23. As before the shape of the ideal NOx line is clearly followed. There is more of a scatter of the torque points demanded and visited particularly at low speed, and the maximum engine speeds reached are not as high as before. The reason for extra scatter is probably due to the torque trimming function giving a greater variation of demanded torques during the transients than occurred using the fuzzy logic controller. However, a greater scatter during transients may be offset by greater adherence of the engine to the ideal operating point during steady state conditions.

Figure 8.24 shows the totalised emissions measured during the test. As in the Fuzzy logic controller test, the NOx emissions increase gradually during the slow speed section of the test and more rapidly during the high speed section. The final value was 5.2 grams. This was a slight improvement on the Fuzzy logic controller result. The HC emissions increased steadily throughout the test finishing up at 1.25 grams, again slightly better than the Fuzzy logic controller result. As before, the particulates increased more rapidly at the end of the test, the final value being 0.35 grams. This was far better than the fuzzy logic controller recorded figure, and also better than the fuzzy logic controller figure corrected for the engine stalls. The total fuel used was 490 grams which was worse than the fuzzy logic controller figure.

The vehicle speeds and distance travelled, Figure 8.25, were very similar to the values obtained in the Fuzzy controller test above. The traces are almost indistinguishable. The emissions in grams per hour are also presented here.

Van Doorne controller

The Van Doorne controller was used in a final test made as similar as possible to those completed using the Fuzzy logic and Transient shaping controllers. The results are presented in Figures 8.26 to

8.29. The vehicle pedal signal shown in Figure 8.26 is notably higher than in either the fuzzy controller or the transient shaping tests. The engine torques and speeds are not unlike those used in either of the two previously described tests. This was perhaps due to the use of the NOx ideal operating line in these tests. The Van Doorne controller typically demanded engine speed torque points in the steady state which were close to the NOx ideal operating line. The complete powertrain behaved in a less oscillatory manner under control of the Van Doorne controller. This may have been due to the lower module of the Van Doorne controller being well tuned and better suited to operation with the upper Van Doorne controller module than with the Fuzzy logic or Transient shaping controller.

Figure 8.27 shows there to be a larger scatter of engine operating points on the torque speed diagram than with the alternative controllers. There is a particularly large cluster of points at low torques between 2000 and 2500 rev/min.

The totalised emissions measured during the test are presented in Figure 8.28. NOx emissions again increase more gradually during the slow speed section of the test and more rapidly towards the end. The final value was 5.6 grams. This was slightly worse than the Fuzzy controller figure which was itself the worse of the two alternative controller figures. The HC emissions increased gradually throughout the test and finished at a value of 1.2 grams. This was better than both of the alternative controller figures. The particulates increased in a similar way to the previous tests and finished off at 0.32 grams slightly less than the better of the two alternative controller figures. Finally the fuel used was 480 grams, a value slightly better than the transient shaping controller result, but not as good as that measured using the fuzzy logic controller.

The vehicle speed and distance travelled, Figure 8.29, are very nearly identical to the previous test traces. The most notable difference is that on the very first acceleration, the dynamometer speed does not seem to have been sustained at the correct value for the duration of the demand. The emissions in grams per hour are also shown on this figure and show less oscillatory behaviour than in the previous test examples.

8.2.2 Chassis dynamometer results

The test vehicle underwent a series of legislative emissions tests at Ford, Dunton in order to evaluate the performance of the alternative controller strategies in practice. The test results are presented in Table 8.1 and are summarised in Figure 8.30 by plotting particulates against the sum of HC and NOx emissions. The reason for presentation in this format is that optimisation of the emissions produced is often a trade off between particulates and NOx. The results produced using the BSFC ideal line show there to be little difference between the performances of the transient shaping and the fuzzy logic controllers. Arguably, the transient shaping controller out performs the fuzzy logic controller. When optimising for low NOx the two results are again quite close together. However, the transient shaping controller seems to have a more definite lead in this case. A large particulates value was recorded using the Van Doorne controller. This made it appear uncompetitive in comparison with the alternative controllers in this set of emissions tests. The HC and NOx readings did however appear more comparable with those produced using the alternative controllers. Steps were taken to ensure that the conditions were as near identical as possible between the tests, and a conditioning cycle was completed prior to the cold soak before each test. The hot test using the Van Doorne controller produced a similar level of particulates to the cold test. However, further vehicle work would confirm the high levels of particulate emissions recorded during testing of the Van Doorne controller.

8.3 Drivability appraisal

The drivability work comprised two appraisals. The first, completed in 1993, was used together with experimental objective data to draw up a set of criteria for the design of the powertrain controllers. This was described in Chapter 3. The second, completed some two years later, was used to compare the performance of a selection of experimental novel controllers, with production vehicles similar to those used in the first appraisal.

The majority of those who took part in the first appraisal were also available for the second. This group is denoted as Group 1. Group 2 are then those who remain and who only took part in one of the appraisals. The number of personnel was not large enough to even out the characteristics of individuals who marked much higher or lower than the average and therefore the data collected from Group 2 is really only valid for comparison of vehicles or controllers in the same appraisal. Discussion of the first appraisal in Chapter 3 includes consideration of the results produced by those in Group 2 who only drove in the first appraisal.

Table 8.2 shows the vehicles used in each of the appraisals and gives a description of the controller set-ups used in each of the experimental vehicle configurations.

8.3.1 Assumptions made and considerations of validity

The conditions of the two appraisals were kept as similar as was possible. The location was the surfaces track at Ford, Dunton on both occasions. The time of year and weather conditions were similar and have been assumed identical for the purposes of the comparison. The production vehicles used for comparison were different vehicles on each of the two occasions. The Nissan Micra was a newer model year for the second appraisal and some minor changes in the design and calibration will probably have been made. It was not possible to obtain a Ford Orion with the correct powertrain for the second appraisal and so a Ford Fiesta was used. This had a similar engine and transmission to that of the production Ford Orion used in the initial appraisal. No production Diesel CVT vehicles were available as comparison vehicles on either of the occasions.

Many of those in Group 1 were directly involved with the project. Perceptions and awareness of CVT vehicles will probably have changed during the two years between the appraisals. The profile of the project and timing of the appraisals at near to each end of the period of work may well have had some impact on those involved.

In order to lessen the effect of the order of completing the appraisal, the appraisers were asked to complete the appraisals of the vehicles in different random orders.

8.3.2 Appraisal results

Figures 8.31 to 8.33 show the results of the appraisals using the data from Group 1. Considering first Figure 8.31 which shows the comparison of the Drivability attributes between the vehicles it can be seen that the assessment of the production vehicles was fairly similar in most cases on each occasion. The most notable exception was the improvement of the Fiesta '95 over the Orion '93 in the category of launch feel. This improvement may have been due, of course, to the Fiesta '95 being a smaller, and therefore perhaps more 'lively' vehicle.

<u>Drivability</u> (Figure 8.31)

In the drivability smoothness and response (forwards) there was little difference between any of the experimental controllers. All of them were given significantly lower ratings than the production vehicles. The Orion0 configuration however was only slightly down compared with the production vehicles. Some additional comments made concerning the novel controller set-ups were to the effect that the lower rating was more to do with response than smoothness. The derated engine used in Orion1, Orion2 and Orion3 may have had some impact here.

The appraisal of drivability smoothness and response (backwards) produced greater differences in the ratings of the experimental controllers than the forwards appraisal. The dynamics and stiffness of the powertrain due to the inclusion of the epicyclic gearset for reverse will have been different. This combined with the experimental controller strategies appears to have improved the situation when compared to the forwards case in the Orion1 and Orion3 configurations. The Orion2 fared worse than before which was perhaps due to the unpredictable feel of a more sensitive set-up. Again all three experimental configurations were rated lower than the baseline Orion0 set-up. As above this may have been due to the derated DI engine when compared with the standard IDI engine.

In the appraisal of the kickdown shift behaviour, the Orion2 set-up gave the best results. This was a more sensitive set-up than Orion1 and Orion3 and this was probably the main reason. Again the production vehicles received the best ratings and the derating of the engine for the experimental controllers may have lowered their ratings compared with the baseline Orion0 set-up.

The tip-in/back-out test was unusual in that the Orion0 baseline configuration produced the best results. This was perhaps due to the combination of fuel injection equipment, IDI engine and hydromechanically controlled CVT compared with production petrol engines. The ratings of the production vehicles were all slightly lower, followed by the Orion1 and Orion3 set-ups. The Orion2 which gave perhaps too much of a jerky response in the vehicle fared worse.

In the overrun/braking to rest test, the production vehicles fared best. The Orion0 was slightly worse possible due to the characteristics of the installation and perhaps due to the different engine braking characteristics of the IDI engine compared with the petrol engines. The overrun/braking to rest characteristics of the vehicles with experimental controllers may have been compromised by the effect of having to move from an ideal line for emissions rather than an ideal line for drivability when moving into the overrun condition. The experimental controllers did however produce acceptable results when compared with the standard rating index (Table 3.2).

The traffic crawl test produced very close results for the four production vehicles and the Orion0 baseline vehicle. The Orion1 and Orion3 configurations fared slightly worse but were acceptable. The Orion2 configuration was unacceptably poor. This was probably again due to the sensitive set-up of the controller producing a less drivable response at low vehicle speeds and low gear ratios.

In the launch feel test, there was more difference in the results from the production vehicles than in most of the other tests. The smallest cars produced the best results followed by the Orion2 experimental configuration and then the Orion '93 production vehicle. The Orion0 baseline and the Orion1 and Orion3 configurations all gave very similar results. Having enough power available for a good immediate response is clearly an issue here. The sensitive set-up of Orion2 helped to off set the effect of a derated engine in quite a heavy and larger (than the Fiesta or Micra) vehicle.

The neutral/drive neutral/reverse engagement smoothness test produced the largest differences between the vehicles and configurations. The Micra performed best, which was not surprising since it was the only vehicle without creep. The shift lever is also an electrical switch only rather than a mechanical link to the transmission. The Orion '93, Fiesta '95 and Orion0 all fared about the same. They all had essentially the same transmission and either production or very close to production engines. All of the experimental set-ups performed poorly on this test. The sudden change from no load at idle to creep load at idle caused problems for the engine idle controller. The fuel injection equipment calibration and set-up on the DI engine was however an early pre-production configuration.

The overall drivability of the production vehicles was good. The Orion0 baseline vehicle calibration was found to be fair. The three experimental set-ups were spread in the borderline and acceptable categories. The Orion1 and Orion2 set-ups produced very close overall results which was perhaps due to the averaging of the advantages and disadvantages of the more controversial Orion2 set-up. Surprisingly, the Orion3 set-up fared significantly better than the Orion1 set-up; there had been little difference between them in any of the first eight categories. The reason may have been due to the more relaxed and less harsh ideal operating line of Orion3, optimised for low fuel consumption rather than low NOx production. This would have utilised lower engine speeds than the Orion1 set-up for the same power demands. It was perhaps difficult for those assessing to completely decouple the noise and vibration of the experimental Diesel vehicle set-ups from the drivability attributes being assessed.

<u>Performance</u> (Figure 8.32)

In the accelerator pedal effort/smoothness test, the production vehicles fared best and all achieved similar ratings. The Orion0 baseline was significantly lower followed by the experimental vehicle configurations. The lowest rating was achieved by the Orion2 set-up and although acceptable was probably due to the pedal set-up being over sensitive at the beginning of its stroke.

The full throttle overtaking/response entering highway test showed the Micra to be best in this category. The Fiesta and Orion '93 were somewhat lower. In the case of the Orion '93 this may have been due to some degree to the size of the vehicle. The baseline Orion0 was marginally better than the Orion1 and Orion2 calibrations. The Orion3 calibration was borderline, the effect of the fuel consumption ideal operating line being perhaps the reason in that less immediate power will have been available at steady state compared with equal power steady state operation on the NOx ideal operating line.

In the 50 km/h tip-in overtaking manoeuvre, the rated order of the vehicles was almost identical to that of the preceding category. The only difference was that the Fiesta fared better than the Orion '93. The Orion0 baseline was not significantly different from the Orion '93. The main reason for the lower performance of the experimental vehicle calibrations in this test was probably the derating of the engine. This effect offset by the high sensitivity controller, the Orion2 calibration was the best of the experimental set-ups. The Orion3 ideal operating line again, as above, was probably the reason why it fared worst.

Fun to drive impression of a vehicle is probably mostly related to power to weight ratio and fast response to changes in driver demand. The Micra performed very well here, followed by the Orion '93 and then the Fiesta '95. It was perhaps surprising that the Fiesta did not beat the Orion. The lower powered Diesel vehicle set-ups fared worst, were not significantly different and the ratings of these may well have been influenced by the noise of the Diesel engine in an experimental vehicle.

In the overall performance feel test, there was little difference between the experimental calibrations. All of them were in the borderline to acceptable rating area. The Orion0 set-up fared only slightly better followed by the Fiesta, Orion '93 and the Micra. Comparison of petrol vehicles with experimental and derated Diesel vehicles probably had the greatest impact on the performance ratings.

NVH (Figure 8.33)

Control of the noise and vibration harshness of the vehicle was outside the scope of this work. NVH attributes were included in the appraisal mainly to try to ensure that the assessors distinguished between them and the issues of drivability and performance. As expected, the assessment of the experimental vehicle produced poor results. Whether or not it was indeed possible to assess transmission noise is questionable, but there is no reason that the transmission should have produced more noise than in the petrol vehicles. Engine presence during ratio change produced low ratings from the Diesel probably due to the high engine speeds needed to produce reasonable powers especially using the derated engine.

Group 2 and total results

The group 2 results are shown in Figures 8.34 to 8.36 but cannot be used to compare the vehicles in the first and second appraisals. They can however be used to compare vehicles and calibrations in the same appraisal. The trends do appear similar to those shown by the group 1 appraisals. Figures 8.37 to 8.39 show the results produced by combining groups 1 and 2 but again it is not strictly valid to compare ratings from the first with the second appraisal.

Results from Chassis Rolls Tests at Ford, Dunton					DI TCi engine, CTXE transmission		
					after catalyst		bag tests
Test Description	HC	CO	NOx	CO2	PM	HC+NOx	Fuel (calc) from bag
	g/km	g/km	g/km	g/km	g/km	g/km	l/100km
VDT cold	0.152	0.675	0.594	216	0.21	0.7466	8.09
VDT hot	0.134	0.458	0.606	209	0.2	0.7402	7.82
FUZZY LOGIC BSFC cold	0.138	0.5	0.692	164	0.09	0.83	6.14
FUZZY LOGIC BSFC hot	0.093	0.323	0.698	155	0.07	0.7907	5.79
FUZZY LOGIC NOx cold	0.123	0.541	0.514	176	0.11	0.6374	6.6
FUZZY LOGIC NOx hot	0.091	0.358	0.549	170	0.1	0.6393	6.33
TRANSIENT SHAPING BSFC cold	0.151	0.554	0.663	160	0.08	0.8141	5.99
TRANSIENT SHAPING BSFC hot	0.089	0.34	0.725	153	0.07	0.814	5.72
TRANSIENT SHAPING NOx cold	0.16	0.589	0.435	173	0.1	0.5945	6.47
TRANSIENT SHAPING NOx hot	0.091	0.349	0.49	160	0.1	0.5815	5.99

Table 8.1 Chassis dynamometer drivecycle emissions results

Micra '93	1993 Nissan Micra NCVT (petrol) used in the first appraisal
Orion '93	1993 Ford Orion CTX (petrol) used in the first appraisal
Orion0 '93	The test vehicle fitted with 1.8 l IDI Diesel engine and CTX transmission
Micra '95	1995 Nissan Micra NCVT (petrol) used in the second appraisal
Fiesta '95	1995 Ford Fiesta CTX (petrol) used in the second appraisal
Orion1 '95	The test vehicle fitted with 1.8 l DI Diesel engine and CTXE transmission Transient shaping controller. NOx ideal line. Pedal sensitivity = 5, busyness = 5
Orion2 '95	The test vehicle fitted with 1.8 l DI Diesel engine and CTXE transmission Fuzzy logic controller. BSFC ideal line. Pedal sensitivity = 10, busyness = 10
Orion3 '95	The test vehicle fitted with 1.8 l DI Diesel engine and CTXE transmission Transient shaping controller. BSFC ideal line. Pedal sensitivity = 5, busyness = 5

Table 8.2 Vehicles used in the drivability appraisals

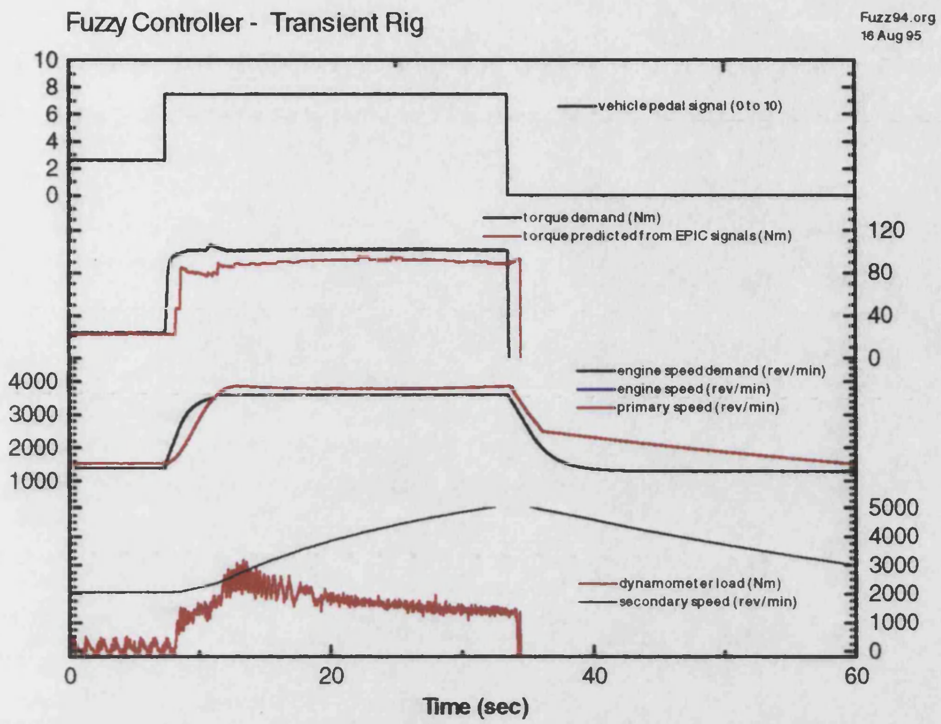

Figure 8.1 VDT controller - engine speed control

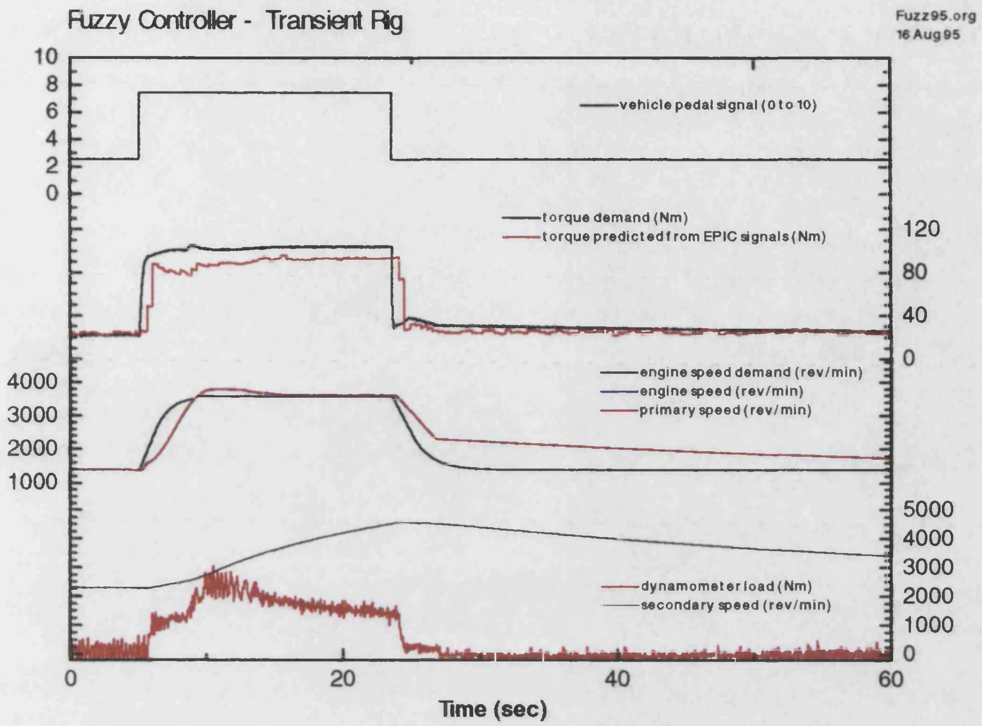

Figure 8.2 Engine speed control with integral term

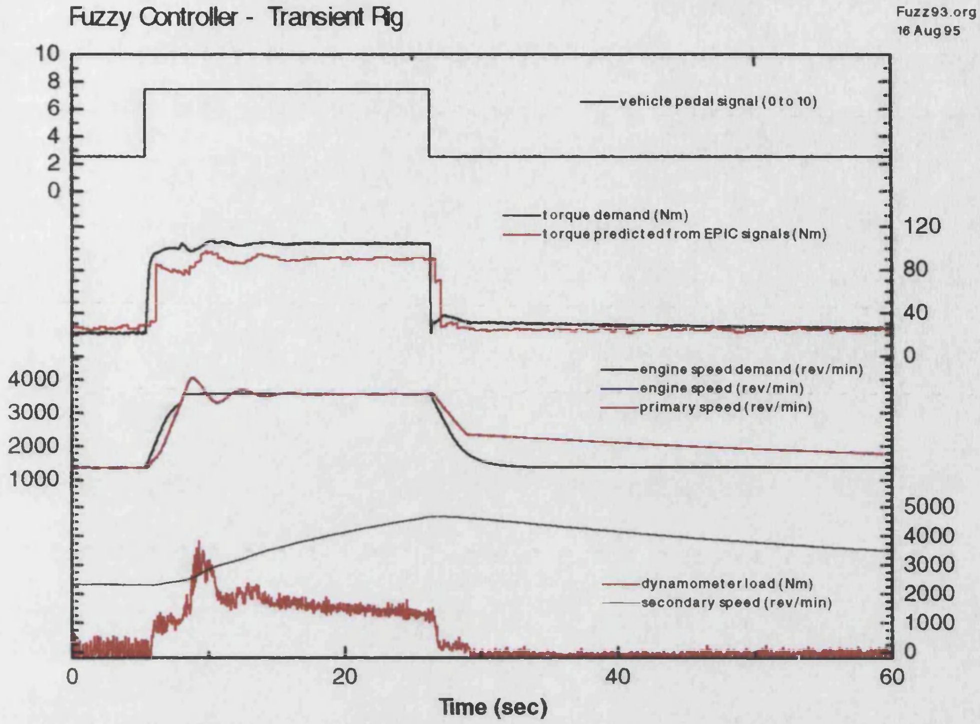

Figure 8.3 Engine speed control with large integral term

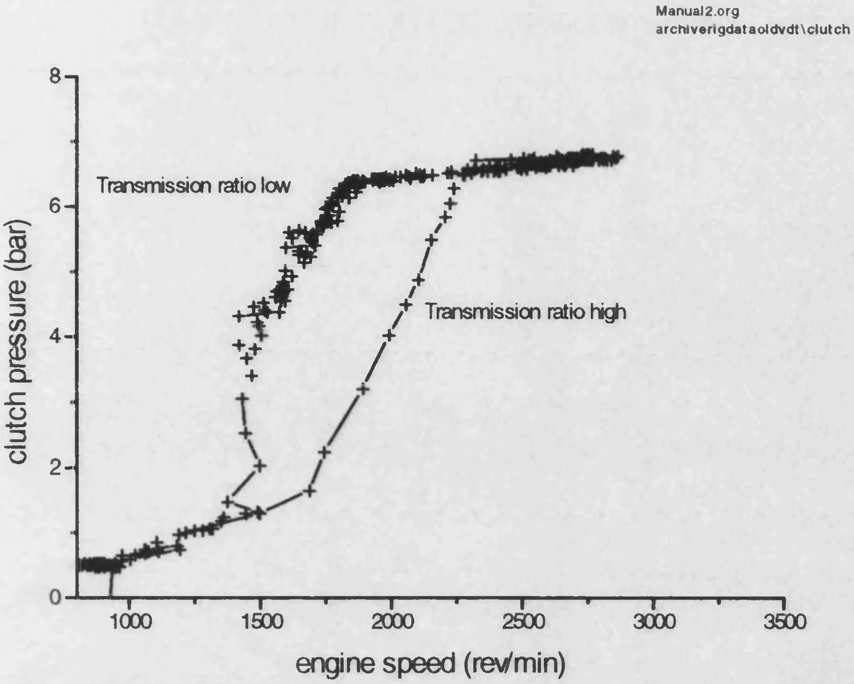

Figure 8.4 Clutch pressure profile with engine speed and transmission ratio

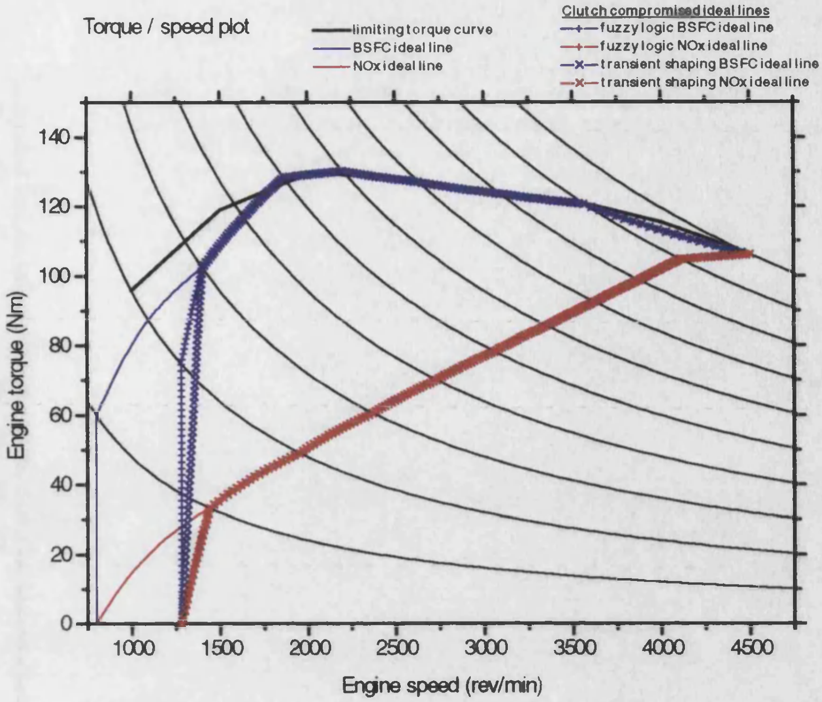

Figure 8.5 Engine ideal operating lines compromised by the clutch limitations

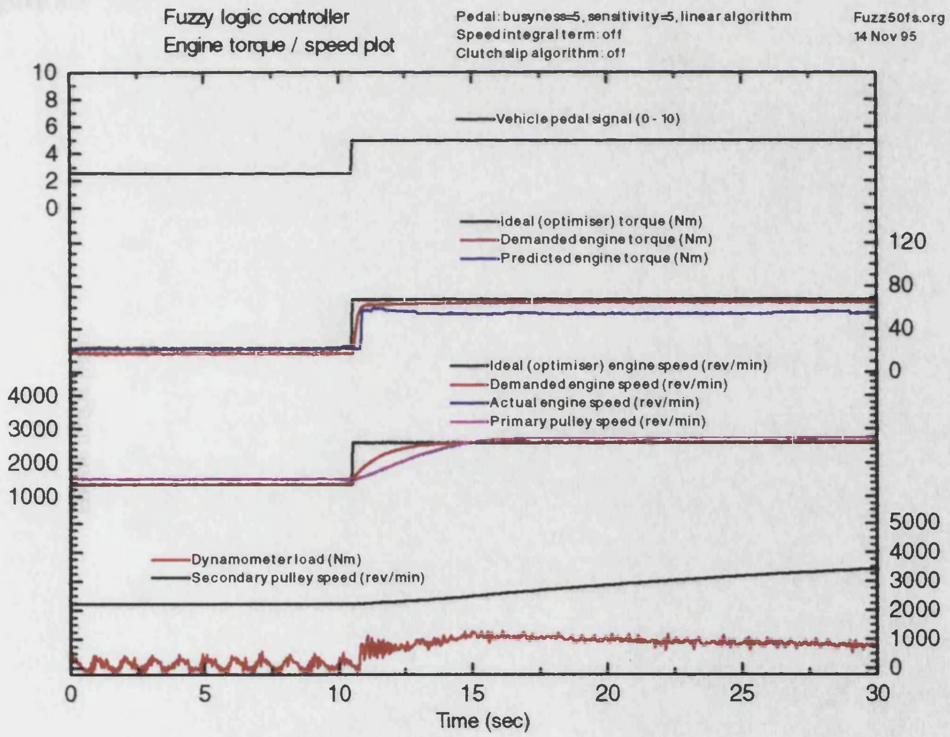

Figure 8.6 Fuzzy logic controller - rig test

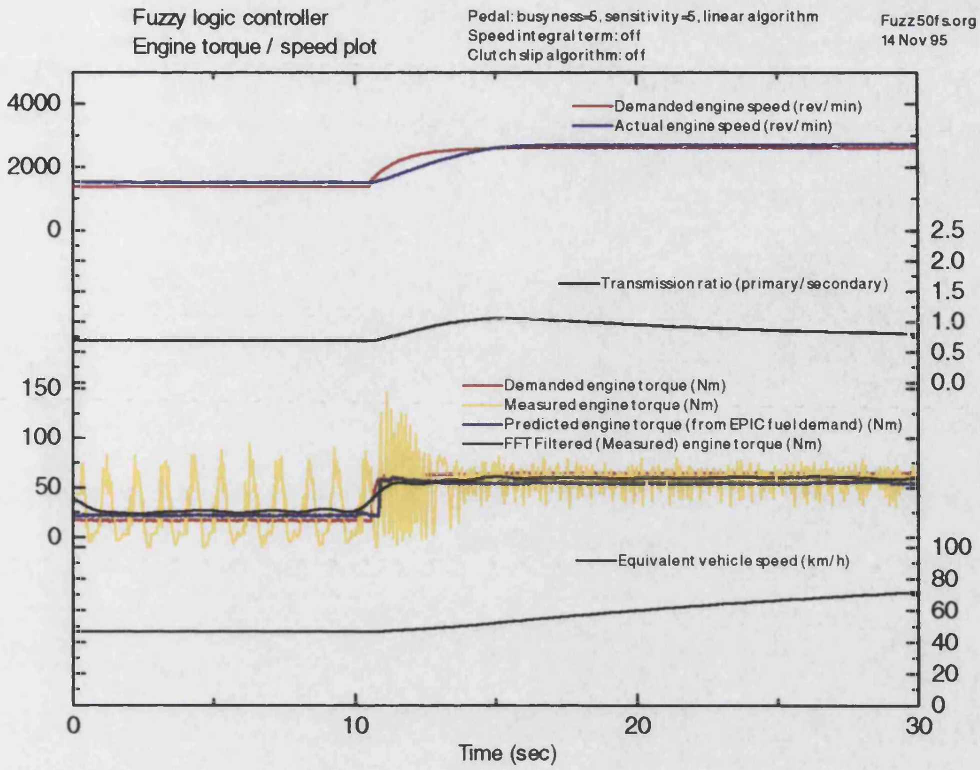

Figure 8.7 Fuzzy logic controller - rig test

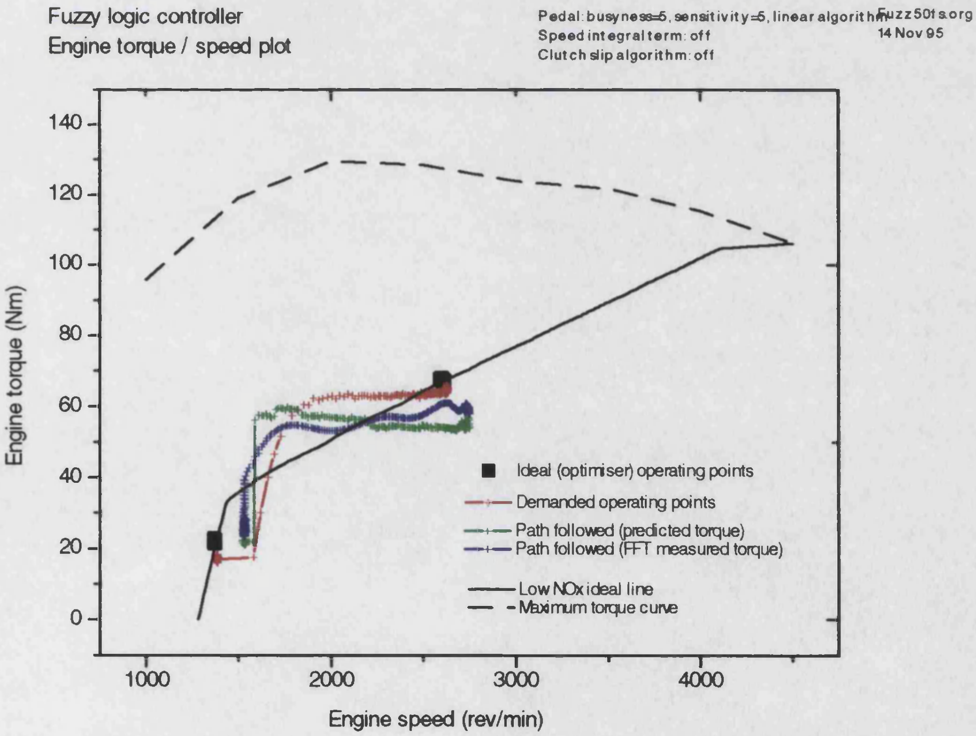

Figure 8.8 Fuzzy logic controller - rig test

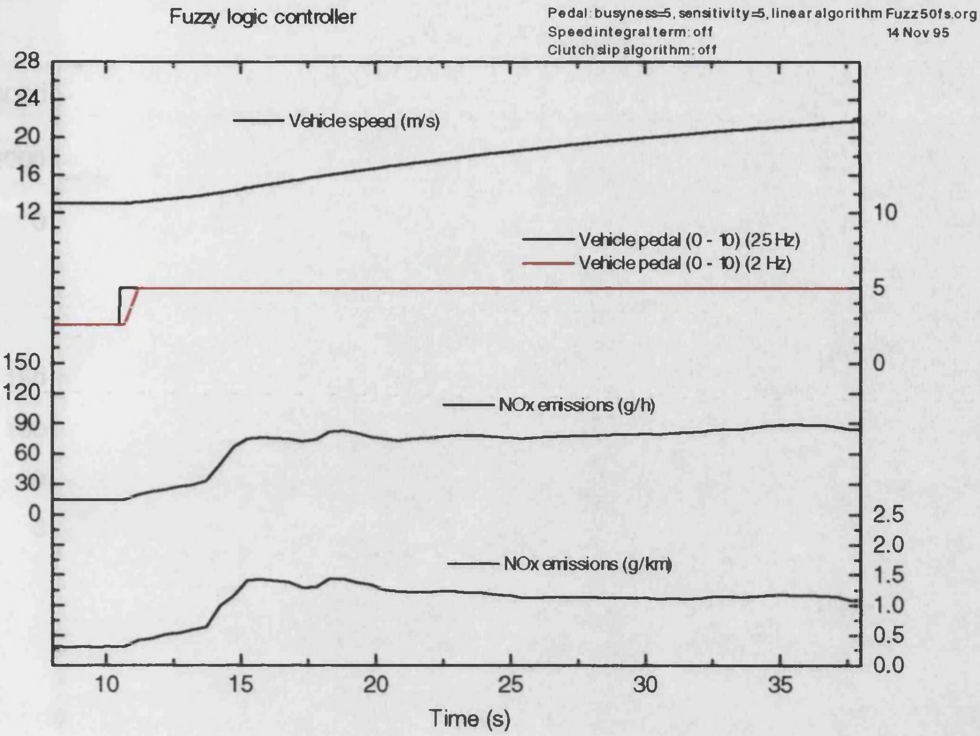

Figure 8.9 Fuzzy logic controller - rig test

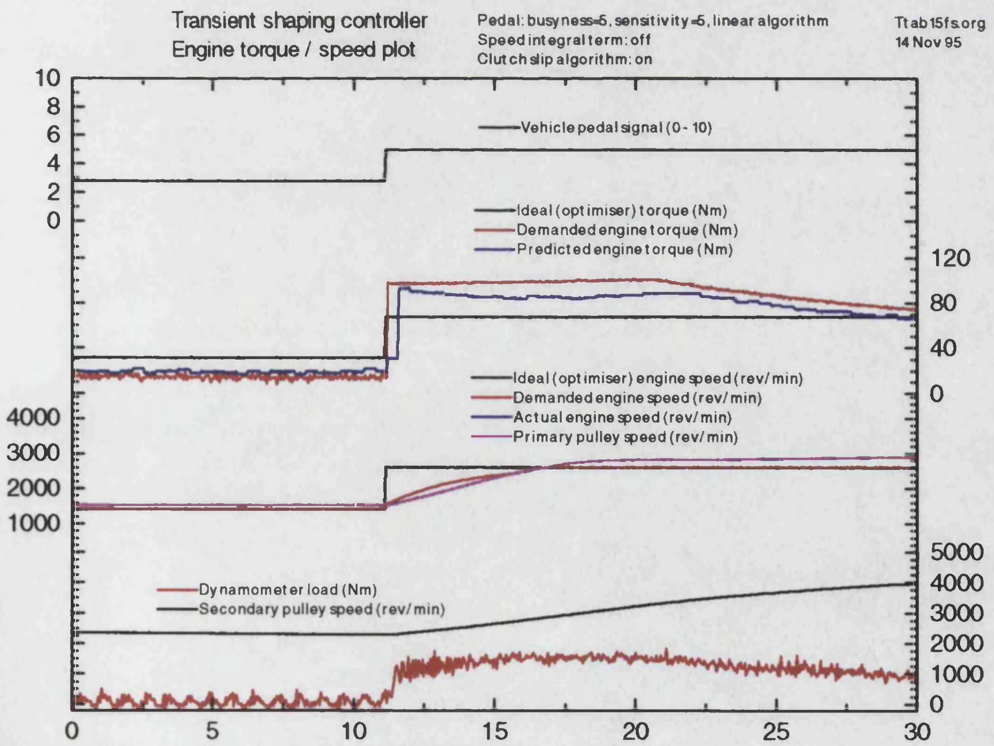

Figure 8.10 Transient shaping controller - rig test

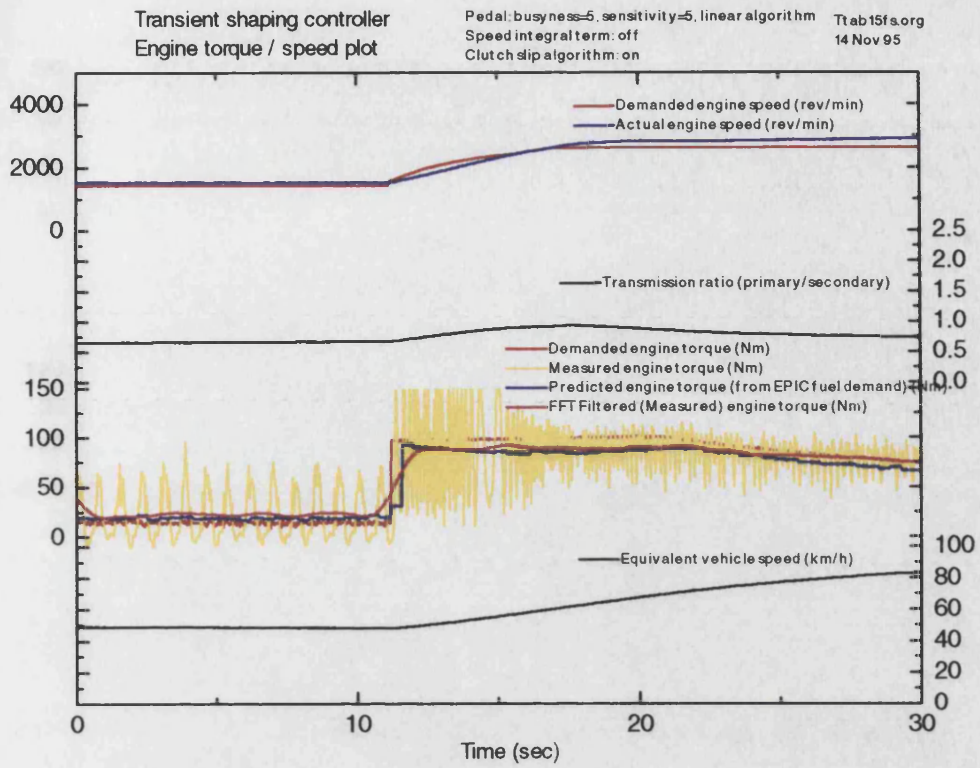

Figure 8.11 Transient shaping controller - rig test

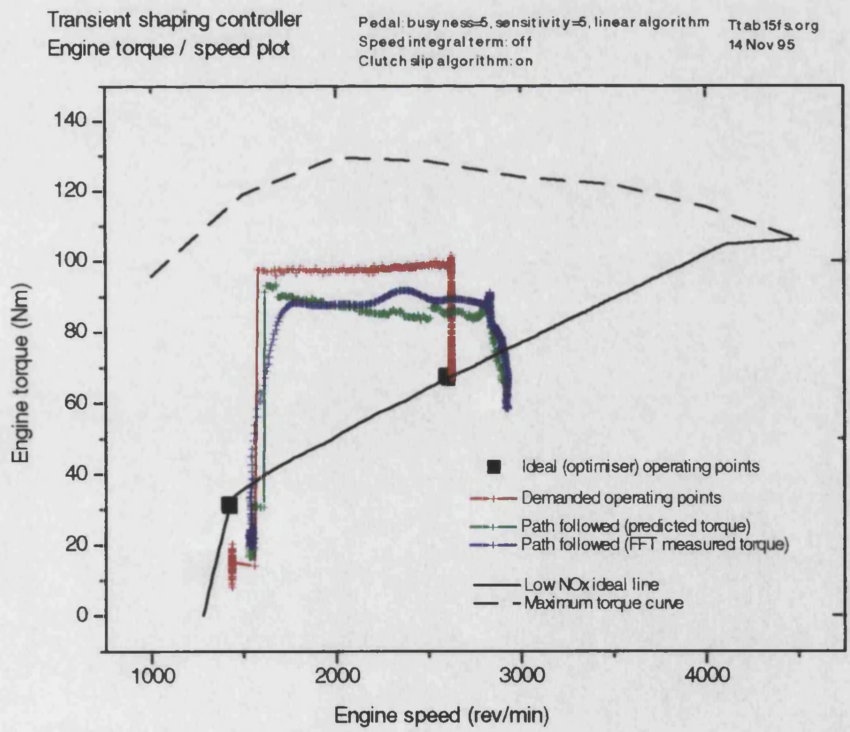

Figure 8.12 Transient shaping controller - rig test

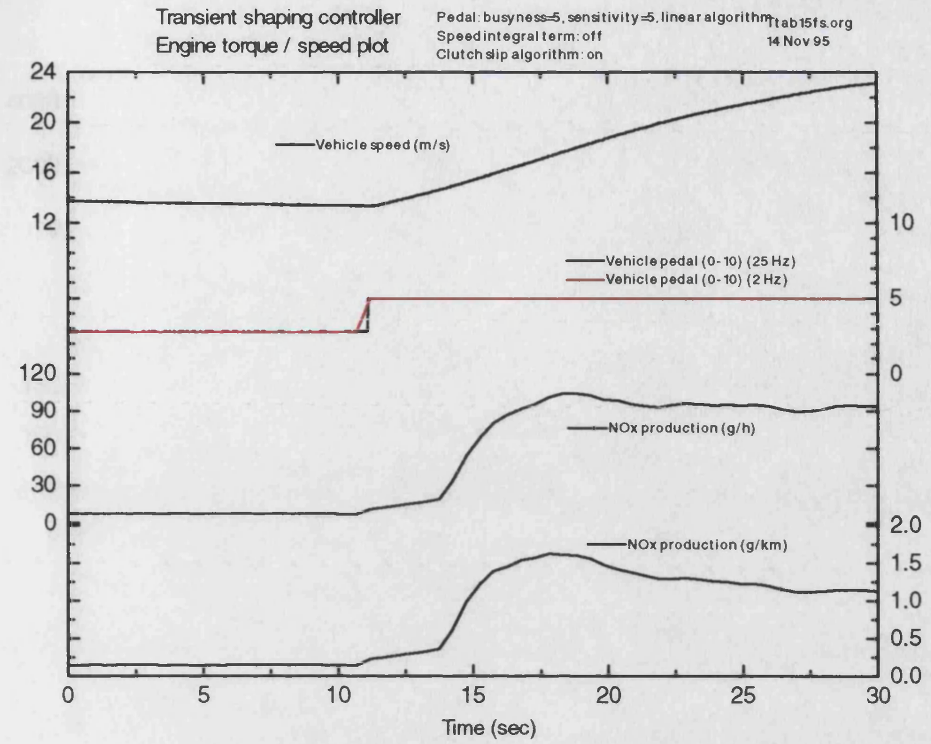

Figure 8.13 Transient shaping controller - rig test

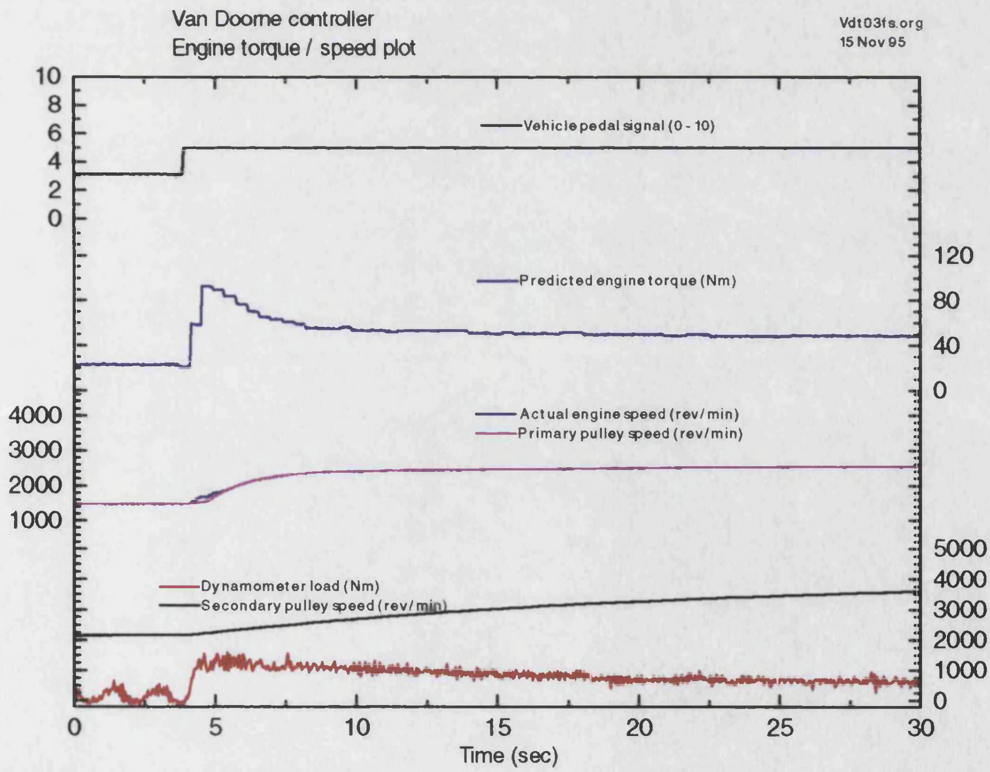

Figure 8.14 Van Doorne controller - rig test

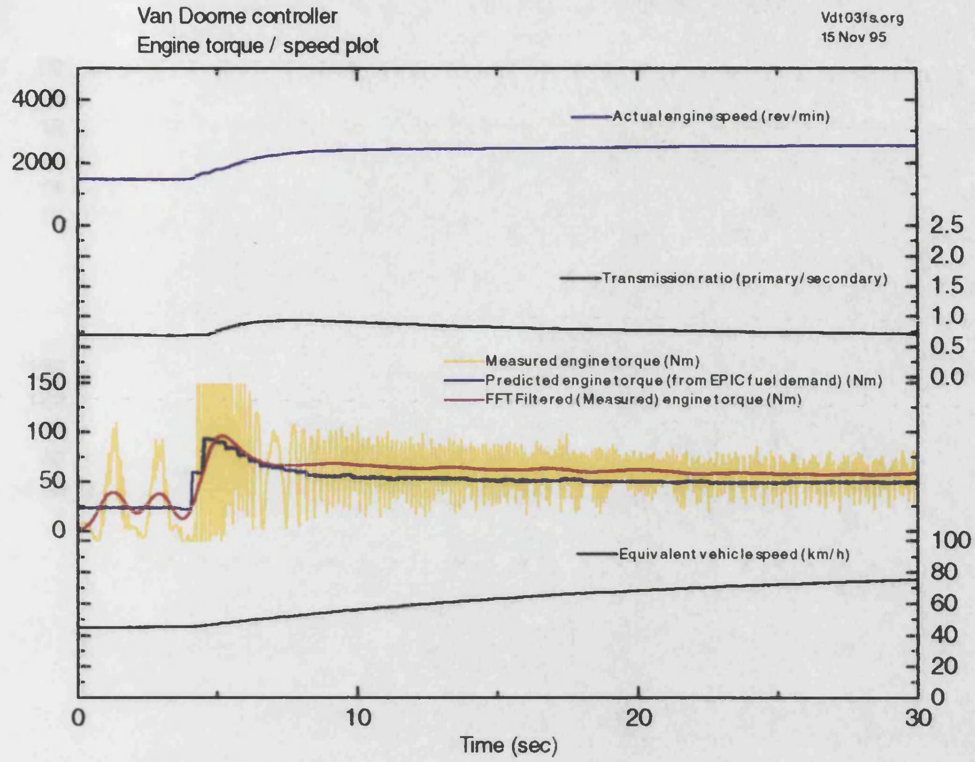

Figure 8.15 Van Doorne controller - rig test

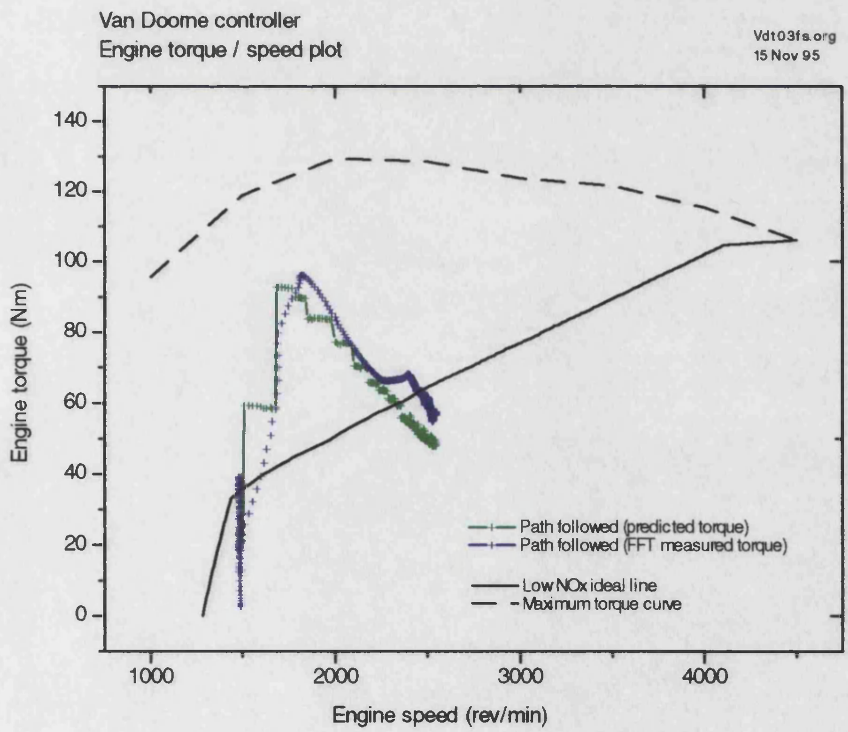

Figure 8.16 Van Doorne controller - rig test

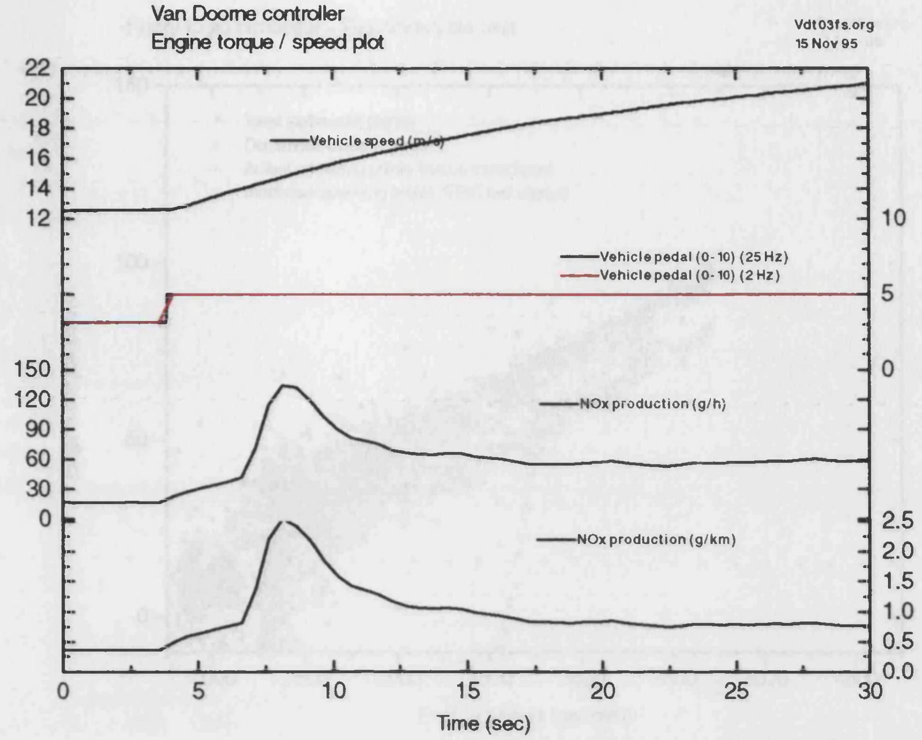

Figure 8.17 Van Doorne controller - rig test

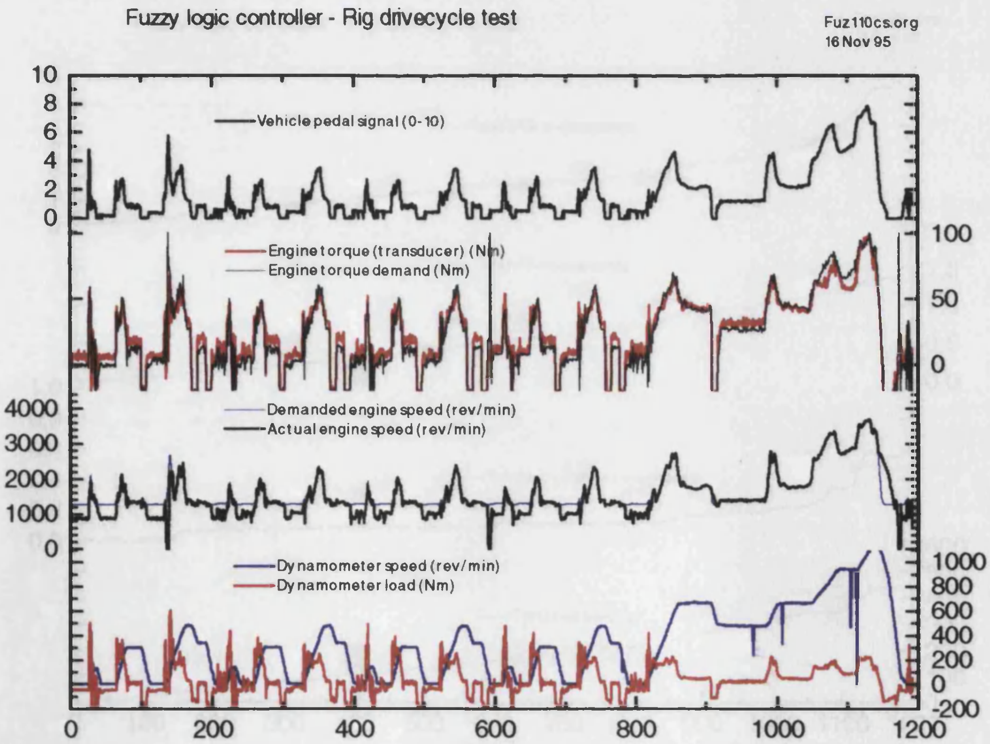

Figure 8.18 Fuzzy logic controller - legislative emissions rig test

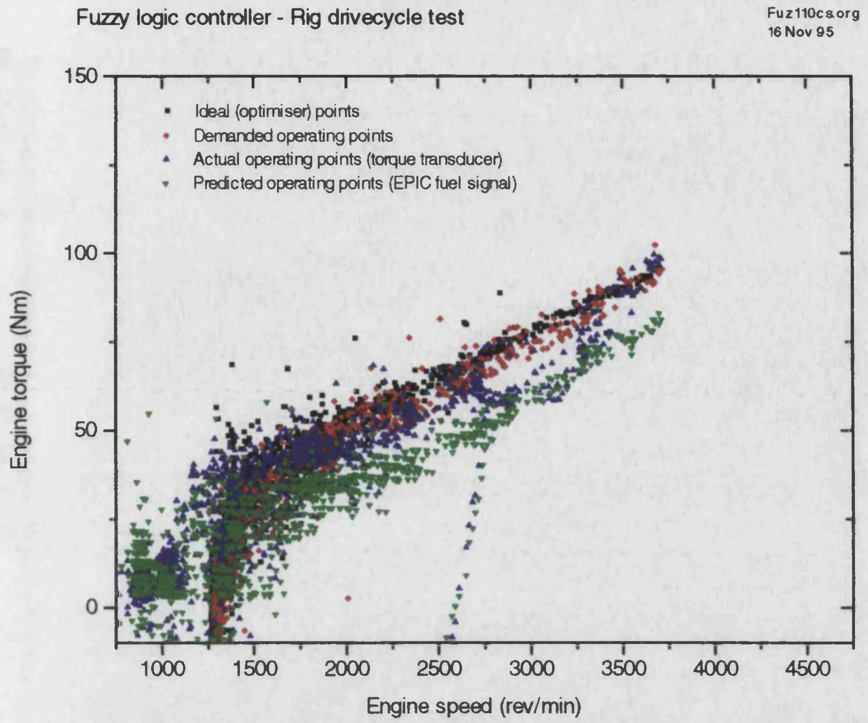

Figure 8.19 Fuzzy logic controller - legislative emissions rig test

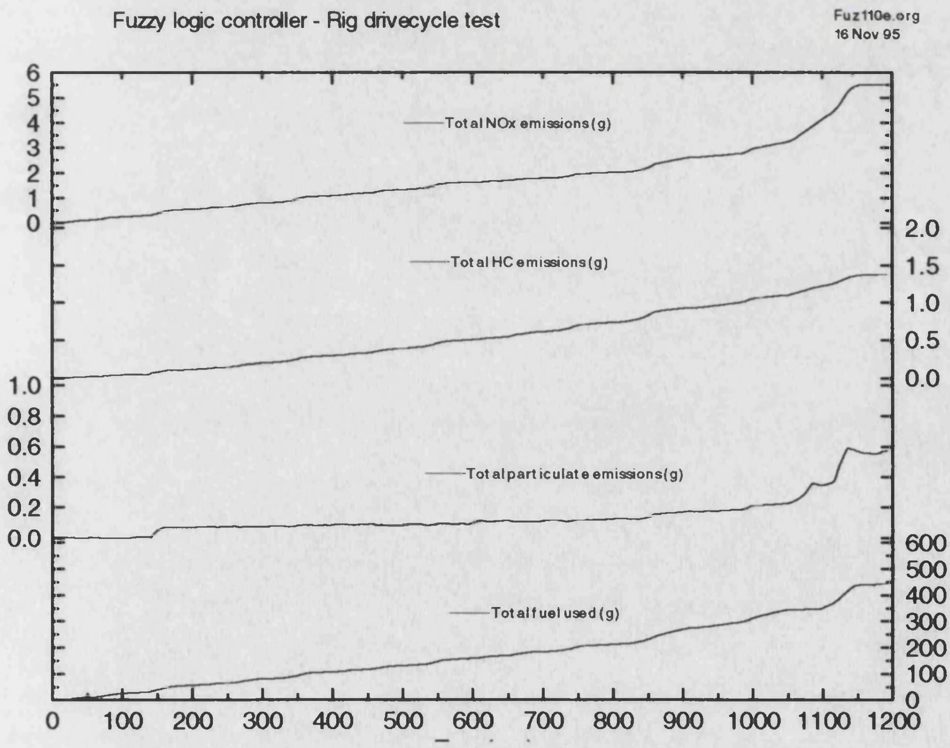

Figure 8.20 Fuzzy logic controller - legislative emissions rig test

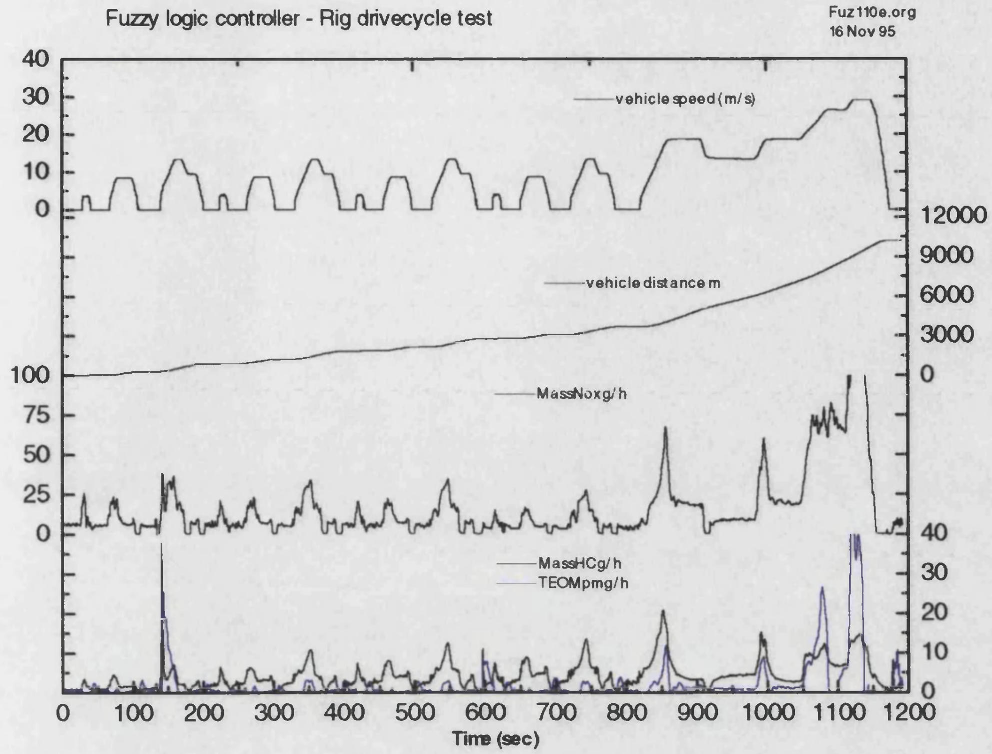

Figure 8.21 Fuzzy logic controller - legislative emissions rig test

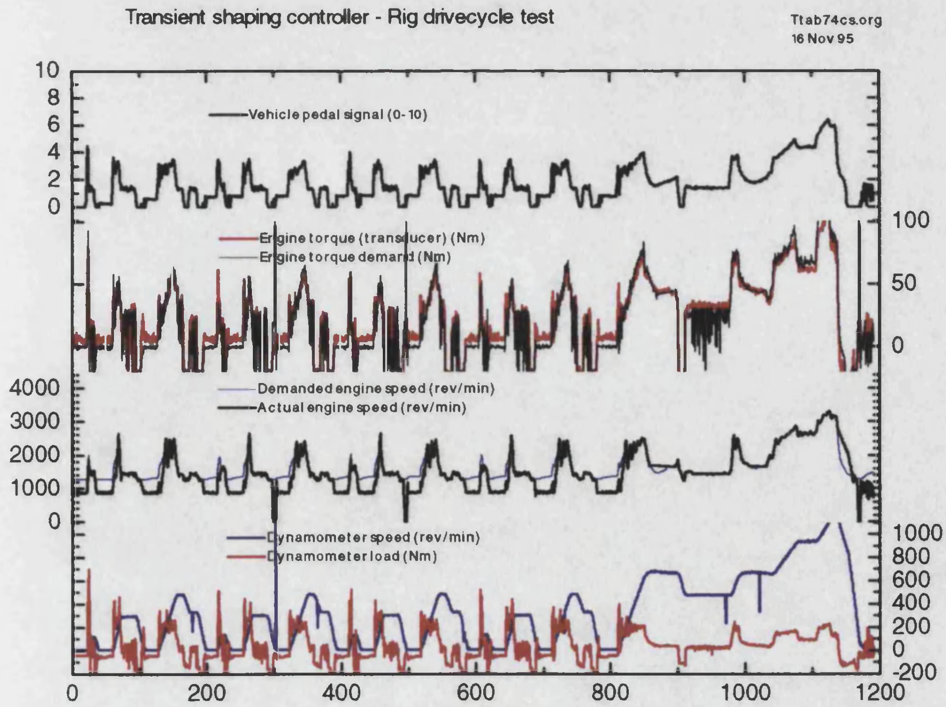

Figure 8.22 Transient shaping controller - legislative emissions rig test

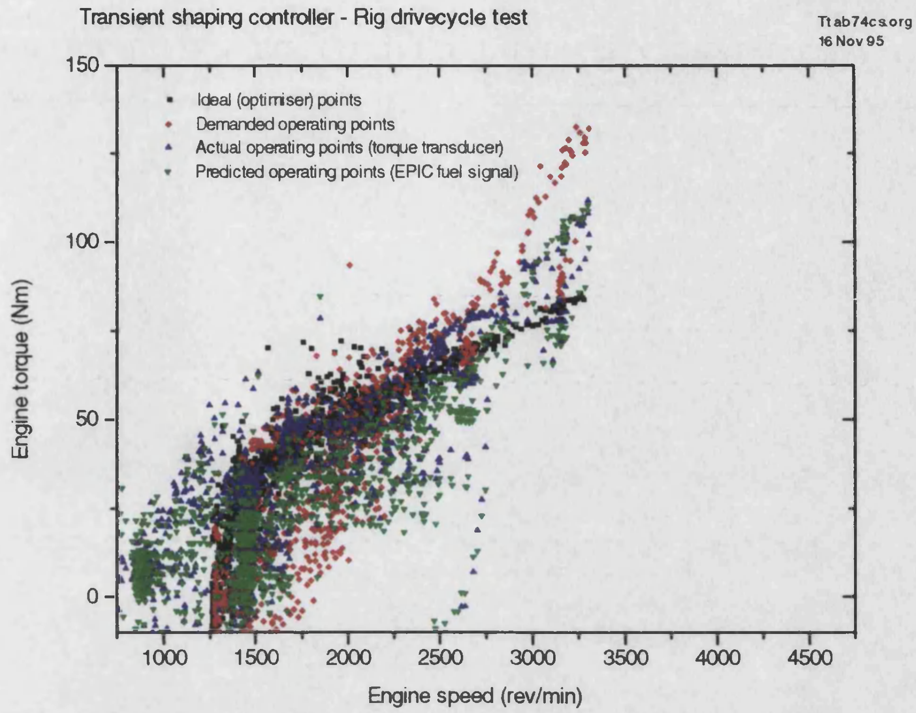

Figure 8.23 Transient shaping controller - legislative emissions rig test

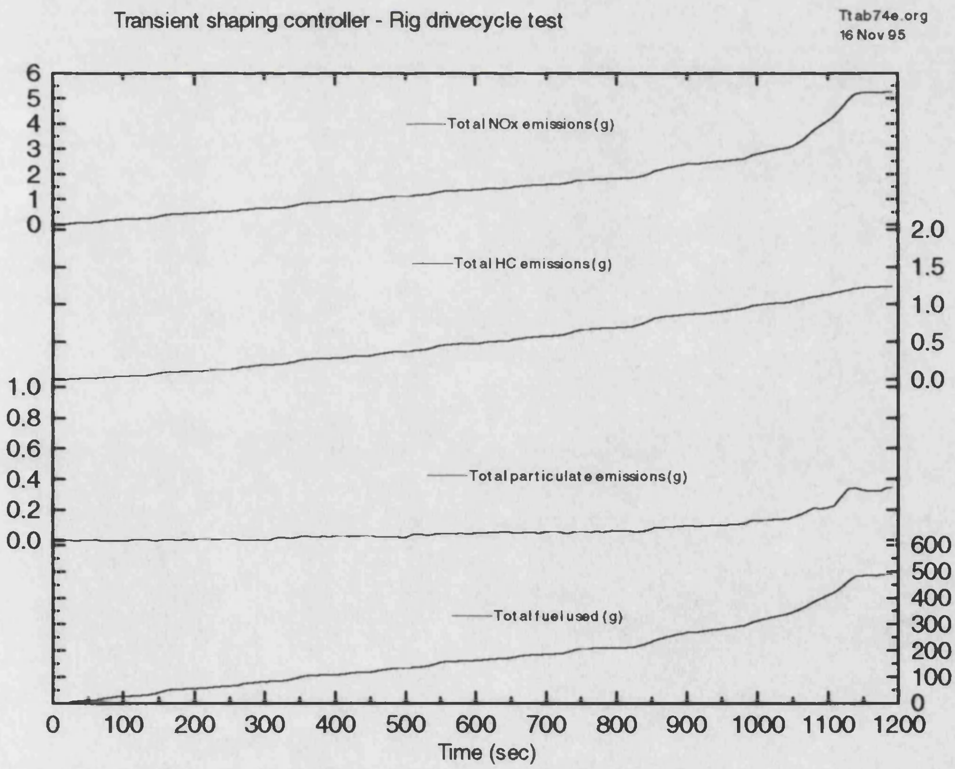

Figure 8.24 Transient shaping controller - legislative emissions rig test

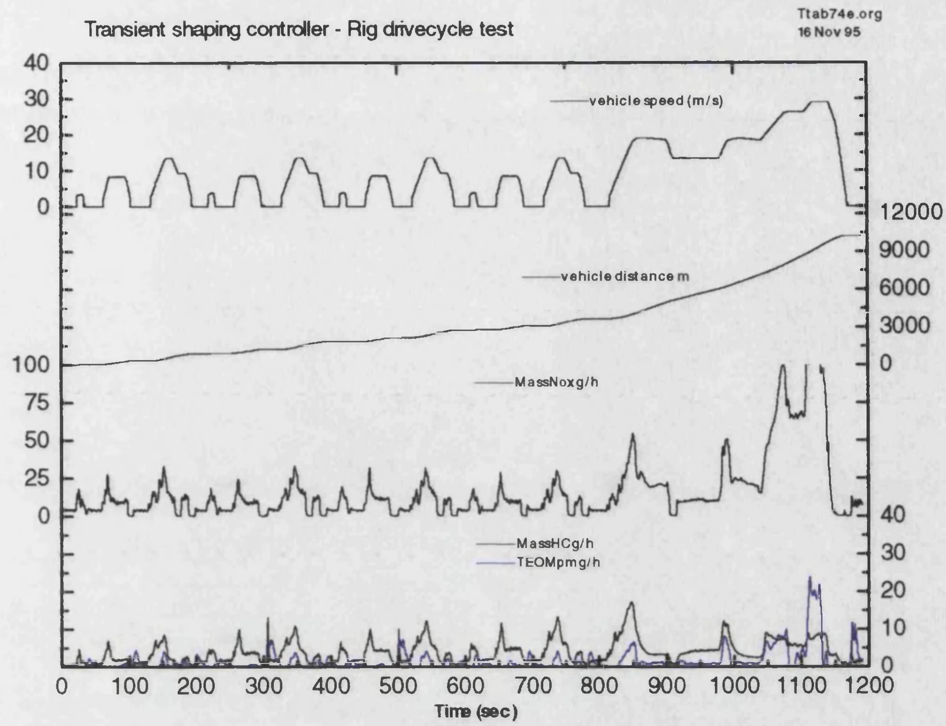

Figure 8.25 Transient shaping controller - legislative emissions rig test

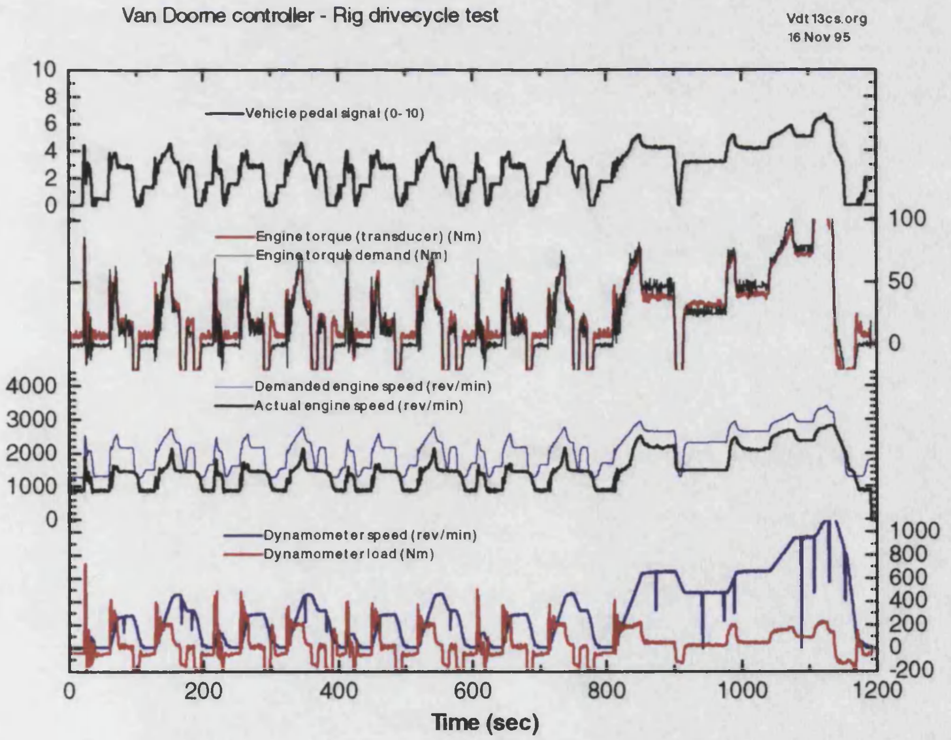

Figure 8.26 Van Doorne controller - legislative emissions rig test

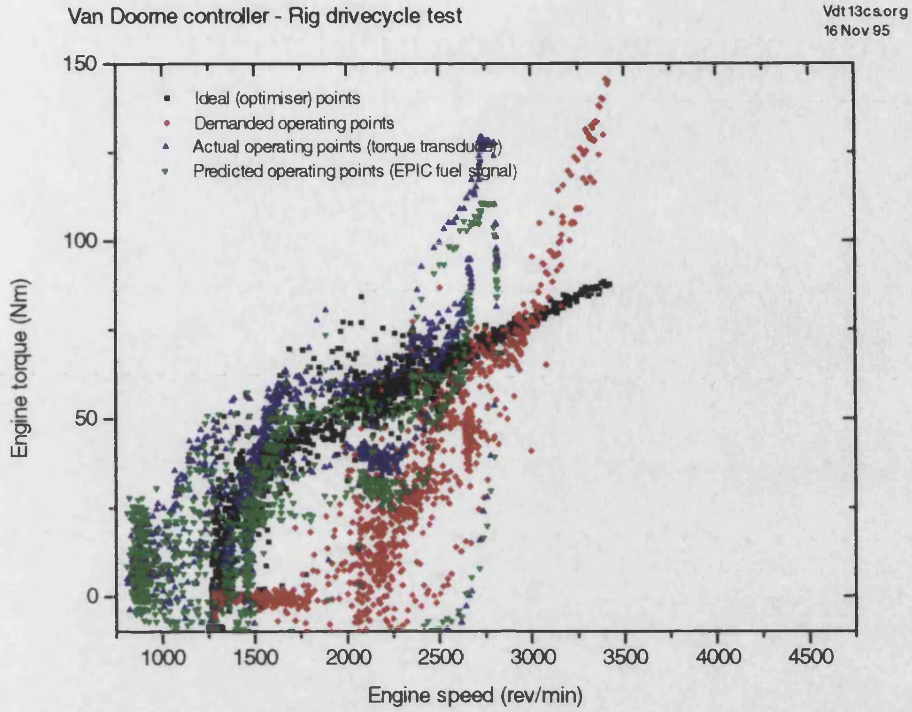

Figure 8.27 Van Doorne controller - legislative emissions rig test

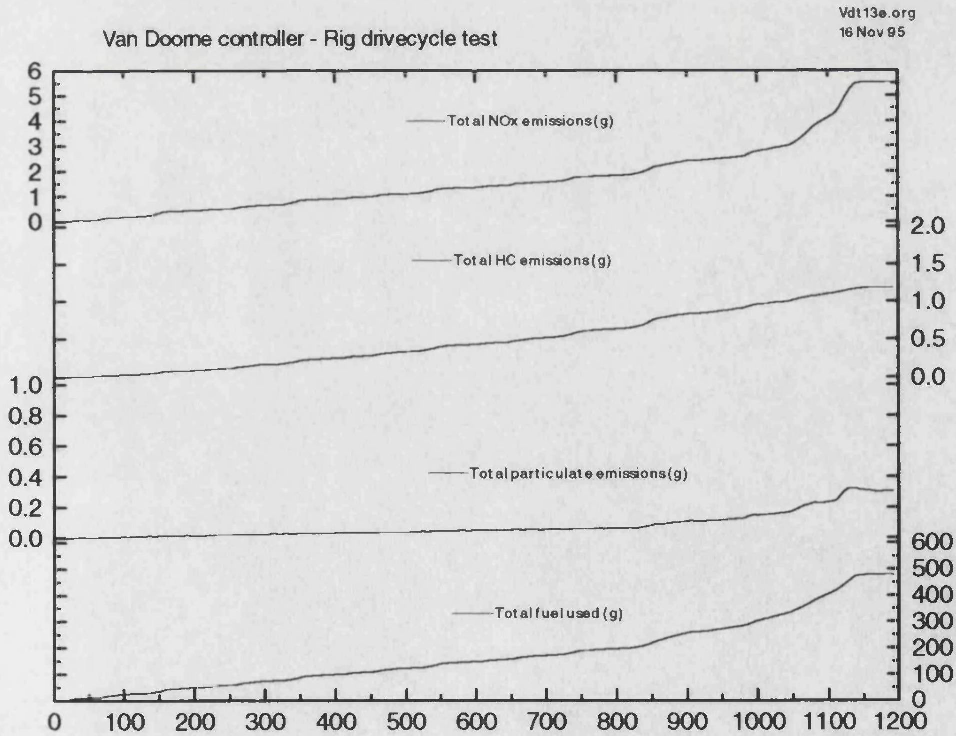

Figure 8.28 Van Doorne controller - legislative emissions rig test

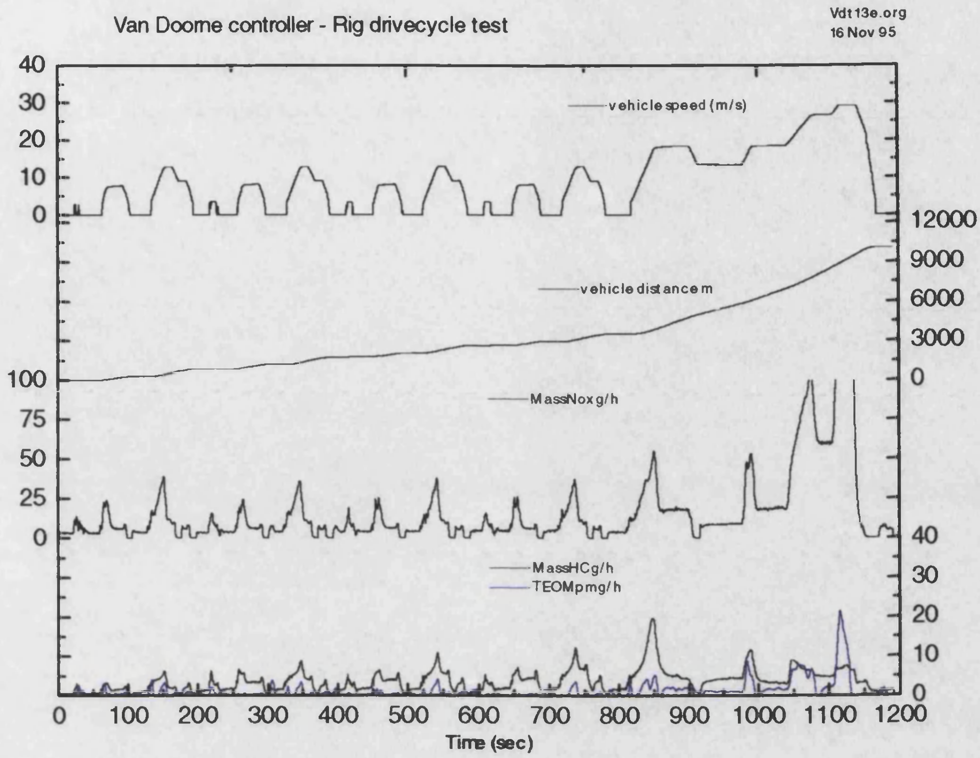

Figure 8.29 Van Doorne controller - legislative emissions rig test

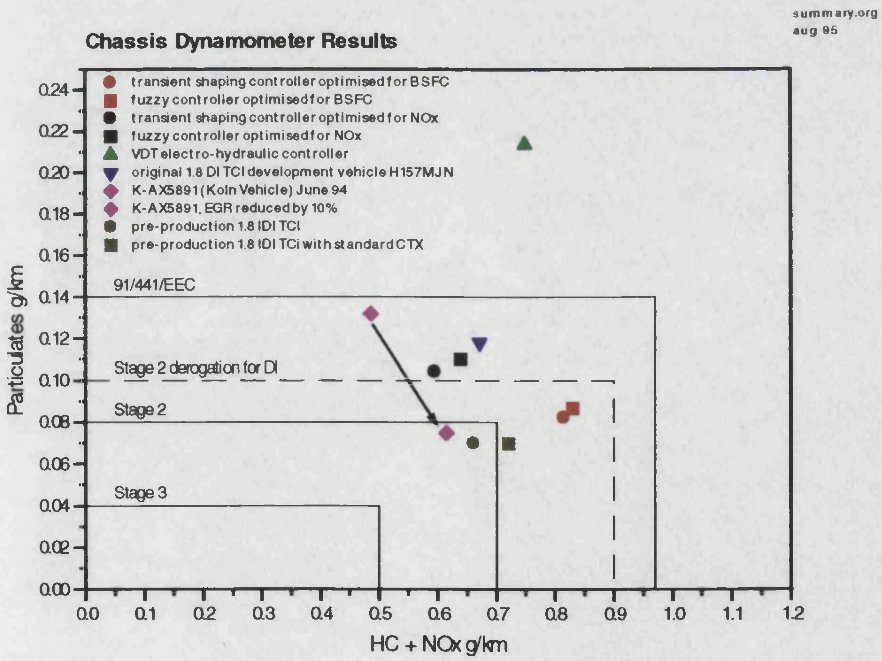

Figure 8.30 Summary of chassis dynamometer legislative emissions tests

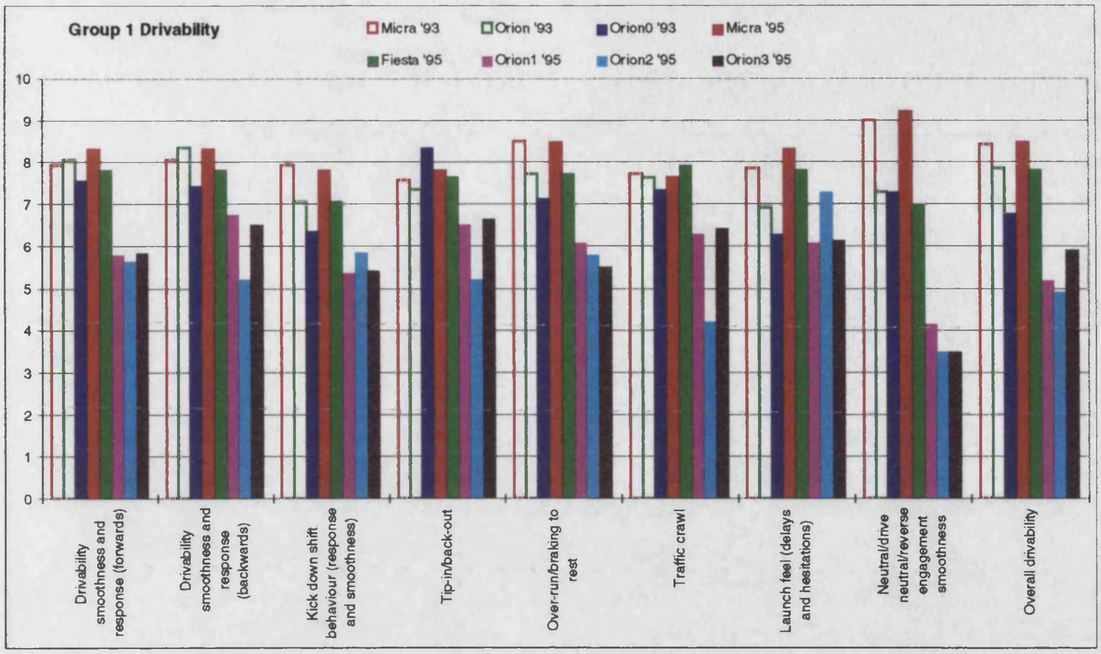

Figure 8.31 Group 1 Vehicle appraisal results - Drivability

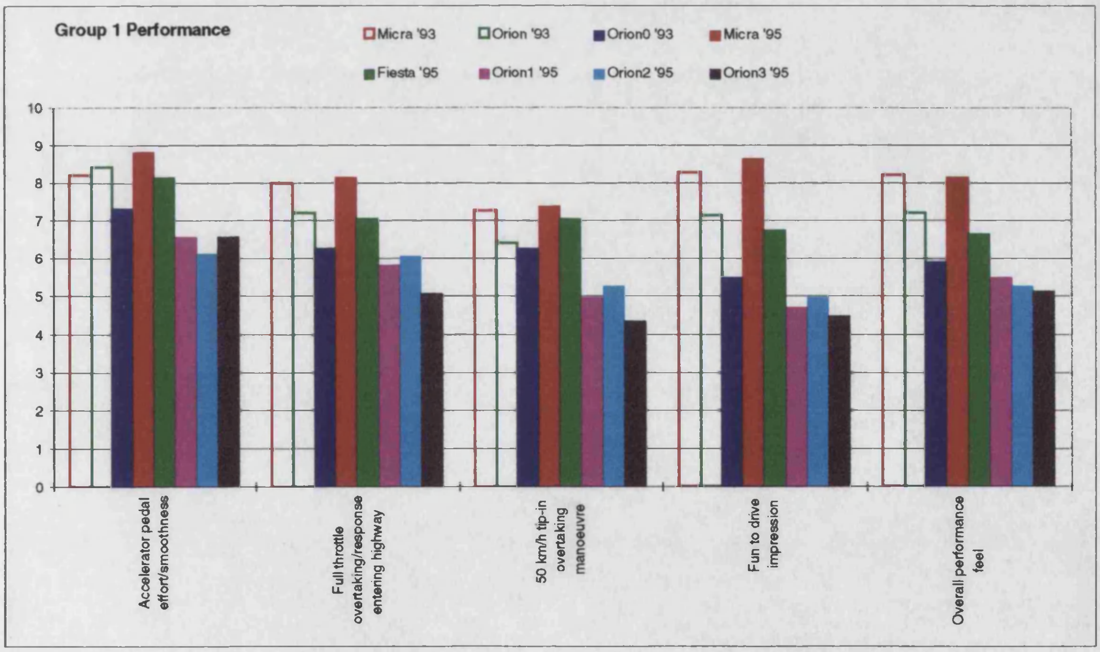

Figure 8.32 Group 1 Vehicle appraisal results - Performance

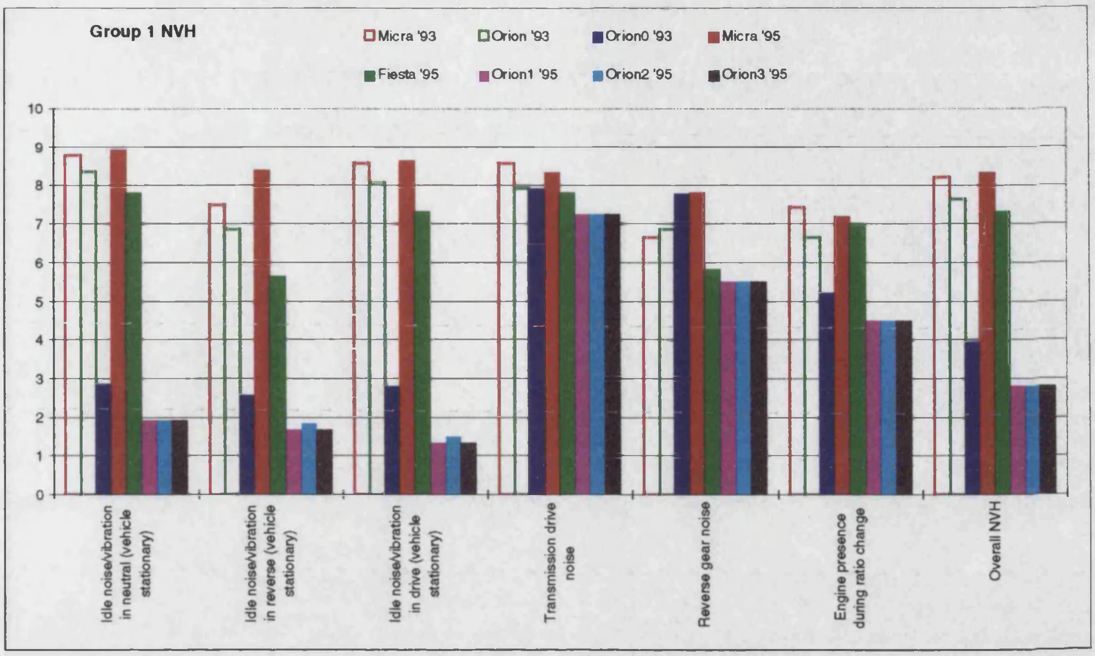

Figure 8.33 Group 1 Vehicle appraisal results - NVH

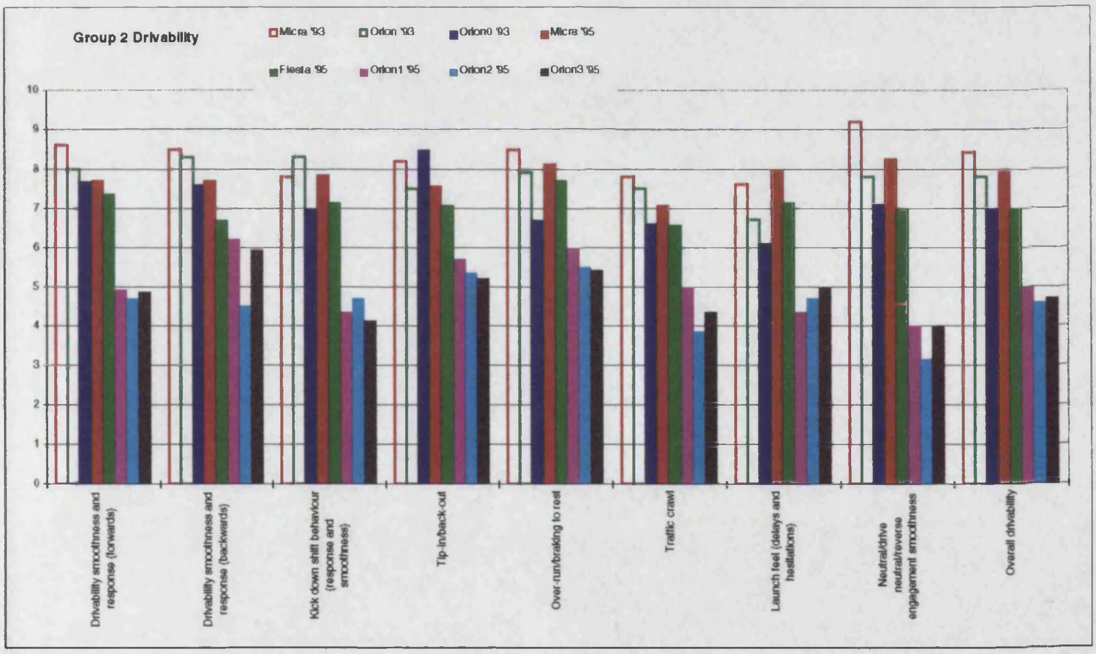

Figure 8.34 Group 2 Vehicle appraisal results - Drivability

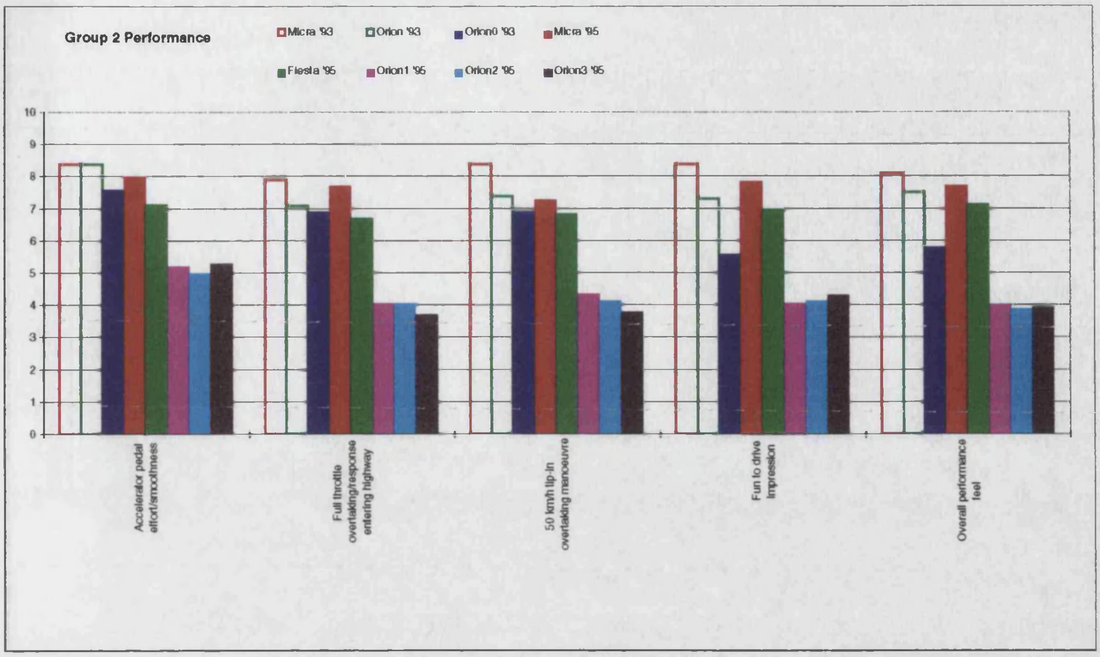

Figure 8.35 Group 2 Vehicle appraisal results - Performance

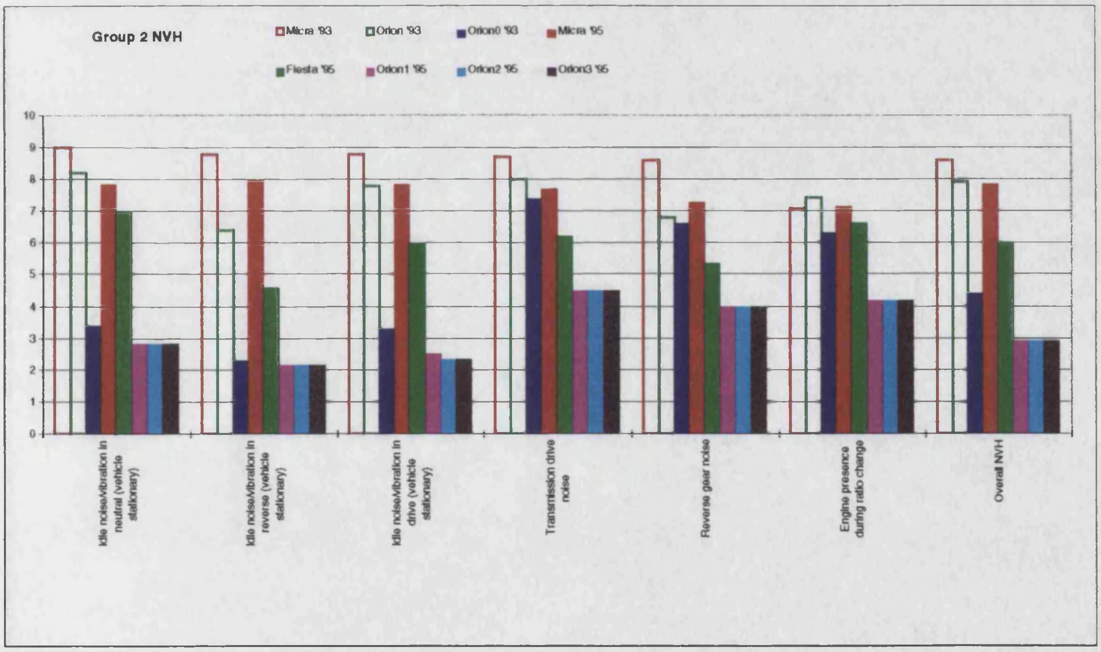

Figure 8.36 Group 2 Vehicle appraisal results - NVH

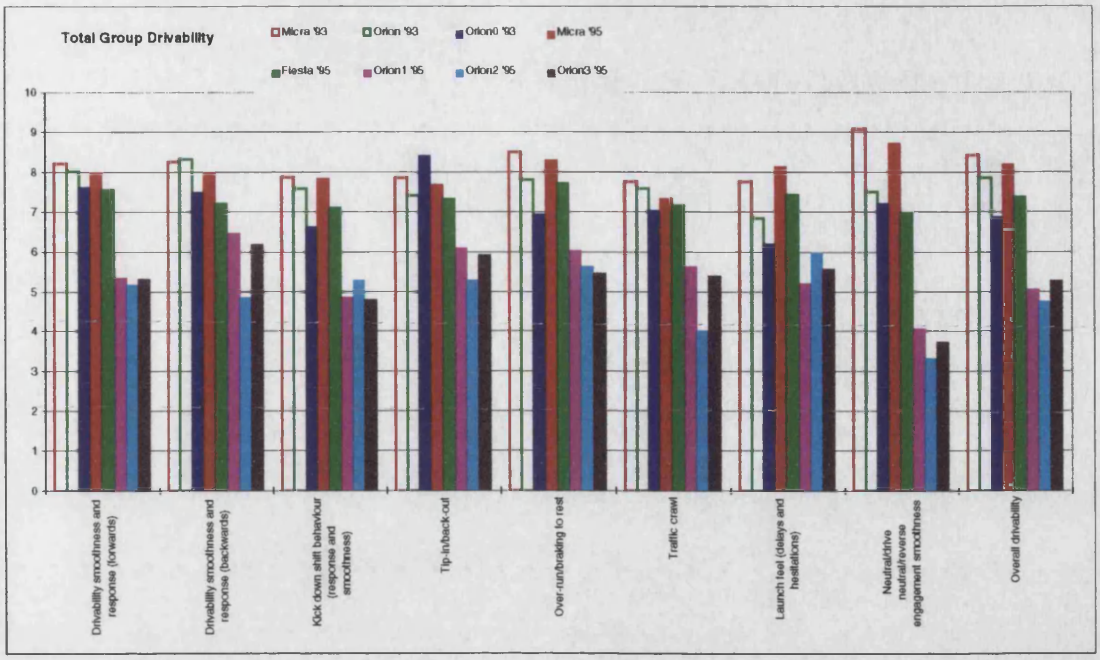

Figure 8.37 Total group Vehicle appraisal results - Drivability

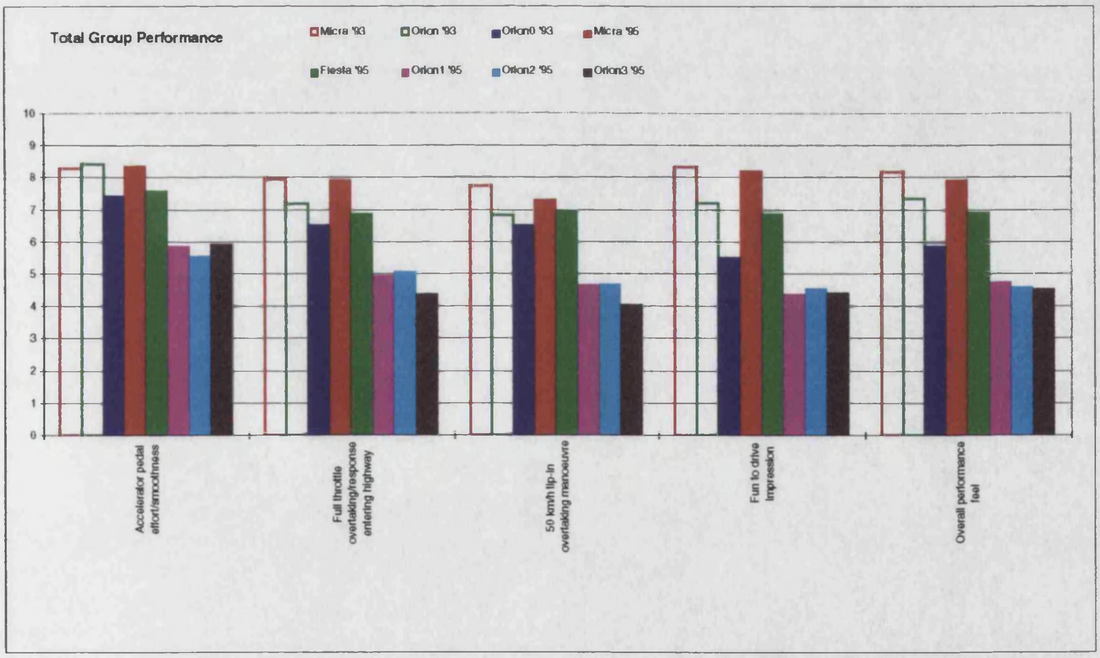

Figure 8.38 Total group Vehicle appraisal results - Performance

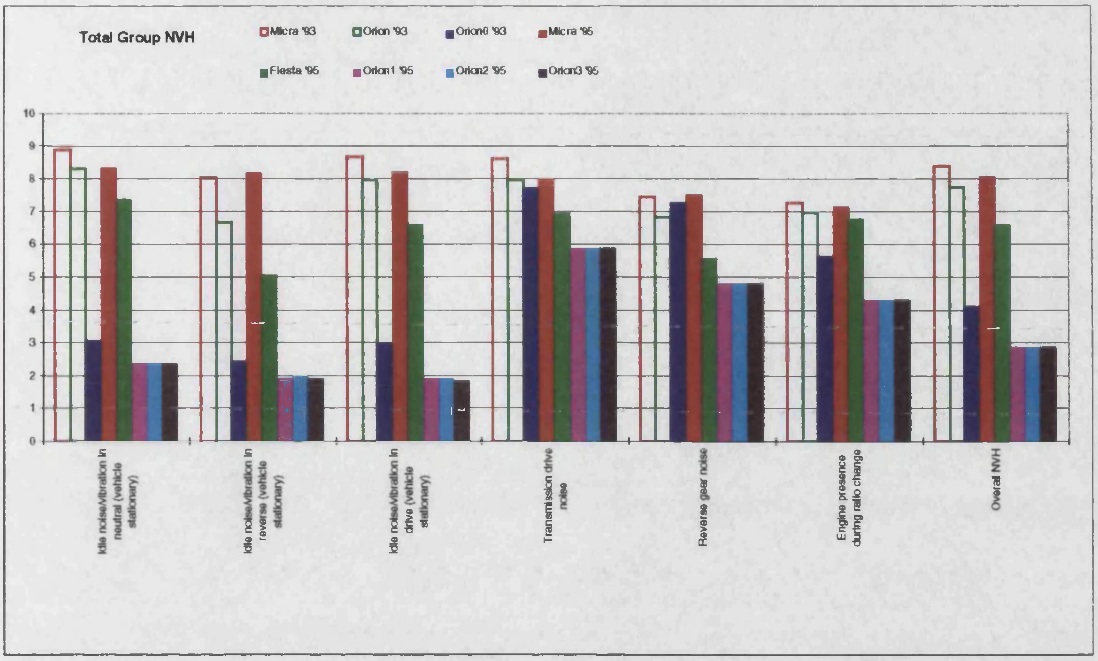

Figure 8.39 Total group Vehicle appraisal results - NVH

9. CONCLUSIONS

9.1 Comparison of controller performance

The advantages of using a CVT as opposed to a stepped ratio transmission within the Diesel powertrain of a medium sized passenger car have been investigated. Existing methods of control of such a powertrain have been analysed and the trade off between emissions and economy control and vehicle drivability considered. Two alternative novel strategies, the Fuzzy logic and Transient shaping controllers, were chosen from a number evaluated in simulation and on the test rig. These strategies were implemented in a test vehicle and shown to demonstrate improved emissions and economy and acceptable drivability over the legislative test when compared to equivalent vehicles with stepped ratio transmissions.

The Fuzzy logic and Transient shaping controllers were shown to be highly flexible and tuneable. They were also robust in operation when implemented on the test rig and in the test vehicle. Both strategies were designed to return the engine to the ideal operating line as steady state powertrain conditions were reached providing the ratio limit of the transmission was not reached. However, the transient shaping controller was designed with special attention to ideal operating line adherence, through the use of the measured engine speed. This characteristic seems to have given the transient shaping controller the advantage in terms of emissions and economy performance. Both alternatives gave an emissions improvement over the legislative vehicle test when compared with equivalent manual vehicles. The measured differences between them reflect both the differences in the strategies and the state of tune of the calibrations.

Assessment of vehicle drivability is made difficult by its subjective nature. The controller calibrations used for the final appraisal were chosen partly to demonstrate and investigate the range of possibilities as well as for comparison against the production vehicles. However, the transient shaping controller did seem to have the advantage over the fuzzy logic controller, here, as in the emissions work. It may have been the more immediate effect of the transient shaping controller torque trimming function which gave it a more responsive feel than the fuzzy logic controller.

The Van Doorne controller and the simulation model of this (the hydraulic controller model) were useful as baseline comparisons for the newly designed controllers. Although Van Doorne did not have opportunity to fully optimise the calibration and matching between the transmission and engine, it was considered that the calibration was aimed generally towards good vehicle drivability and that this was reasonable. Good matching between the Van Doorne controller and the transmission hydraulics and lower level control modules led to a damped, non-oscillatory response from the drive train. The general use of high engine speeds and low engine torques during steady state conditions, by the Van Doorne controller led to reasonable emissions results for NOx but less remarkable fuel economy results.

9.2 Drivability and emissions/economy issues

The choice of ideal operating line was shown to have considerable impact upon both emissions / economy and drivability. The BSFC line, whilst good for fuel consumption, had the effect of making the vehicle feel less responsive. This was due to the low engine speeds generally used and the fact that large engine speed changes were necessary to move the engine to a high speed where large amounts of power could be developed. For the same reasons the NOx line was better for drivability. However, due to the experimental nature of the test vehicle, high engine speeds resulted in the poor NVH characteristics of the vehicle being made more apparent.

9.3 Future work

The work completed by Micklem (1994) and Guebeli (1993), showed the scope for further efficiency optimisation of the CTXE transmission. The recommendations fell into the areas of the hydraulic pump and operating pressures for the variable speed unit, and the general design of the hardware, for example, the decision to have two clutches with an epicyclic gear set to enable vehicle reverse. Some of the modelling work presented in Chapter 7, supports their recommendations concerning the transmission operating pressures. It is also apparent from the subject of, and the discussion in, this thesis that efficiency of the complete powertrain must be considered in advance of either the individual engine or transmission efficiencies. Automatic transmissions have traditionally been matched with engines originally and primarily developed for use with manual transmissions. It is now time to consider an integrated approach to powertrain design and to design prime movers to be used in particular with the automatic transmissions of today.

Clearly drivability of vehicles is a complex issue which has been the subject of much work prior to that presented here. The linking of subjective vehicle assessment with the more objective data acquisition and analysis is considered valuable in producing powertrain controller requirements. Drivability of Diesel vehicles with CVTs is further complicated by the fact that only a minority of passenger cars in production incorporate either and none both. Gasoline vehicles with manual transmissions tend to be the accepted normality, certainly in the European market.

The way in which we travel and the effect this has on the environment we live in is receiving increasing attention both from ourselves and from governments and legislative bodies. This work has highlighted one approach in a field where much work continues, much has been achieved and there is much more to be achieved.

APPENDIX A

A summary of European emissions legislation for light duty Diesel vehicles

EEC Passenger car 91/441/EEC

CO g/km	HC + NOx g/km	Particulates g/km
2.72	0.97	0.14

DI Diesel derogation of 40% for all pollutants until 1994

Stage 2 (1995/6)

CO g/km	HC + NOx g/km	Particulates g/km
1.0	0.9	0.1

Stage 3 Proposal* (1999)

CO g/km	HC g/km	NOx g/km	Particulates g/km
0.5	0.15	0.35	0.04

* The figures given under Stage 3 are the Ford Motor Company forecasts for future emissions legislation.

Glossary

CTX	The continuously variable transmission manufactured by the Ford Motor Co. Ltd. and based upon the Van Doorne push belt continuously variable transmission.
CTXE	The electrohydraulically controlled version of the Ford CTX transmission.
CVT	Continuously variable transmission.
VSU	Variable speed unit. The part of the transmission which enables the continuously variable ratio range. In the Van Doorne transmission, the variable speed unit is comprised of the belt and pulleys.

REFERENCES

AA Magazine (1994)	All the fun of the fair - CVTs pitted against ordinary autos. Autumn 1994 - Issue 10.
Abate M, Dosio N, (1990)	Use of Fuzzy Logic for Engine Idle Speed Control. SAE 900594
Autocar & Motor (1992)	CVT. 8 January 1992.
Autocar & Motor (1993)	The Autocar Twin Test - Nissan Micra 1.3 CVT vs Rover Metro 1.4 CVT. 3 March 1993.
Autocar & Motor (1994)	The Autocar 30000 mile test - Nissan Micra 1.3 CVT. Autocar & Motor. 6 April 1994.
Bacon A, Shayler PJ, Ma T, (1992)	Potential for engine control using neural networks. IMechE C448/057
Brace CJ, Deacon M, Vaughan ND, Burrows CR, Horrocks RW, (1996)	Operating point optimiser for integrated Diesel/CVT powertrain. University of Bath, Ford Motor Company. Application of Powertrain and Fuel Technologies to Meet Emissions Standards for 21st Century. IMechE C517.
Brace CJ, Deacon M, Vaughan ND, Charlton SJ, Burrows CR, (1993/4)	Prediction of Drive Cycle Emissions of a Turbocharged Passenger Car Diesel Engine. Submitted for IMechE Fifth International Conference on Turbocharging and Turbochargers June 1994
Charlton S J, Cox A, Somerville B J, Watts M J, Horrocks R W (1992)	An investigation of the emission characteristics of the passenger car IDI diesel engine. University of Bath, Ford Motor Company Ltd. IMechE 1992 C448/025
Chauhan R, (1993)	Automotive Systems Architecture. Lucas Engineering Centre. Autotech 1993. IMechE C462/4/100
Christenson BC, Beachley NH, Frank AA, (1975)	The fuel-saving potential of cars with CVTs and an optimal control algorithm.
Cuypers MH, (1984)	Metal V-belt and V-chain traction drives. International Symposium on Advanced and Hybrid Vehicles, Strathclyde
Deacon M, (1994)	Appraisal and test of three vehicles with continuously variable transmissions. University of Bath, School of Mechanical Engineering Report No. 033/1994
Deacon M, (1994)	Testing of a vehicle fitted with the CTXE transmission. University of Bath, School of Mechanical Engineering Report No. 035/1994
Deacon M, Brace CJ, Guebeli M, Vaughan ND, Burrows CR, Dorey RE, (1994)	A modular approach to the computer simulation of a passenger car powertrain incorporating a Diesel engine and continuously variable transmission. IEE International conference on Control (1994) University of Warwick.
Department of Transport, (1994)	Fuel consumption of new vehicles
Dongen van L A M, (1982)	Efficiency characteristics on manual and automatic passenger car transmissions. SAE 820741.
Gemeinholzer G, (1990)	Oil cooled multiple disc clutches. Hoerbiger & Co. Germany.
Guebeli M, Dorey RE, (1990)	Real time powertrain simulation for dynamic engine testing using a hydrostatic dynamometer. IEE Colloquium on Power Train Control. 1990.
Guebeli M, (1993)	Optimum Efficiency Control of the CTX Powertrain, PhD Thesis, University Of Bath
Guebeli M, Micklem JD, Burrows CR, (1992)	Maximum transmission efficiency of a steel belt continuously variable transmission. 6th International Power transmission and gearing conference. Phoenix, Arizona. 1992 ASME.
Guibet J C, Douaud A, (1992)	The reduction of photochemical pollution and gaseous emissions having a greenhouse effect. Impact of existing and coming engines - fuel technologies. SAE 923052.
Hendriks E, (1993)	Qualitative and Quantitative Influence of a Fully Electronically Controlled CVT on Fuel Economy and Vehicle Performance SAE 930668.
Hendriks E, Heegde ter P, Prooijen van T, (1988)	Aspects of a metal Pushing V-belt for Automotive Car Application. SAE paper 881734
Hojo Y, Iwatsuki K, Oba H, Ishikawa K, (1992)	Toyota Five Speed Automatic Transmission with application of modern control theory. Toyota Motor Corporation. Aisin AW Co Ltd. SAE 1992.
Hopfner U, (1991)	Will energy consumption and exhaust emissions force a reduction of mobility - A review up to 2005. SAE 917120.
Horowitz A, (1980)	Evaluation of Novel and Powerful Continuously Variable V-Band Transmissions in Comparison with Current Variable and Fixed Drives, 1980 ASME 80- C2/DET-121
Howard G, (1992)	The doubtful future of the CVT. Car Design and Technology, April 1992, pp 44-48
Ironside JM, Stubbs PWR, (1980)	Continuously Variable Transmission Control IEEE Vehicular Technology Society 80CH1601-4
Kamei E, Namba H, Osaki K, Ohba M, (1987)	Application of Reduced Order Model to Automotive Engine Control System. Transactions of the ASME Vol.109

REFERENCES

AA Magazine (1994)	All the fun of the fair - CVTs pitted against ordinary autos. Autumn 1994 - Issue 10.
Abate M, Dosio N, (1990)	Use of Fuzzy Logic for Engine Idle Speed Control. SAE 900594
Autocar & Motor (1992)	CVT. 8 January 1992.
Autocar & Motor (1993)	The Autocar Twin Test - Nissan Micra 1.3 CVT vs Rover Metro 1.4 CVT. 3 March 1993.
Autocar & Motor (1994)	The Autocar 30000 mile test - Nissan Micra 1.3 CVT. Autocar & Motor. 6 April 1994.
Bacon A, Shayler PJ, Ma T, (1992)	Potential for engine control using neural networks. IMechE C448/057
Brace CJ, Deacon M, Vaughan ND, Burrows CR, Horrocks RW, (1996)	Operating point optimiser for integrated Diesel/CVT powertrain. University of Bath, Ford Motor Company. Application of Powertrain and Fuel Technologies to Meet Emissions Standards for 21st Century. IMechE C517.
Brace CJ, Deacon M, Vaughan ND, Charlton SJ, Burrows CR, (1993/4)	Prediction of Drive Cycle Emissions of a Turbocharged Passenger Car Diesel Engine. Submitted for IMechE Fifth International Conference on Turbocharging and Turbochargers June 1994
Charlton S J, Cox A, Somerville B J, Watts M J, Horrocks R W (1992)	An investigation of the emission characteristics of the passenger car IDI diesel engine. University of Bath, Ford Motor Company Ltd. IMechE 1992 C448/025
Chauhan R, (1993)	Automotive Systems Architecture. Lucas Engineering Centre. Autotech 1993. IMechE C462/4/100
Christenson BC, Beachley NH, Frank AA, (1975)	The fuel-saving potential of cars with CVTs and an optimal control algorithm.
Cuypers MH, (1984)	Metal V-belt and V-chain traction drives. International Symposium on Advanced and Hybrid Vehicles, Strathclyde
Deacon M, (1994)	Appraisal and test of three vehicles with continuously variable transmissions. University of Bath, School of Mechanical Engineering Report No. 033/1994
Deacon M, (1994)	Testing of a vehicle fitted with the CTXE transmission. University of Bath, School of Mechanical Engineering Report No. 035/1994
Deacon M, Brace CJ, Guebeli M, Vaughan ND, Burrows CR, Dorey RE, (1994)	A modular approach to the computer simulation of a passenger car powertrain incorporating a Diesel engine and continuously variable transmission. IEE International conference on Control (1994) University of Warwick.
Department of Transport, (1994)	Fuel consumption of new vehicles
Dongen van L A M, (1982)	Efficiency characteristics on manual and automatic passenger car transmissions. SAE 820741.
Gemeinholzer G, (1990)	Oil cooled multiple disc clutches. Hoerbiger & Co. Germany.
Guebeli M, Dorey RE, (1990)	Real time powertrain simulation for dynamic engine testing using a hydrostatic dynamometer. IEE Colloquium on Power Train Control. 1990.
Guebeli M, (1993)	Optimum Efficiency Control of the CTX Powertrain, PhD Thesis, University Of Bath
Guebeli M, Micklem JD, Burrows CR, (1992)	Maximum transmission efficiency of a steel belt continuously variable transmission. 6th International Power transmission and gearing conference. Phoenix, Arizona. 1992 ASME.
Guibet J C, Douaud A, (1992)	The reduction of photochemical pollution and gaseous emissions having a greenhouse effect. Impact of existing and coming engines - fuel technologies. SAE 923052.
Hendriks E, (1993)	Qualitative and Quantitative Influence of a Fully Electronically Controlled CVT on Fuel Economy and Vehicle Performance SAE 930668.
Hendriks E, Heegde ter P, Prooijen van T, (1988)	Aspects of a metal Pushing V-belt for Automotive Car Application. SAE paper 881734
Hojo Y, Iwatsuki K, Oba H, Ishikawa K, (1992)	Toyota Five Speed Automatic Transmission with application of modern control theory. Toyota Motor Corporation. Aisin AW Co Ltd. SAE 1992.
Hopfner U, (1991)	Will energy consumption and exhaust emissions force a reduction of mobility - A review up to 2005. SAE 917120.
Horowitz A, (1980)	Evaluation of Novel and Powerful Continuously Variable V-Band Transmissions in Comparison with Current Variable and Fixed Drives, 1980 ASME 80- C2/DET-121
Howard G, (1992)	The doubtful future of the CVT. Car Design and Technology, April 1992, pp 44-48
Ironside JM, Stubbs PWR, (1980)	Continuously Variable Transmission Control IEEE Vehicular Technology Society 80CH1601-4
Kamei E, Namba H, Osaki K, Ohba M, (1987)	Application of Reduced Order Model to Automotive Engine Control System. Transactions of the ASME Vol.109